Domain decomposition and multi-scale computations of singularities in mechanical structures

Thi Bach Tuyet Dang

ÉCOLE POLYTECHNIQUE

ÉCOLE DOCTORALE DE L'ÉCOLE POLYTECHNIQUE

LABORATOIRE DE MÉCANIQUE DES SOLIDES

THÈSE présentée par :

Thi Bach Tuyet DANG

soutenue le : **29 Avril 2013**

pour obtenir le grade de : **Docteur de l'École Polytechnique**

Discipline : **MÉCANIQUE**

Calcul multi-échelle de singularités et applications en mécanique de la rupture

THÈSE dirigée par :

Jean Jacques MARIGO	Professeur, L'École Polytechnique
Laurence HALPERN	Professeure, Université Paris XIII

RAPPORTEURS :

Francoise KRASUCKI	Professeure, Université de Montpellier
Radhi ABDELMOULA	Maitre de conference, Université Paris XIII

JURY :

Francoise KRASUCKI	Professeure, Université de Montpellier
Radhi ABDELMOULA	Maitre de conference, Université Paris XIII
Marc DAMBRINE	Professeur, Université de PAU
Quoc Son NGUYEN	Directeur de Recherches, CNRS
Jean-Jacques MARIGO	Professeur, École Polytechnique
Laurence HALPERN	Professeure, Université Paris XIII

Calcul multi-échelle de singularités et applications en mécanique de la rupture

DANG Thi Bach Tuyet

Abstract

A major issue in fracture mechanics is to model the nucleation of a crack in a sound material. There are two difficulties: the first one is to propose a law able to predict that nucleation; the second is a purely numerical issue. It is indeed difficult to compute with a good accuracy all the mechanical quantities like the energy release rate associated with a crack of small length which appears at the tip of a notch. The classical finite element method leads to inaccurate results because of the overlap of two singularities which cannot be correctly captured by this method: one due to the tip of the notch, the other due to the tip of the crack. A specific method of approximation based on asymptotic expansions is preferable as it is developed in analog situations with localized defects. The first chapter of the thesis is devoted to the presentation of this Matched Asymptotic Method (shortly, the **MAM**) in the case of a defect (which includes the case of a crack) located at the tip of a notch in the simplified context of antiplane linear elasticity.

The main goal of the thesis is to use these asymptotic methods to predict the nucleation or the propagation of defects (like cracks) near those singular points. The second chapter of the thesis will be devoted to this task. This requires, of course, to overcome the first issue by introducing a criterion for nucleation. This delicate issue has not received a definitive answer at the present time and it was considered for a long time as a problem which could not be solved in the framework of Griffith theory of fracture. The main invoked reason is that the release of energy due to a small crack tends to zero when the length of the crack tends to zero. Therefore, if one follows the Griffith criterion which stands that the crack can propagate only when the energy release rate reaches a critical value characteristic of the material, no nucleation is possible because the energy release rate vanishes when there is no preexisting crack. This "drawback" of Griffith's theory was one of the motivations which led Francfort and Marigo to replace the Griffith criterion by a principle of least energy. It turns out that this principle of global minimization of the energy is really able to predict the nucleation of cracks in a sound body. However, the nucleation is necessarily brutal in the sense that a crack of finite length suddenly appears at a critical loading. Moreover the system has to cross over an energy barrier which can be high when the minimum is "far". Another way to overcome the issue of the crack nucleation is to leave the pure Griffith setting by considering cohesive cracks. Indeed, since any cohesive force model contains a critical stress, it becomes possible to nucleate crack without invoking global energy minimization. Accordingly, we propose to revisit the problem of nucleation of a crack at the tip of a notch by comparing the three criteria. One of our goal is to use the **MAM** to obtain semi-analytical expressions for the critical loading at which a crack appears and the length of the nucleated crack.

Specifically, the thesis is organized as follows. Chapter 1 is devoted to the description of the **MAM** on a generic anti-plane linear elastic problem where the body contains a defect near the tip of a notch. We first decompose the solution into two expansions: one, the *outer expansion*, valid far enough from the tip of the notch, the other, the *inner expansion*, valid in a neighborhood of the tip of the notch. These expansions contain a sequence of inner and outer terms which are solutions of inner and outer problems and which are interdependent by the matching conditions. Moreover each term contains a regular and a singular part. We explain how all the terms and the coefficients entering in their singular and regular parts are sequentially determined. The chapter finishes by an example where the exact solution is obtained in a closed form and hence where we can verify the relevance of the **MAM**. In Chapter 2, the **MAM** is applied to the case where the defect is a crack. Its main goal is to compute with a good accuracy the energy release rate associated with a crack of small length near the tip of the notch. Indeed, it is a real issue in the case of a genuine notch (by opposition to a crack) because the energy release rate starts from 0 when the length of the nucleated crack is 0, then is rapidly increasing

with the length of the crack before reaching a maximum and finally is decreasing. Accordingly, after the setting of the problem, one first explains how one computes the energy release rate by the FEM and why the numerical results are less accurate when the crack length is small. Then, one uses the **MAM** to compute the energy release rate for small values of the crack length and one shows, as it was expected, that the smaller the size of the defect, the more accurate is the approximation by the **MAM** at a certain order. It even appears that one can obtain very accurate results by computing a small number of terms in the matched asymptotic expansions. We discuss also the influence of the angle of the notch on the accuracy of the results, this angle playing an important role in the process of nucleation (because, in particular, the length at which the maximum of the energy release rate is reached depends on the angle of the notch). It turns out that when the notch is sufficiently sharp, *i.e.* sufficiently close to a crack, it suffices to calculate the first two non trivial terms of the expansion of the energy release rate to capture with a very good accuracy the dependence of the energy release rate on the crack length.

Then a cohesive model, the so-called Dugdale model, is considered in the last section of the chapter. Combining the **MAM** with the $G - \theta$ method allows us to calculate in an almost closed form the nucleation and the evolution of the crack, namely the relations between the external load and the lengths of the non-cohesive zone and the cohesive zone. Specifically, it turns out that the inner problem can be seen as an Hilbert problem which can be solved with the help of complex potentials. Thus, the access to the solution is reduced to a few quadratures which are computed numerically. One obtains so an analytical expression of the critical load at which a "macroscopic" crack will appear in the body after an unstable stage of propagation of the nucleated crack. The order of magnitude of that critical load is directly associated with the power of the singularity of the solution before nucleation which is itself a known function of the angle of the notch.

Chapter 3 proposes a generalization of all the previous results in the plane elasticity setting. Specifically, the goal is still to study the nucleation of non cohesive or cohesive cracks at the angle of a notch in the case of a linearly elastic isotropic material but now by considering plane displacements. Moreover, we will consider as well pure mode I situation as mixed modes cases. In the first part of the chapter we use the global minimization principle in the case of a non cohesive crack. In the second part we consider Dugdale cohesive force model. In both cases the **MAM** is used to compensate the non accuracy of the finite element method. All the derived results can be seen as simple generalizations of those developed in the antiplane case. Indeed, from a conceptual and qualitative viewpoint, we obtain essentially the same types of properties. However, from a technical point of view, the **MAM** is more difficult to apply in plane elasticity because the sequence of singularities can be obtained only by solving transcendental equations. Therefore, the numerical procedure becomes more expansive. Moreover, from the analytical point of view, the calculations become much more intricate and consequently a part of these calculations are given in the appendix.

Résumé

Un enjeu majeur de mécanique de la rupture est de modéliser l'initiation d'une fissure dans une structure saine. Il y a deux difficultés: la première est de proposer une loi capable de prédire la nucléation, la seconde est d'ordre purement numérique. En ce qui concerne ce deuxième point, il est en effet difficile de calculer avec une bonne précision toute quantité comme le taux de restitution d'énergie associée à une fissure de faible longueur qui apparaît en fond d'entaille. La méthode des éléments finis classique conduit à des résultats inexacts en raison de la superposition de deux singularités (l'une due à l'entaille, l'autre à la pointe de la fissure) qui ne peuvent être correctement capturées par cette méthode. Une méthode spécifique d'approximation basée sur des développements asymptotiques est préférable comment il a déjà été constaté dans des situations analogues présentant des défauts localisés. Le premier chapitre de la thèse est consacré à la présentation de cette méthode asymptotique dite Méthode des Développements Asymptotiques Raccordés (**MAM**) dans le cas d'un défaut (ce qui inclut le cas d'une fissure) situé à l'extrémité d'une entaille. Cette première étude est faite dans le cadre simplifié de l'élasticité linéaire antiplane avant d'être étendue à l'élasticité plane dans le troisième chapitre.

Un objectif majeur est d'utiliser cette méthode asymptotique pour prédire la nucléation ou la propagation d'une fissure à proximité d'un point singulier. Le deuxième chapitre de la thèse sera consacré à cette tâche. Cela nécessite, bien sûr, de lever la première difficulté en proposant un critère de nucléation physiquement raisonnable. Cette délicate question n'a pas reçu de réponse définitive à l'heure actuelle et a été considérée pendant longtemps comme un problème qui ne pouvait être résolu dans le cadre de la théorie de Griffith. La principale raison invoquée est que le taux de restitution de l'énergie dû à une petite fissure tend vers zéro lorsque la longueur de la fissure tend vers zéro. Par conséquent, si l'on suit le critère de Griffith qui stipule que la fissure peut se propager que lorsque le taux de libération d'énergie atteint une valeur caractéristique du matériau, il n'y a pas de nucléation possible. Ce "défaut" de la théorie de Griffith fut l'une des motivations qui conduit Francfort et Marigo à remplacer le critère de Griffith par un principe de minimisation de l'énergie. Il s'avère que ce principe de minimum global de l'énergie est vraiment en mesure de prédire la nucléation des fissures dans un corps sain. Cependant, la nucléation est nécessairement brutale dans le sens où une fissure de longueur finie apparaît brutalement à une charge critique et de plus il faut que le système franchisse une barrière d'énergie qui peut être d'autant plus haute que le minimum est "loin". Une autre façon de rendre compte de la nucléation de fissures est de quitter le cadre de la théorie de Griffith en introduisant le concept de forces cohésives. L'intérêt d'une telle approche est qu'elle contient automatiquement la notion de contrainte critique qui permet de régir naturellement la nucléation sans passer par le principe de minimisation globale de l'énergie. En résumé, nous proposons de traiter le problème de la nucléation d'une fissure à la pointe d'une entaille de trois façons et de comparer les trois critères correspondants. L'un de nos objectifs est aussi d'utiliser la **MAM** pour obtenir des expressions semi-analytiques pour la charge critique à partir de laquelle une fissure apparaît ainsi que la longueur de la fissure une fois nucléée.

De façon précise, la thèse est organisée comme suit. Le chapitre 1 est consacré à la description de la **MAM** sur un problème générique d'élasticité linéaire antiplane où la structure contient un défaut situé au voisinage de la pointe d'une entaille. Nous avons d'abord décomposé la solution en deux développements: l'un, le *développement* extérieur, valable assez loin de la pointe de l'entaille, l'autre, le *développement* intérieur, valable au voisinage de la pointe de l'entaille. Ces développements contiennent une séquence de termes "intérieurs" et "exterieurs" qui sont solutions de problèmes "intérieurs" et "extérieurs" reliés les uns aux autres par des conditions de raccord. En outre, chaque terme contient une partie régulière et une partie singulière. Nous expliquons ensuite comment tous les termes et les

coefficients qui entrent dans les parties singulières et régulières sont déterminés séquentiellement. Le chapitre se termine par un exemple où la solution exacte est connue et peut donc être développée directement avant d'être comparée à celle fournie par la **MAM**.

Dans le chapitre 2, la **MAM** est appliquée au cas où le défaut est une fissure. Le premier objectif est de calculer avec une bonne précision le taux de restitution d'énergie associée à une fissure non cohésive de faible longueur située près de la pointe de l'entaille. En effet, il s'agit d'un véritable problème dans le cas où l'entaille n'est elle-même pas une fissure parce que le taux de restitution d'énergie est voisin de 0 lorsque la longueur de la fissure nucléée est voisine de 0, puis augmente rapidement avec la longueur de la fissure avant d'atteindre un maximum pour finalement redécroître. On explique d'abord comment le taux de restitution d'énergie est calculé par la Méthode des Elémenst Finis et pourquoi les résultats numériques sont moins précis lorsque la longueur de la fissure est faible. Ensuite, on utilise la **MAM** pour calculer le taux de restitution d'énergie pour les petites valeurs de la longueur de la fissure et on montre, comme il était prévu, que plus la taille de la fissure est petite, plus le résultat fourni par la **MAM** à un ordre donné est précis. Il s'avère même que l'on peut obtenir des résultats très précis en calculant seulement un petit nombre de termes. Nous discutons aussi de l'influence de l'angle de l'entaille sur l'exactitude des résultats. Cet angle joue un rôle important dans le processus de nucléation (parce que, en particulier, la longueur à partir de laquelle le maximum du taux de restitution d'énergie est atteinte dépend de l'angle de l'entaille). Lorsque l'angle de l'entaille est suffisamment grand, il suffit de calculer les deux premiers termes non triviaux du développement du taux de restitution d'énergie pour obtenir avec une très bonne précision la dépendance du taux de restitution d'énergie avec la longueur de fissure.

Nous considérons ensuite le cas des fissures cohésives en introduisant le modèle de forces cohésives de Dugdale. En combinant la **MAM** avec la méthode $G - \theta$, nous obtenons un système de deux équations non linéaires couplées régissant l'évolution des longueurs de la zone non-cohésive et la zone cohésive en fonction du chargement. Il s'avère que le problème intérieur fourni par la **MAM** est un problème de Hilbert qui peut être résolu par la méthode des potentiels complexes. Ce faisant, la résolution se ramène à de simples quadratures qui sont calculées numériquement. On obtient ainsi, de façon quasiment analytique, la charge critique à partir de laquelle la petite fissure se propage de façon instable pour donner lieu à une fissure "macroscopique". En particulier, l'ordre de grandeur de cette charge critique est directement relié à l'exposant de la singularité de la solution avant fissuration qui est lui-même fonction de l'angle de l'entaille.

Le chapitre 3 propose une généralisation de toutes les méthodes et résultats précédents au cas de l'élasticité plane. De façon précise, le but est toujours d'étudier la nucléation de fissures cohésives ou non cohésives à l'angle d'une entaille dans un milieu linéairement élastique et isotrope, mais maintenant en considérant des déplacements plans. De plus, il s'agit de traiter les conditions de nucléation aussi bien sous mode I pur que sous mode mixte. Dans la première partie du chapitre, nous utilisons le principe de minimisation globale pour traiter le cas des fissures non cohésives, alors que dans la deuxième partie nous utilisons le modèle de Dugdale pour traiter le cas des fissures cohésives. Dans les deux cas, la **MAM** est mise en œuvre pour pallier le manque de précision de la méthode des éléments finis. Tous les résultats qui sont obtenus peuvent être considérés comme de simples généralisations de ceux développés dans le cas antiplan. En effet, d'un point de vue conceptuel et qualitatif, nous obtenons essentiellement le même type de propriétés. Toutefois, d'un point de vue technique, la **MAM** est plus délicate d'application en élasticité plane parce que l'obtention de la suite des fonctions singulières passe par la résolution d'équations transcendantes. Ce faisant, la mise en œuvre numérique est sensiblement plus coûteuse. De plus, d'un point de vue analytique, les calculs et les démonstartions sont beaucoup plus lourds et une partie est donc passée en annexe.

Acknowledgments

Firstly, I would like to thank my first thesis advisor Jean-Jacques MARIGO. I am deeply indebted to him for his many invaluable guidance, advice, inspiration and the constant support during my years of thesis.

Secondly, I am very grateful to my second thesis advisor Laurence HALPERN for her precious advice, support and for her very important suggestions and discussions.

I would like to thank Francoise KRASUCKI and Radhi ABDELMOULA for accepting to be reporters and for their careful reading of the thesis.

And I would like to thank Marc DAMBRINE for agreeing to be part of my jury.

The fortune gave me chance to meet BUI Huy Duong in LMS and then I have discussed with him a lots about the method of Muskhelishvili. I would like to express my gratitude to BUI Huy Duong for many interesting discussions and highly valuable advice.

I would like to thank Giuseppe GEYMONAT for his very important discussions and help when i met many difficulties in studying the singularity behavior of Bi-Laplace function.

I would like also to thank director of LMS for giving me the office, many support for working during my stay in LMS. Then, i am also truly thankful to the secretaries of LMS for many precious help.

Many thanks sent to researchers in LMS, Andrei CONSTANTINESCU, Thien Nga LE, NGUYEN Quoc Son, LUONG Minh Phong, etc . . . , for many precious discussions.

I also want to thank Michel ZINSMEISTER for helping the vietnamese students in the PUF program.

Finally, i would like to thank all my friends LE Minh Bao, LUU Duy Hao, NGUYEN Truong Giang, TRAN Thuong Van Du, Roberto ALESSI, Paul SICSIC, TRAN Huong Lan, TRAN Ngoc Diem My, NGUYEN Dinh Liem, LE Thi Van Anh, ONG Thanh Hai, NGUYEN Dang Ky, LE Thanh Hoang Nhat, BUI Xuan Thang, LE Kim Ngan, NGUYEN Van Dang, HOANG Van Ha, etc . . . for helping me in many ways in life, specially, Pierre Alexandre DELATTRE for all great encouragement that he gave me and for all his help . Many deep thanks go to my parents for raising, encouraging and for their love.

Introduction

A major issue in fracture mechanics is how to model the initiation of a crack in a sound material, see [Bourdin et al., 2008]. There are two difficulties: the first one is to propose a law able to predict that nucleation; the second is a purely numerical issue. Indeed, it is difficult to compute with a good accuracy the energy release rate associated with a crack of small length which appears at the tip of a notch, see [Marigo, 2010]. The classical finite element method leads to inaccurate results because of the overlap of two singularities which cannot be correctly captured by this method: one due to the tip of the notch, the other due to the tip of the crack. A specific method of approximation based on asymptotic expansions is preferable as it is developed in analog situations with localized defects, see for instance [Abdelmoula and Marigo, 2000; Abdelmoula et al., 2010; Bilteryst and Marigo, 2003; Bonnaillie-Noel et al., 2010; Bonnaillie-Noel et al., 2011; David et al., 2012; Geymonat et al., 2011; Leguillon, 1990; Marigo and Pideri, 2011; Vidrascu et al., 2012].

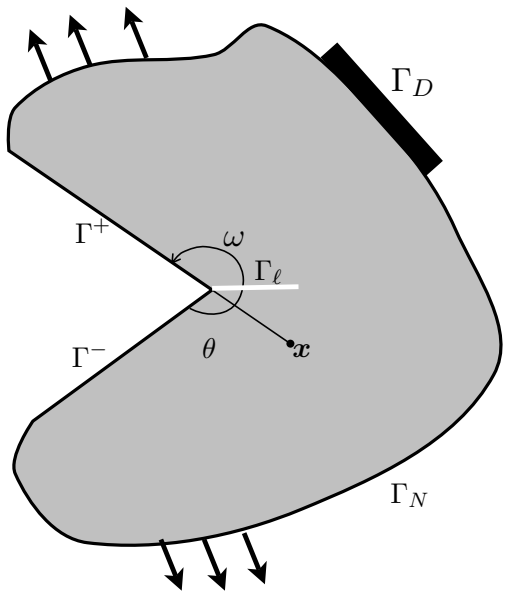

Figure 1: The notched body with a small crack of length ℓ at the corner of the notch

The first chapter is devoted to the presentation of this Matched Asymptotic Method (shortly, the **MAM**) in the case of a defect (which includes the case of a crack) located at the tip of a notch in

the simplified context of antiplane linear elasticity. Therefore, our approach can be considered as a particular case of the previous works which have been devoted to the study of elliptic problems in corner domains, like [Dauge, 1988; Dauge et al., 2010; Grisvard, 1985; Grisvard, 1986]. Specifically, if one denotes by ℓ the small parameter characterizing the size of the defect and u_ℓ the displacement field solution of the static problem posed on an elastic body submitted to an anti-plane loading, the method consists in postulating that u_ℓ admits two expansions with respect to the small parameter: the inner one close to the defect and the outer one far from the defect. These two expansions have to be matched by the so-called matching conditions which consists in giving a sequence of relations between the behavior of the inner expansions "at infinity" with the behavior of the outer expansions "at the tip of the notch".

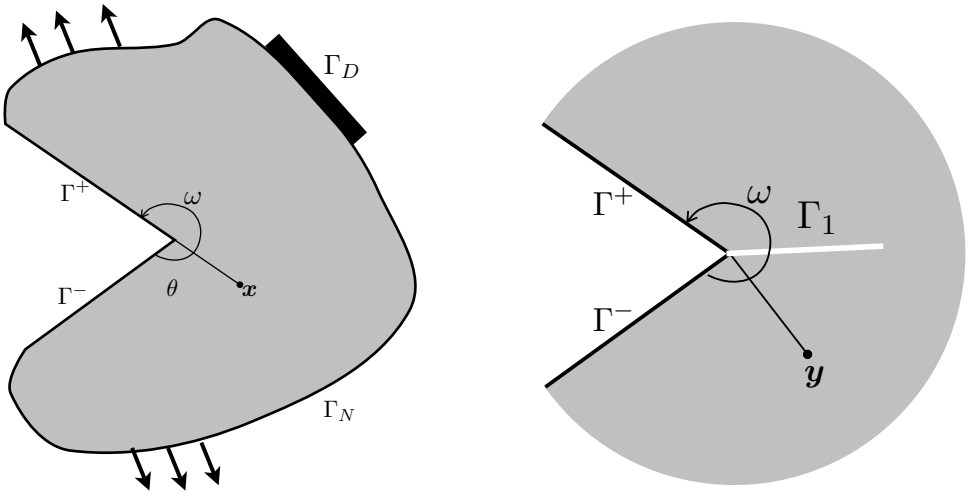

Figure 2: Left: the outer domain where the outer terms of the asymptotic expansions are defined (there is no more crack); Right: the inner domain where the inner terms are defined (there is no more boundary except the edges of the notch)

The specificity of this approach when it is applied to the case of a notch (or more generally to the case where the solution without defect is singular at the point where the defect will occur) is that the presence of singularities change the form of the expansions. Indeed, u_ℓ can no more be expanded in powers of ℓ. In the anti-plane isotropic elastic setting, the outer expansion of u_ℓ can be written in terms of the powers of ℓ^λ where λ is the exponent of the singularity of the solution without defect. (The inner expansion can contain a term involving $\ln(\ell)$ according to the type of boundary conditions which are applied on the defect. In our case where the defect is stress free or is submitted to equilibrated forces, this logarithmic term disappears.) This exponent is well-known and simply reads as $\lambda = \pi/\omega$ where ω is the angle of the notch. Accordingly, the inner out outer expansions can read as

$$\text{Outer expansion:} \quad u_\ell(\mathbf{x}) = \sum_{i\in\mathbb{N}} \ell^{i\lambda} u^i(\mathbf{x}),$$

$$\text{Inner expansion:} \quad u_\ell(\mathbf{x}) = \sum_{i\in\mathbb{N}} \ell^{i\lambda} v^i(\mathbf{x}/\ell).$$

One of the main difficulties of the **MAM** is that the successive terms of the expansions u^i and v^i become more and more singular. That requires to separate their singular part (corresponding to fields with infinite energy) to their regular part (corresponding to fields with finite energy) to obtain well-posed problems. Accordingly, the determination of each part is made separately: the knowledge of the singular parts up to the order i allows one to determine the ith regular part which in turn gives higher order singular parts. Thus, one can obtain by induction all the terms.

One can consider that our study completes the previous ones in the sense that we propose to effectively determine all the terms of the inner and outer expansions. To this end, two methods will be proposed. The first one consists in solving sequentially the different terms. Its drawback is that one must recalculate all the terms as soon as one changes a parameter of the problem (the loading, the overall geometry or the defect). On the contrary, the second method is based on the linearity of the problem and allows one to solve independently and once and for all a sequence of inner problems and a sequence of outer problems. In particular, we will be able to calculate in a closed form the different coefficients entering in the inner expansion in the case of a cavity or a crack.

But the major difference of the present work by comparison with previous ones is that we want to use these asymptotic methods to predict the nucleation and the propagation of cracks near those singular points. The second chapter will be devoted to this task. That requires, of course, to introduce a criterion of nucleation. This delicate issue has not received a definitive answer at the present time and it was considered for a long time as a problem which could not be solved in the framework of Griffith theory of fracture the main ingredients of which are briefly recalled, see [Bui, 1978; Cherepanov, 1979; Lawn, 1993; Leblond, 2000] for more details.

Griffith's theory of fracture [Griffith, 1920] remains the most used in Engineering, [Bui, 1978], [Lawn, 1993], [Leblond, 2000]. Its main advantage is its simplicity in terms of material behavior, because it only requires the identification of the two elastic coefficients, namely the Young modulus E and the Poisson ratio ν, and the surface energy density $\mathsf{G_c}$ for an isotropic brittle material. However, there exist several ways to set the problem of crack propagation while staying within the framework of Griffith's assumptions. (This lack of uniqueness is in fact the mark that none of those ways is perfect.) We are interested here in two of them. The first one, called in this work the *G-law*, which is also the most used, is the law based on the concept of critical energy release rate requiring that a crack can propagate only when the potential energy release rate $\mathcal{G}$ is equal to $\mathsf{G_c}$. One of the drawbacks of the energy release rate criterion is its incapacity to account for crack initiation in a body which does not contain a preexisting crack. The reason is that the release of energy due to a small crack tends to zero when the length of the crack tends to zero, as it was generically proved in [Chambolle et al., 2008; Francfort and Marigo, 1998]. Therefore, if one follows the Griffith criterion, no nucleation is possible because the energy release rate vanishes when there is no preexisting crack. This "drawback" of the *G-law* was one of the motivations which led Francfort and Marigo to replace the Griffith criterion by a principle of least energy. This revisited Griffith energy principle stated first in [Francfort and Marigo, 1998], the so-called *FM-law*, is equivalent to the critical energy release rate criterion and hence to the

G-law in a certain number of cases, as it is will be briefly shown in this work and as it is clearly proved in [Francfort and Marigo, 1998; Marigo, 2010]. But it is (in general) quite different as far as the crack initiation is concerned. In particular, with the least energy principle, it becomes possible to predict the onset of cracking in a sound body. However, the price to pay is that the onset of cracking is necessarily brutal in the sense that a crack of finite length appears at a critical load. The reason is that the elastic response (without any crack) is always a (local) minimum of the energy. Therefore the body has to jump from a local minimum to another (local or global) minimum. This revisited Griffith theory, which simply consists in formalizing the seminal Griffith idea, provided the adequate mathematical framework to obtain new results by inserting fracture mechanics into a modern variational approach, [Dal Maso and Toader, 2002], [Francfort and Larsen, 2003], [Dal Maso et al., 2005].

In the first part of Chapter 2 we do not leave Griffith's setting and will continue to compare the two formulations in the case of a two-dimensional body which contains a notch the opening ω of which is taken as a parameter. (The limit case $\omega = 2\pi$ corresponds to an initial crack.) We will show that the latter, the *FM-law*, based on energy minimization, enjoys the fundamental property of delivering a continuous response with respect to the parameter ω whereas the former one, the *G-law*, formulated in terms of the energy release rate, does not. This major difference appears precisely when it is question of crack initiation and this result greatly militates in favor of the minimization principle. Assuming that the crack will appear (or propagate) at the tip of the notch (or of the preexisting crack) and that the crack path is known, the problem consists in determining, for a given ω, the evolution $\ell_\omega(t)$ of the crack length with the loading parameter t. The evolution depends of course on ω and on the chosen criterion of propagation. Since the concept of crack in Continuum Mechanics— where a crack is considered as a surface of discontinuity— is an idealization of the reality, a criterion of initiation or of propagation can be considered as physically acceptable only if it is stable under small perturbations. In other words, the law is acceptable only if it delivers a response which continuously depends on the geometrical or material parameters of the problem. In the present case that means that the initiation and the propagation of a crack from the tip of a notch whose angle is close to 2π must be close to those corresponding to the evolution from a preexisting crack. In mathematical terms that means that the function $t \mapsto \ell_\omega(t)$ must converge (in a sense to be precised) to $t \mapsto \ell_{2\pi}(t)$ when ω goes to 2π. Unfortunately, the critical energy release rate criterion does not enjoy this continuity property. On the contrary, the least energy criterion does.

Let us summarize here the reasons of these differences (they will be developed in Chapter 2 in an anti-plane elasticity setting and in Chapter 3 in a plane elasticity setting). Since the singularity at the tip of a notch ($\omega < 2\pi$) is "weak", the energy release rate $\mathcal{G}_\omega(t, \ell)$ associated with a crack of small length ℓ (starting from the tip of the notch) goes to 0 when ℓ goes to 0, *i.e.* $\lim_{\ell \to 0} \mathcal{G}_\omega(t, \ell) = 0, \forall t$. Consequently, no crack will appear if we use the critical energy release rate criterion, *i.e.* $\ell_\omega(t) = 0\ \forall t$. On the other hand, if we consider a preexisting crack ($\omega = 2\pi$), then the singularity is strong enough so that $\mathcal{G}_{2\pi}(t, 0) = \mathcal{G}^0_{2\pi} t^2$ with $\mathcal{G}^0_{2\pi} > 0$ (in general). Consequently, the critical energy release rate criterion predicts that the crack will propagate at a (finite) critical loading $t_{2\pi} = \sqrt{\mathsf{G_c}/\mathcal{G}^0_{2\pi}}$. What happens for

$t > t_{2\pi}$ depends on the convexity properties of the potential energy as a function of ℓ, but in any case there is no continuity of the response with respect to ω at $\omega = 2\pi$. In contrast, we will show that this continuity property holds if we define the evolution from the least energy criterion. In particular, when $\omega < 2\pi$, the least energy criterion predicts that a crack of finite length ℓ^0_ω suddenly appears at $t = t_\omega$, then propagates continuously with t. Moreover, we prove that $\lim_{\omega\to 2\pi} \ell^0_\omega = 0$ and $\lim_{\omega\to 2\pi} t_\omega = t_{2\pi}$ and that the height of the energy barrier tends to 0 with ω.

The proofs of those continuity properties with respect to ω were given in [Marigo, 2010] in the restricted setting of anti-plane elasticity and will be extended in Chapter 3 to plane elasticity. Note that a quasi-static assumption is adopted throughout the analysis even though the nucleation of the crack is brutal. It is of course a strong assumption to neglect inertial effects in such a situation, but it is also a limitation due to Griffith's assumption on the surface energy. Indeed, as far as the initiation of a crack at the tip of a notch is concerned, Griffith's criterion remains unable to predict the initiation in dynamics, because the singularity is of the same type as in statics and hence the energy release rate vanishes also in dynamics.

In addition to this qualitative comparisons between the two laws, one goal of this work is to obtain quantitative results. In particular, we want to have some estimates of the critical load at which a crack is nucleated with the *FM-law* and the length of this initial crack. The **MAM** is a good candidate for doing that. Indeed, it allows us to have good estimates of the mechanical quantities for small values of the crack length. The question which is *a priori* open is to know how many terms are necessary to obtain accurate estimates of those quantities. The answer will be given in Chapters 2 and 3.

However, several criticisms can be made against the *FM-law* and the principle of least energy when it is applied to predict the crack initiation. One of them is that the body must cross over an energy barrier to jump from one well to the other. The presence of that energy barrier (which ensures the stability of the elastic response) is essentially due to the fact that Griffith's theory does not contain a critical stress and allow singular stress fields. Accordingly, a remedy consists in introducing this concept of critical stress by leaving Griffith's setting. It is the essence of cohesive force models ([Needleman, 1992], [Del Piero, 1999], [Del Piero and Truskinovsky, 2001], [Laverne and Marigo, 2004], [Charlotte et al., 2006], [Ferdjani et al., 2007]) in the spirit of Dugdale's and Barenblatt's works, cf. [Dugdale, 1960], [Barenblatt, 1962] and [Bourdin et al., 2008]. Indeed, since any cohesive force model contains a critical stress, it becomes possible to nucleate crack without invoking global energy minimization. Since there exists a great number of cohesive force models, the first issue is to choose one of them. By sake of simplicity in this first attempt, we propose to use the simplest ones, namely Dugdale's model. In this model, the surface energy density is a linear function of the jump of the displacement as long as this jump is lower than a critical value δ_c, then becomes constant and equal to the usual Griffith surface energy density $\mathsf{G_c}$. That means that in terms of the cohesive forces, the cohesive force between the lips of the crack remains constant and equal to σ_c as long as the jump of the displacement is lower than δ_c and then vanishes as in Griffith's model, cf Figure 3. Accordingly, this model contains both an internal length δ_c and a critical stress σ_c. Specifically, the scenario of nucleation of a crack if one

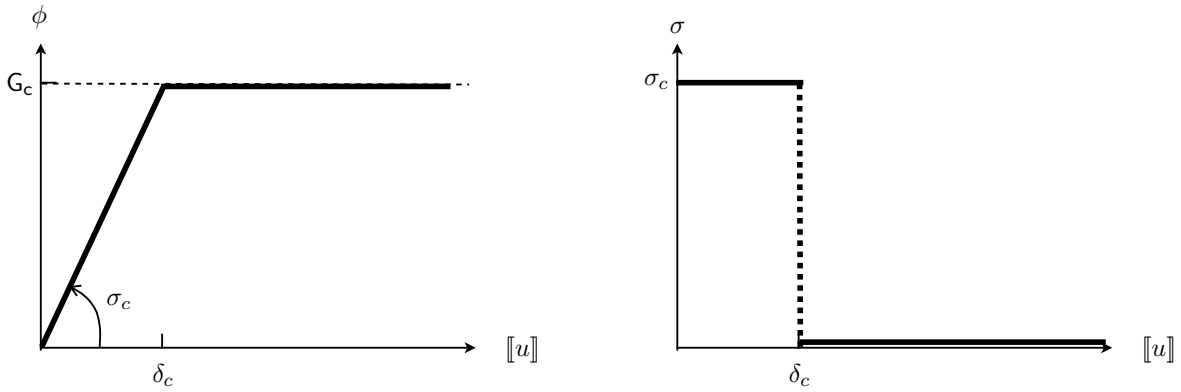

Figure 3: Dugdale's cohesive force model: the surface energy density (left) and the cohesive force (right) in terms of the jump of the displacement $[\![u]\!]$ across the crack

adopts the Dugdale's model consists in the following stages:

1. Because of the notch, the displacement field solution of the pure elastic problem is singular at the tip of the notch and the stress field goes to infinity when one approaches that tip. However, since the cohesive force model contains a critical stress and does not allow such a singularity, a crack will appear as soon as a load is applied. One assumes that the crack path is a segment line which starts from the tip of the notch and will grow in a direction which is known in advance (by reason of symmetry, for instance).

2. In the first stage of the loading, this crack will be cohesive in the sense that a cohesive stress σ_c will act between the lips of the crack;

3. The length of that first cohesive crack is also governed by the concept of critical stress. Indeed, this length must be adjusted in such a manner that the stress field remains less than the critical stress σ_c everywhere in the body. That requires that there does not exist a singularity at the tip of that cohesive crack and that condition gives the equation for determining the crack length [Ferdjani et al., 2007; Abdelmoula et al., 2010].

4. In the same time the jump of the displacement increases and is maximal at the tip of the notch. At a critical load, the jump of the displacement will reach the critical value δ_c and hence a non cohesive crack will appear.

5. After this critical loading, the crack will continue to grow but will now contain two parts: a still cohesive part and a non cohesive part. Then the problem consists in finding the evolution of the two corresponding lengths or equivalently of the position of the corresponding tips l and ℓ, see Figure 4. It turns out that, in general, this phase of propagation is unstable in the sense that one cannot observe such a quasi-static evolution without decrease of the loading. In such a case, one considers that this critical load corresponds to the phase of nucleation and that after this load a “macroscopic" crack is appeared.

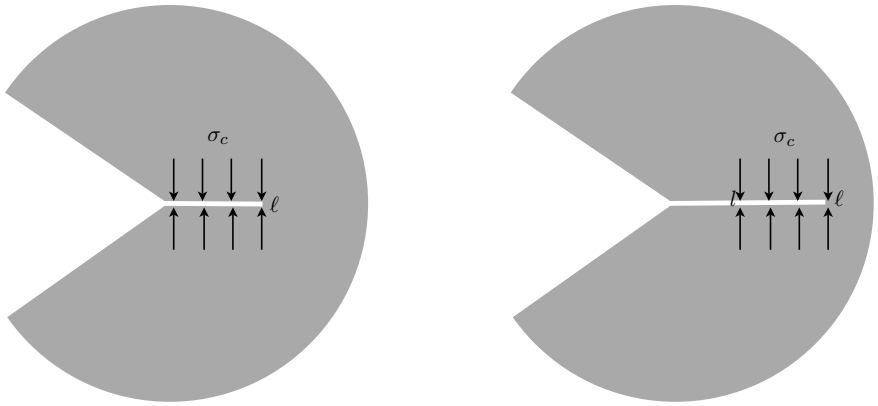

Figure 4: Scenario of the nucleation of a crack at the tip of a notch with Dugdale's model. First (left), growth of a cohesive crack; then (right), onset and propagation of a non cohesive crack.

The study of the nucleation of a crack by using Dugdale's surface energy will be done in the second part of Chapter 2. The fact that the cohesive force is a material constant before the jump of the displacement reaches a critical value leads to linear problems at given positions of the two crack tips. In this setting, the **MAM** will allow us to obtain quasi-analytical results. Specifically, it turns out that the inner problem can be seen as an Hilbert's problem which can be solved with the help of complex potentials. Thus, the access to the solution is reduced to a few quadratures which are computed numerically. One obtains so an analytical expression of the critical load at which a "macroscopic" crack will appear in the body after an unstable stage of propagation of the nucleated crack. The order of magnitude of that critical load is directly associated with the power of the singularity of the solution before nucleation which is itself a known function of the angle of the notch.

The last goal of Chapter 2 will be to compare the predictions of *FM-law* and of Dugdale's model for the nucleation of a crack at a notch. In particular, it will be interesting to see the influence of the material parameters as well as the size of the body or the angle of the notch.

The anti-plane elasticity is a comfortable framework to develop all the ideas because the equilibrium equation is reduced to Laplace's equation and one eliminates some technical questions. Indeed, the singularities of the Laplacian and more generally all the properties of the Laplace operator are well-known in two dimensions. However, from a practical point of view, we cannot be satisfied by a so restricted framework and it is necessary to investigate at least the plane elasticity setting. Chapter 3 proposes a partial generalization of the methods and results developed in the first two chapters in that plane elasticity setting. Specifically, the goal is still to study the nucleation of non cohesive or cohesive cracks at the angle of a notch in the case of a linearly elastic isotropic material but now by considering plane displacements. Moreover, we will consider as well pure mode I situation as mixed modes cases. In the first part of the chapter we use the global minimization principle in the case of a non cohesive crack. In the second part we consider Dugdale cohesive force model. In both cases the **MAM** is used to compensate for the non accuracy of the finite element method.

Chapter 1

Matching asymptotic method in presence of singularities in antiplane elasticity

1.1 Introduction

We use matching asymptotic expansions to treat the anti-plane elastic problem associated with a small defect located at the tip of a notch. In a first part, we develop the asymptotic method for any type of defect and present the sequential procedure which allows us to calculate the different terms of the inner and outer expansions at any order. That requires in particular to separate in each term its singular part from its regular part.

Specifically, the chapter is organized as follows. Section 1.2 is devoted to the description of the **MAM** on a generic anti-plane linear elastic problem where the body contains a defect near the tip of a notch. We first decompose the solution into two expansions: one, the *outer expansion*, valid far enough from the tip of the notch, the other, the *inner expansion*, valid in a neighborhood of the tip of the notch. These expansions contain a sequence of inner and outer terms which are solutions of inner and outer problems and which are interdependent by the matching conditions. Moreover each term contains a regular and a singular part. We explain how all the terms and the coefficients entering in their singular and regular parts are sequentially determined. The section finishes by an example where the exact solution is obtained in a closed form and hence where we can verify the relevance of the **MAM**.

In Section 1.3, we introduce another decomposition of the expansions of inner and outer problems. That leads to solve two sequences of inner or outer problems which are independent of each other. That allows us to solve these problems once and for all, the inner ones being characteristic of the defect whereas the outer ones are characteristic of the whole structure without its defect. This new method is illustrated by solving the inner problems in the case of a cavity or of a crack. In both cases the solution is obtained in a closed form with the help, in the case of crack, of the theory of complex potentials.

1.2 The Matched Asymptotic Method

1.2.1 The real problem

Here, we are interested in a case where a small geometrical defect of size ℓ (like a crack or a void) is located near the corner of a notch, see Figure 1.1. The geometry of the notch is characterized by its angle ω, see Figure 1.2. The tip of the notch is taken as the origin of the space and we will consider two scales of coordinates: the “macroscopic" coordinates $\mathbf{x} = (x_1, x_2)$ which are used in the outer domain and the “microscopic" coordinates $\mathbf{y} = \mathbf{x}/\ell = (y_1, y_2)$ which are used in the neighborhood of the tip of

the notch where the defect is located, see Figure 1.2. In the case of a crack, the axis x_1 is chosen in such a way that the crack corresponds to the line segment $(0,\ell)\times\{0\}$. The unit vector orthogonal to the (x_1,x_2) plane is denoted $\mathbf{e}_3$.

The natural reference configuration of the *sound* two-dimensional body is Ω_0 while the associated body which contains a defect of size ℓ is Ω_ℓ. One denotes by Γ_ℓ the part of the boundary of Ω_ℓ which is due to the defect, *i.e.*

$$\Gamma_\ell = \partial\Omega_\ell \setminus \partial\Omega_0, \tag{1.1}$$

Γ_ℓ is contained in a disk of center $(0,0)$ and radius ℓ. In the case of a crack, Γ_ℓ is the crack itself, *i.e.* $\Gamma_\ell = (0,\ell)\times\{0\}$. The two edges of the notch are denoted by Γ^+ and Γ^- and in order to simplify the presentation one assumes that they are not modified by the introduction of the defect, see Figure 1.1. When one uses polar coordinates (r,θ), the pole is the tip of the notch and the origin of the polar angle is the edge Γ^-. Accordingly, we have

$$r=|\mathbf{x}|, \quad \Gamma^- = \{(r,\theta), 0<r<r^*, \quad \theta=0\}, \qquad \Gamma^+ = \{(r,\theta), 0<r<r^*, \quad \theta=\omega\}. \tag{1.2}$$

This body is made of an elastic isotropic material whose shear modulus is $\mu>0$. It is submitted to a loading such that the displacement field at equilibrium $\mathbf{u}_\ell$ be antiplane, *i.e.*

$$\mathbf{u}_\ell(\mathbf{x}) = u_\ell(x_1,x_2)\mathbf{e}_3$$

where the subscript ℓ is used in order to recall that the real displacement depends on the size of the defect. We assume that the body forces are zero and then u_ℓ must be a harmonic function in order to satisfy the equilibrium equations in the bulk:

$$\Delta u_\ell = 0 \quad \text{in} \quad \Omega_\ell. \tag{1.3}$$

The edges of the notch are free while Γ_ℓ is submitted to a density of (antiplane) surface forces. Accordingly, the boundary conditions on Γ_ℓ and $\Gamma^\pm$ read as

$$\frac{\partial u_\ell}{\partial \nu} = 0 \quad \text{on} \quad \Gamma^\pm, \qquad \frac{\partial u_\ell}{\partial \nu} = \frac{g(\mathbf{y})}{\ell} \quad \text{on} \quad \Gamma_\ell. \tag{1.4}$$

In (1.4), ν denotes the unit outer normal vector to the domain and we assume that the density of (antiplane) surface forces depends on the microscopic variable $\mathbf{y}$ and has a magnitude of the order of $1/\ell$.

The remaining part of the boundary of Ω_ℓ is divided into two parts: Γ_D where the displacement is prescribed and Γ_N where (antiplane) surface forces are prescribed. Specifically, we have

$$u_\ell = f(\mathbf{x}) \quad \text{on} \quad \Gamma_D, \qquad \frac{\partial u_\ell}{\partial \nu} = h(\mathbf{x}) \quad \text{on} \quad \Gamma_N. \tag{1.5}$$

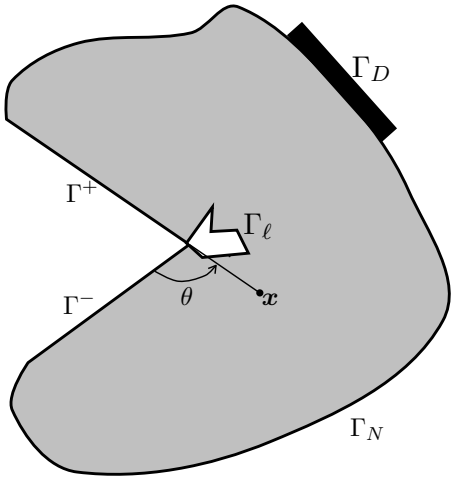

Figure 1.1: The domain Ω_ℓ for the real problem

The following Proposition is a characterization of functions which are harmonic in an angular sector and whose normal derivatives vanish on the edges of the sector. It is of constant use throughout the Chapter 1 and Chapter 2.

Proposition 1.1. *Let r_1 and r_2 be such that $0 \leq r_1 < r_2 \leq +\infty$ and let $\mathcal{D}_{r_1}^{r_2}$ be the angular sector*

$$\mathcal{D}_{r_1}^{r_2} = \{(r,\theta) \ : \ r \in (r_1, r_2), \quad \theta \in (0,\omega)\}.$$

Then any function u which is harmonic in $\mathcal{D}_{r_1}^{r_2}$ and which satisfies the Neumann condition $\partial u/\partial\theta = 0$ on the sides $\theta = 0$ and $\theta = \omega$ can be read as

$$u(r,\theta) = a_0 \ln(r) + d_0 + \sum_{n\in\mathbb{N}_*} \left(a_n r^{-n\lambda} + d_n r^{n\lambda} \right) \cos(n\lambda\theta) \tag{1.6}$$

with

$$\lambda = \frac{\pi}{\omega}, \tag{1.7}$$

whereas the a_n's and the d_n's constitute two sequences of real numbers which are characteristic of u.

Proof. Since the normal derivative vanishes at $\theta = 0$ and $\theta = \omega$, $u(r,\theta)$ can be read as the following Fourier series:

$$u(r,\theta) = \sum_{n\in\mathbb{N}} f_n(r) \cos(n\lambda\theta).$$

In order that u is harmonic, the functions f_n must satisfy $r^2 f_n'' + r f_n' - n^2\lambda^2 f_n = 0$, for each n. One easily deduces that $f_0(r) = a_0 \ln(r) + d_0$ and $f_n(r) = a_n r^{-n\lambda} + d_n r^{n\lambda}$ for $n \geq 1$. □

1.2.2 The basic ingredients of the MAM

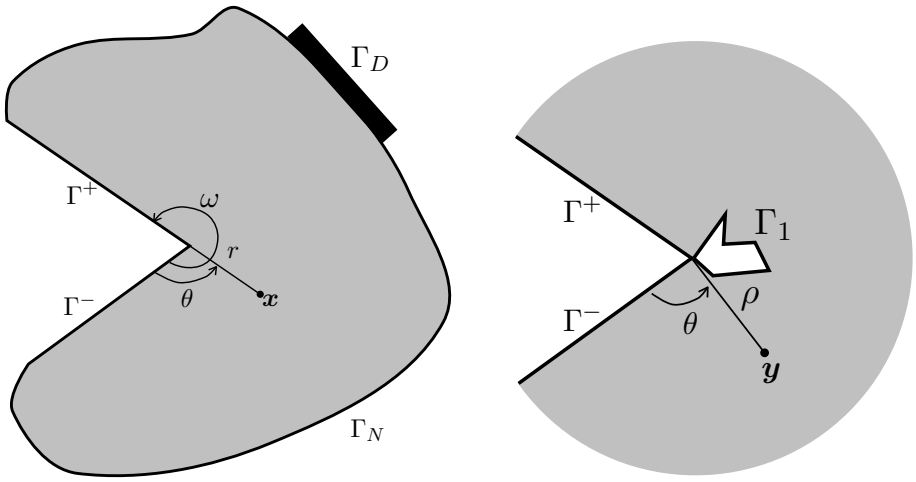

Figure 1.2: The domains Ω_0 and Ω^∞ for, respectively, the outer (left) and the inner (right) problems

When the length ℓ of the defect is small by comparison with the characteristic length of the body (in this section, this characteristic length is not precised), then it is necessary to make an asymptotic analysis of the problem rather than to try to obtain directly an approximation by classical finite element methods. In the case of a crack for instance, because of the overlap of two singularities (one at the tip of the notch and the other at the tip of the crack), it is difficult and even impossible to obtain accurate results without using a relevant asymptotic method. Here we will use the matched asymptotic expansion technique which consists in making two asymptotic expansions of the field u_ℓ in terms of the small parameter ℓ. The first one, called the inner expansion, is valid in the neighborhood of the tip of the notch, while the other, called the outer expansion, is valid far from this tip. These two expansions are matched in an intermediate zone.

The outer expansion

Far from the tip of the notch, *i.e.* for $r \gg \ell$, we assume that the real displacement field u_ℓ can be expanded as follows

$$u_\ell(\mathbf{x}) = \sum_{i \in \mathbb{N}} \ell^{i\lambda} u^i(\mathbf{x}). \tag{1.8}$$

In (1.8), even if this expansion is valid far enough from $r = 0$ only, the fields u^i must be defined in the whole outer domain Ω_0 which corresponds to the sound body, see Figure 1.2-left. Inserting this expansion into the set of equations constituting the real problem, one obtains the following equations that the u^i's must satisfy:

The first outer problem $i = 0$

$$\begin{cases} \Delta u^0 = 0 & \text{in } \Omega_0 \\ \dfrac{\partial u^0}{\partial \nu} = 0 & \text{on } \Gamma^+ \cup \Gamma^- \\ \dfrac{\partial u^0}{\partial \nu} = h(\mathbf{x}) & \text{on } \Gamma_N \\ u^0 = f(\mathbf{x}) & \text{on } \Gamma_D \end{cases} \tag{1.9}$$

The other outer problems $i \geq 1$

$$\begin{cases} \Delta u^i = 0 & \text{in } \Omega_0 \\ \dfrac{\partial u^i}{\partial \nu} = 0 & \text{on } \Gamma^+ \cup \Gamma^- \\ \dfrac{\partial u^i}{\partial \nu} = 0 & \text{on } \Gamma_N \\ u^i = 0 & \text{on } \Gamma_D \end{cases} \tag{1.10}$$

Moreover, the behavior of u^i in the neighborhood of $r = 0$ is singular and the singularity will be given by the matching conditions.

The inner expansion

Near the tip of the notch, *i.e.* for $r \ll 1$, we assume that the real displacement field u_ℓ can be expanded as follows

$$u_\ell(\mathbf{x}) = \ln(\ell) \sum_{i \in \mathbb{N}} \ell^{i\lambda} w^i(\mathbf{y}) + \sum_{i \in \mathbb{N}} \ell^{i\lambda} v^i(\mathbf{y}), \qquad \mathbf{y} = \frac{\mathbf{x}}{\ell}. \tag{1.11}$$

In (1.11), even if this expansion is valid only in the neighborhood of $r = 0$, the fields v^i and w^i must be defined in an infinite inner domain Ω^∞. The domain Ω^∞ is the infinite angular sector $\mathcal{D}_0^\infty$ of the (y_1, y_2) plane from which one removes the rescaled defect of size 1, see Figure 1.2-right. Accordingly, the rescaled boundary Γ_1 of the defect reads as

$$\Gamma_1 = \partial\Omega^\infty \setminus \partial\mathcal{D}_0^\infty. \tag{1.12}$$

(In the case of a crack, one has $\Gamma_1 = (0,1) \times \{0\}$.) Inserting this expansion into the set of equations constituting the real problem, one obtains the following equations that the v^i's must satisfy:

The first inner problem $i = 0$

$$\begin{cases} \Delta v^0 = 0 & \text{in } \Omega^\infty \\ \dfrac{\partial v^0}{\partial \theta} = 0 & \text{on } \theta = 0 \text{ and } \theta = \omega \\ \dfrac{\partial v^0}{\partial \nu} = g(\mathbf{y}) & \text{on } \Gamma_1 \end{cases} \tag{1.13}$$

The other inner problems $i \geq 1$

$$\begin{cases} \Delta v^i = 0 & \text{in } \Omega^\infty \\ \dfrac{\partial v^i}{\partial \theta} = 0 & \text{on } \theta = 0 \text{ and } \theta = \omega \\ \dfrac{\partial v^i}{\partial \nu} = 0 & \text{on } \Gamma_1 \end{cases} \tag{1.14}$$

The w^i's must satisfy, for every $i \geq 0$ the same equations as the v^i's for $i \geq 1$. To complete the set of equations one must add the behavior at infinity of the v^i's and the w^i's. This behavior will be given by the matching conditions with the outer problems.

Matching conditions

Since all the displacement fields u^i are harmonic in the sector $\mathcal{D}_0^{r_2}$ and satisfy homogeneous Neumann boundary conditions on the edges of this angular sector, we can use Proposition 1.1. Accordingly, in $\mathcal{D}_0^{r_2}$ the field u^i can read as

$$u^i(\mathbf{x}) = a_0^i \ln(r) + d_0^i + \sum_{n\in\mathbb{N}_*} \left(a_n^i r^{-n\lambda} + d_n^i r^{n\lambda} \right) \cos(n\lambda\theta). \tag{1.15}$$

In the same way for the inner expansion, since all the displacement fields v^i and w^i are harmonic in the sector $\mathcal{D}_1^{\infty}$ of the $\mathbf{y}$ plane and satisfy homogeneous Neumann boundary conditions on the edges of this angular sector, we can use Proposition 1.1 with the macroscopic coordinates $\mathbf{x}$ and r replaced by the microscopic coordinates $\mathbf{y}$ and $\rho = |\mathbf{y}| = r/\ell$. Accordingly, in $\mathcal{D}_1^{\infty}$ the fields v^i and w^i can read as

$$v^i(\mathbf{y}) = c_0^i \ln(\rho) + b_0^i + \sum_{n\in\mathbb{N}_*} \left(c_n^i \rho^{-n\lambda} + b_n^i \rho^{n\lambda} \right) \cos(n\lambda\theta), \tag{1.16}$$

$$w^i(\mathbf{y}) = \mathsf{e}_0^i \ln(\rho) + \mathsf{f}_0^i + \sum_{n\in\mathbb{N}_*} \left(\mathsf{e}_n^i \rho^{-n\lambda} + \mathsf{f}_n^i \rho^{n\lambda} \right) \cos(n\lambda\theta). \tag{1.17}$$

The outer expansion and the inner expansion are both valid in any intermediate zone $\mathcal{D}_{r_1}^{r_2}$ such that $\ell \ll r_1 < r_2 \ll 1$. Inserting (1.15) into the outer expansion (1.8) with $r = \ell\rho$ leads to

$$u_\ell(\mathbf{x}) = \sum_{i\in\mathbb{N}} \ln(\ell)\ell^{i\lambda} a_0^i + \sum_{i\in\mathbb{N}} \ell^{i\lambda} \Big(a_0^i \ln(\rho) + d_0^i + \sum_{n\in\mathbb{N}_*} \left(a_n^{i+n} \rho^{-n\lambda} + d_n^{i-n} \rho^{n\lambda} \right) \cos(n\lambda\theta) \Big) \tag{1.18}$$

with the convention that $d_n^{i-n} = 0$ when $n > i$. Inserting (1.16) and (1.17) into the inner expansion (1.11) leads to

$$\begin{aligned} u_\ell(\mathbf{x}) \;&=\; \sum_{i\in\mathbb{N}} \ln(\ell)\ell^{i\lambda} \Big(\mathsf{e}_0^i \ln(\rho) + \mathsf{f}_0^i + \sum_{n\in\mathbb{N}_*} \left(\mathsf{e}_n^i \rho^{-n\lambda} + \mathsf{f}_n^i \rho^{n\lambda} \right) \cos(n\lambda\theta) \Big) \\ &+\; \sum_{i\in\mathbb{N}} \ell^{i\lambda} \Big(c_0^i \ln(\rho) + b_0^i + \sum_{n\in\mathbb{N}_*} \left(c_n^i \rho^{-n\lambda} + b_n^i \rho^{n\lambda} \right) \cos(n\lambda\theta) \Big). \end{aligned} \tag{1.19}$$

Both expansions (1.18) and (1.19) are valid provided that $1 \ll \rho \ll 1/\ell$. By identification one gets the following properties for the coefficients of the inner and outer expansions, see Table 1.1:

Remark 1.1. *One deduces from Table 1.1 that the fields w^i are constant in the whole inner domain:*

$$w^i(\mathbf{y}) = a_0^i, \qquad \forall \mathbf{y} \in \Omega^\infty, \quad \forall i \geq 0. \tag{1.20}$$

Therefore, these fields will be determined once the constants a_0^i will be known.

$\mathsf{e}_n^i = 0$	$i \geq 0,\ n \geq 0$
$\mathsf{f}_0^i = a_0^i$	$i \geq 0$
$\mathsf{f}_n^i = 0$	$i \geq 0,\ n \geq 1$
$a_n^i = 0$	$n > i \geq 0$
$c_n^i = a_n^{i+n}$	$i \geq 0,\ n \geq 0$
$b_n^i = 0$	$n > i \geq 0$
$d_n^i = b_n^{i+n}$	$i \geq 0,\ n \geq 0$

Table 1.1: The relations between the coefficients of the inner and outer expansions given by the matching conditions

1.2.3 Determination of the different terms of the inner and outer expansions

The singular behavior of the u^i's and the v^i's

We deduce from the matching conditions the behavior of u^i in the neighborhood of $r = 0$ and the behavior of v^i at infinity. In particular, one obtains the form of their singularities. Let us first precise what one means by singularity.

Definition 1.1. *A field u defined in Ω_0 is said* regular *in Ω_0 if $u \in H^1(\Omega_0)$, i.e. $u \in L^2(\Omega_0)$ and $\nabla u \in L^2(\Omega_0)^2$. It is said* singular *otherwise.*

A field u defined in the unbounded sector Ω^∞ is said regular *in Ω^∞ if $\nabla u \in L^2(\Omega^\infty)^2$ and $\lim_{\rho\to\infty} u(\rho,\theta) = 0$. It is said* singular *otherwise.*

By virtue of the analysis of the previous subsection, the field u^0 can be read in a neighborhood of the tip of the notch as

$$u^0(\mathbf{x}) = a_0^0 \ln(r) + \sum_{n\in\mathbb{N}} b_n^n r^{n\lambda} \cos(n\lambda\theta). \tag{1.21}$$

Since $\ln(r)$ is singular in Ω_0 whereas $r^{n\lambda}\cos(n\lambda\theta)$ is regular (for $n \geq 0$) in Ω_0 in the sense of Definition 1.1, $a_0^0 \ln(r)$ can be considered as the singular part of the field u^0. Accordingly, one can decompose u^0 into its singular and its regular part as follows

$$u^0(\mathbf{x}) = u_S^0(\mathbf{x}) + \bar{u}^0(\mathbf{x}), \tag{1.22}$$

$$u_S^0(\mathbf{x}) = a_0^0 \ln(r), \quad \bar{u}^0 \in H^1(\Omega_0). \tag{1.23}$$

In the same way, for $i \geq 1$, the field u^i can be read in a neighborhood of the tip of the notch as

$$u^i(\mathbf{x}) = a_0^i \ln(r) + \sum_{n=1}^{i} a_n^i r^{-n\lambda} \cos(n\lambda\theta) + \sum_{n\in\mathbb{N}} b_n^{i+n} r^{n\lambda} \cos(n\lambda\theta). \tag{1.24}$$

Since $r^{-n\lambda}\cos(n\lambda\theta)$ is singular (for $n \geq 0$) in the sense of Definition 1.1, one can decompose u^i into its singular and its regular part as follows

$$u^i(\mathbf{x}) = u^i_S(\mathbf{x}) + \bar{u}^i(\mathbf{x}), \tag{1.25}$$

$$u^i_S(\mathbf{x}) = a^i_0 \ln(r) + \sum_{n=1}^{i} a^i_n r^{-n\lambda}\cos(n\lambda\theta), \quad \bar{u}^i \in H^1(\Omega_0). \tag{1.26}$$

For the fields v^i of the inner expansion, one has to study their behavior at infinity. By virtue of the analysis of the previous subsection, the field v^i for $i \geq 0$ can be read for large ρ as

$$v^i(\mathbf{y}) = a^i_0 \ln(\rho) + \sum_{n=0}^{i} b^i_n \rho^{n\lambda}\cos(n\lambda\theta) + \sum_{n\in\mathbb{N}_*} a^{i+n}_n \rho^{-n\lambda} cos(n\lambda\theta). \tag{1.27}$$

The field $\ln(\rho)$ as well as the fields $\rho^{n\lambda}\cos(n\lambda\theta)$, for $n \geq 0$, are singular in Ω^∞ in the sense of Definition 1.1 (even the constant field 1 corresponding to $n = 0$ is singular). Since the fields $\rho^{-n\lambda}\cos(n\lambda\theta)$ are regular when $n \geq 1$, $a^i_0 \ln(\rho) + \sum_{n=0}^{i} b^i_n \rho^{n\lambda}\cos(n\lambda\theta)$ can be considered as the singular part of the field v^i. Accordingly, one can decompose v^i into its singular and its regular part as follows

$$v^i(\mathbf{y}) = v^i_S(\mathbf{y}) + \bar{v}^i(\mathbf{y}), \tag{1.28}$$

$$v^i_S(\mathbf{y}) = a^i_0 \ln(\rho) + \sum_{n=0}^{i} b^i_n \rho^{n\lambda}\cos(n\lambda\theta), \quad \nabla\bar{v}^i \in L^2(\Omega^\infty), \quad \lim_{|\mathbf{y}|\to\infty} \bar{v}^i(\mathbf{y}) = 0. \tag{1.29}$$

Remark 1.2. *This analysis of the singularities shows that the singular parts of the fields u^i and v^i will be known once the coefficients a^i_n and b^i_n will be determined for $0 \leq n \leq i$.*

The problems giving the regular parts $\bar{u}^i$ and $\bar{v}^i$

We are now in position to set the inner and outer problems giving the fields v^i and u^i. Since, by construction, the singular parts of these fields are harmonic and satisfy the homogeneous Neumann boundary conditions on the edges of the notch, their regular parts must verify the following boundary value problems.

The first outer problem, $i = 0$

Find $\bar{u}^0$ regular in Ω_0 such that

$$\begin{cases} \Delta\bar{u}^0 = 0 & \text{in } \Omega_0 \\ \dfrac{\partial\bar{u}^0}{\partial\nu} = 0 & \text{on } \Gamma^+ \cup \Gamma^- \\ \dfrac{\partial\bar{u}^0}{\partial\nu} = h - \dfrac{\partial u^0_S}{\partial\nu} & \text{on } \Gamma_N \\ \bar{u}^0 = f - u^0_S & \text{on } \Gamma_D \end{cases} \tag{1.30}$$

The other outer problems, $i \geq 1$

Find $\bar{u}^i$ regular in Ω_0 such that

$$\begin{cases} \Delta \bar{u}^i = 0 & \text{in } \Omega_0 \\ \dfrac{\partial \bar{u}^i}{\partial \nu} = 0 & \text{on } \Gamma^+ \cup \Gamma^- \\ \dfrac{\partial \bar{u}^i}{\partial \nu} = -\dfrac{\partial u_S^i}{\partial \nu} & \text{on } \Gamma_N \\ \bar{u}^i = -u_S^i & \text{on } \Gamma_D \end{cases} \tag{1.31}$$

The first inner problem, $i = 0$

Find $\bar{v}^0$ regular in Ω^∞ such that

$$\begin{cases} \Delta \bar{v}^0 = 0 & \text{in } \Omega^\infty \\ \dfrac{\partial \bar{v}^0}{\partial \nu} = 0 & \text{on } \Gamma^+ \cup \Gamma^- \\ \dfrac{\partial \bar{v}^0}{\partial \nu} = g - \dfrac{\partial v_S^0}{\partial \nu} & \text{on } \Gamma_1 \end{cases} \tag{1.32}$$

The other inner problems, $i \geq 1$

Find $\bar{v}^i$ regular in Ω^∞ such that

$$\begin{cases} \Delta \bar{v}^i = 0 & \text{in } \Omega^\infty \\ \dfrac{\partial \bar{v}^i}{\partial \nu} = 0 & \text{on } \Gamma^+ \cup \Gamma^- \\ \dfrac{\partial \bar{v}^i}{\partial \nu} = -\dfrac{\partial v_S^i}{\partial \nu} & \text{on } \Gamma_1 \end{cases} \tag{1.33}$$

Let us study first the outer problems. We have the following Proposition which is a direct consequence of classical results for the Laplace equation:

Proposition 1.2. *Let $i \geq 0$. For a given singular part u_S^i, i.e. if the coefficients a_n^i are known for all n such that $0 \leq n \leq i$, then there exists a unique solution $\bar{u}^i$ of* (1.31) *(or of* (1.30) *when $i = 0$). Consequently, since the coefficients b_n^{i+n} are included in the regular part $\bar{u}^i$ of u^i, see* (1.24)*, they are determined for all $n \geq 0$.*

Let us consider now the inner problems. We obtain the following

Proposition 1.3. *Let $i \geq 0$. For given b_n^i with $0 \leq n \leq i$, there exists a regular solution $\bar{v}^i$ for the i-th inner problem if and only if the coefficient a_0^i is such that*

$$a_0^0 = -\frac{1}{\omega} \int_{\Gamma_1} g(s) ds, \qquad a_0^i = 0 \quad \textit{for} \quad i \geq 1. \tag{1.34}$$

Moreover, if this condition is satisfied, then the solution is unique and therefore the coefficients a_n^{i+n} are determined for all $n \geq 0$.

Proof. The inner problems are pure Neumann problems in which no Dirichlet boundary conditions are imposed to the v^i's. Consequently, they admit a solution (if and) only if the Neumann data satisfy a global compatibility condition. Let us re-establish that condition. Let Ω^R be the part of Ω^∞ included

in the ball of radius $R > 1$, *i.e.* $\Omega^R = \Omega^\infty \cap \{\mathbf{y} \,:\, |\mathbf{y}| < R\}$. Let us consider first the case $i = 0$. Integrating the equation $\Delta v^0 = 0$ over Ω^R and using the boundary conditions leads to

$$0 = \int_{\partial\Omega^R} \frac{\partial v^0}{\partial \nu} ds = \int_0^\omega \frac{\partial v^0}{\partial \rho}(R,\theta) R\, d\theta + \int_{\Gamma_1} g(s) ds. \tag{1.35}$$

Using (1.27), one gets $R\dfrac{\partial v^0}{\partial \rho}(R,\theta) = a_0^0 + \sum_{n\in\mathbb{N}_*} n\lambda\big(-c_n^0 R^{-n\lambda} + b_n^0 R^{n\lambda}\big)\cos(n\lambda\theta)$. Since $\int_0^\omega \cos(n\lambda\theta)d\theta = 0$ for all $n \geq 1$, after inserting in (1.35) one obtains the desired condition for a_0^0. One proceeds exactly in the same manner for $i \geq 1$ and one obtains the desired condition because the integral over Γ_1 vanishes.

If the compatibility condition (1.34) is satisfied, then one proves the existence of a regular solution for $\bar{v}^i$ by standard arguments. Note however that, since $\nabla\bar{v}^i$ belongs to $L^2(\Omega^\infty)$, $\bar{v}^i$ tends to a constant at infinity and this constant is fixed to 0 by the additional regularity condition. As far as the uniqueness is concerned, the solution of this pure Neumann problem is unique up to a constant and the constant is fixed by the condition that $\bar{v}^i$ vanishes at infinity.

Once v^i is determined, one obtains the coefficients a_n^{i+n} by virtue of Proposition 1.1 and (1.27). □

Remark 1.3. *If the forces applied to the boundary of the defect are equilibrated, i.e. if* $\int_{\Gamma_1} g(s)ds = 0$, *then all the coefficients* a_0^i *vanish and hence the terms in* $\ln(\ell)$ *disappear in the inner expansion. There is no more logarithmic singularities in the* u^i*'s and the* v^i*'s.*

The construction of the outer and inner expansions

Equipped with the previous results, we are in position to explain how one can determine the different terms of the two expansions. Let us explain first how one obtains the first terms.

S1 One obtains a_0^0 by (1.34) and hence one knows u_S^0.

S2 Knowing u_S^0, one determines $\bar{u}^0$ and hence u^0 by solving (1.30), see Proposition 1.2.

S3 Knowing u^0, one calculates b_n^n for $n \geq 0$ as a regular part of u^0, see the next subsection for the practical method. Hence, one knows v_S^0.

S4 Knowing v_S^0, one determines $\bar{v}^0$ and hence v^0 by solving (1.32), see Proposition 1.3.

S5 Knowing v^0, one calculates a_n^n for $n \geq 1$ as a regular part of v^0, see the next subsection for the practical method. Hence, since $a_0^1 = 0$, one knows u_S^1.

Then one proceeds by induction. Let $i \geq 1$. Assuming that the following properties hold true:

H1 u^j and v^j have been determined for $0 \leq j \leq i-1$,

H2 b_n^j is known for $0 \leq n \leq j \leq i-1$,

H3 a_n^{j+n} and b_n^{j+n} are known for $0 \leq j \leq i-1$ and $n \geq 0$,

H4 a_n^j is known for $0 \leq n \leq j \leq i$,

let us prove that they remain true for $i+1$.

R1 Knowing a_n^i for $0 \leq n \leq i$, one knows u_S^i. Knowing u_S^i, one determines $\vec{u}^i$ and hence u^i by solving (1.31), see Proposition 1.2.

R2 Knowing u^i, one calculates b_n^{i+n} for $n \geq 0$ as a regular part of u^i, see the next subsection for the practical method. Hence, one knows v_S^i.

R3 Since b_0^i is known and since $b_n^i = b_n^{j+n}$ with $j = i-n$, one knows b_n^i for $0 \leq n \leq i$.

R4 Knowing v_S^i, one determines $\vec{v}^i$ and hence v^i by solving (1.33), see Proposition 1.3.

R5 One knows that $a_0^i = 0$. Knowing v^i, one calculates a_n^{i+n} for $n \geq 1$ as a regular part of v^i, see the next subsection for the practical method.

R6 Since $a_0^{i+1} = 0$ and since $a_n^{i+1} = a_n^{j+n}$ with $j = i+1-n$, one knows a_n^{i+1} for $0 \leq n \leq i+1$.

This iterative method is summarized in Table 1.2.

a_n^i / b_n^i	i=0	i=1	i=2	i=3	i=4
n=0	(1.34) /Outer 0	0 / Outer 1	0 / Outer 2	0 / Outer 3	0 / Outer 4
n=1	0	Inner 0 / Outer 0	Inner 1 / Outer 1	Inner 2 / Outer 2	Inner 3 / Outer 3
n=2	0	0	Inner 0 / Outer 0	Inner 1/ Outer 1	Inner 2 / Outer 2
n=3	0	0	0	Inner 0 / Outer 0	Inner 1 / Outer 1
n=4	0	0	0	0	Inner 0 / Outer 0

Table 1.2: Summary of the inductive method to obtain the coefficients a_n^i and b_n^i: in the corresponding cell is indicated the problem which must be solved

The practical method for determining the coefficients a_n^i and b_n^i for $0 \leq n \leq i$

Throughout this section, $\mathcal{C}_r$ denotes the arc of circle of radius r starting on Γ^- and ending on Γ^+:

$$\mathcal{C}_r = \{(r, \theta) \ : \ 0 \leq \theta \leq \omega\}.$$

The coefficients a_n^i and b_n^i can be obtained by path integrals (which are path independent) as it is proved in the following Proposition.

Proposition 1.4. *Let $i \geq 0$ and let us assume that the i^{th} inner and outer problems are solved and thus that $\bar{v}^i$ and $\bar{u}^i$ are known. Then*

1. *For $n \geq 1$, a_n^{i+n} is given by the following path integral over $\mathcal{C}_\rho$ which is independent of ρ provided that $\rho > 1$:*

$$a_n^{i+n} = \frac{2\rho^{n\lambda}}{\omega} \int_0^\omega \bar{v}^i(\rho, \theta) \cos(n\lambda\theta) d\theta \tag{1.36}$$

2. *For $n \geq 0$, b_n^{i+n} is given by the following path integral over $\mathcal{C}_r$ which is independent of r provided that $0 < r < r^*$:*

$$b_0^i = \frac{1}{\omega} \int_0^\omega \bar{u}^i(r, \theta) d\theta, \qquad b_n^{i+n} = \frac{2r^{-n\lambda}}{\omega} \int_0^\omega \bar{u}^i(r, \theta) \cos(n\lambda\theta) d\theta \quad \textit{for} \quad n \geq 1 \tag{1.37}$$

Proof. The proofs are identical for the two families of coefficients and then one gives only the proof for b_n^{i+n}. By virtue of (1.24), the regular part $\bar{u}^i$ of u^i is given by

$$\bar{u}^i(r, \theta) = \sum_{p \in \mathbb{N}} b_p^{i+p} r^{p\lambda} \cos(p\lambda\theta)$$

for $0 < r < r^*$. Since $\int_0^\omega \cos(p\lambda\theta) d\theta$ is equal to ω if $p = 0$ and is equal to 0 otherwise, one obtains the expression for b_0^i. For $n \geq 1$, since $\int_0^\omega \cos(p\lambda\theta) \cos(n\lambda\theta) d\theta$ is equal to $\omega/2$ if $p = n$ and is equal to 0 otherwise, one obtains the expression for b_n^{i+n}. □

1.2.4 Verification in the case of a small cavity

This subsection is devoted to the verification of the construction of the **MAM** presented in the previous subsections on an example where the exact solution is obtained in a closed form and hence can be directly expanded. Specifically, we consider a Laplace's problem posed in a domain which consists in an angular sector delimited by two arc of circles. The radius of the outer circle is equal to 1 while the radius of the inner circle is ℓ, see Figure 1.3. Thus,

$$\Omega_\ell = \{\mathbf{x} = r\cos\theta \mathbf{e}_1 + r\sin\theta \mathbf{e}_2 \ : \ r \in (\ell, 1), \ \theta \in (0, \omega)\}.$$

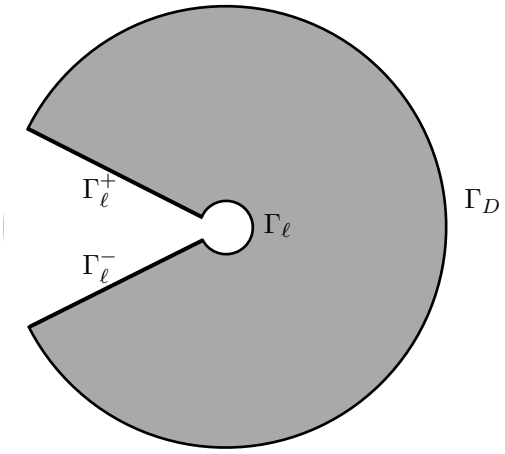

Figure 1.3: The domain Ω_ℓ in the case of a cavity

The sides of the notch and the inner circle are free and hence the boundary conditions on those parts of the boundary read as

$$\frac{\partial u_\ell}{\partial \nu} = 0 \quad \text{on} \quad \Gamma_\ell^+ \cup \Gamma_\ell^- \cup \Gamma_\ell, \tag{1.38}$$

where

$$\Gamma_\ell^\pm = \{(r,\theta) : \ell < r < 1, \theta = 0 \text{ or } \omega\}, \qquad \Gamma_\ell = \{(r,\theta) : r = \ell, 0 \le \theta \le \omega\}.$$

(Note that $\Gamma_\ell^\pm$ depend on ℓ, contrarily to the assumption made in the remaining part of this chapter. But that has no influence on the results.) The displacement is prescribed on the outer boundary Γ_D so that:

$$u_\ell(\mathbf{x}) = \cos\lambda\theta \quad \text{on} \quad \Gamma_D, \qquad \lambda = \frac{\pi}{\omega}. \tag{1.39}$$

Note that Γ_N is empty. Assuming that there exists no body force, the exact solution of this anti-plane elastic problem is given by

$$u_\ell(\mathbf{x}) = \Big(\frac{\ell^{2\lambda}}{1+\ell^{2\lambda}} r^{-\lambda} + \frac{1}{1+\ell^{2\lambda}} r^{\lambda}\Big) \cos\lambda\theta. \tag{1.40}$$

Using the well-known expansion of $1/(1+\epsilon) = \sum_{i\in\mathbb{N}} (-1)^i \epsilon^i$, one easily obtains the expansion of $u_\ell(\mathbf{x})$ at a given $\mathbf{x}$:

$$u_\ell(\mathbf{x}) = r^\lambda \cos\lambda\theta + \sum_{n\in\mathbb{N}^*} \ell^{2n\lambda}(r^{-\lambda} - r^{\lambda}) \cos\lambda\theta. \tag{1.41}$$

Thus (1.41) corresponds to the outer expansion where the odd terms vanish and the even terms are given by

$$u^0(\mathbf{x}) = r^\lambda \cos\lambda\theta, \qquad u^{2n}(\mathbf{x}) = (-1)^n (r^\lambda - r^{-\lambda}) \cos\lambda\theta, \quad \forall n \ge 1. \tag{1.42}$$

To obtain the inner expansion, one replaces r by $\ell\rho$ in (1.40) and gets

$$u_\ell(\ell\mathbf{y}) = \frac{\ell^\lambda}{1+\ell^{2\lambda}}(\rho^{-\lambda}+\rho^\lambda)\cos\lambda\theta. \tag{1.43}$$

Expanding $1/(1+\epsilon)$ as before, one obtains the following expansion of $u_\ell(\ell\mathbf{y})$ at given $\mathbf{y}$

$$u_\ell(\ell\mathbf{y}) = \sum_{n\in\mathbb{N}}(-1)^n\ell^{(2n+1)\lambda}(\rho^{-\lambda}+\rho^\lambda)\cos\lambda\theta \tag{1.44}$$

which corresponds to the inner expansion where the even terms vanish and the odd terms are given by

$$v^{2n+1}(\mathbf{y}) = (-1)^n(\rho^{-\lambda}+\rho^\lambda)\cos\lambda\theta, \quad \forall n \geq 0. \tag{1.45}$$

It remains to check that we recover the same expansions by following the procedure described in the previous subsections. Since $g=0$, one knows that $a_0^i = 0$ for all i and that there does not exist a logarithmic singularity, see Remark 1.3. Let us detail the first steps of the procedure

S1 By (1.34), $a_0^0 = 0$ and hence $u_S^0 = 0$.

S2 Hence (1.30) reads as: $\Delta u^0 = 0$ in Ω_0, $\partial u^0/\partial\theta = 0$ on $\theta \in \{0,\omega\}$, $u^0 = \cos\lambda\theta$ on $r=1$. The unique solution in $H^1(\Omega_0)$ is u^0 given by (1.42).

S3 By (1.37), one gets $b_1^1 = 1$ and $b_n^n = 0$ for $n \neq 1$. Hence $v_S^0 = 0$.

S4 Since $v_S^0 = 0$ and $g=0$, (1.32) gives $\bar{v}^0 = 0$ and hence $v^0 = 0$.

S5 By (1.36), $a_n^n = 0$ for $n \geq 1$.

S6 By (1.26), $u_S^1 = 0$.

S7 By (1.31), $\bar{u}^1 = 0$ and hence $u^1 = 0$.

S8 By (1.37), one gets $b_n^{n+1} = 0$ for all n. Hence $v_S^1 = \rho^\lambda\cos\lambda\theta$.

S9 Hence (1.33) for $i=1$ reads as: $\Delta\bar{v}^1 = 0$ in Ω^∞, $\partial\bar{v}^1/\partial\theta = 0$ on $\theta\in\{0,\omega\}$, $\partial\bar{v}^1/\partial\rho = -\lambda\cos\lambda\theta$ on $\rho=1$. The unique regular solution is $\bar{v}^1 = \rho^\lambda\cos\lambda\theta$ and hence v^1 is really given by (1.45).

S10 By (1.36), $a_1^2 = 1$ and $a_n^{n+1} = 0$ for $n \neq 1$.

S11 By (1.26), $u_S^2 = r^{-\lambda}\cos\lambda\theta$.

S12 Hence (1.31) for $i=2$ reads as: $\Delta\bar{u}^2 = 0$ in Ω_0, $\partial\bar{u}^2/\partial\theta = 0$ on $\theta\in\{0,\omega\}$, $\bar{u}^2 = -\cos\lambda\theta$ on $r=1$. The unique solution in $H^1(\Omega_0)$ is $\bar{u}^2 = -r^\lambda\cos\lambda\theta$ and hence u^2 is given by (1.42).

...

Proceeding by induction, one finally recovers the expected expansions. The end of the verification is left to the reader.

1.3 Another method for determining the inner and outer expansions

1.3.1 Another decomposition which allows to treat independently the inner and outer problems

Throughout this section, we assume that we are in a situation such that the singularity in $\ln(r)$ vanishes, see Remark 1.3. Accordingly, the first outer term u^0 contains no singular part ($u^0_S = 0, \bar{u}^0 = u^0$) and u^0 is the unique solution in $H^1(\Omega_0)$ of (1.9). That solution depends on the loading characterized by h and f. Note that (1.9) is posed on the domain without the defect and hence u^0 does not depend on the defect. There is, in general, no particular method to find it and hence we will assume that u^0 has been determined. Consequently, by virtue of the previous analysis, the coefficients b^n_n for $n \geq 0$ are assumed to be known.

Le us consider now the other outer terms, *i.e.* u^i for $i \geq 1$. From the previous part, we know that the outer term u^i is decomposed into its singular part u^i_S and its regular part $\bar{u}^i$. Moreover $\bar{u}^i$ is determined in terms of u^i_S by virtue of (1.31), see also Proposition 1.2. Recalling that there is no logarithmic singularity, by virtue of (1.26) u^i_S is given by

$$u^i_S(\mathbf{x}) = \sum_{n=1}^{i} a^i_n r^{-n\lambda} \cos(n\lambda\theta).$$

Inserting this expression into (1.31), the regular part $\bar{u}^i$ must satisfy the following problem:

$$\begin{cases} \Delta \bar{u}^i = 0 & \text{in } \Omega_0 \\ \dfrac{\partial \bar{u}^i}{\partial \nu} = 0 & \text{on } \Gamma^+ \cup \Gamma^- \\ \dfrac{\partial \bar{u}^i}{\partial \nu} = -\displaystyle\sum_{n=1}^{i} a^i_n \Big[\frac{\partial (r^{-n\lambda}\cos(n\lambda\theta))}{\partial \nu}\Big] & \text{on } \Gamma_N \\ \bar{u}^i = -\displaystyle\sum_{n=1}^{i} a^i_n r^{-n\lambda}\cos(n\lambda\theta) & \text{on } \Gamma_D \end{cases} \tag{1.46}$$

By linearity, $\bar{u}^i$ can be decomposed into the following linear combination

$$\bar{u}^i = \sum_{n=1}^{i} a^i_n \bar{U}^n$$

where the fields $\bar{U}^n$ for $n \geq 1$ are solutions of the following family of problems:

$$\begin{cases} \Delta \bar{U}^n = 0 & \text{in } \Omega_0 \\ \dfrac{\partial \bar{U}^n}{\partial \nu} = 0 & \text{on } \Gamma^+ \cup \Gamma^- \\ \dfrac{\partial \bar{U}^n}{\partial \nu} = -\dfrac{\partial (r^{-n\lambda}\cos(n\lambda\theta))}{\partial \nu} & \text{on } \Gamma_N \\ \bar{U}^n = -r^{-n\lambda}\cos(n\lambda\theta) & \text{on } \Gamma_D \end{cases} . \tag{1.47}$$

Clearly the problem (1.47) giving $\bar{U}^n$ is self-contained and does not depend on the other outer or inner terms. Hence, the family of problems (1.47), for $n \geq 1$, can be viewed as a set of "elementary" problems depending on the outer geometry Ω_0 (and hence independent of the defect) which can be solved once and for all for a given outer geometry and a given partition of the boundary into Dirichlet and Neumann parts. Moreover, one can obtain their solution explicitly in some particular geometries such as a circular plate with a arbitrary radius R, see the example below. By virtue of Proposition 1.1, $\bar{U}^n$ can be expanded in the neighborhood of the tip of the notch. Since it is a regular field which belongs to $H^1(\Omega_0)$, this expansion can read as

$$\bar{U}^n(r,\theta) = \sum_{p\in\mathbb{N}} K_p^n r^{p\lambda}\cos(p\lambda\theta) \tag{1.48}$$

and hence is characterized by the coefficients $\{K_p^n\}_{p\in\mathbb{N}}$. Using Proposition 1.4, (1.37) allows us to deduce those coefficients by path integrals:

$$K_0^n = \frac{1}{\omega}\int_0^\omega \bar{U}^n(r,\theta)d\theta, \tag{1.49}$$

$$K_p^n = \frac{2r^{-p\lambda}}{\omega}\int_0^\omega \bar{U}^n(r,\theta)\cos(p\lambda\theta)d\theta \ , \quad \forall p \geq 1. \tag{1.50}$$

Therefore the outer term u^i can be expressed as a the following linear composition which involve the coefficients $\{a_n^i\}_{1\leq n\leq i}$ and the "elementary" fields $\bar{U}^n$. Specifically, one has

$$u^i(\mathbf{x}) = \sum_{n=1}^{i} a_n^i\big(r^{-n\lambda}\cos(n\lambda\theta) + \bar{U}^n(\mathbf{x})\big).$$

So, assuming that the fields $\bar{U}^n$ are known, u^i for $i \geq 1$ will be perfectly determined once the coefficients $\{a_n^i\}_{1\leq n\leq i}$ will be known. The method for determining these coefficients will be discussed after the discussion on the inner problems.

Let us first consider v^0. Since there is no logarithmic singularity, the singular part of v^0 is reduced to the constant b_0^0 which is given by u^0, see (1.29) and (1.37). Accordingly,

$$v^0 = b_0^0 + \bar{v}^0$$

where $\bar{v}^0$ is the unique solution of

$$\begin{cases} \Delta \bar{v}^0 = 0 & \text{in } \Omega^\infty \\ \dfrac{\partial \bar{v}^0}{\partial \nu} = 0 & \text{on } \Gamma^+ \cup \Gamma^- \\ \dfrac{\partial \bar{v}^0}{\partial \nu} = g & \text{on } \Gamma_1 \end{cases}. \tag{1.51}$$

Hence, v^0 essentially depends on the external loading g. In the case where $g = 0$ (for instance for a non cohesive crack), on gets $\bar{v}^0 = 0$ and hence v^0 is the constant b_0^0 given by u^0. In any case, we will assume that v^0 has been determined.

Let us consider v^i, for $i \geq 1$. It contains a singular part v_S^i and a regular part $\bar{v}^i$. Moreover $\bar{v}^i$ is determined in terms of v_S^i by virtue of (1.33), see also Proposition 1.2. Recalling that there is no logarithmic singularity, by virtue of (1.29) v_S^i is given by

$$v_S^i(\mathbf{y}) = \sum_{n=0}^{i} b_n^i \rho^{n\lambda} \cos(n\lambda\theta).$$

Inserting this expression into (1.33), the regular part $\bar{v}^i$ must satisfy the following problem:

$$\begin{cases} \Delta \bar{v}^i = 0 & \text{in } \Omega^\infty \\ \dfrac{\partial \bar{v}^i}{\partial \nu} = 0 & \text{on } \Gamma^+ \cup \Gamma^- \\ \dfrac{\partial \bar{v}^i}{\partial \nu} = -\displaystyle\sum_{n=0}^{i} b_n^i \frac{\partial(\rho^{n\lambda}\cos(n\lambda\theta))}{\partial \nu} & \text{on } \Gamma_1 \\ \bar{v}^i \to 0 & \text{at } \infty \end{cases} \tag{1.52}$$

By linearity, v^i can be decomposed into the following linear combination

$$v^i(\mathbf{y}) = \sum_{n=0}^{i} b_n^i \Big(\rho^{n\lambda} \cos(n\lambda\theta) + \bar{V}^n(\mathbf{y}) \Big) \tag{1.53}$$

where the fields $\bar{V}^n$ for $n \geq 0$ are solutions of the following family of problems:

$$\begin{cases} \Delta \bar{V}^n = 0 & \text{in } \Omega^\infty \\ \dfrac{\partial \bar{V}^n}{\partial \nu} = 0 & \text{on } \Gamma^+ \cup \Gamma^- \\ \dfrac{\partial \bar{V}^n}{\partial \nu} = -\dfrac{\partial(\rho^{n\lambda}\cos(n\lambda\theta))}{\partial \nu} & \text{on } \Gamma_1 \\ \bar{V}^n \to 0 & \text{at } \infty \end{cases} \tag{1.54}$$

The problem (1.54) giving $\bar{V}^n$ depends only on the angle of the notch and the geometry of the defect. It is independent of the geometry and the loading of the whole body. Accordingly, the family

of problems (1.54) can be considered as "elementary problems" which are characteristic of the defect (for a given notch angle). They can be solved once and for all for a given notch and a given defect whatever the remaining part of the body. One can obtain their solution explicitly in some particular geometries, such as a circular cavity or a non cohesive crack, see the examples below.

By virtue of Proposition 1.1, $\bar{V}^n$ can be expanded for large ρ as follows (see (2.16)):

$$\bar{V}^n(\mathbf{y}) = \sum_{p\in\mathbb{N}_*} T_p^n \rho^{-p\lambda}\cos(p\lambda\theta) \tag{1.55}$$

where the coefficients $\{T_p^n\}_{p\in\mathbb{N}_*}$ are calculated by path integrals by virtue of Proposition 1.4. Specifically, one gets

$$T_p^n = \frac{2\rho^{p\lambda}}{\omega}\int_0^\omega \bar{V}^n(\rho,\theta)\cos(p\lambda\theta)d\theta. \tag{1.56}$$

Assuming that all the "elementary" inner and outer terms $\bar{U}^n$ and $\bar{V}^n$ have been determined, it remains to determine the coefficients a_n^i and b_n^i in order that the inner and outer expansions be obtained. That leads to the following Proposition:

Proposition 1.5. *Let us assume that u^0 is known and hence $\{b_n^n\}_{n\in\mathbb{N}}$ are known. Then, $\forall i \geq 1$, $a_0^i = 0$ and the coefficients $\{b_n^{i+n}\}$ are given in terms of a_n^{i+n} by*

$$b_0^i = \sum_{p=1}^i a_p^i K_0^p \quad \textit{for} \quad n=0 \tag{1.57}$$

$$b_n^{i+n} = \sum_{p=1}^i a_p^i K_n^p \quad \textit{for} \quad n\geq 1 \tag{1.58}$$

Symmetrically the coefficients $\{a_n^{i+n}\}_{p\in\mathbb{N}_*}$ are given in terms of b_n^{i+n} by

$$a_n^{i+n} = \sum_{p=1}^i b_p^i T_n^p \quad \textit{for} \quad n\geq 1 \tag{1.59}$$

Proof. $\forall i \geq 1$, using (1.37) gives

$$b_0^i = \frac{1}{\omega}\int_0^\omega \sum_{p=1}^i a_p^i \bar{U}^p(r,\theta)d\theta$$

The behavior of $\bar{U}^n(r,\theta)$ near the notch tip as mentioned in (1.48) gives us

$$b_0^i = \frac{1}{\omega}\sum_{p=1}^i a_p^i \int_0^\omega \Big(K_0^p + K_1^p r^\lambda\cos(\lambda\theta) + \dots\Big)d\theta$$

The orthogonal property of the basis $\{\cos(p\lambda\theta)\}_{p\in\mathbb{N}}$ leads to (1.57). Similarly, we can obtain (1.58) and (1.59). □

1.3.2 The construction of the coefficients a_n^{i+n} and b_n^{i+n}

Let's us explain the process of the construction. The following steps are independent and they can be considered as the initial input of the process.

(i) Once u^0 is determined, one knows b_n^n by (1.37). Reminding that when the compatibility (1.35) is satisfied and $g = 0$, then $v^0(\mathbf{y}) = b_0^0$. Therefore $a_n^n = 0$ and $a_0^i = 0\ \forall i \geq 0$.

(ii) The problem (1.47) for $\bar{U}^n$ depends on the outer geometry. It can be solved independently and once it is known, the coefficients $\{K_p^n\}_{p\in\mathbb{N}}$ are given by (1.49) and (1.50).

(iii) Symmetrically, $\bar{V}^n$ is given by the problem (1.54) defined on the inner (infinite) domain which contains the defect. Once $\bar{V}^n$ is known, the coefficients $\{T_p^n\}_{p\in\mathbb{N}_*}$ are given by (1.56).

Then one can determine the other coefficients by induction.

a_n^i / b_n^i	i=0	i=1	i=2	i=3	i=4
n=0	0 /step $i=0$	0 / 0	0 / step $i=2$	0 / step $i=3$	0 /step $i=4$
n=1	0	0/step $i=0$	step $i=1$ / 0	step $i=2$ / step $i=2$	step $i=3$/step $i=3$
n=2	0	0	0 / step $i=0$	step $i=1$/ 0	step $i=2$ / step $i=2$
n=3	0	0	0	0 / step $i=0$	step $i=1$ / 0
n=4	0	0	0	0	0/ step $i=0$

Table 1.3: The iterative method for calculating the coefficients a_n^i and b_n^i

(S1) Considering first $i = 1$, we have $b_n^{1+n} = a_1^1 K_n^1 = 0,\ \forall n \geq 0$ and $a_n^{1+n} = b_1^1 T_n^1,\ \forall n \geq 1$ where b_1^1 is obtained by (i) and T_n^1 by (iii).

(Si) Considering $i \geq 1$, we have $b_n^{i+n} = \sum_{p=1}^i a_p^i K_n^p$ and $a_n^{i+n} = \sum_{p=1}^i b_p^i T_n^p$ where the a_p^i's and the b_p^i's have been obtained at the previous steps whereas the K_n^p's are obtained by (ii) and the T_n^p's by (iii).

(Si+1) The process for calculating the coefficients remains true at the step $i+1$.

(a) Knowing a_n^{i+n} from step i, one can determine $b_0^{i+1} = \sum_{p=1}^i a_p^{(i+1-p)+p} K_0^p$ and $b_n^{i+1+n} = \sum_{p=1}^i a_p^{(i+1-p)+p} K_n^p$ with $a_p^{(i+1-p)+p},\ (p = \overline{1..i})$ corresponds to the coefficients a_n^{i+n} from the step 1 to step i.

(b) One knows b_n^{i+n} from step i, (1.58) at step $i+1$ can be written $a_n^{i+1+n} = \sum_{p=1}^i b_p^{(i+1-p)+p} T_n^p$. Similarly, $b_p^{(i+1-p)+p},\ (p = \overline{1..i})$ are specified from the step 1 to step i.

This procedure of construction is schematized in Table 1.3.

1.3.3 Example of calculation of the sequence of coefficients

In order to illustrate the above procedure, one considers the case of a crack in the particular geometry studied in chapter 2, see Figure 2.1. The angle of the notch is characterized by the parameter ϵ:

$$\omega = 2\pi - 2\arctan(\epsilon).$$

The goal is first to obtain the values of b_n^{i+n} and a_n^{i+n} by this technique. The initial input of the process is given in step 1 and the inductive process in step 2.

1. Step 1:

   (a) The b_n^n's are obtained from u^0 which is computed with the code COMSOL (by the finite element method). Their values for $1 \leq n \leq 5$ are given in Table 2.2.

   (b) The elementary displacements $\bar{U}^1$ and $\bar{V}^1$ are also computed with COMSOL. They give the coefficients $\{K_p^1\}_{p\in\mathbb{N}}$ and $\{T_p^1\}_{p\in\mathbb{N}_*}$ which can calculated by (1.50) and (1.56). Their values for $1 \leq p \leq 3$ or $1 \leq p \leq 5$ are given in Table 1.4. (Note that the values corresponding to the even p vanish by reason of symmetry of the structure and the loading.) Note also that the values of $\{T_p^1\}$ seems independent of the angle of the notch. This property will be discussed in Section 1.3.6 where the inner displacement $\bar{V}^1$ is obtained in a closed form.

ϵ	K_0^1	K_1^1	K_2^1	K_3^1	T_1^1	T_2^1	T_3^1	T_4^1	T_5^1
0	0	-0.6067	0	-0.2692	0.5016	0	-0.1260	0	0.0630
0.1	0	-0.5567	0	-0.2641	0.5020	0	-0.1261	0	0.0630
0.2	0	-0.4991	0	-0.2542	0.5021	0	-0.1260	0	0.0630
0.3	0	-0.4341	0	-0.2394	0.5021	0	-0.1258	0	0.0629
0.4	0	-0.3621	0	-0.2198	0.5020	0	-0.1257	0	0.0628

Table 1.4: The computed values of the coefficients $\{K_p^1\}_{p:\overline{1:3}}$ and $\{T_p^1\}_{p:\overline{1:5}}$ which are derived respectively from $\bar{U}^1$ and $\bar{V}^1$

2. Step 2: The values of $\{a_n^{1+n}\}$, $\{b_n^{1+n}\}$ and $\{a_n^{2+n}\}$, $\{b_n^{2+n}\}$ are given in Table 1.5. They are directly deduced from Step 1.

ϵ	$a_1^2 = b_1^1 T_1^1$	$a_2^3 = b_1^1 T_2^1$	$b_1^3 = a_1^2 K_1^1$
0	-0.3930	0	0.2384
0.1	-0.3756	0	0.2091
0.2	-0.3559	0	0.1776
0.3	-0.3342	0	0.1451
0.4	-0.3106	0	0.1125

Table 1.5: The computed values of the coefficients $\{a_n^{1+n}\}_{n:\overline{1:2}}$, $\{b_n^{1+n}\}_{n:\overline{1:2}}$ and $\{a_n^{2+n}\}_{n=1}$, $\{b_n^{2+n}\}_{n:\overline{1:2}}$ by the technique proposed in Proposition 1.5

ϵ	$a_1^3 = b_1^2 T_1^1 + b_2^2 T_1^2$	$b_0^2 = a_1^2 K_0^1$	$b_1^3 = a_1^2 K_1^1$	$b_2^4 = a_1^2 K_2^1$
0	0	0	0.2384	0
0.1	0	0	0.2091	0
0.2	0	0	0.1776	0
0.3	0	0	0.1451	0
0.4	0	0	0.1125	0

Table 1.6: The computed values of the coefficients $\{a_n^{2+n}\}_{n=1}$ and $\{b_n^{2+n}\}_{n:\overline{1:2}}$ by the technique proposed in Proposition 1.5

Remark 1.4. *The process of identification of all the coefficients $\{a_n^{i+n}\}$ and $\{b_n^{i+n}\}$ by the two methods can accumulate the errors from the prior computations. Therefore a good precision of each term is highly required. This is of course the case when the elementary problems can be solved analytically. Otherwise, the risk is that the higher order are badly evaluated and consequently that the asymptotic expansions can be used for small values of the parameter and up to a certain order only.*

The end of this chapter is devoted to particular cases where the outer or inner elementary problems admit solutions in a closed form. Specifically, one first considers the case where the outer domain is an angular sector and then the cases where the defect is a circular cavity or a non cohesive crack. The case of a cohesive crack will be partially treated in the next chapter.

1.3.4 The analytic form of the $\bar{U}^n$'s in the case where Ω_0 is an angular sector

Let us assume that the outer domain consists in the angular sector $\mathcal{D}_0^R$, *i.e.*

$$\Omega_0 = \{(r,\theta) \ : \ r \in (0,R), \quad \theta \in (0,\omega)\}.$$

The edges $\theta = 0$ and $\theta = \omega$ are free whereas the boundary $r = R$ is of Dirichlet type. In such a case the $\bar{U}^n$'s for all $n \geq 1$ can be obtained in a closed form. Indeed, by virtue of (1.47), $\bar{U}^n$ is the unique

element of $H^1(\Omega_0)$ which satisfies

$$\begin{cases} \Delta \bar{U}^n = 0 & \text{in } (0,R)\times(0,\omega) \\ \dfrac{\partial \bar{U}^n}{\partial \theta} = 0 & \text{on } (0,R)\times\{0,\omega\}\ . \\ \bar{U}^n = -R^{-n\lambda}\cos(n\lambda\theta) & \text{on } \{R\}\times(0,\omega) \end{cases} \tag{1.60}$$

Searching the solution (which is unique) under the form $\bar{U}^n(r,\theta) = f(r)\cos(n\lambda\theta)$, one easily finds

$$\bar{U}^n(\mathbf{x}) = -\frac{r^{n\lambda}}{R^{2n\lambda}}\cos(n\lambda\theta), \qquad \lambda = \frac{\pi}{\omega}. \tag{1.61}$$

Using (1.49), one deduces the coefficients K_p^n. Specifically, one gets

$$K_p^n = \begin{cases} 0 & \text{if} \quad p \neq n \\ -R^{2n\lambda} & \text{if} \quad p = n \end{cases}.$$

These solutions can be used whatever the defect at the tip of the notch.

1.3.5 The analytic form of the $\bar{V}^n$'s in the case of a circular cavity

Supposing the defect has the form of a small circular cavity of a radius ℓ, we can make a reference to the equation (1.54) in the case of Γ_1 being a circle cavity with a unit radius, then the analytic form of $\bar{V}^n$ can be read as following :

$$\bar{V}^n(\rho,\theta) = \rho^{-n\lambda}\cos(n\lambda\theta) \quad \text{for} \quad n \geq 1 \tag{1.62}$$

Consequently, the coefficients T_p^n are simply given by

$$\text{for} \quad n \geq 1, \qquad T_p^n = \begin{cases} 1 & \text{if} \quad p = n \\ 0 & \text{otherwise} \end{cases}.$$

The relations between a_n^{i+n} and b_n^{i+n} in this case can be illustrated in the Table 1.7 and Table 1.8. Finally, we can see that the coefficients a_n^i and b_n^i just depend on the outer problems, see Table 1.8. Therefore, in the case of a circular cavity, the determination of u_ℓ needs only to compute the solution of the outer problems. When the outer geometry has a particular form and has special boundary conditions which allows us to obtain analytic form for $\bar{U}^n$ (like the angular sector studied in the previous section), the solution u_ℓ will be defined analytically.

a_n^i / b_n^i	i=0	i=1	i=2	i=3	i=4
n=0	0 /b_0^0	0 / 0	0 /$b_1^1 K_0^1$	0 /0	0 /$b_1^3 K_0^1 + b_2^2 K_0^2$
n=1	0	0/b_1^1	b_1^1 / 0	0/$b_1^1 K_1^1$	b_1^3/0
n=2	0	0	0 / b_2^2	0/ 0	b_2^2 / $b_1^1 K_2^1$
n=3	0	0	0	0 / b_3^3	0 / 0
n=4	0	0	0	0	0/ b_4^4

Table 1.8: The final relations giving a_n^{i+n} and b_n^{i+n} when the defect is a circular cavity (to be compared with Table 1.7)

a_n^i / b_n^i	i=0	i=1	i=2	i=3	i=4
n=0	0 /b_0^0	0 / 0	0 /$a_1^2 K_0^1$	0 /$a_1^3 K_0^1 + a_2^3 K_0^2$	0 /$a_1^4 K_0^1 + a_2^4 K_0^2 + a_3^4 K_0^3$
n=1	0	0/b_1^1	b_1^1 / 0	b_1^2/$a_1^2 K_1^1$	b_1^3/$a_1^3 K_1^1 + a_2^3 K_1^2$
n=2	0	0	0 / b_2^2	0/ 0	b_2^2 / $a_1^2 K_2^1$
n=3	0	0	0	0 / b_3^3	0 / 0
n=4	0	0	0	0	0/ b_4^4

Table 1.7: The first relations giving a_n^{i+n} and b_n^{i+n} when the defect is a circular cavity

1.3.6 The analytic solution for the $\bar{V}^n$'s in the case of a crack

The case where the defect at the tip of the notch is a crack is of great practical importance. It turns out that, provided that the crack path is a segment line and the lips of the crack are free (no cohesive crack), the inner elementary problems $\bar{V}^n$ can be obtained in a closed form. This section is devoted to the construction of this analytical solution by using a conformal transform and the theory of complex potentials. One obtains then an Hilbert's problem which can be solved in a closed form.

Let us consider the inner problem (1.54). Since $\bar{V}^n$ is an harmonic function, it can be seen as a real part of a holomorphic function in the complex plane $z = y_1 + iy_2$. The domain Ω^∞ will be transformed into the domain denoted $\bar{\Omega}^\infty$ by using the conform mapping $Z = z^{2\lambda}$ with $Z = Z_1 + iZ_2,\ (Z_1, Z_2) \in \bar{\Omega}^\infty$ and $\bar{V}^n$ will be now considered as a function of the coordinates Z in $\bar{\Omega}^\infty$. We denote the holomorphic function by $f(Z) = \bar{V}^n(Z_1, Z_2) + i\bar{W}^n(Z_1, Z_2)$ where $\bar{W}^n$ is the imaginary part of $f(Z)$. The equation (1.54) becomes:

$$\begin{cases} \Delta \bar{V}^n = 0 & \text{in } \bar{\Omega}^\infty \\ \dfrac{\partial \bar{V}^n}{\partial \nu} = 0 & \text{on } \bar{\Gamma}^+ \cup \bar{\Gamma}^- \\ \dfrac{\partial \bar{V}^n}{\partial Z_2} = \dfrac{n}{2} Z_1^{\frac{n}{2}-1} \sin(\dfrac{n\pi}{2}) & \text{on } \bar{\Gamma}_1 \\ \bar{V}^n \to 0 & \text{at } \infty \end{cases} \tag{1.63}$$

Introducing $F(Z) = if^{'}(Z)$, one gets:

$$F(Z) = \frac{\partial \bar{V}^n}{\partial Z_2}(Z_1, Z_2) + i\frac{\partial \bar{V}^n}{\partial Z_1}(Z_1, Z_2)$$

where the real part of $F(Z)$ is given on a half-line $(-\infty, 1) \times \{0\}$ as follows:

$$\frac{\partial \bar{V}^n}{\partial Z_2}(t,0) = \begin{cases} 0 & \text{if} \quad -\infty < t < 0 \\ \frac{n}{2} t^{\frac{n}{2}-1} \sin(\frac{n\pi}{2}) & \text{if} \quad 0 < t < 1 \end{cases} \tag{1.64}$$

Using the results of Hilbert's problem, see Appendix 1.5, one obtains:

$$F(Z) = \frac{1}{2\pi i\sqrt{Z-1}} \int_0^1 \frac{n t^{\frac{n}{2}-1} \sin(\frac{n\pi}{2})}{X(t^+)(t-Z)} dt + C^\star \tag{1.65}$$

where $C^\star\sqrt{Z-1}$ represents the behavior of $F(Z)$ at infinity. Therefore, the last condition in (1.63) gives $C^\star = 0$ and finally, $F(Z)$ can be read as:

$$F(Z) = n \sin\frac{n\pi}{2} \; \frac{1}{2\pi\sqrt{Z-1}} \int_0^1 \frac{t^{\frac{n}{2}-1}\sqrt{1-t}}{t-Z} dt. \tag{1.66}$$

Remarking that $F(Z) = 0$ when n is an even integer number, let us consider odd numbers and set $n = 2m+1, \; m \in \mathbb{N}$. From now, we can write that

$$F(Z) = (2m+1)\sin(m+\frac{\pi}{2}) \frac{1}{2\pi\sqrt{Z-1}} \int_0^1 \frac{t^{m-\frac{1}{2}}\sqrt{1-t}}{t-Z} dt, \quad m \in \mathbb{N} \tag{1.67}$$

Hence, $f(Z) = -i\int_1^Z F(Y)dY + f(1)$ and $\bar{V}^n(Z)$ is the real part of $f(Z)$. Taking the integral of (1.67) with respect to Z gives

$$\begin{aligned} f(Z) &= -i\frac{(-1)^m(2m+1)}{2\pi} \int_1^Z \frac{1}{\sqrt{Y-1}} \Big[\int_0^1 \frac{t^{m-\frac{1}{2}}\sqrt{1-t}}{t-Y} dt \Big] dY + f(1) & (1.68) \\ &= -i\frac{(-1)^m(2m+1)}{2\pi} \int_0^1 \Big[t^{m-\frac{1}{2}}\sqrt{1-t} \int_1^Z \frac{1}{(t-Y)\sqrt{Y-1}} dY \Big] dt + f(1) & (1.69) \\ &= 2i\frac{(-1)^m(2m+1)}{2\pi} \int_0^1 t^{m-\frac{1}{2}} \arctan\sqrt{\frac{Z-1}{1-t}} dt + f(1) & (1.70) \end{aligned}$$

Besides, since

$$\arctan\sqrt{\frac{Z-1}{1-t}} = \frac{1}{2i}\ln\Big(\frac{1+i\sqrt{\frac{Z-1}{1-t}}}{1-i\sqrt{\frac{z-1}{1-t}}}\Big) = \frac{1}{2i}\ln\Big(\frac{\sqrt{1-t}+\mathrm{i}\sqrt{Z-1}}{\sqrt{1-t}-i\sqrt{Z-1}}\Big), \tag{1.71}$$

setting

$$\varrho = \Big|\frac{\sqrt{1-t}+i\sqrt{Z-1}}{\sqrt{1-t}-i\sqrt{Z-1}}\Big|, \qquad \vartheta = \arg\Big(\frac{\sqrt{1-t}+i\sqrt{Z-1}}{\sqrt{1-t}-i\sqrt{Z-1}}\Big),$$

and remarking that

$$\frac{\sqrt{1-t}+i\sqrt{Z-1}}{\sqrt{1-t}-i\sqrt{Z-1}}=\varrho e^{\mathrm{i}\vartheta},$$

then we obtain

$$\arctan\sqrt{\frac{Z-1}{1-t}}=\frac{1}{2i}\Big[\ln(\varrho)+i(\vartheta+2\lambda\pi)\Big]\quad\text{with}\quad k\in\mathbb{N}. \tag{1.72}$$

That gives us

$$\bar{V}^{2m+1}(Z)=\mathrm{Re}f(Z)=\frac{(-1)^m(2m+1)}{2\pi}\int_0^1 t^{m-\frac{1}{2}}\ln(\varrho)dt+f(1)\quad\forall m\in\mathbb{N} \tag{1.73}$$

Moreover,

$$\sqrt{Z-1}=\pm\Big[\sqrt{\frac{(Z_1-1)+\sqrt{(1-Z_1)^2+Z_2^2}}{2}}+\mathrm{i}\ \mathrm{sgn}(Z_2)\sqrt{\frac{(Z_1-1)+\sqrt{(Z_1-1)^2+Z_2^2}}{2}}\Big]$$

Then, we obtain two values of ϱ, denoted by ϱ_1 and ϱ_2, which are derived from function $\sqrt{Z-1}$ and can be written as :

$$\begin{aligned}\varrho_1 &= \sqrt{\frac{(1-t)^2+2(1-t)(Z_1-1)+(Z_1-1)^2+Z_2^2}{\Big[1-t+\sqrt{2(1-t)}\sqrt{1-Z_1+\sqrt{(Z_1)^2+Z_2^2}}\mathrm{sgn}(Z_2)+\sqrt{(Z_1-1)^2+Z_2^2}\Big]^2}}\\ \varrho_2 &= \sqrt{\frac{(1-t)^2+2(1-t)(Z_1-1)+(Z_1-1)^2+Z_2^2}{\Big[t-1+\sqrt{2(1-t)}\sqrt{1-Z_1+\sqrt{(Z_1)^2+Z_2^2}}\mathrm{sgn}(Z_2)-\sqrt{(Z_1-1)^2+Z_2^2}\Big]^2}}\end{aligned}$$

In order to define $\ln(\varrho)$, we choose the principle square root which corresponds to ϱ_1. Then, $\bar{V}^{2m+1}$ can be written as :

$$\bar{V}^{2m+1}(Z)=C_m\int_0^1 t^{m-\frac{1}{2}}\ln\Big(\frac{(1-t)^2+2(1-t)\mathrm{Re}(Z-1)+|Z-1|^2}{\Big[1-t+\sqrt{2(1-t)}\sqrt{|Z|-\mathrm{Re}(Z-1)}\mathrm{sgn}(\mathrm{Im}(Z))+|Z-1|^2\Big]^2}\Big)dt \tag{1.74}$$

with $C_m=\frac{(-1)^m(2m+1)}{4\pi},\ \forall m\in\mathbb{N}$.

Besides, we know that the formula for T_p^n in (1.56) is valid for all $\rho>0$ and then when $\rho\to\infty$. We also know that when Z goes to infinity,

$$\arctan\sqrt{\frac{1-t}{Z-1}}=\frac{\sqrt{1-t}}{\sqrt{Z-1}}-\frac{1}{3}\Big[\frac{\sqrt{1-t}}{\sqrt{Z-1}}\Big]^3+\frac{1}{5}\Big[\frac{\sqrt{1-t}}{\sqrt{Z-1}}\Big]^5-\frac{1}{7}\Big[\frac{\sqrt{1-t}}{\sqrt{Z-1}}\Big]^7+O\Big(\Big[\frac{\sqrt{1-t}}{\sqrt{Z-1}}\Big]^9\Big) \tag{1.75}$$

and $\arctan\sqrt{\frac{Z-1}{1-t}}+\arctan\sqrt{\frac{1-t}{Z-1}}=\frac{\pi}{2}$, then we can get the asymptotic expansion of $\arctan\sqrt{\frac{Z-1}{1-t}}$ when Z is close to infinity as :

$$\arctan\sqrt{\frac{Z-1}{1-t}}=\frac{\pi}{2}-\frac{\sqrt{1-t}}{\sqrt{Z-1}}+\frac{1}{3}\Big[\frac{\sqrt{1-t}}{\sqrt{Z-1}}\Big]^3-\frac{1}{5}\Big[\frac{\sqrt{1-t}}{\sqrt{Z-1}}\Big]^5+O\Big(\Big[\frac{\sqrt{1-t}}{\sqrt{Z-1}}\Big]^7\Big) \tag{1.76}$$

Using the binomial series for $(Z-1)^{-1/2}$ for large Z, we have:

$$\begin{aligned}(Z-1)^{-1/2} &= \frac{1}{\sqrt{Z}}\Big[1-\frac{1}{Z}\Big]^{-1/2} \\ &= \frac{1}{\sqrt{Z}}\Big[1+\frac{1}{2}\frac{1}{Z}+\frac{-\frac{1}{2}\Big(-\frac{1}{2}-1\Big)}{2!}\frac{1}{Z^2}+\frac{-\frac{1}{2}\Big(-\frac{1}{2}-1\Big)\ldots\Big(-\frac{1}{2}-k+1\Big)}{k!}\frac{1}{Z^k}+\ldots\Big]\end{aligned}$$

or

$$\frac{1}{\sqrt{Z-1}}=\frac{1}{Z^{1/2}}+\frac{1}{2}\frac{1}{Z^{3/2}}+\frac{3}{8}\frac{1}{Z^{5/2}}+\frac{5}{16}\frac{1}{Z^{7/2}}+\frac{35}{128}\frac{1}{Z^{9/2}}+O\Big(\frac{1}{Z^5}\Big) \tag{1.77}$$

Finally, from (1.76) and (1.77), we can see that the asymptotic expansion of $\arctan\Big(\sqrt{\frac{Z-1}{1-t}}\Big)$:

$$\begin{aligned}\arctan\Big(\sqrt{\frac{Z-1}{1-t}}\Big) &= \frac{\pi}{2}-\sqrt{1-t}\Big[\frac{1}{Z^{1/2}}+\frac{1}{2}\frac{1}{Z^{3/2}}+\frac{3}{8}\frac{1}{Z^{5/2}}+\ldots\Big]+\frac{(\sqrt{1-t})^3}{3}\Big[\frac{1}{\sqrt{Z}}+\frac{1}{2}\frac{1}{Z^{3/2}}+\ldots\Big]^3 \\ &+ \ \ldots \qquad (1.78) \\ &= \frac{\pi}{2}-\sqrt{1-t}\Big[\frac{1}{Z^{1/2}}+\frac{1}{2}\frac{1}{Z^{3/2}}+\frac{3}{8}\frac{1}{Z^{5/2}}+\ldots\Big]+\frac{(\sqrt{1-t})^3}{3}\Big[\frac{1}{Z^{3/2}}+\frac{3}{2}\frac{1}{Z^{5/2}}+\ldots\Big] \\ &+ \ \ldots \qquad (1.79)\end{aligned}$$

Setting

$$\alpha_m=\frac{\sqrt{\pi}\Gamma(m+\frac{1}{2})}{\Gamma(m+2)},\quad \beta_m=\frac{\sqrt{\pi}\Gamma(m+\frac{1}{2})}{\Gamma(m+3)},\quad \gamma_m=\frac{3\sqrt{\pi}\Gamma(m+\frac{1}{2})}{\Gamma(m+4)}, \tag{1.80}$$

where $\Gamma(.)$ is the Gamma function and hence

$$\Gamma(m+\frac{1}{2})=\frac{\sqrt{\pi}(2m)!}{4^m m!},\quad \Gamma(m+i)=(m+i-1)!,\quad \text{when}\quad i\in\mathbb{N}.$$

Then (1.70) becomes

$$\begin{aligned}f(Z) &= i\frac{(-1)^m(2m+1)}{\pi}\Big[(m+\frac{1}{2})\frac{\pi}{2}-\frac{\alpha_m}{2}\Big(\frac{1}{Z^{1/2}}+\frac{1}{2}\frac{1}{Z^{3/2}}+\frac{3}{8}\frac{1}{Z^{5/2}}\Big)+\frac{\beta_m}{4}\Big(\frac{1}{Z^{3/2}} \\ &+ \ \frac{3}{2}\frac{1}{Z^{5/2}}\Big)-\frac{\gamma_m}{8}\Big(\frac{1}{Z^{5/2}}+\ldots\Big)+\ldots\Big]+f(1)+\ldots \qquad (1.81)\end{aligned}$$

Using the mapping $Z=z^{2\lambda}$ or $Z=\rho^{2\lambda}e^{i2\lambda\Theta}$ where $\Theta=\theta-\frac{\omega}{2}$ and inserting into (1.81) gives us that :

$$\begin{aligned}f(Z) &= i\frac{(-1)^m(2m+1)}{\pi}\Big[(m+\frac{1}{2})\frac{\pi}{2}-\frac{\alpha_m}{2}\Big(\frac{e^{-ik\Theta}}{\rho^k}+\frac{1}{2}\frac{e^{-i3k\Theta}}{\rho^{3k}}+\frac{3}{8}\frac{e^{-i5k\Theta}}{\rho^{5k}}\Big) \\ &+ \ \frac{\beta_m}{4}\Big(\frac{e^{-i3k\Theta}}{\rho^{3k}}+\frac{3}{2}\frac{e^{-i5k\Theta}}{\rho^{5k}}\Big)-\frac{\gamma_m}{8}\Big(\frac{e^{-i5k\Theta}}{\rho^{5k}}+\ldots\Big)\ldots\Big]+f(1)+\ldots \\ &= i\frac{(-1)^m(2m+1)}{\pi}\Big[(m+\frac{1}{2})\frac{\pi}{2}-\frac{\alpha_m}{2}\frac{e^{-ik\Theta}}{\rho^k}+\frac{\beta_m-\alpha_m}{4}\frac{e^{-i3k\Theta}}{\rho^{3k}}+\frac{6\beta_m-3\alpha_m}{16}\frac{e^{-i5k\Theta}}{\rho^{5k}}+\ldots\Big] \\ &+ \ f(1)+\ldots \qquad (1.82)\end{aligned}$$

From (1.82) we can derive the asymptotic expansion for $\bar{V}^{2m+1}(\mathbf{y})$ at infinity:

$$\begin{aligned}\bar{V}^{2m+1}(\mathbf{y}) &= \frac{(-1)^{m+1}(2m+1)}{\pi}\Big[(m+\frac{1}{2})\frac{\pi}{2} - \frac{\alpha_m}{2}\rho^{-k}\cos(k\theta) + \frac{\alpha_m-\beta_m}{4}\rho^{-3k}\cos(3k\theta) \\ &+ \frac{6\beta_m - 3\alpha_m - 2\gamma_m}{16}\rho^{-5k}\cos(5k\theta) + \dots\Big] + \mathrm{Re}f(1) \end{aligned} \tag{1.83}$$

The condition at infinity gives that $\lim_{\rho\to\infty}\bar{V}^{2m+1} = 0$. Hence,

$$\mathrm{Re}f(1) = \frac{(-1)^m(2m+1)}{\pi}(m+\frac{1}{2})\frac{\pi}{2}.$$

Moreover, by virtue of (1.56), we can easily get that $T_{2p}^{2m+1} = 0$ for $p \in \mathbb{N}_*$, whereas the first coefficients $\{T_{2p+1}^{2m+1}\}_{p\in\mathbb{N}}$, namely T_1^{2m+1}, T_1^{2m+1} and T_3^{2m+1}, are given by

$$\begin{aligned} T_1^{2m+1} &= -\frac{\alpha_m}{2}.\frac{(-1)^{m+1}(2m+1)}{\pi}, \\ T_3^{2m+1} &= \frac{\alpha_m-\beta_m}{4}.\frac{(-1)^{m+1}(2m+1)}{\pi}, \\ T_5^{2m+1} &= -\frac{6\beta_m-3\alpha_m-2\gamma_m}{16}.\frac{(-1)^{m+1}(2m+1)}{\pi}, \dots \end{aligned} \tag{1.84}$$

where α_m and β_m are given by (1.80). Table 1.9 gives the coefficients $\{T_p^1\}_{p\in\mathbb{N}_*}$ (which correspond to $m = 0$). Comparing with Table 1.4 allows us to validate these analytic results.

T_1^1	T_3^1	T_5^1
0.5	$-\frac{1}{8}$	$\frac{1}{16}$

Table 1.9: The values of the coefficients T_1^1, T_3^1 and T_5^1 by the analytic method

One can conclude that the coefficients $\{T_p^1\}_{p=\overline{1:5}}$ do not depend on the notch angle. Accordingly, The method based on the calculation of the two independent families $\{\bar{U}^n\}$ and $\{\bar{V}^n\}$ becomes much more advantageous.

Conclusion

We have proposed a technique for solving the inner problems and the outer problems independently. The flexibility of the method can be applied in various form of the inner or outer geometries. In particular, the values of the coefficient $\{T_p^n\}$ in case of a crack (or any other defect which allows to calculate exactly and once and for all those coefficients) do not change even one changes the outer domain and the boundary conditions. Therefore the amount of work is reduced by a half because we have just to solve the outer problems.

1.4 Conclusion and Perspectives

We have presented here a general method based on matched asymptotic expansions which can be applied to determine the mechanical fields and all related mechanical quantities in the case of a defect located at the tip of a notch. In the anti-plane setting where the problem was addressed, we have explained how it is possible to calculate all the terms of both expansions by solving by induction the family of inner and outer problems coupled by the matching conditions. The crucial point, point which is specific to the fact that the defect is located at the tip of a notch, is the presence of more and more singular terms (which are more and more singular) when we consider higher orders in the expansions. It is necessary to isolate these singular terms and to calculate them separately by a relevant method so that each problem becomes well-posed.

With the method presented in Section 1.2, the inner and outer problems are interdependent and must be solved sequentially. The drawback of such a procedure is that one has to recalculate each term when the loading or the geometry or the defect are changed. Accordingly, we have proposed in Section 1.3 another method based on the linearity of the problems which allows one to calculate certain terms once and for all. In particular, we have obtained in a closed form the solution of the family of “elementary" inner problems in the cases of a cavity or a crack. Those solutions are intrinsic to the corresponding defect and can be used whatever the geometry and the loading of the whole body. Therefore, they can be used as a plug and play device for solving a variety of structures having such a type of defects.

Both methods were presented here in an anti-plane elasticity setting. From a practical viewpoint, it is absolutely necessary to extend them at least to plane elasticity. There is no conceptual difficulty to do that, except that the sequence of singularities at a corner are known explicitly in the anti-plane case but not in the plane case. Accordingly, the development of the method becomes more delicate from a practical viewpoint. The chapter 3 will be partially devoted to this task. Another interesting extension should be to consider non linear problems. The issue is, of course, that we loose then the possibility to use the principle of superposition and to solve each problem independently. The case of cohesive cracks enters in this category and will be addressed in the next chapter.

1.5 Appendix: the Hilbert problem

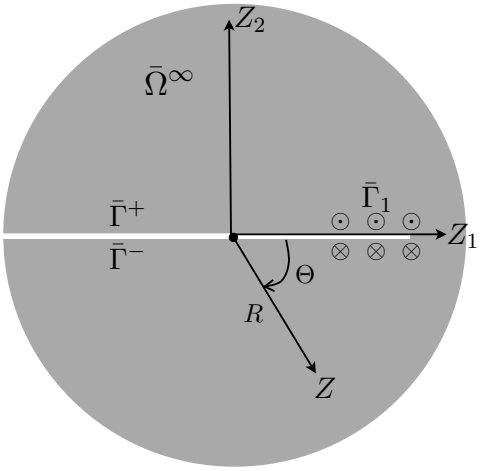

Figure 1.4: The Hilbert problem

Let Vdenote for a displacement field satisfying the Laplace's equation in an infinite domain $\bar{\Omega}^{\infty}$, see Figure 1.4

$$\Delta V = 0 \quad \text{in} \quad \bar{\Omega}^{\infty} \tag{1.85}$$

In general, the homogeneous condition is prescribed on the semi-infinite line $\bar{\Gamma}^+ \cup \bar{\Gamma}^-$, while on $\bar{\Gamma}_1$, a Neumann condition is given in terms of a function of Z_1,

$$\frac{\partial V}{\partial Z_2} = 0 \quad \text{on} \quad \bar{\Gamma}^+ \cup \bar{\Gamma}^-, \qquad \frac{\partial V}{\partial Z_2} = h(Z_1) \quad \text{on} \quad \bar{\Gamma}_1. \tag{1.86}$$

The condition of V at infinity is given as a function of R and Θ as follows,

$$V \to C\sqrt{R}\sin\frac{\Theta}{2} \quad \text{at infinity} \tag{1.87}$$

where C is a constant. The problem above can be posed in the complex plane $Z = Z_1 + iZ_2$ by introducing the holomorphic function $f(Z)$ such that

$$f(Z) = V(Z_1, Z_2) + iW(Z_1, Z_2).$$

Therefore $V(Z_1, Z_2)$ is the real part of $f(Z)$. Setting $F(Z) = if'(Z) = V_{,2} + iV_{,1}$, we have

$$\begin{cases} F(t^+) + \overline{F(t^+)} = 0 & \text{for} \quad t \in \bar{\Gamma}^+ \cup \bar{\Gamma}^- \\ F(t^+) + \overline{F(t^+)} = 2\dfrac{\partial V}{\partial Z_2} = 2h(Z_1) & \text{for} \quad t \in \bar{\Gamma}_1 \end{cases} \tag{1.88}$$

where $F(t^{\pm}) = \lim_{\delta\to 0,\delta>0} F(t\pm i\delta)$. Furthermore, since $\overline{F(t^+)} = F(t^-)$, the conditions on $\bar{\Gamma}^+\cup\bar{\Gamma}^-\cup\bar{\Gamma}_1$ can read as:

$$F(t^+) + F(t^-) = 2h(Z_1). \tag{1.89}$$

Let us denote by $(b,0)$ the position of the tip of $\bar{\Gamma}_1$ in the Z-coordinates. Choosing an analytic function such that $X(Z)\sim 1/\sqrt{Z}$ at infinity,

$$X(Z) = \frac{1}{\sqrt{Z-b}} \tag{1.90}$$

we can see that $X(t^+) = -X(t^-)$. Clearly, one has $\big(Z-b\big)^{-\frac{1}{2}} = |Z-b|\, e^{-\frac{i\alpha}{2}}$, where $\alpha = \arg\big(Z-b\big)$. When Z goes from the upper side of the crack around the point $\big(b,0\big)$ to the lower side of the crack, α increases by -2π. Therefore, $\big(Z-b\big)^{-\frac{1}{2}}$ must be multiplied by $e^{i\pi} = -1$. Thus $X(t^+) = -X(t^-)$. Dividing (1.89) by $X(t^+)$, we obtain:

$$\frac{F(t^+)}{X(t^+)} - \frac{F(t^-)}{X(t^-)} = \frac{2h(Z_1)}{F(t^+)} \tag{1.91}$$

The formula of Plemelj gives us:

$$\frac{F(Z)}{X(Z)} = \frac{1}{2\pi i}\int_a^b \frac{h(t)}{F(t^+)(t-Z)}dt + C^\star \tag{1.92}$$

or

$$F(Z) = \frac{X(Z)}{2\pi i}\int_a^b \frac{2h(t)}{X(t^+)(t-Z)}dt + C^\star X(Z) \tag{1.93}$$

where the term $C^\star X(Z)$ represents the behavior of $F(Z)$ at infinity. Since at infinity $V^1(R,\Theta)$ behaves like $C\sqrt{R}\sin\frac{\Theta}{2}$, one deduces that:

$$F(Z) \approx \frac{C}{2R}\sqrt{Z} \quad \text{at infinity} \tag{1.94}$$

Finally, the analytic function $F(Z)$ can be read as:

$$F(Z) = \frac{C}{2\sqrt{Z-b}} + \frac{1}{2\pi\lambda\sqrt{Z-b}}\int_a^b \frac{2h(t)\sqrt{b-t}}{t-Z}dt. \tag{1.95}$$

The formula of $F(Z)$ in (1.95) gives also the (transformed) stress $\sigma_{32}+i\sigma_{31} = \mu(V_{,2}+iV_{,1})$ in domain $\bar{\Omega}^\infty$. Accordingly, we can see that there exits a singularity at the tip $(b,0)$ of $\bar{\Gamma}_1$ which corresponds to the factor of $\frac{1}{\sqrt{Z-b}}$. Therefore, the value of the stress intensity factor and the jump of the displacement at position $(a,0)$ can be easily deduced from the analytic formula $F(Z)$.

1.5.1 Stress intensity factor $\mathcal{K}$

In mode III, $\mathcal{K}$ is formally defined as:

$$\mathcal{K} := \lim_{Z_1 \to b} \sqrt{2\pi(Z_1 - b)} Re\big(F(Z1, 0)\big). \tag{1.96}$$

Therefore, one deduces from (1.95)

$$\mathcal{K} = \sqrt{2\pi}\Big(\frac{C}{2} - \frac{1}{2\pi\lambda}\int_a^b \frac{2h(t)}{\sqrt{b-t}}dt\Big) \tag{1.97}$$

1.5.2 The jump of the displacement V at position $(a, 0)$

Note that the homogeneous Neumann condition is given on $\bar{\Gamma}^+ \cup \bar{\Gamma}^-$, in particular $V_{,2} = 0$ on $\bar{\Gamma}^{\pm}$. We also have

$$F(Z) := if'(Z) = -i\Big(\frac{C}{2\sqrt{b-Z}} + \frac{1}{2\pi\lambda\sqrt{b-Z}}\int_a^b \frac{2h(t)\sqrt{b-t}}{t-Z}dt\Big)$$

Moreover, $f(Z) := V_{,1} - iV_{,2} = V_{,1}$ on $\Gamma^{\pm}$ because an homogeneous Neumann condition is given on $\Gamma^{\pm}$. Consequently, the jump of the displacement V can be determined at any point $(a, 0)$ on the lips of the crack by integrating the function $f(Z)$ and taking into account that the jump at $(b, 0)$ is equal to 0. It can be read as:

$$[\![V]\!](a, 0) = \int_a^b \Big(\frac{C}{\sqrt{b-Z_1}} + \frac{1}{\pi\lambda\sqrt{b-Z_1}}\int_a^b \frac{2h(t)\sqrt{b-t}}{t-Z_1}dt\Big)dZ_1 \tag{1.98}$$

Chapter 2

Application to the nucleation of a crack in mode III

2.1 Introduction

In the present chapter, the **MAM** is applied to the case where the defect is a crack, first in the non cohesive case, then in the cohesive case. In the case of a non cohesive crack, the first issue is to estimate with a good accuracy any mechanical quantity like the energy release rate associated with a crack of small length near the tip of the notch. Indeed, it is a real issue in the case of a genuine notch (by opposition to a crack) because the energy release rate starts from 0 when the length of the nucleated crack is 0, then is rapidly increasing with the length of the crack before to reach a maximum and finally is decreasing.

Accordingly, after the setting of the problem, one first explains in Section 2.2 how one computes the energy release rate by the FEM and why the numerical results are less accurate when the crack length is small. Then, one uses the **MAM** to compute the energy release rate for small values of the crack length and one shows, as it was expected, that the smaller the size of the defect, the more accurate is the approximation by the **MAM** at a certain order. It even appears that one can obtain very accurate results by computing a small number of terms in the matched asymptotic expansions. We discuss also the influence of the angle of the notch on the accuracy of the results, this angle playing an important role in the process of nucleation (because, in particular, the length ℓ_{m} at which the maximum of the energy release rate is reached depends on the angle of the notch). It turns out that when the notch is sufficiently sharp, *i.e.* sufficiently close to a crack, it suffices to calculate the first two non trivial terms of the expansion of the energy release rate to capture with a very good accuracy the dependence of the energy release rate on the crack length.

In section 2.3, we study the problem of crack nucleation at the tip of a notch. We first introduce the two competing evolution laws, *i.e.* the *G-law* and the *FM-law*: the first one is the usual Griffith's law based on the criterion of critical energy release rate, the second is that introduced in [Francfort and Marigo, 1998] and which is based on the concept of energy minimization. We recall some general results previously established in [Marigo, 2010] and extend them in the present case of a notch-shaped body in an antiplane setting. By virtue of the good approximation given by the **MAM**, we are able to solve the evolution problem in a quasi closed form, the solution depending only on two coefficients that one must compute by the FEM. That allows us to make a qualitative and quantitative comparison of the two laws.

In Section 2.4, we consider the case of a cohesive crack whose behavior is governed by the Dugdale model. Since such a model contains a critical stress, it is no more necessary to introduce a specific

nucleation criterion. Indeed, owing to the singularity due to the notch, a cohesive crack is nucleated at the beginning of the loading. Then, the cohesive crack will grow until the crack "opening" at the tip of the notch reaches the critical value associated with Dugdale's model, [Dugdale, 1960]. At this moment a "true" non cohesive crack is created and we will see that an instability occurs. So, the main goal is to determine the loading at which this instability happens. Assuming that the internal length of the material (which is contained in Dugdale's model) is small by comparison with the overall dimension of the body and taking that length as a small parameter, we propose to use the **MAM** to obtain an approximate value of this critical load.

Finally, the results predicted by the two models of Griffith and Dugdale are compared.

2.2 The case of a non cohesive crack

2.2.1 Setting of the problem

In this section, the method is applied to the case where the defect is a non cohesive crack. Specifically, let Ω be the rectangle $(-H, L) \times (-H, +H)$. We remove from Ω the following sector $\mathcal{N}$:

$$\mathcal{N} = \{\mathbf{x} = (x_1, x_2) \, : \, -H < x_1 \leq 0, |x_2| \leq \epsilon |x_1|)\}, \tag{2.1}$$

where ϵ is a given parameter in $(0, 1)$. We obtain so the notch-shaped body $\Omega_0 = \Omega \backslash \mathcal{N}$. Finally we remove from Ω_0 the line segment $\Gamma_\ell = (0, \ell) \times \{0\}$ and obtains the cracked body Ω_ℓ, see Figure 2.1. The angle ω of the notch is given in terms of the parameter ϵ by

$$\omega = 2\pi - 2 \arctan(\epsilon).$$

The boundary Γ_D where the displacement are prescribed corresponds to the sides $D^\pm$ and D_L. Specifically, the boundary conditions read as

$$u_\ell(\mathbf{x}) = \begin{cases} +H & \text{on} \quad D^+ = \{-H\} \times [\epsilon H, H] \\ -H & \text{on} \quad D^- = \{-H\} \times [-H, -\epsilon H] \\ 0 & \text{on} \quad D_L = \{L\} \times [-H, H] \end{cases} \tag{2.2}$$

whereas the remaining parts of the boundary (including the lips of the crack) are free. Accordingly, we have

$$\frac{\partial u_\ell}{\partial x_2} = \begin{cases} 0 & \text{on} \quad \Gamma_\ell = (0, \ell) \times \{0\} \\ 0 & \text{on} \quad N^\pm = (-H, L) \times \{\pm H\} \end{cases} \tag{2.3}$$

and

$$\frac{\partial u_\ell}{\partial n} = 0 \quad \text{on} \quad \Gamma^\pm = \{(x_1, x_2) \quad -H < x_1 < 0, x_2 = \pm \epsilon x_1\}. \tag{2.4}$$

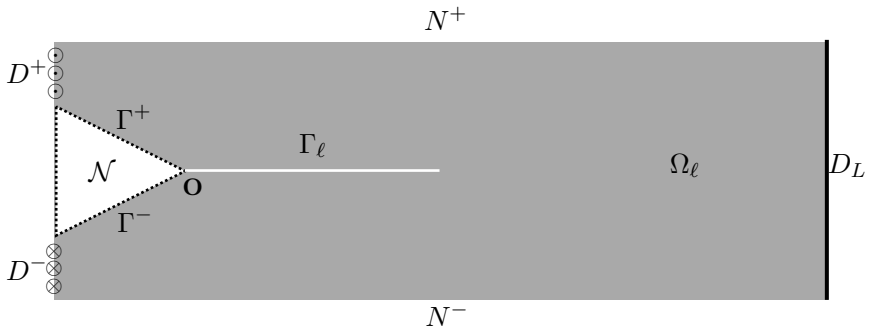

Figure 2.1: The cracked notch-shaped body Ω_ℓ and its different parts of the boundary.

Remark 2.1. *The amplitude of the prescribed displacement is normalized to H so that u_ℓ have the dimension of a length. The fact that the amplitude is equal to the height H has no importance in the present context of linearized elasticity. We will introduce a time dependent amplitude of the prescribed displacement when we will study the propagation of the crack. Then the prescribed displacement will take "reasonable" values, controlled by the toughness of the material.*

Remark 2.2. *The case $\epsilon = 0$ corresponds to a body with an initial crack of length H and this limit case is also considered is this paper. On the other hand, $\epsilon = 1$ corresponds to a corner with an angle of $\pi/2$, the sides $D^\pm$ being reduced to the points $(-H, \pm H)$. This limit case will not be considered here.*

Remark 2.3. *We only consider the case where the crack path is the line segment $(0, L)\times\{0\}$. It is a rather natural assumption by virtue of the symmetry of the geometry and the loading. An interesting extension should be to consider non symmetric geometry or loading and hence to take the direction of the crack as a parameter. This extension is reserved for future works.*

Let us examine the singularities of ∇u_ℓ (in the sense that ∇u_ℓ is not bounded) according to whether $\ell = 0$ and according to whether $\epsilon = 0$.

1. **When $\epsilon > 0$ and $\ell = 0$.** Then ∇u_0 is infinite at the tip of the notch and in its neighborhood reads as
$$\nabla u_0(\mathbf{x}) = \frac{\lambda b_1^1}{r^{1-\lambda}}\Big(\cos(\lambda\theta)\mathbf{e}_r - \sin(\lambda\theta)\mathbf{e}_\theta\Big) + \text{regular terms}.$$
2. **When $\epsilon > 0$ and $\ell > 0$.** Then ∇u_ℓ is no more infinite at the tip of the notch but becomes infinite at the tip of the crack, with the usual singularity in $1/\sqrt{r}$, see [Bui, 1978]. Specifically,

∇u_ℓ reads as

$$\nabla u_\ell(\mathbf{x}) = \frac{K_\ell}{\mu\sqrt{2\pi r'}}\Big(\sin\Big(\frac{\theta'}{2}\Big)\mathbf{e}_r + \cos\Big(\frac{\theta'}{2}\Big)\mathbf{e}_\theta\Big) + \text{regular terms.} \tag{2.5}$$

In (2.5) (r', θ') denotes the polar coordinate system such that $\mathbf{x} = (\ell + r'\cos\theta')\mathbf{e}_1 + r\sin\theta'\mathbf{e}_2$ and the angular function of θ' is normalized so that K_ℓ be the usual stress intensity factor. K_ℓ depends on ℓ and is "strongly" influenced by the presence of the notch when ℓ is small. (In fact, K_ℓ goes to 0 when ℓ goes to 0 as we will see below.) So, even if the stresses are only singular at the tip of the crack, there is a kind of overlapping of the previous singularity at the tip of the notch. This phenomenon renders the computations by the finite element method less accurate when ℓ is small.

3. **When $\epsilon = 0$.** Then the notch is already a crack and it is unnecessary to treat separately $\ell = 0$ and $\ell > 0$. In any case ∇u_ℓ has the classical singularity in $1\sqrt{r}$ as in (2.5) and there is no more an overlapping of two singularities. The computations by the finite element method are accurate in the full range of values of ℓ.

2.2.2 The issue of the computation of the energy release rate

The main goal of this section is to obtain accurate values for the *elastic energy* $\mathcal{P}_\ell$ stored in the cracked body and for its derivative with respect to ℓ, the so-called *energy release rate* $\mathcal{G}_\ell$, when ℓ is small. By definition, the elastic energy is given by

$$\mathcal{P}_\ell = \frac{1}{2}\int_{\Omega_\ell} \mu\nabla u_\ell \cdot \nabla u_\ell dx. \tag{2.6}$$

By virtue of Clapeyron's formula, the elastic energy stored in the body when the body is at equilibrium is equal to one half the work done by the external loads over the prescribed displacement on $D^\pm$. Therefore, using the symmetry of u_ℓ, the elastic energy can also read as the following integral over D^+:

$$\mathcal{P}_\ell = -\int_{\epsilon H}^{H} \mu H \frac{\partial u_\ell}{\partial x_1}(-H, x_2)dx_2 \tag{2.7}$$

which involves only the displacement field far from the tip of the notch.

By definition, see [Bourdin et al., 2008; Leblond, 2000], the *energy release rate* $\mathcal{G}_\ell$ is the opposite of the derivative of the elastic energy with respect to the length of the crack:

$$\mathcal{G}_\ell = -\frac{d\mathcal{P}_\ell}{d\ell}. \tag{2.8}$$

Even if $\mathcal{P}_\ell$ involves the ℓ dependent displacement field u_ℓ, its derivative does not involve the derivative $du_\ell/d\ell$ but can be expressed in terms of u_ℓ only. This property is a consequence of the fact that

u_ℓ satisfies the equilibrium equations. Specifically, $\mathcal{G}_\ell$ can be computed either with the help of path integrals like the $\mathcal{J}$ integral of Rice [Rice, 1968] or by using the so-called $G-\theta$ method developed in [Destuynder and Djaoua, 1981]. We recall below the main ingredients of both methods when $0<\ell<L$. The cases $\ell=0$ and $\ell=L$ are treated separately.

In the former method, the integral $\mathcal{J}_\mathcal{C}$ over the path $\mathcal{C}$ is defined by

$$\mathcal{J}_\mathcal{C}=\int_\mathcal{C}\left(\frac{\mu}{2}\nabla u_\ell\cdot\nabla u_\ell n_1-\mu\frac{\partial u_\ell}{\partial n}\frac{\partial u_\ell}{\partial x_1}\right)ds,$$

where $\mathbf{n}$ denotes the outer normal of the path. This integral is (theoretically) path-independent and equal to $\mathcal{G}_\ell$ provided that the path $\mathcal{C}$ starts from the lip of the crack, circumvents the tip of the crack and finishes on the lip of the crack like in Figure 2.2, see [Bui, 1978]. This path independency is used to obtain Irwin's formula [Irwin, 1958; Leblond, 2000]. Indeed, taking for path the circle $\mathcal{C}_{r'}$ centered at the tip of the crack with radius r', using (2.5) and passing to the limit when $r'\to 0$, one obtains the following link between the energy release rate and the stress intensity factor K_ℓ introduced in (2.5):

$$\mathcal{G}_\ell=\lim_{r'\to 0}\mathcal{J}_{\mathcal{C}_{r'}}=\frac{K_\ell^2}{2\mu}.$$

For the computations, one can benefit of the particularities of the geometry and the loading to choose

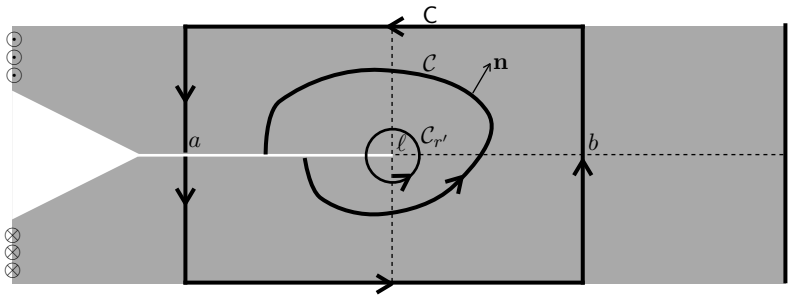

Figure 2.2: Examples of path for which $\mathcal{J}_\mathcal{C}$ is equal to $\mathcal{G}_\ell$.

a path made of line segments parallel to the axes like the path C in Figure 2.2. Specifically, let us set

$$\mathsf{C}=\{a\}\times(-H,0)\cup[a,b]\times\{-H\}\cup\{b\}\times(-H,H)\cup[a,b]\times\{+H\}\cup\{a\}\times(0,H)\quad\text{with}\quad 0<a<\ell<b<L.$$

Then $\mathcal{J}_\mathsf{C}=\mathcal{G}_\ell$. Therefore, since $n_1=0$ and $\partial u_\ell/\partial n=0$ on the sides $x_2=\pm H$ and by virtue of the symmetry of u_ℓ, $\mathcal{G}_\ell$ can read as

$$\mathcal{G}_\ell=\mu\int_{\{b\}\times(0,H)}\left(\left(\frac{\partial u_\ell}{\partial x_2}\right)^2-\left(\frac{\partial u_\ell}{\partial x_1}\right)^2\right)dx_2-\mu\int_{\{a\}\times(0,H)}\left(\left(\frac{\partial u_\ell}{\partial x_2}\right)^2-\left(\frac{\partial u_\ell}{\partial x_1}\right)^2\right)dx_2. \tag{2.9}$$

From a theoretical point of view, a and b can be chosen arbitrarily provided that they satisfy the constraints above. Indeed, the integral over the line segment $x_1=a$ (resp. $(x_1=b)$) does not depend

on a (resp. on b) because u_ℓ is harmonic and satisfy homogeneous Neumann boundary conditions on $N^\pm$ and Γ_ℓ. (This verification is left to the reader, see [Marigo, 2010, Proposition 8] for a proof.) However, from a numerical point of view, it is no more true because the computed displacement field does not satisfy exactly the equilibrium equations. Consequently, the computed values of $\mathcal{G}_\ell$ depend on the choice of a and b. Moreover, since the integral over the line a involves the gradient of the displacement, this integral can be badly approximated when ℓ is small because of the singularity.

The $G-\theta$ method is based on a change of variables which sends the ℓ-dependent domain Ω_ℓ onto a fix domain. In essence, it is the basic method to prove that $\ell \mapsto \mathcal{P}_\ell$ is differentiable, see [Destuynder and Djaoua, 1981] for the genesis of this method and [Chambolle et al., 2010] for a discussion on a generalization of the concept of energy release rate. In turn the $G-\theta$ approach gives a practical method to compute the energy release rate, see [Chambolle et al., 2010; Destuynder and Djaoua, 1981]. Specifically, for a given $\ell > 0$, with a Lipschtiz continuous vector field $\boldsymbol{\theta}$ defined on Ω_ℓ one associates the following volume integral $\mathsf{G}_{\boldsymbol{\theta}}$:

$$\mathsf{G}_{\boldsymbol{\theta}} = \int_{\Omega_\ell} \left(\sum_{i,j=1}^{2} \mu \frac{\partial \theta_i}{\partial x_j} \frac{\partial u_\ell}{\partial x_i} \frac{\partial u_\ell}{\partial x_j} - \frac{\mu}{2} \nabla u_\ell \cdot \nabla u_\ell \, \mathrm{div}\boldsymbol{\theta} \right) dx.$$

One can prove that, if $\boldsymbol{\theta}$ is such that $\boldsymbol{\theta}(\ell, 0) = \mathbf{e}_1$ and $\boldsymbol{\theta} \cdot \mathbf{n} = 0$ on $\partial\Omega_\ell$, then $\mathsf{G}_{\boldsymbol{\theta}}$ is independent of $\boldsymbol{\theta}$ and equal to $\mathcal{G}_\ell$. Of course, this result of independency holds only when u_ℓ is the true displacement field. If it is numerically approximated, then $\mathsf{G}_{\boldsymbol{\theta}}$ becomes $\boldsymbol{\theta}$ dependent. In our case, owing to the simplicity of the geometry, we can use a very simple vector field $\boldsymbol{\theta}$ which renders the computations easier. Specifically, let $\boldsymbol{\theta}$ be given by

$$\boldsymbol{\theta}(\mathbf{x}) = \begin{cases} \mathbf{0} & \text{if } x_1 < 0 \\ \dfrac{x_1}{\ell} \mathbf{e}_1 & \text{if } 0 \le x_1 \le \ell \\ \dfrac{L - x_1}{L - \ell} \mathbf{e}_1 & \text{if } \ell \le x_1 < L \end{cases}, \tag{2.10}$$

then it satisfies the required conditions and hence $\mathsf{G}_{\boldsymbol{\theta}} = \mathcal{G}_\ell$. Accordingly, owing to the symmetry, one gets

$$\mathcal{G}_\ell = \frac{\mu}{L-\ell} \int_\ell^L \int_0^H \left(\left(\frac{\partial u_\ell}{\partial x_2} \right)^2 - \left(\frac{\partial u_\ell}{\partial x_1} \right)^2 \right) dx_2 dx_1 - \frac{\mu}{\ell} \int_0^\ell \int_0^H \left(\left(\frac{\partial u_\ell}{\partial x_2} \right)^2 - \left(\frac{\partial u_\ell}{\partial x_1} \right)^2 \right) dx_2 dx_1. \tag{2.11}$$

Comparing (2.11) with (2.9), (2.11) can be seen as an average of all the line integrals appearing in (2.9) when a and b vary respectively from 0 to ℓ and to ℓ and L. Accordingly, one can expect that (2.11) gives more accurate computations than (2.9) when ℓ is small.

2.2.3 Numerical results obtained for $\mathcal{G}_\ell$ by the FEM

All the computations based on the finite element method are made with the industrial code COMSOL. They are made after introducing dimensionless quantities. Specifically, in all the computations, the dimensions of the body are $H = 1$ and $L = 5$, the shear modulus $\mu = 1$ and $\mathsf{G_c} = 1$. That does not restrict the generality of the study because the scale dependences are known in advance. Indeed, if we denote with a tilde all quantities computed with the normalized coefficients, then the true physical quantities read as

$$\ell = H\tilde{\ell}, \quad u_\ell = H\tilde{u}_\ell, \quad \mathcal{P}_\ell = \mu H^2 \tilde{\mathcal{P}}_\ell, \quad \mathcal{G}_\ell = \mu H \tilde{\mathcal{G}}_\ell. \tag{2.12}$$

For a given $\tilde{\ell} \in (0, 5)$ and a given $\epsilon \in (0, 1)$, we use the symmetry of the body and of the load to mesh

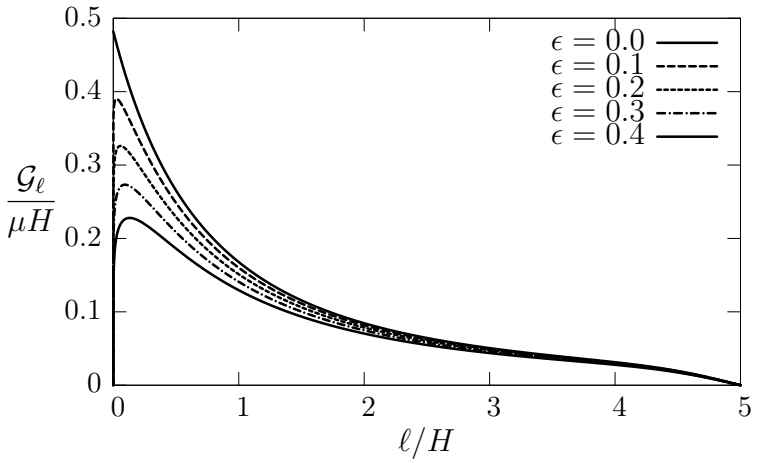

Figure 2.3: Computation by the Finite Element Method of the energy release rate $\mathcal{G}_\ell$ as a function of the crack length ℓ for five values of the notch angle.

only its upper half and prescribe $\tilde{u}_\ell = 0$ on the segment $\tilde{\ell} \leq \tilde{x}_1 \leq 5, \tilde{x}_2 = 0$. We use 6-nodes triangular elements, *i.e.* quadratic Lagrange interpolations. The mesh is refined near the singular corners and a typical mesh contains 25000 elements and 50000 degrees of freedom. We compute the discretized solution (still denoted) $\tilde{u}_\ell$ by solving the linear system. Then, the energy $\tilde{\mathcal{P}}_\ell$ and the energy release rate $\tilde{\mathcal{G}}_\ell$ are obtained by a post-treatment. The energy is obtained by a direct integration of the elastic energy density over the body. The derivative of the energy is obtained by using the formula (2.11), which needs to integrate the different parts of the elastic energy density over the two rectangles $(0, \tilde{\ell}) \times (0, 1)$ and $(\tilde{\ell}, 5) \times (0, 1)$. For a given ϵ, we compute $\tilde{\mathcal{P}}_\ell$ and $\tilde{\mathcal{G}}_\ell$ for $\tilde{\ell}$ varying from 0.001 to 5, first by steps of 0.001 in the interval $(0, 0.05)$, then by steps of 0.002 in the interval $(0.05, 0.2)$, finally by steps of 0.01 in the interval $(0.2, 5)$. The computations can be considered as sufficiently accurate for $\tilde{\ell} \geq 0.002$ even

if this lower bound depends on ϵ, the computations being less accurate for small (but non-zero) values of ϵ. Below this value, if we try to refine the mesh near the corner of the notch, the results become mesh-sensitive, the linear system becomes bad-conditioned. Since only the part of the graph of $\tilde{\mathcal{G}}_\ell$ close to $\tilde{\ell} = 0$ is interesting when ϵ is small, we cannot obtain accurate results when ϵ is too small.(Of course, this remark does not apply when $\epsilon = 0$, because $\tilde{\ell} = 0$ is no more a "singular" case.)

The cases $\tilde{\ell} = 0$ and $\tilde{\ell} = 5$ with $\epsilon \neq 0$ are treated with specific meshes. We have only to compute $\tilde{u}_0$, $\tilde{\mathcal{P}}_0$, $\tilde{u}_L$ and $\tilde{\mathcal{P}}_L$ because one knows that $\tilde{\mathcal{G}}_0 = \tilde{\mathcal{G}}_L = 0$.

The case $\epsilon = 0$ is treated separately by adapting the previous methods. In particular, for calculating $\tilde{\mathcal{G}}_\ell$, the second integral in (2.11) is replaced by an integral over the rectangle $(-1, 0) \times (0, 1)$ and this integral is divided by $1 + \tilde{\ell}$ and no more by $\tilde{\ell}$. Moreover, the mesh is refined only near the tip of the crack, $\tilde{\ell} = 0$ is no more a particular case and the computations of $\tilde{\mathcal{G}}_\ell$ are accurate in the full range of $\tilde{\ell}$.

Let us highlight the main features of the numerical results plotted in Figure 2.3. These properties will be the basic assumptions from which we will study the crack propagation in the end of the present section.

P1 For $\epsilon = 0$, $\mathcal{G}_\ell/\mu H$ is monotonically decreasing from 0.4820 to 0 when ℓ/H grows from 0 to 5.

P2 For $\epsilon > 0$, $\mathcal{G}_\ell/\mu H$ starts from 0 at $\ell/H = 0$, then is rapidly increasing. This growth is so important (for instance, $\mathcal{G}_\ell/\mu H = 0.1443$ when $\ell/H = 0.002$ for $\epsilon = 0.4$) that it cannot be correctly captured by the FEM.

P3 Still for $\epsilon > 0$, $\mathcal{G}_\ell$ is monotonically increasing as long as $\ell \leq \ell_{\mathsf{m}}$. At $\ell = \ell_{\mathsf{m}}$, $\mathcal{G}$ takes its maximal value G_{m}. Those values which depend on ϵ are given in the table below. It turns out that ℓ_{m}/H is rather small.

ϵ	0	0.1	0.2	0.3	0.4
ℓ_{m}/H	0	0.024	0.058	0.092	0.130
$\mathsf{G}_{\mathsf{m}}/\mu H$	0.4820	0.3900	0.3260	0.2733	0.2279

P4 For $\epsilon > 0$ again, $\mathcal{G}_\ell$ is monotonically decreasing from G_{m} to 0 when ℓ grows from ℓ_{m} to $5H$.

2.2.4 Application of the MAM to the non cohesive case

We are in the case where $g = 0$ on Γ_ℓ. Therefore, by virtue of Proposition 1.3, all the coefficients a_0^i vanish and there is no logarithmic singularities.

Here the asymptotic variable is chosen to be $\tilde{\ell} = \ell/H$ instead of ℓ in order that all the terms of the expansions have the dimension of a displacement. We applied the Matched asymptotic expansion up

to a required order for the solution in order to capture the rapid increase starting from 0 at $\ell/H = 0$. The solution can be approximated in a similar series as follows:

$$\textbf{Outer expansion} \quad u_\ell(\mathbf{x}) = u^0(\mathbf{x}) + \tilde{\ell}^\lambda u^1(\mathbf{x}) + \tilde{\ell}^{2\lambda} u^2(\mathbf{x}) + \tilde{\ell}^{3\lambda} u^3(\mathbf{x}) + \dots$$
$$\textbf{Inner expansion} \quad u_\ell(\mathbf{x}) = v^0(\mathbf{y}) + \tilde{\ell}^\lambda v^1(\mathbf{y}) + \tilde{\ell}^{2\lambda} v^2(\mathbf{y}) + \tilde{\ell}^{3\lambda} v^3(\mathbf{y}) + \dots$$

with

$$\lambda = \frac{\pi}{\omega} \qquad \text{and} \qquad \omega = 2\pi - 2\arctan(\epsilon). \tag{2.13}$$

Let us briefly recall the procedure to obtain the different terms of both expansions in the present case, see chapter 1 for the details in a general setting.

The outer terms $u^i(\mathbf{x})$ are defined in the domain Ω_0 and the inner terms $v^i(\mathbf{y})$ are defined in the infinite domain

$$\Omega^\infty = \{(r,\theta) : 0 < r < \infty, 0 < \theta < \omega\} \setminus \Gamma_1$$

with $\Gamma_1 = [0,1] \times \{0\}$ since the defect is a crack. The first term $u^0(\mathbf{x})$ which belongs to $H^1(\Omega_0)$ can be approximated accurately by numeric methods such as FEM. The problem for u^0 reads as:

$$\begin{cases} \Delta u^0 = 0 & \text{in} \quad \Omega_0 \\ u^0 = \pm 1 & \text{on} \quad D^\pm \\ u^0 = 0 & \text{on} \quad D_L \\ \dfrac{\partial u^0}{\partial n} = 0 & \text{on } \partial\Omega_0 \setminus \left(D^+ \cup D^- \cup D_L\right) \end{cases} \tag{2.14}$$

Moreover, $v^0(\mathbf{y}) = 0$ as it is proved in Chapter 1 when there is no force applied to the defect. In fact, it was proved that v^0 is the constant b_0^0. But $b_0^0 = u^0(0,0)$ by virtue of (1.37) and since $u^0(0,0) = 0$ by symmetry, one gets $v^0 = 0$.

The higher order terms, *i.e.* with $i \geq 1$, are decomposed into singular and regular parts:

$$u^i(\mathbf{x}) = \sum_{n=1}^{i} a_n^i r^{-n\lambda} \cos(n\lambda\theta) + \bar{u}^i(\mathbf{x}), \quad \text{with} \quad \bar{u}^i \in H^1(\Omega_0) \tag{2.15}$$

$$v^i(\mathbf{y}) = \sum_{n=0}^{i} b_n^i \rho^{n\lambda} \cos(n\lambda\theta) + \bar{v}^i(\mathbf{y}), \quad \text{with} \quad \nabla\bar{v}^i \in L^2(\Omega^\infty) \text{ and } \lim_{|\mathbf{y}|\to\infty} \bar{v}^i(\mathbf{y}) = 0 \tag{2.16}$$

We have seen that the regular part $\bar{u}^i$ is determined once the singular part u_S^i is known or equivalently

once the coefficients $\{a_n^i\}_{1\le n\le i}$ are known. Specifically, the governed equation for $\bar{u}^i(\mathbf{x})$ can read as:

$$\begin{cases} \Delta \bar{u}^i = 0 & \text{in} \quad \Omega_0 \\ \bar{u}^i = \pm \displaystyle\sum_{n=1}^{i} a_n^i r^{-n\lambda} \cos(n\lambda\theta) & \text{on} \quad D^{\pm} \cup D_L \\ \dfrac{\partial \bar{u}^i}{\partial n} = -\dfrac{\partial}{\partial \nu} \displaystyle\sum_{n=1}^{i} a_n^i r^{-n\lambda} \cos(n\lambda\theta) & \text{on} \quad N^{\pm} \\ \dfrac{\partial \bar{u}^i}{\partial n} = 0 & \text{on} \quad \Gamma^{\pm} \end{cases} \tag{2.17}$$

Similarly, once the coefficients $\{b_n^i\}_{0\le n\le i}$ are known, the regular part $\bar{v}^i(\mathbf{y})$ is given by:

$$\begin{cases} \Delta \bar{v}^i = 0 & \text{in} \quad \Omega^{\infty} \\ \dfrac{\partial \bar{v}^i}{\partial n} = -\dfrac{\partial}{\partial \nu} \displaystyle\sum_{n=1}^{i} b_n^i \rho^{n\lambda} \cos(n\lambda\theta) & \text{on} \quad \Gamma_1 \\ \dfrac{\partial \bar{v}^i}{\partial n} = 0 & \text{on} \quad \Gamma^{\pm} \\ \lim\limits_{\rho\to\infty} \bar{v}^i = 0 & \text{at infinity} \end{cases} \tag{2.18}$$

In turn the coefficients a_n^i and b_n^i are defined from the outer fields u^j and the inner fields v^j by path integrals (independent of the path), see Proposition 1.4. Specifically, for $n \ge 1$, the coefficients a_n^{i+n} are given by

$$a_n^{i+n} = \frac{2\rho^{n\lambda}}{\omega} \int_0^{\omega} \bar{v}^i(\rho,\theta) \cos(n\lambda\theta) d\theta \tag{2.19}$$

where the radius ρ must be greater than 1 so that the path does not cross the crack Γ_1. Symmetrically, for $n \ge 0$, the coefficients b_n^{i+n} are given by

$$b_0^i = \frac{1}{\omega} \int_0^{\omega} \bar{u}^i(r,\theta) d\theta, \qquad b_n^{i+n} = \frac{2r^{-n\lambda}}{\omega} \int_0^{\omega} \bar{u}^i(r,\theta) \cos(n\lambda\theta) d\theta \quad \text{for} \quad n \ge 1 \tag{2.20}$$

where the radius r must be small enough so that the path does not reach the upper and lower sides $N^{\pm}$ of Ω_0.

Remark 2.4. *Theoretically, the integrals* (2.19)-(2.20) *are path independent and hence do not depend of ρ and r respectively provided that these radii satisfy the conditions above. However, this path independency holds true only for the exact fields $\bar{v}^i$ and $\bar{u}^i$. Since those fields are only approximate by the FEM, the integrals are in fact path dependent. So that, the value of the coefficients a_n^{i+n} and b_n^{i+n} depends on chosen path $\mathcal{C}_\rho$ or $\mathcal{C}_r$ in practice. It turns out that in all our computations the differences in the results with respect to the paths are small and can be neglected.*

By symmetry of the geometry and the loading, the real field u_ℓ is an odd function of x_2, *i.e.*

$$u_\ell(x_1, -x_2) = -u_\ell(x_1, x_2), \qquad u_\ell(r, \omega - \theta) = -u_\ell(r, \theta).$$

Therefore, all the fields u^i, $\bar{u}^i$, v^i, $\bar{v}^i$ admit the same symmetry. One deduces from Proposition 1.4 the following

Proposition 2.1. *All the coefficients b_{2n}^{i+2n} and a_{2n}^{i+2n} vanish.*

Proof. Let us remark that b_{2n}^{i+2n} and a_{2n}^{i+2n} are defined in (1.36) and (1.37) by integral with respect to θ over $[0, \omega]$. To see the properties of symmetry in these integrals, one must make the change of variable $\theta \mapsto \alpha = \theta - \omega/2$. In such a case $\cos(2n\lambda\theta)$ becomes an even function of α. Accordingly, $\bar{u}^i(., \theta) \cos 2n\lambda\theta$ is an odd function of α and that implies the vanishing of the coefficients b_{2n}^{i+2n}. The same arguments can be used for $\bar{v}^i \cos 2n\lambda\theta$ to obtain that a_{2n}^{i+2n} vanishes. □

Consequently, all the odd terms of the outer expansion and all the even terms of the inner expansions vanish, *i.e.* $u^{2i+1} = 0$ and $v^{2i} = 0$ for all $i \in \mathbb{N}$. Indeed, that property can be shown by the following inductive process:

P0 (For $i = 0$), one can see that $v^0 = 0$ and $u^1 = 0$ because $b_0^0 = 0$ and $a_1^1 = 0$. The second reason is deduced from $v^0 = 0$. Hence $a_n^n = 0, \ \forall n \in \mathbb{N}_*$.

Pj Supposing that $u^{2i+1} = 0$ and $v^{2i} = 0$ is true for $i = j \geq 0$.

Pj+1 This step is to check that the conclusion is still valid for $i = j + 1$. $u^{2(j+1)+1}$ is investigated firstly. One has $u_n^{2(j+1)+1} \equiv 0$ if and only if $a_n^{2j+3} \equiv 0$, for $n = \overline{1 : 2j + 3}$. Moreover, one can write $a_n^{2j+3} = a_n^{n+(2j+3-n)}$. When n is an even number, it is trivial to get $a_n^{n+(2j+3-n)} = 0$. And when n is an odd number, one can get $2j + 3 - n$ is an even number. Consequently, $a_n^{n+(2j+3-n)} = 0$ because $v^{2i} = 0$ in the previous step Pj. Similarly, in order to show $v^{2(j+1)} \equiv 0$, b_n^{2j+2} must be proved to equal 0 for $n = \overline{0 : 2j + 2}$. When n is an even number, b_n^{2j+2} will equal 0 because of $b_{2n}^{i+2n} = 0, \ \forall n \in \mathbb{N}$. When n is an odd number, one also concludes that $b_n^{2j+2} = 0$ because $b_n^{2j+2} = b_n^{n+(2j+2-n)} = 0$ which is deduced from $u_n^{2i+1} = 0$ in the step Pj too.

In the same way, the inductive process can be followed to prove that $u^{2i+1} = 0$ and $v^{2i} = 0$ which holds for all $i \in \mathbb{N}$.

Finally, the solution admits the following expansions:

$$\textbf{Outer expansion} \quad : \quad u_\ell(\mathbf{x}) = \sum_{i\in\mathbb{N}} \tilde{\ell}^{2i\lambda} u^{2i}(\mathbf{x}), \tag{2.21}$$

$$\textbf{Inner expansion} \quad : \quad u_\ell(\mathbf{x}) = \sum_{i\in\mathbb{N}} \tilde{\ell}^{(2i+1)\lambda} v^{2i+1}(\mathbf{y}) \tag{2.22}$$

and all the following coefficients vanish by symmetry:

$$a_n^i = 0 \quad \text{when } n \text{ or } i-n \text{ are even}, \qquad b_n^i = 0 \quad \text{when } n \text{ is even or } i-n \text{ is odd}. \tag{2.23}$$

The process of calculation for u^{2i} and v^{2i+1}

This process follows the process of interaction between outer expansions and inner expansions which means the couple of u^i, v^i is defined one after one and step by step. In addition, one can apply the second method proposed in Section 1.3 which allows to define the outer expansions and inner expansions independently in the meaning of the independent family of problems constructs u^i and v^i.

S0 At this step, the first regular term u^0 according to (2.14) is found. Accordingly, the value of b_n^n is defined according to Proposition 1.4.

$$b_n^n = \frac{2r^{-n\lambda}}{\omega} \int_0^\omega u^0(r,\theta)\cos(n\lambda\theta)d\theta \tag{2.24}$$

In practice, the integral is taken on a path $\mathcal{C}_r$ with a chosen $r = 0.2$.

S2i The regular part of u^{2i} obeys (2.17) where $a_n^{(2i-n)+n}$ (for an odd n) is given from the previous step by calculating terms by terms. Deducing from u^{2i}, the coefficients b_n^{2i+n} (for $n = 2m+1$) are determined, such as:

$$b_{2m+1}^{2i+(2m+1)} = \frac{2r^{-(2m+1)\lambda}}{\omega} \int_0^\omega \bar{u}^{2i}(r,\theta)\cos\big((2m+1)\lambda\theta\big)d\theta \tag{2.25}$$

S2i+1 The term v^{2i+1} is defined once $b_n^{(2i+1-n)+n}$ (with n is odd) are given for $\overline{n = 0 : 2i+1}$. Obviously, $b_n^{(2i+1-n)+n}$ (with n is odd) are determined from u^0 to $\bar{u}^{2i}$. As a result, the undetermined coefficients relating to v^{2i+1}, such as a_n^{2i+1+n} with $n = 2m+1 (m \in \mathbb{N})$, will be specified then,

$$a_{2m+1}^{2i+1+(2m+1)} = \frac{2\rho^{(2m+1)\lambda}}{\omega} \int_0^\omega \bar{v}^{2i+1}(\rho,\theta)\cos\big((2m+1)\lambda\theta\big)d\theta \tag{2.26}$$

Using the FEM in Comsol, the infinite domain Ω^∞ has its radius equals 20 and the contour C_ρ in above integral has $\rho = 2$.

The results for these coefficients are given in the table 2.1 and 2.2.

2.2.5 Evaluation of the energy release rate by the MAM

By virtue of (2.7), one can expand $\mathcal{P}_\ell$ by using the outer expansion of u_ℓ. Using (2.21), one gets

$$\mathcal{P}_\ell = \sum_{i\in\mathbb{N}} P_{2i} \left(\frac{\ell}{H}\right)^{2i\lambda} \mu H^2, \tag{2.27}$$

where the coefficients P_{2i} of the expansions are dimensionless. The expansion of the energy release rate can be immediately deduce from that of the energy:

$$\mathcal{G}_\ell = -\sum_{i\in\mathbb{N}_*} 2i\lambda P_{2i} \left(\frac{\ell}{H}\right)^{2i\lambda-1} \mu H \tag{2.28}$$

and it is not necessary to use the path integrals $\mathcal{J}_\mathcal{C}$ or the $G-\theta$ method. Let us remark that

$$\mathcal{G}_0 = \begin{cases} 0 & \text{if } \epsilon \neq 0 \\ -P_2\mu H = K_0^2/2 > 0 & \text{if } \epsilon = 0 \end{cases} \tag{2.29}$$

because $\lambda < 1/2$ in the former case while $\lambda = 1/2$ in the latter.

To obtain the i^{th} term of the expansion of $\mathcal{P}_\ell$ and $\mathcal{G}_\ell$, one must determine both the singular part u_S^i and the regular part $\bar{u}^i$ of u^i. The singular part involves the coefficients a_n^i for $1 \leq n \leq i$ which are obtained as the regular parts of the v^j's for $j \leq i$, see Section 1.2.3. Therefore, one must also solve the inner problems and hence determine the coefficients b_n^i for $0 \leq n \leq i$. In practise, these coefficients are obtained by using Proposition 1.4 after the inner and the outer problems have been solved with a finite element method. The advantage is that those problems do not contain a small defect and the accuracy is guaranteed. The drawback is that one has to solve more and more problems to obtain accurate values of $\mathcal{G}_\ell$ when ℓ/H is not small.

ϵ	a_1^2	P_2	a_1^4	a_3^4	P_4	a_1^6	a_3^6	a_5^6	P_6
0	-0.3930	-0.4820	0.1888	0.0987	0.3282	-0.1365	-0.0537	-0.0494	-0.2013
0.1	-0.3756	-0.4413	0.1766	0.0943	0.3001	-0.1279	-0.0507	-0.0472	-0.1931
0.2	-0.3559	-0.3957	0.1619	0.0893	0.2673	-0.1165	-0.0470	-0.0446	-0.1787
0.3	-0.3342	-0.3486	0.1453	0.0838	0.2320	-0.1029	-0.0427	-0.0418	-0.1603
0.4	-0.3106	-0.3005	0.1273	0.0778	0.1952	-0.0880	-0.0380	-0.0389	-0.1385

Table 2.1: The computed values of the (non zero) coefficients a_n^i for $1 \leq n \leq i \leq 6$ and of the leading terms P_2, P_4 and P_6 of the expansion of the potential energy for several values of the angle of the notch

ϵ	b_1^1	b_1^3	b_3^3	b_1^5	b_3^5	b_5^5
0	-0.7834	0.2384	-0.2059	-0.1943	0.1058	-0.0172
0.1	-0.7482	0.2091	-0.2085	-0.1730	0.0992	-0.0283
0.2	-0.7089	0.1777	-0.2081	-0.1489	0.0905	-0.0379
0.3	-0.6657	0.1451	-0.2045	-0.1232	0.0800	-0.0454
0.4	-0.6187	0.1125	-0.1977	-0.0974	0.0683	-0.0508

Table 2.2: The computed values of the (non-zero) coefficients b_n^i for $1 \leq n \leq i \leq 5$ for several values of the angle of the notch

The tables 2.1 and 2.2 give the computed values of the first coefficients of the inner and outer expansions (still with $H = 1$, $L = 5$, $\mu = 1$). These tables contain all the terms which are necessary to compute the expansions of the energy up to the sixth order, *i.e.* P_{2i} for $i \in \{0, 1, 2, 3\}$. (Note that P_0 does not appear in the expansion of $\mathcal{G}_\ell$.) The graphs of $\ell \mapsto \mathcal{G}_\ell$ obtained from these expansions are plotted on Figure 2.4 in the cases $\epsilon = 0.2$ and $\epsilon = 0.4$. They are compared with the values obtained directly by the finite element code Comsol. One can bring out from these comparisons the following conclusions:

C1 For very small values of ℓ, the first non trivial term (corresponding to $i = 1$ in (2.28)) of the Matched Asymptotic Expansion (denoted by **MAM** 2 on Figure 2.4) is sufficient to well approximate $\mathcal{G}_\ell$ while the FEM is unable to deliver accurate values.

C2 For values of ℓ of the order of ℓ_{m}, at least the first two non trivial terms (corresponding to $i = 1$ and 2 in (2.28)) of the MAM (denoted by **MAM** 4 on Figure 2.4), are necessary to capture the change of monotonicity of $\mathcal{G}_\ell$. Indeed, the first term being monotonically increasing is unable, alone, to capture that change of behavior.

C3 Still for values of ℓ of the order of ℓ_{m}, the first two terms are really sufficient to well approximate $\mathcal{G}_\ell$ provided that ℓ_{m}/H is sufficiently small. Specifically, the first two terms are sufficient as long as $\ell/H < 0.2$.

C4 Accordingly, one can use the approximation of $\mathcal{G}_\ell$ by the first two non trivial terms of MAE in the range $[0, 2\ell_{\mathsf{m}}]$ of ℓ when $\epsilon \in (0, 0.4)$.

C5 As ℓ/H grows beyond 0.2, one must add more and more terms of the MAE to well approximate $\mathcal{G}_\ell$. Consequently, in the range of "large" values of ℓ/H, the direct FEM is accurate and hence is better to use.

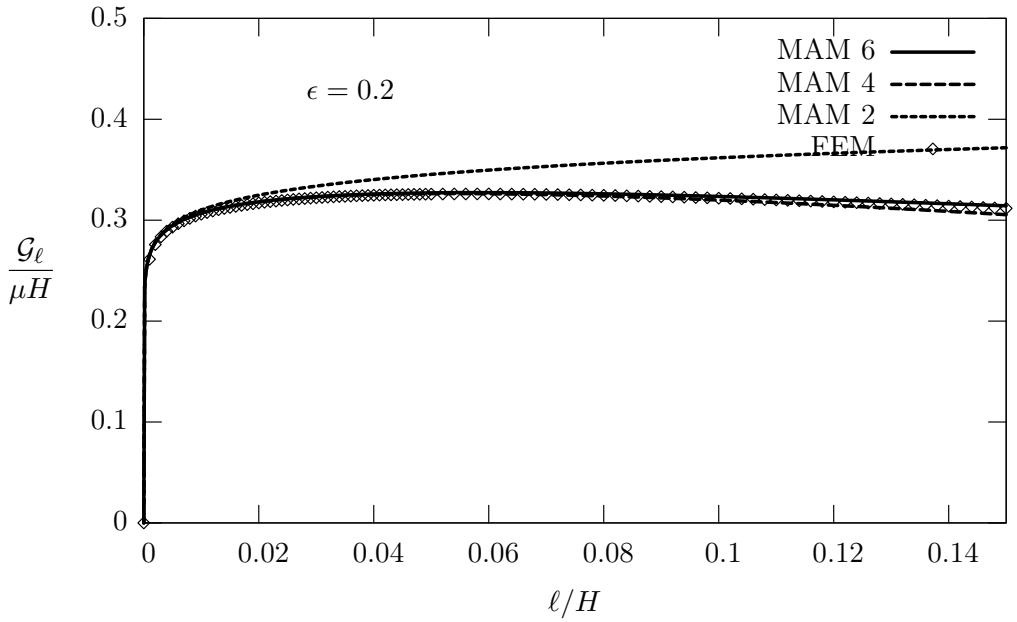
0.5
0.4
0.3
0.2
0.1
0
$\frac{\mathcal{G}_\ell}{\mu H}$
$\epsilon = 0.2$
MAM 6
MAM 4
MAM 2
FEM
0
0.02
0.04
0.06
0.08
0.1
0.12
0.14
ℓ/H

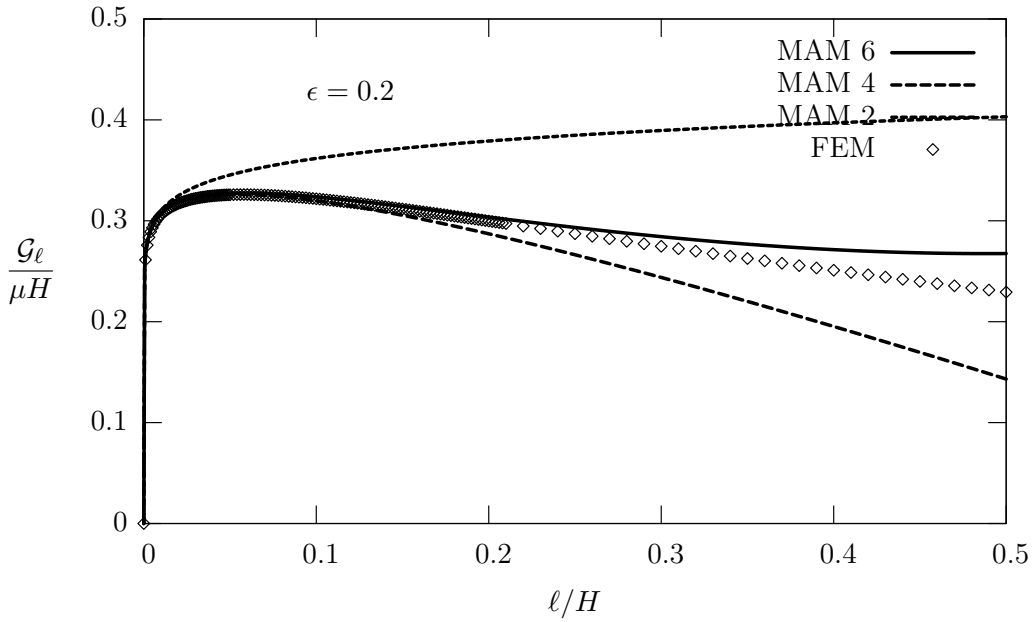
0.5
0.4
0.3
0.2
0.1
0
$\frac{\mathcal{G}_\ell}{\mu H}$
$\epsilon = 0.2$
MAM 6
MAM 4
MAM 2
FEM
0
0.1
0.2
0.3
0.4
0.5
ℓ/H

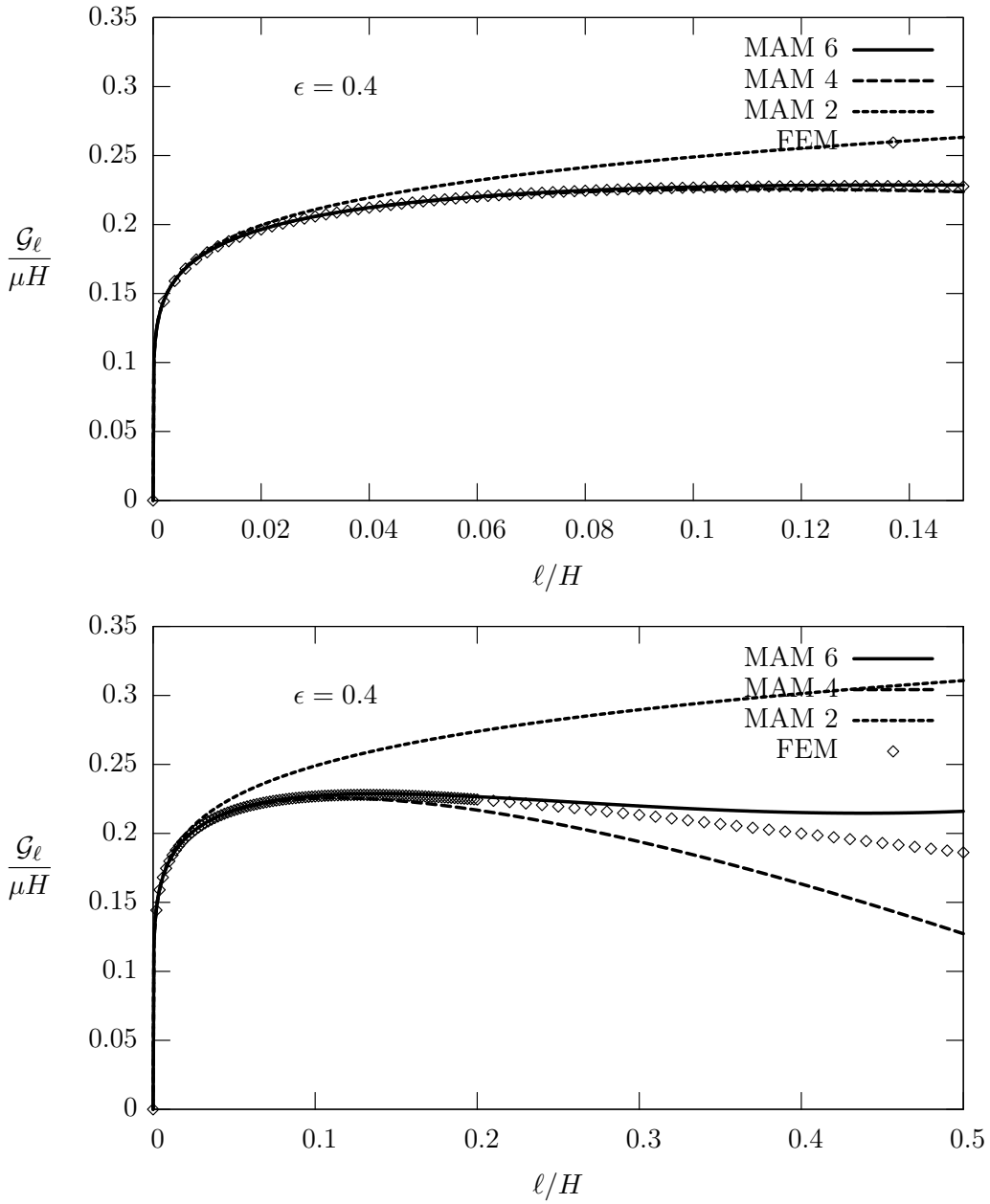

Figure 2.4: Comparisons of the graph of $\mathcal{G}_\ell$ obtained by the Matched Asymptotic Method or by the finite element code COMSOL in the cases $\epsilon = 0.2$ (page 64) and $\epsilon = 0.4$ (this page). The diamonds correspond to the points obtained by FEM while the curves MAM $2i$, $i \in \{1, 2, 3\}$, correspond to the values obtained by considering the first i non trivial terms in the expansion of $\mathcal{G}_\ell$.

2.3 Application to the nucleation of a non cohesive crack

The theoretical and numerical results obtained in the previous sections are used here to study the delicate issue of the nucleation of a crack in a sound body or the most classical question of the onset of a preexisting crack. Specifically, we consider the notched body Ω_0 which either contains a preexisting crack $\ell_0 > 0$ or is sound, *i.e.* $\ell_0 = 0$. We have also to distinguish different cases according to whether $\epsilon = 0$ or $\epsilon > 0$. The nucleation or the onset of cracking is governed by either the so-called *G-law* or the so-called *FM-law* and one goal of this section is to compare those laws. The interested reader can also refer to [Bourdin et al., 2008; Francfort and Marigo, 1998; Negri, 2008; Negri and Ortner, 2008; Marigo, 2010] where other comparisons between *G-law* and *FM-law* are proposed.

The notched body is submitted to a time-dependent loading process which consists in a monotonically increasing amplitude of the displacement prescribed on the sides $D^{\pm}$. Specifically, one considers the following boundary conditions

$$u = \pm tH \quad \text{on} \quad D^{\pm}, \qquad t \geq 0, \tag{2.30}$$

the other remaining unchanged. (Note that the "time" parameter t is dimensionless.) The evolution problem consists in finding the time evolution of the length of the crack, *i.e.* $t \mapsto \ell(t)$ for $t \geq 0$, under the initial condition $\ell(0) = \ell_0 \in [0, L)$. For that, we first remark that, for a given time $t \geq 0$ and a given crack length $\ell \in [0, L]$, the displacement field which equilibrates the body reads as

$$u(t, \ell) = t u_\ell, \tag{2.31}$$

where u_ℓ is the displacement field introduced in Section 2.2.1. Accordingly, the potential energy and the energy release rate at time t with a crack length ℓ can read as

$$\mathcal{P}(t, \ell) = t^2 \mathcal{P}_\ell, \qquad \mathcal{G}(t, \ell) = t^2 \mathcal{G}_\ell, \tag{2.32}$$

where $\mathcal{P}_\ell$ and $\mathcal{G}_\ell$ are given by (2.6) and (2.8).

The two evolutions law are based on the crucial Griffith's assumption [Griffith, 1920] concerning the surface energy associated with a crack. Specifically, one assumes that there exists a material constant $\mathsf{G_c} > 0$ such that the surface energy of the body with a crack of length ℓ reads as

$$\mathcal{S}(\ell) = \mathsf{G_c} \ell. \tag{2.33}$$

Accordingly, the total energy of the body at equilibrium at time t with a crack of length ℓ reads as

$$\mathcal{E}(t, \ell) := \mathcal{P}(t, \ell) + \mathcal{S}(\ell) = t^2 \mathcal{P}_\ell + \mathsf{G_c} \ell. \tag{2.34}$$

2.3.1 The two evolution laws

Let us briefly introduce the two evolution laws, the reader interested by the details should refer to [Marigo, 2010]. The first one, called the *G-law*, is the usual Griffith law based on the critical potential energy release rate criterion, see [Bui, 1978; Leblond, 2000; Nguyen, 2000]. In essence, this law only investigates smooth (*i.e.* at least continuous) evolutions of the crack length with the loading. It consists in the three following items:

Definition 2.1 (*G-law*)**.** *Let $\ell_0 \in [0, L]$. A continuous function $t \mapsto \ell(t)$ is said satisfying (or solution of) the* G-law *in the interval $[t_0, t_1]$ with the initial condition $\ell(t_0) = \ell_0$, if the three following properties hold*

1. **Irreversibility:** *$t \mapsto \ell(t)$ is not decreasing;*
2. **Energy release rate criterion:** *$\mathcal{G}(t, \ell(t)) \leq \mathsf{G_c}, \quad \forall t \in [t_0, t_1]$;*
3. **Energy balance:** *$\ell(t)$ is increasing only if $\mathcal{G}(t, \ell(t)) = \mathsf{G_c}$, i.e. if $\mathcal{G}(t, \ell(t)) < \mathsf{G_c}$ at some t, then $\ell(t') = \ell(t)$ for every t' in a certain neighborhood $[t, t + h)$ of t.*

The third item implies that the release of potential energy is equal to the created surface energy when the crack propagates what justifies its name of energy balance. Consequently, if $t \mapsto \ell(t)$ is absolutely continuous, then the third item is equivalent to $\frac{\partial \mathcal{E}}{\partial \ell}(t, \ell(t))\dot{\ell}(t) = 0$ for almost all t and the following equality holds for almost all t:

$$\frac{d}{dt}\mathcal{E}(t, \ell(t)) = \frac{\partial \mathcal{E}}{\partial t}(t, \ell(t)). \tag{2.35}$$

A major drawback of the *G-law* is to be unable to take into account discontinuous crack evolutions, what renders it useless in many situations as we will see in the next subsection. It must be replaced by another law which admits discontinuous solutions. Another motivation of changing the *G-law* is to reinforce the second item by introducing a full stability criterion, see [Francfort and Marigo, 1998; Nguyen, 2000; Bourdin et al., 2008]. Specifically, let us consider the following local stability condition

$$\forall t \geq 0, \exists h(t) > 0 \quad : \quad \mathcal{E}(t, \ell(t)) \leq \mathcal{E}(t, l) \quad \forall l \in [\ell(t), \ell(t) + h(t)], \tag{2.36}$$

which requires that the total energy at t is a "unilateral" local minimum. (The qualifier unilateral is added because the irreversibility condition leads to compare the energy at t with only that corresponding to greater crack length, see [Bourdin et al., 2008]). Taking $l = \ell(t) + h$ with $h > 0$ in (2.36), dividing by h and passing to the limit when $h \to 0$, we recover the critical energy release rate criterion. Thus,

the second item can be seen as a first order stability condition, weaker than (2.36). A stronger requirement consists in replacing local minimality by global minimality. It was the condition introduced by [Francfort and Marigo, 1998] in the spirit of the original Griffith idea [Griffith, 1920] and that we will adopt here. Thus, the second evolution law, called *FM-law*, consists in the three following items

Definition 2.2 (*FM-law*)**.** *A function $t \mapsto \ell(t)$ (defined for $t \geq 0$ and with values in $[0, L]$) is said satisfying (or solution of) the* FM-law *if the three following properties hold*

1. **Irreversibility:** *$t \mapsto \ell(t)$ is not decreasing;*
2. **Global stability:** $\mathcal{E}(t, \ell(t)) \leq \mathcal{E}(t, l), \quad \forall t \geq 0$ *and* $\forall l \in [\ell(t), L]$*;*
3. **Energy balance:** $\mathcal{E}(t, \ell(t)) = \mathcal{E}(0, \ell_0) + \displaystyle\int_0^t \frac{\partial \mathcal{E}}{\partial t'}(t', \ell(t'))\ dt', \quad \forall t \geq 0.$

Let us note that the irreversibility condition is unchanged, while the energy balance condition is now written as the integrated form of (2.35), what does not require that $t \mapsto \ell(t)$ be continuous. Note also that the energy balance implies $\ell(0) = \ell_0$ because $0 = \mathcal{E}(0, \ell(0)) - \mathcal{E}(0, \ell_0) = \mathsf{G_c}(\ell(0) - \ell_0)$, and that the second item is automatically satisfied at $t = 0$ because $\mathcal{E}(0, l) = \mathsf{G_c} l$.

2.3.2 The main properties of the *G-law* and the *FM-law*

We recall or establish in this subsection some results for the two evolution laws under the assumptions of monotonicity of $\ell \mapsto \mathcal{G}_\ell$ resulting of the numerical computations, see **P1**–**P4** in Section 2.2.3. Some of those results have a general character and have been previously established in [Bourdin et al., 2008; Francfort and Marigo, 1998; Marigo, 2010] while the other ones are specific to the present problem. In the case of properties which have already been obtained, we simply recall them without proofs.

Let us first consider the case when the notch is in fact a crack. Then, the two laws are equivalent by virtue of

Proposition 2.2. *In the case $\epsilon = 0$, since $\ell \mapsto \mathcal{G}_\ell$ is decreasing from $\mathcal{G}_0 > 0$ to 0 when ℓ goes from 0 to L (see Property* **P1***), the* G-law *and the* FM-law *admit the same and unique solution. Specifically, the preexisting crack begins to propagate at time $\mathsf{t_i}$ such that $\mathsf{t_i}^2 \mathcal{G}_{\ell_0} = \mathsf{G_c}$. Then the crack propagates continuously and $\ell(t)$ is such that $t^2 \mathcal{G}_{\ell(t)} = \mathsf{G_c}$. Since $\mathcal{G}_L = 0$, the crack will not reach the end L in a finite time.*

Proof. See [Marigo, 2010, Proposition 18]. □

In the case of a guenuine notch, as far as the nucleation and the propagation of a crack with the *G-law* are concerned, we have

Proposition 2.3. *In the case $\epsilon > 0$, according to $\ell_0 = 0$ or $\ell_0 \in (0, \ell_\mathsf{m})$ or $\ell_0 \in [\ell_\mathsf{m}, L)$, the crack evolution predicted by the* G-law *is as follows*

1. *If $\ell_0 = 0$, since $\mathcal{G}_0 = 0$, the unique solution to* G-law *is $\ell(t) = 0$ for all t, i.e.* **there is no crack nucleation**;

2. *If $\ell_0 \in (0, \ell_\mathsf{m})$, then the preexisting crack begins to propagate at time $\mathsf{t_i}$ such that $\mathsf{t_i}^2\mathcal{G}_{\ell_0} = \mathsf{G_c}$ after what there is no more (continuous) solution to* G-law, **the propagation is necessarily discontinuous**;

3. *If $\ell_0 \in [\ell_\mathsf{m}, L)$, since $\ell \mapsto \mathcal{G}_\ell$ is monotonically decreasing in the interval (ℓ_m, L), the situation is the same as in Proposition 2.2. There exists a unique solution for the* G-law*: the crack begins to propagate at $\mathsf{t_i}$ (still given by $\mathsf{t_i}^2\mathcal{G}_{\ell_0} = \mathsf{G_c}$) and then propagates continuously until L which is reached asymptotically.*

Proof. Let us give the sketch of the proof for the first two items.

1. Since $\ell_0 = 0$ and $\mathcal{G}_0 = 0$, then for all $t \geq 0$ one gets $0 = \mathcal{G}(t, 0) < \mathsf{G_c}$ and hence $\ell(t) = 0$ is a solution. The uniqueness follows from the initial condition and the energy balance.

2. Since $0 < \ell_0 < \ell_\mathsf{m}$, then $\mathcal{G}_{\ell_0} > 0$ and hence $t^2\mathcal{G}_{\ell_0} = \mathcal{G}(t, \ell_0) \leq \mathsf{G_c}$ if and only if $t \in [0, \mathsf{t_i}]$. Since the inequality is strict when $t \in [0, \mathsf{t_i})$, then $\ell(t) = 0$ is the unique solution in this interval because of the initial condition and the energy balance. By continuity, it is also the unique solution in the closed interval $[0, \mathsf{t_i}]$. On the other hand, since $\mathcal{G}(t, \ell_0) > \mathsf{G_c}$ when $t > \mathsf{t_i}$, the crack must begin to propagate at $\mathsf{t_i}$.

   Let us show that no (continuous) evolution can satisfy the *G-law* for $t > \mathsf{t_i}$. Indeed, by construction $\mathcal{G}(\mathsf{t_i}, \ell(\mathsf{t_i})) = \mathsf{t_i}^2\mathcal{G}_{\ell_0} = \mathsf{G_c}$. But since $\ell(t) \geq \ell_\mathsf{i}$ for $t > \mathsf{t_i}$ and since $\ell \mapsto \mathcal{G}_\ell$ is monotonically increasing in the neighborhood of $\ell_0 < \ell_\mathsf{m}$, one gets for $t \in (\mathsf{t_i}, \mathsf{t_i} + h)$ and a sufficiently small $h > 0$:

$$\ell_0 < \ell(t) < \ell_\mathsf{m}, \qquad \mathcal{G}(t, \ell(t)) > \mathcal{G}(\mathsf{t_i}, \ell_0) = \mathsf{G_c}.$$

   Therefore the energy release rate criterion cannot be satisfied by a continuous evolution in a neighborhood of $\mathsf{t_i}$. The unique possibility is that the length of the crack jumps from ℓ_0 to some $\ell_\mathsf{i} > \ell_\mathsf{m}$ at time $\mathsf{t_i}$. But that requires to reformulate the *G-law*.

The proof of the third item is the same as in the previous Proposition and hence one can refer to [Marigo, 2010, Proposition18]. □

Let us now consider the *FM-law*. It is proved in [Marigo, 2010, Proposition 3] (see also [Francfort and Marigo, 1998, Proposition 4.14]) that, in the case of a monotonically increasing loading, the *FM-law* is equivalent to a minimization problem of the total energy at each time. Specifically, one gets

Lemma 2.1. *Let $\ell_0 \in [0, L)$ be the initial length of the crack. A function $t \mapsto \ell(t)$ satisfies the* FM-law *if and only if, at each t, $\ell(t)$ is a minimizer of $l \mapsto \mathcal{E}(t, l)$ over $[\ell_0, L]$. Therefore, the* FM-law *admits at least one solution and each solution grows from ℓ_0 to L.*

This property holds true for any $\epsilon \geq 0$. In the case $\epsilon > 0$ one deduces the following

Proposition 2.4. *In the case $\epsilon > 0$, according to $\ell_0 \in [0, \ell_{\mathsf{m}})$ or $\ell_0 \in [\ell_{\mathsf{m}}, L)$, the crack evolution predicted by the* FM-law *is as follows*

1. *If $\ell_0 \in [0, \ell_{\mathsf{m}})$, then the nucleation (if $\ell_0 = 0$) or the propagation of the preexisting crack (if $\ell_0 \neq 0$) starts at time $\mathsf{t_i} > 0$ and at this time the crack length* **jumps** *instantaneously from ℓ_0 to ℓ_{i}. The length ℓ_{i} is the unique length in (ℓ_{m}, L) such that*

$$\int_{\ell_0}^{\ell_{\mathsf{i}}} \mathcal{G}_\ell d\ell = (\ell_{\mathsf{i}} - \ell_0)\mathcal{G}_{\ell_{\mathsf{i}}} \quad \textit{or equivalently} \quad \mathcal{P}_{\ell_0} - \mathcal{P}_{\ell_{\mathsf{i}}} = (\ell_{\mathsf{i}} - \ell_0)\mathcal{G}_{\ell_{\mathsf{i}}} \tag{2.37}$$

   while the time $\mathsf{t_i}$ is given by

$$\mathsf{t_i}^2 \mathcal{G}_{\ell_{\mathsf{i}}} = \mathsf{G_c}. \tag{2.38}$$

   After this jump, the crack propagates continuously from ℓ_{i} to L, the evolution satisfying then the G-law, *i.e.*

$$t^2 \mathcal{G}_{\ell(t)} = \mathsf{G_c}, \quad \forall t > \mathsf{t_i}.$$

2. *If $\ell_0 \in [\ell_{\mathsf{m}}, L)$, since $\ell \mapsto \mathcal{G}_\ell$ is monotonically decreasing in the interval (ℓ_{m}, L), the situation is the same as in Proposition 2.2. There exists a unique solution for the* FM-law *which is the same as for the* G-law*: the crack begins to propagate at $\mathsf{t_i}$ such that $\mathsf{t_i}^2 \mathcal{G}_{\ell_0} = \mathsf{G_c}$ and then propagates continuously until L which is reached asymptotically.*

Remark 2.5. *Before the proof of this Proposition, let us comment and interpret the equation* (2.37) *giving the jump of the crack at $\mathsf{t_i}$.*

- *Let us first prove that ℓ_{i} is well defined by* (2.37)*. Let $\ell \mapsto g(\ell)$ be the function defined for $\ell \in (\ell_{\mathsf{m}}, L)$ by*

$$g(\ell) = \int_{\ell_0}^{\ell} \mathcal{G}_\delta \, dl - (\ell - \ell_0)\mathcal{G}_\ell.$$

Its derivative is given by $g'(\ell) = -(\ell - \ell_0)\mathcal{G}'_\ell$ *and hence is positive because* $\mathcal{G}_\ell$ *is decreasing in* (ℓ_{m}, L). *Since* $\mathcal{G}_\ell < \mathsf{G}_{\mathsf{m}} := \mathcal{G}_{\ell_{\mathsf{m}}}$, *one gets* $g(\ell_{\mathsf{m}}) < 0$ *whereas* $g(L) > 0$ *because* $\mathcal{G}_L = 0$. *Therefore, there exists a unique* $\ell \in (\ell_{\mathsf{m}}, L)$ *such that* $g(\ell) = 0$, *what is precisely the definition of* ℓ_{i}.

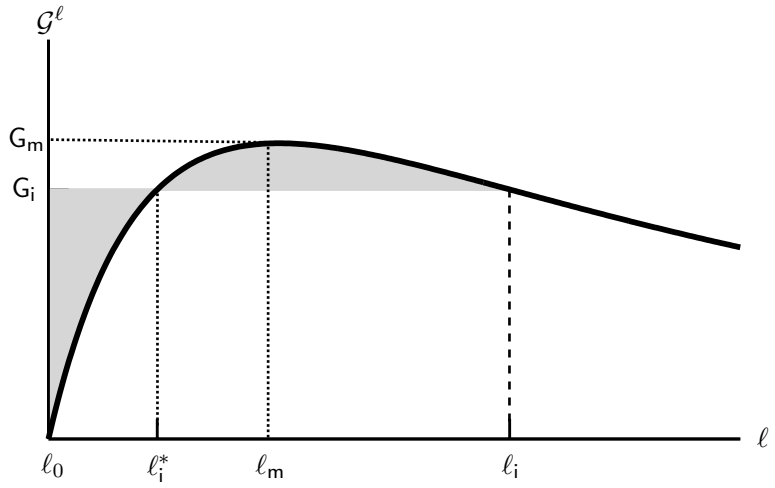

Figure 2.5: Graphical interpretation of the criterion of crack nucleation given by *FM-law* and which obeys to the Maxwell rule of equal areas.

- *The equation* (2.37) *giving* ℓ_{i} *has a graphical interpretation. Indeed, the integral over* $(\ell_0, \ell_{\mathsf{i}})$ *represents the area under the graph of* $\ell \mapsto \mathcal{G}_\ell$ *between the lengths* ℓ_0 *and* ℓ_{i}. *On the other hand the product* $(\ell_{\mathsf{i}} - \ell_0)\mathcal{G}_{\ell_{\mathsf{i}}}$ *represents the area of the rectangle whose height is* $\mathsf{G}_{\mathsf{i}} := \mathcal{G}_{\ell_{\mathsf{i}}}$. *Therefore, since these two areas are equal, the two gray areas of Figure 2.5 are also equal. This rule of equality of the areas determines* ℓ_{i} *and, by essence, the line* $\mathcal{G} = \mathsf{G}_{\mathsf{i}}$ *is the classical Maxwell line which appears in any problem of minimization of a non convex function.*

- *Note that* ℓ_{i} **is independent of the toughness** G_{c} **and of the shear modulus** μ **of the material**. *It is a characteristic of the structure and merely depends on the geometry and the type of loading. Here, it depends on* ϵ, H *and* L. *For a given* ϵ *and a given ratio* L/H, ℓ_{i} *is proportional to* H, $\ell_{\mathsf{i}} = \tilde{\ell}_{\mathsf{i}} H$. *This property is a consequence of the Griffith assumption on the surface energy.*

- **The critical loading amplitude** t_{i} **depends on the toughness and on the size of the body**. *Since* $\mathcal{G}_{\ell_{\mathsf{i}}} = \tilde{\mathcal{G}}_{\ell_{\mathsf{i}}} \mu H$, t_{i} *varies like* $1/\sqrt{H}$. *This size effect is also a consequence of the Griffith assumption on the surface energy.*

- *By virtue of* (2.37) *and* (2.38)*,* **the energy balance holds at time** t_i *even if the crack jumps at this time, i.e. the total energy of the body just before the jump is equal to the total energy just after. Indeed, those energies are respectively given by*

$$\mathcal{E}(\mathsf{t}_\mathsf{i}-,\ell_0) = {\mathsf{t}_\mathsf{i}}^2\mathcal{P}_{\ell_0} + \mathsf{G}_\mathsf{c}\ell_0, \qquad \mathcal{E}(\mathsf{t}_\mathsf{i}+,\ell_\mathsf{i}) = {\mathsf{t}_\mathsf{i}}^2\mathcal{P}_{\ell_\mathsf{i}} + \mathsf{G}_\mathsf{c}\ell_\mathsf{i}.$$

Using (2.37)*,* (2.38) *and the equality* $\mathcal{P}_{\ell_0} - \mathcal{P}_{\ell_\mathsf{i}} = \int_{\ell_0}^{\ell_\mathsf{i}} \mathcal{G}_\ell d\ell$*, one obtains* $\mathcal{E}(\mathsf{t}_\mathsf{i}-,\ell_0) = \mathcal{E}(\mathsf{t}_\mathsf{i}+,\ell_\mathsf{i})$*.*

Proof of Proposition 2.4. We just prove the first part of the Proposition and the reader should refer to [Marigo, 2010, Proposition 18] for the proof of the second part. Let $\ell_0 \in [0, \ell_\mathsf{m})$. By virtue of Lemma 2.1, $\ell(t)$ is a minimizer of $\ell \mapsto \mathcal{E}(t,\ell)$ over $[\ell_0, L]$. (The minimum exists because the energy is continuous and the interval is compact.) Let ℓ_i, t_i be given by (2.37)-(2.38), let $\mathsf{G}_\mathsf{i} = \mathcal{G}_{\ell_\mathsf{i}}$ and let ℓ_i^* be the other length such that $\mathcal{G}_{\ell_\mathsf{i}^*} = \mathsf{G}_\mathsf{i}$, see Figure 2.5. Let us first remark that the function $\ell \mapsto \bar{g}(\ell)$ defined on $[\ell_0, L]$ by

$$\bar{g}(\ell) := \mathsf{G}_\mathsf{i}(\ell - \ell_0) - \big(\mathcal{P}_{\ell_0} - \mathcal{P}_\ell\big)$$

is non negative and vanishes only at ℓ_0 and ℓ_i. Indeed, its derivative is $\bar{g}'(\ell) = \mathsf{G}_\mathsf{i} - \mathcal{G}_\ell$. Hence, $\bar{g}$ is first increasing from 0 when ℓ grows from ℓ_0 to ℓ_i^*, then decreasing to 0 when ℓ grows from ℓ_i^* to ℓ_i, and finally increasing again from 0 when ℓ grows from ℓ_i to L.

Let us show that ℓ_0 is the unique minimizer of the total energy when $t < \mathsf{t}_\mathsf{i}$. From (2.37) and (2.38), one gets for all $\ell \in [\ell_0, L]$ and all $t \le \mathsf{t}_\mathsf{i}$:

$$\mathcal{E}(t,\ell) - \mathcal{E}(t,\ell_0) = -t^2(\mathcal{P}_{\ell_0} - \mathcal{P}_\ell) + \mathsf{G}_\mathsf{c}(\ell - \ell_0) \ge t^2\bar{g}(\ell) \ge 0.$$

Moreover, the inequalities above are equalities if and only if $\ell = \ell_0$ when $t < \mathsf{t}_\mathsf{i}$ and the result follows. Using the same estimates, one deduces that ℓ_0 and ℓ_i are the two minimizers of the total energy at $t = \mathsf{t}_\mathsf{i}$.

Let us show now that the minimizer is in the open interval (ℓ_i, L) when $t > \mathsf{t}_\mathsf{i}$. From (2.37) and (2.38), one gets for all $\ell \in [\ell_0, \ell_\mathsf{i})$ and all $t > \mathsf{t}_\mathsf{i}$:

$$\mathcal{E}(t,\ell) - \mathcal{E}(t,\ell_\mathsf{i}) = t^2(\mathcal{P}_\ell - \mathcal{P}_{\ell_\mathsf{i}}) - \mathsf{G}_\mathsf{c}(\ell_\mathsf{i} - \ell) > {\mathsf{t}_\mathsf{i}}^2\big(\mathcal{P}_\ell - \mathcal{P}_{\ell_\mathsf{i}} - \mathsf{G}_\mathsf{i}(\ell_\mathsf{i} - \ell)\big) = {\mathsf{t}_\mathsf{i}}^2\big(\bar{g}(\ell) - \bar{g}(\ell_\mathsf{i})\big) = {\mathsf{t}_\mathsf{i}}^2\bar{g}(\ell) \ge 0.$$

Hence, the minimizer cannot be in $[\ell_0, \ell_\mathsf{i})$. Since the derivative of the total energy at $\ell = \ell_\mathsf{i}$ is equal to $\mathsf{G}_\mathsf{c} - t^2\mathsf{G}_\mathsf{i} < 0$, ℓ_i is not the minimizer. In the same manner, since the derivative of the total energy at $\ell = L$ is equal to $\mathsf{G}_\mathsf{c} - t^2\mathcal{G}_L = \mathsf{G}_\mathsf{c} > 0$, L cannot be the minimizer. Therefore, the minimizer is in the interval (ℓ_i, L) when $t > \mathsf{t}_\mathsf{i}$. Hence, it must be such that the derivative of the total energy vanishes.

Accordingly, one gets $t^2\mathcal{G}_{\ell(t)} = \mathsf{G_c}$. Since $\ell \mapsto \mathcal{G}_\ell$ is monotonically decreasing from $\mathsf{G_i}$ to 0 when ℓ goes from ℓ_i to L, there exists a unique $\ell(t) \in (\ell_\mathsf{i}, L)$ such that $\mathcal{G}_{\ell(t)} = \mathsf{G_c}/t^2 < \mathsf{G_i}$. The proof of the first part is complete. □

2.3.3 Computation of the crack nucleation by the MAM

Let us consider the cases where ϵ is sufficiently small in order that $\ell \mapsto \mathcal{G}_\ell$ be well approximated by the first two non trivial terms of its MAE for ℓ in the interval $[0, 2\ell_\mathsf{m}]$, see **C4**. Accordingly, one has

$$\frac{\mathcal{G}_\ell}{\mu H} \approx 2\lambda\,|P_2| \left(\frac{\ell}{H}\right)^{2\lambda-1} - 4\lambda\,|P_4| \left(\frac{\ell}{H}\right)^{4\lambda-1}. \tag{2.39}$$

where one uses the fact that $P_2 < 0$ and $P_4 > 0$. Therefore, the length ℓ_m where $\mathcal{G}_\ell$ is maximal and the maximum $\mathsf{G_m}$ are approximated by

$$\frac{\ell_\mathsf{m}}{H} \approx \left(\frac{(2\lambda-1)\,|P_2|}{2(4\lambda-1)\,|P_4|}\right)^{\frac{1}{2\lambda}}, \qquad \frac{\mathsf{G_m}}{\mu H} \approx \frac{4\lambda^2\,|P_2|}{4\lambda-1} \left(\frac{(2\lambda-1)\,|P_2|}{2(4\lambda-1)\,|P_4|}\right)^{\frac{2\lambda-1}{2\lambda}}. \tag{2.40}$$

If we compare with the values obtained by the FEM (see **P3**), one sees that the agreement is very good for the maximum $\mathsf{G_m}$, less for ℓ_m. The reason is that the localization of ℓ_m by the FEM is quite imprecise because the graph of $\mathcal{G}_\ell$ is very flat near ℓ_m: for instance, for $\epsilon = 0.3$, $\mathcal{G}_\ell$ computed at $\tilde{\ell} = 0.092$ is equal to 0.27327 while it is equal to 0.27307 at $\tilde{\ell} = 0.082$, *i.e.* with a relative difference less than 10^{-4}.

ϵ	0	0.1	0.2	0.3	0.4
λ	0.5	0.5164	0.5335	0.5511	0.5689
ℓ_m/H by FEM	0	0.024	0.058	0.092	0.130
ℓ_m/H by **MAM** 4	0	0.0255	0.0533	0.0823	0.1124
$\mathsf{G_m}/\mu H$ by FEM	0.4820	0.3900	0.3260	0.2733	0.2279
$\mathsf{G_m}/\mu H$ by **MAM** 4	0.4820	0.3917	0.3264	0.2724	0.2257
ℓ_i by **MAM** 4	0	0.0499	0.1020	0.1544	0.2067
$\mathsf{G_i}/\mu H$ by **MAM** 4	0.4820	0.3877	0.3195	0.2635	0.2157
$\mathsf{t_i}/\mathsf{t_c}$ by **MAM** 4	1.440	1.606	1.769	1.916	2.153

Table 2.3: Comparisons of the values of ℓ_m and $\mathsf{G_m}$ obtained by the FEM with those obtained by **MAM** 4, and values of the length of the crack, the energy release rate and the loading at which the crack nucleates.

If one uses **MAM** 4 for calculating the nucleation, then one gets the

Proposition 2.5. *In the case of a genuine notch $\epsilon > 0$,*

1. *if the body does not contain a preexisting crack ($\ell_0 = 0$), then the time $\mathsf{t_i}$ at which the crack nucleates and the length ℓ_i of the nucleated crack at this time are approximated with the* **MAM** *4*

by

$$\frac{\ell_{\mathsf{i}}}{H} \approx 2^{\frac{1}{2\lambda}} \frac{\ell_{\mathsf{m}}}{H} \approx \left(\frac{(2\lambda-1)\,|P_2|}{(4\lambda-1)\,|P_4|} \right)^{\frac{1}{2\lambda}} \quad , \tag{2.41}$$

$$\mathsf{t_i}^2 \approx \frac{1}{\lambda\ 2^{\frac{1}{2\lambda}}} \frac{\mathsf{G_c}}{\mathsf{G_m}} \approx \frac{\mathsf{t_c}^2}{8\lambda^3} \left(\frac{4\lambda-1}{|P_2|} \right)^{2-\frac{1}{2\lambda}} \left(\frac{4P_4}{2\lambda-1} \right)^{1-\frac{1}{2\lambda}} \quad , \tag{2.42}$$

where $\mathsf{t_c}^2 = \mathsf{G_c}/\mu H$*;*

2. *if the body contains a preexisting crack of length* ℓ_0 *such that* $0 < \ell_0 < \ell_{\mathsf{m}}$*, then the length* ℓ_{i} *at which the crack jumps at the onset of the propagation is the unique solution greater than* ℓ_{m} *of*

$$0 = |P_2| \left((2\lambda-1)\ell_{\mathsf{i}}^{2\lambda} - 2\lambda\ell_0\ell_{\mathsf{i}}^{2\lambda-1} + \ell_0^{2\lambda} \right) H^{2\lambda} - P_4 \left((4\lambda-1)\ell_{\mathsf{i}}^{4\lambda} + 4\lambda\ell_0\ell_{\mathsf{i}}^{4\lambda-1} - \ell_0^{4\lambda} \right), \tag{2.43}$$

while the time $\mathsf{t_i}$ *at which the onset occurs is given by* $\mathsf{t_i}^2 = \mathsf{G_c}/\mathcal{G}_{\ell_{\mathsf{i}}}$*. Therefore,* ℓ_{i} *and* $\mathsf{t_i}$ *decrease from the values given by* (2.41) *to* ℓ_{m} *and* $\sqrt{\mathsf{G_c}/\mathsf{G_m}}$ *given by* (2.40) *when* ℓ_0 *runs from* 0 *to* ℓ_{m}*.*

Proof. When $\ell_0 = 0$, if one uses **MAM** 4, then (2.37) reads as

$$0 = (2\lambda-1)\,|P_2| \left(\frac{\ell_{\mathsf{i}}}{H} \right)^{2\lambda} - (4\lambda-1)\,|P_4| \left(\frac{\ell_{\mathsf{i}}}{H} \right)^{4\lambda}.$$

Using (2.40), one deduces (2.41) after some calculations left to the reader. In the same manner, (2.43) is a direct consequence of (2.37) and (2.39). The monotonicity of ℓ_{i} and $\mathsf{t_i}$ with respect to ℓ_0 is easily checked from the graphical interpretation of (2.43), see Figure 2.5. □

Therefore, since $1/2 < \lambda < 1$ for a genuine notch, the length of the nucleated crack ℓ_{i} is less than $2\ell_{\mathsf{m}}$ while the critical time $\mathsf{t_i}$ is not greater than $2^{1/4}\sqrt{\mathsf{G_c}/\mathsf{G_m}}$. For very sharp notch, *i.e.* when ϵ is small, then $2\lambda \approx 1 + \epsilon/\pi$ and

$$\ell_{\mathsf{i}} \approx \frac{\epsilon\,|P_2|}{\pi P_4} H, \quad \mathsf{t_i}^2 \approx \frac{\mathsf{G_c}}{|P_2|\,\mu H},$$

where $P_2 \approx -0.4820$ and $P_4 \approx 0.3282$. In other words, we recover the response associated with a crack when the notch angle tends to 2π, the *FM-law* delivers an evolution which depends continuously of the parameter ϵ, in contrast with the *G-law*.

As long as the dependence of $\mathsf{t_i}$ on ℓ_0 is concerned, it turns out that the *FM-law* predicts that the variation of $\mathsf{t_i}$ is small when ℓ_0 goes from 0 to ℓ_{m} as one can see on Figure 2.6 for $\epsilon = 0.4$. Indeed, $\mathsf{t_i}/\mathsf{t_c}$ decreases from 2.153 to 2.105 when ℓ_0 varies from 0 to $\ell_{\mathsf{m}} = 0.112\,H$. That constitutes also a strong difference with the prediction of the *G-law* for which $\mathsf{t_i}$ goes to infinity when ℓ_0 goes to 0.

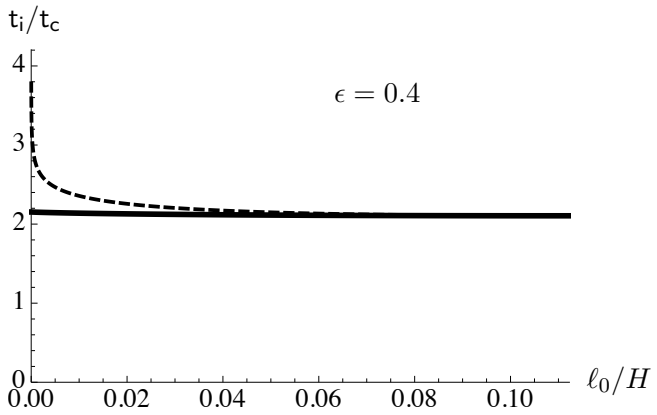

Figure 2.6: Time at which a preexisting crack starts in function of its length in the case where the notch parameter $\epsilon = 0.4$. Plain line: from the *FM-law*; dashed line: from the *G-law*

2.4 The case of a cohesive crack

2.4.1 Dugdale cohesive model

Dugdale model is formulated in energetic terms by considering the surface energy density ϕ. In Dugdale's model ϕ depends in a non-trivial manner on the displacement jump, while in Griffith's model ϕ is assumed to be constant, see Figure 2.7. In our anti-plane setting, the displacement field at equilibrium $\mathbf{u}$ reads as

$$\mathbf{u}(\mathbf{x}) = u(x_1, x_2)\mathbf{e}_3$$

and hence the component u alone is non zero and can be discontinuous. Accordingly, the surface energy density can be read as follows:

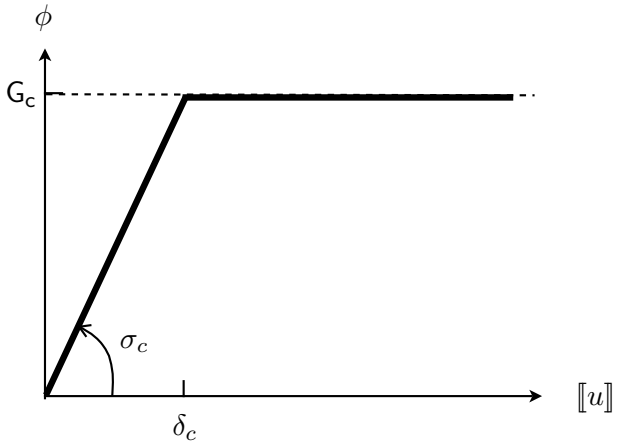

Figure 2.7: Densities of surface energy in model of Dugdale and Griffith

$$\phi([\![u]\!]) = \begin{cases} \dfrac{\mathsf{G_c}}{\delta_c}[\![u]\!] & \text{if} \quad [\![u]\!] \leq \delta_c \\ \mathsf{G_c} & \text{if} \quad [\![u]\!] \geq \delta_c \end{cases} \tag{2.44}$$

In equation (2.44), δ_c is a material characteristic length and $[\![u]\!]$ denotes for the jump of the displacement. Assuming that u is discontinuous across the axis $x_2 = 0$, one has

$$[\![u]\!](x_1) = \lim_{x_2 \to 0^+} u(x_1, x_2) - \lim_{x_2 \to 0^-} u(x_1, x_2).$$

Therefore, the surface energy density ϕ is a linear function of the jump discontinuity of the displacement as long as this latter one is less than the critical value δ_c and becomes a constant, like in Griffith's theory, when the displacement jump is beyond that critical value. The so-called cohesive force σ_c is given by the ratio $\mathsf{G_c}/\delta_c$,

$$\sigma_c = \frac{\mathsf{G_c}}{\delta_c}.$$

From equation (2.44), the normal stress σ_{32} on the crack lips is equal to σ_c if $[\![u]\!] < \delta_c$ and will vanish if $[\![u]\!] > \delta_c$. Thus, the crack lips are divided into two zones: a cohesive zone where the cohesive forces are equal to σ_c and a non-cohesive zone where $[\![u]\!] > \delta_c$ and where the free stress conditions are imposed.

Remark 2.6. *In the context of the variational approach to fracture, [*Charlotte et al., 2006*] uses the loss of stability of elastic response as the criterion of crack initiation. This stability criterion can be assimilated as a local minimum energy principle. Accordingly, a sample under an uniaxial traction will break once the stress reaches the critical value σ_c and hence σ_c can be also considered as the rupture limit stress of the material.*

The same crack notch-shaped body as in the non cohesive case is considered, see Fig. 2.8.

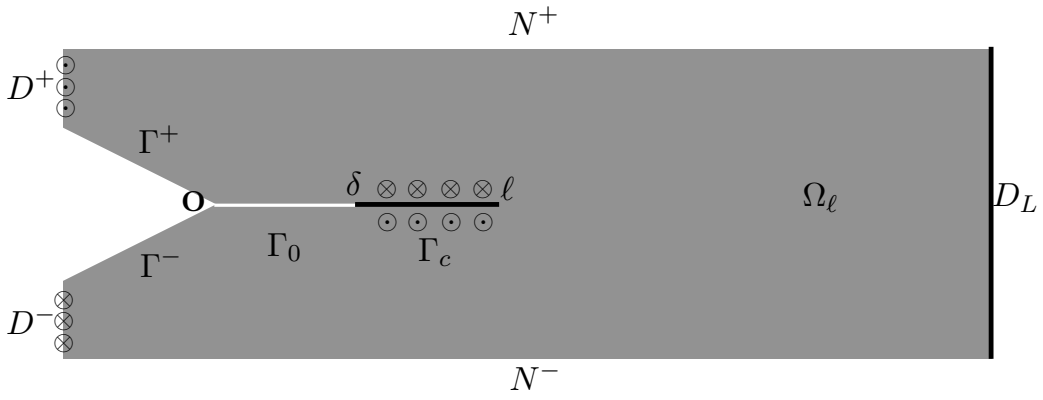

Figure 2.8: The cracked notch-shaped body Ω_ℓ, the different parts of the boundary and the two parts of the crack: the non cohesive part Γ_0 and the cohesive part Γ_c.

The type of load is the same as in the previous section and the displacement is controlled on the sides $D^{\pm}$. The amplitude of the displacement with now be denoted by U and hence the Dirichlet boundary conditions read as:

$$u(\mathbf{x}) = \begin{cases} +U & \text{on} \quad D^{+} \\ -U & \text{on} \quad D^{-} \\ 0 & \text{on} \quad D_L \end{cases}. \tag{2.45}$$

On $N^{\pm}$ and on the edges of the notch, the stress is set to be free,

$$\frac{\partial u}{\partial n} = 0 \quad \text{on} \quad N^{\pm} \cup \Gamma^{\pm}. \tag{2.46}$$

As soon as U is positive, the pure elastic problem posed on the uncracked body admits a solution u^0 which is in $H^1(\Omega_0)$ but not in $H^2(\Omega_0)$. Indeed, because of the presence of the notch, the gradient of $u^0(\mathbf{x})$ tends to infinity when the point $\mathbf{x}$ tends to the tip of the notch. Consequently, since the Dugdale's model contains a critical stress, this solution u^0 which leads to unbounded stresses is not admissible. A crack must appear. By reason of symmetry, we assume that the crack will starts at the tip of the notch and then propagates along the axis $x_2 = 0$. Accordingly, denoting by ℓ the current position of the tip of the crack, the crack is the interval $\Gamma_\ell = (0, \ell) \times \{0\}$. The displacement is not discontinuous across the axis $x_2 = 0$ in front of the crack tip, *i.e.* $[\![u]\!](x_1) = 0$ for $x_1 > \ell$. If one assumes that $x_1 \mapsto [\![u]\!](x_1)$ is continuous, then the jump of the displacement vanishes at the tip of the crack, *i.e.* $[\![u]\!](\ell) = 0$. Still by continuity, the jump of the displacement is less than the critical value δ_c of Dugdale's model in some neighborhood of the crack tip. Consequently, there exists cohesive forces of intensity σ_c on the lips of the crack in that neighborhood of the crack tip. One can then consider two situations:

1. The jump of the displacement is less than δ_c all along Γ_ℓ and hence all the crack is cohesive. One can expect that such a situation holds for small values of U;

2. The jump of the displacement is greater than δ_c in a first part of Γ_ℓ close to the tip of the notch and less than δ_c in the second part close to the crack tip. In such a case the second part of the crack is cohesive, but not the first one. One can expect that such a situation holds for large values of U.

Since the first situation can be viewed as a particular case of the second one, we consider generically the second. Hence, the crack is divided into two parts, the cohesive part and the non-cohesive part,

$$\Gamma_\ell = \Gamma_0 \cup \Gamma_c$$

with

$$\Gamma_0 = (0, \delta) \times \{0\}, \qquad \Gamma_c = [\delta, \ell) \times \{0\}.$$

The associated body containing the crack Γ_ℓ is denoted by $\Omega_\ell = \Omega_0 \setminus \Gamma_\ell$. The two edges of the notch are denoted by Γ^+ and Γ^- in Figure 2.8. When one uses polar coordinates (r, θ), the pole is the tip of the notch and the origin of the polar angle is the edge Γ^-. Accordingly, we have:

$$r = \|\mathbf{x}\|, \quad \Gamma^- = \{(r, \theta), 0 < r < r^*,\ \theta = 0\}, \quad \Gamma^+ = \{(r, \theta), 0 < r < r^*,\ \theta = \omega\}.$$

Assuming that there is no body forces, the equilibrium condition requires that u satisfy the Laplace's equation:

$$\Delta u = 0 \quad \text{in} \quad \Omega_\ell \tag{2.47}$$

and the edges of the notch are stress free.

By virtue of Dugdale's model and owing to the assumptions made on the crack and on the external loading, the conditions on the lips of the crack read as:

$$\mu \frac{\partial u}{\partial n} = 0 \quad \text{on} \quad \Gamma_0 \quad \text{and} \quad \mu \frac{\partial u}{\partial x_2} = \sigma_c \quad \text{on} \quad \Gamma_c \tag{2.48}$$

Note that these conditions hold true both on the upper lip and the lower lip of the crack. In particular, on the cohesive part of the crack, since the outer normal to the upper lip is $-\mathsf{e}_2$ and the outer normal to the lower lip is $+\mathsf{e}_2$, these lips are in fact submitted to opposite forces: $-\sigma_c$ for the upper, $+\sigma_c$ for the lower. The sign of these forces comes from Dugdale's model and the implicit assumption that the jump of the displacement is positive all along Γ_c. Hence these forces tend to close the lips of the crack.

Finally, the field u has to satisfy the following set of equations:

$$\begin{cases} \Delta u = 0 & \text{in} \quad \Omega_\ell \\ u = \pm U & \text{on} \quad D^\pm \\ u = 0 & \text{on} \quad D_L \\ \mu \dfrac{\partial u}{\partial n} = 0 & \text{on} \quad \Gamma_0 \cup \Gamma^\pm \cup N^\pm \\ \mu \dfrac{\partial u}{\partial x_2} = \sigma_c & \text{on} \quad \Gamma_c \end{cases} \tag{2.49}$$

Consequently, for a given position δ and ℓ of the tips of the crack, this problem is an elastic linear problem which admits a unique solution in $H^1(\Omega_\ell)$. It remains to find the positions δ and ℓ of the tips of the crack. This is the goal of the next section.

2.4.2 Study of the crack nucleation

The variational formulation of the evolution of the two crack tips

Let us assume that, for given δ and ℓ, the displacement field solution of (2.49) is known. Then, the total energy of the body is the function of $U,\ \delta,$ and ℓ given by

$$\mathcal{E}(U,\delta,\ell) = \frac{\mu}{2}\int_{\Omega_\ell} \nabla u.\nabla u dx + \int_{\Gamma_c} \sigma_c [\![u]\!] dx_1 + \mathsf{G_c}\delta. \tag{2.50}$$

Let us remark that the cohesive energy is included in the total energy which is hence the sum of the elastic and the surface energy. Note also that Griffith's model can be seen as a limit case of Dugdale model when $\ell = \delta$ and hence $\Gamma_c = \emptyset$. Indeed, in such a case the second term on the right hand side of (2.49) disappears and the surface energy is reduced to the third term which is precisely Griffith's surface energy.

The evolution of the two tips δ and ℓ of the non-cohesive and cohesive zones when the external load U grows from 0 to "infinity" is governed by an energetic criterion which is stated in the following definition

Definition 2.3 (*D-law*)**.** *For a given U, the positions δ and ℓ of the tips of the non cohesive and cohesive zones are such that the total energy is a* **local minimum***. Specifically, δ and ℓ have to satisfy*

$$(i) \qquad 0 \le \delta < \ell < L \tag{2.51}$$

$$(ii) \quad \exists \epsilon > 0,\ \forall (\delta^*,\ell^*)\ :\ 0 \le \delta^* < \ell^* < L,\ |\delta^* - \delta| + |\ell^* - \ell| \le \epsilon \quad ,$$
$$\mathcal{E}(U,\delta,\ell) \le \mathcal{E}(U,\delta^*,\ell^*) \qquad . \tag{2.52}$$

In the sequel, we will refer to this local minimization principle of the total energy as the *D-law*. Note that we have *a priori* excluded the case $\delta = \ell$ which corresponds to the case where there is no cohesive zone. In such a situation the stress should be infinite at δ. This is in fact forbidden by the cohesive law as we will see below. So, we exclude directly this case to save time. On the other hand, the case $\delta = 0$ is allowed because it corresponds to the case where a non cohesive case has not still nucleated. Such a situation holds true for small values of the loading U. We have also excluded the case $\ell < L$ because we are only interested by the beginning of the crack propagation.

Note also that we have not introduced in this criterion any condition of irreversibility. Of course, such a condition is physically necessary. Indeed, once a non cohesive crack is created, it is in principle impossible that this crack disappears except if one tries to account for healing effects. Accordingly, one should require that at least δ be an increasing function of time. This condition was introduced both

in *G-law* and in *FM-law*. Moreover the irreversibility condition was automatically satisfied by *FM-law* in the case of a monotonically increasing loading, see Lemma 2.1. In the case of *D-law*, to simplify the presentation, this condition is not required *a priori* but will be checked *a posteriori*. As far as the evolution of the cohesive zone is concerned, the question of the irreversibility is much more delicate. A complete model should contain internal variables which take into account all the history of the jump of the displacement up to the present time. Such complete models are presented for instance in [Jaubert and Marigo, 2006; Abdelmoula et al., 2010]. But here, still to simplify the presentation, we do not consider such complete models and we will simply check *a posteriori* whether ℓ is also an increasing function of time.

In such a simplified setting, *D-law* leads to the following Proposition

Proposition 2.6. *By virtue of* D-law*, at a given U, the positions δ and ℓ of the tips of the non cohesive and cohesive zones must satisfy the following set of conditions:*

$$\textit{Condition for } \delta \quad : \quad \begin{cases} \dfrac{\partial \mathcal{E}}{\partial l}(U,0,\ell) \geq 0 \quad \textit{if} \quad \delta = 0 \\ \\ \dfrac{\partial \mathcal{E}}{\partial l}(U,\delta,\ell) = 0 \quad \textit{if} \quad \delta > 0 \end{cases} ; \tag{2.53}$$

(2.54)

$$\textit{Condition for } \ell \quad : \quad \frac{\partial \mathcal{E}}{\partial \ell}(U,\delta,\ell) = 0. \tag{2.55}$$

Proof. These conditions are direct consequences of the definition 2.6. Note that there are only necessary conditions so that (δ, ℓ) be a local minimum. □

One sees that the determination of δ and ℓ requires that one has previously obtained the two partial derivatives of the total energy with respect to δ and ℓ at given U. These partial derivatives are the so-called *energy release rates*. Note that here, because of the cohesive forces and contrarily to Griffith's case, there exist *two* energy release rates. Each one corresponds to the release of the total energy due to an increase of the associated crack tip, the other crack tip and the loading being kept constant. The next subsections are devoted to the determination and the interpretation of these energy release rates. Accordingly, for conciseness of the notations we set

$$\mathcal{G}_\delta := \frac{\partial \mathcal{E}}{\partial \delta}(U,\delta,\ell), \qquad \mathcal{G}_\ell := \frac{\partial \mathcal{E}}{\partial \ell}(U,\delta,\ell).$$

Calculation of the energy release rate $\mathcal{G}_\delta$

The calculation of $\mathcal{G}_\delta$ is easier than that of $\mathcal{G}_\ell$ because there is no singularity at the tip of the non-cohesive zone. This fundamental property comes from the fact that both on Γ_c and Γ_0 the boundary

conditions are of Neumann type (contrarily to the tip ℓ where there are Dirichlet conditions in front of the crack and Neumann conditions on the lips of the crack). The consequence of this lack of singularity is that we can obtain $\mathcal{G}_\delta$ by using classical formula for differentiating the energy. Indeed, recalling that the energy reads as

$$\mathcal{E}(U,\delta,\ell) = \int_{\Omega_\ell} \frac{\mu}{2} \nabla u(U,\delta,\ell) \cdot \nabla u(U,\delta,\ell) dx + \int_\delta^\ell \sigma_c [\![u(U,\delta,\ell)]\!](x_1) dx_1 + \mathsf{G_c}\delta,$$

where $u(U,\delta,\ell)$ stands for the displacement at equilibrium for given (U,δ,ℓ), we can directly take the derivative under the integral sign in both integrals. Moreover since one bound depends on δ, one has also to use the Reynolds transport theorem, [Marsden and Hughes, 1983]. Omitting to make explicit the dependence on (U,δ,ℓ), one gets

$$\mathcal{G}_\delta = -\int_{\Omega_\ell} \mu \nabla u \nabla (\frac{\partial u}{\partial \delta}) dx - \int_\delta^\ell \sigma_c [\![\frac{\partial u}{\partial \delta}]\!] dx_1 + \sigma_c [\![u]\!](\delta) - \mathsf{G_c}, \tag{2.56}$$

where $\partial u/\partial\delta$ represents the variation of the displacement due to a unit propagation of the non cohesive crack tip at given U and ℓ. Let us consider the two terms in the right hand side of (2.56) which involve $\partial u/\partial\delta$. After an integration by parts, one gets

$$\int_{\Omega_\ell} \mu \nabla u \nabla (\frac{\partial u}{\partial \delta}) dx + \int_\delta^\ell \sigma_c [\![\frac{\partial u}{\partial \delta}]\!] dx_1 \quad = \quad -\int_{\Omega_\ell} \mu \Delta u \frac{\partial u}{\partial \delta} dx + \int_{\partial\Omega_\ell} \mu \frac{\partial u}{\partial n} \frac{\partial u}{\partial \delta} ds + \int_\delta^\ell \sigma_c [\![\frac{\partial u}{\partial \delta}]\!] dx_1$$

Using the fact that u satisfies (2.49) and hence that $\partial u/\partial\delta = 0$ on $D^\pm \cup D_L$ leads to

$$\int_{\Omega_\ell} \mu \nabla u \nabla (\frac{\partial u}{\partial \delta}) dx + \int_\delta^\ell \sigma_c [\![\frac{\partial u}{\partial \delta}]\!] dx_1 = 0.$$

Inserting into (2.56) gives the desired expression for $\mathcal{G}_\delta$:

$$\mathcal{G}_\delta = \sigma_c [\![u]\!](\delta) - \mathsf{G_c}. \tag{2.57}$$

Therefore the condition for δ in Proposition 2.6 simply reads as

$$\text{Condition for } \delta : \quad \begin{cases} [\![u]\!](0) \le \delta_c & \text{if} \quad \delta = 0 \\ \\ [\![u]\!](\delta) = \delta_c & \text{if} \quad \delta > 0 \end{cases}. \tag{2.58}$$

We have finally the rather natural conditions that

(i) a non cohesive crack does not exist as long as the jump of the displacement at the tip of the notch is less than the critical value δ_c given by Dugdale's model;

(ii) once the non cohesive crack exists, the position of its tip is such that the jump of the displacement at the tip is equal to δ_c.

Calculation of the energy release rate $\mathcal{G}_\ell$

Taking the derivative with respect to ℓ of the total energy for $\mathcal{G}_\ell$ meets some difficulties like in the Griffith's case. Indeed, one has to take the derivative of an integral over a domain which depends on the parameter. Moreover, the integrand itself depends on the parameter and has a singularity which will move with the parameter. Therefore, the calculation of the derivative can no more be achieved by usual transport theorem like in the calculation of $\mathcal{G}_\delta$. One must proceed as in Griffith's case and make a change of variable in order to send the variable domain onto a fix domain, see Section 2.2.2. In other words, one has to adapt the $G-\theta$ method to that situation. It is the goal of this subsection.

The difference with the Griffith's case is that one must choose a change of variable such that the moving tip ℓ_h be sent to the fix tip ℓ without changing the tip δ. Indeed, since we are only interested by the partial derivative of the energy with respect to ℓ at given δ, the tip δ must remain unchanged after the change of variable. Accordingly we consider a vector field $\mathbf{v}(\mathbf{x}) = v(\mathbf{x})\mathbf{e}_1$ (which plays here the role of the vector field $\boldsymbol{\theta}$ in Griffith's case) where $\mathbf{x} \mapsto v(\mathbf{x})$ is smooth and must satisfy

$$v(\mathbf{x}) = 1 \text{ at } \mathbf{x} = (\ell, 0) \quad \text{and} \quad v(\mathbf{x}) = 0 \text{ outside the ball of center } (\ell, 0) \text{ and radius } r_0 < \ell - \delta. \quad (2.59)$$

Consequently, one has

$$v(\delta, 0) = 0.$$

For a small h, let $\Gamma_{\ell+h}$ be the virtual crack of length $\ell + h$. This new crack is decomposed into the same non cohesive part Γ_0 (as the previous one) and a cohesive crack Γ_c^h which has changed and has now a length equal to $\ell + h - \delta$. Specifically, one has

$$\Gamma_{\ell+h} = \Gamma_0 \cup \Gamma_c^h \qquad \text{with} \quad \Gamma_c^h = [\delta, \ell + h) \times \{0\}. \quad (2.60)$$

The associated cracked domain is now $\Omega_{\ell+h}$. Let Φ_h be the direct diffeomorphism from Ω_ℓ onto $\Omega_{\ell+h}$ defined by

$$\mathbf{x} \mapsto \mathbf{x}^h = \Phi_h(\mathbf{x}) := (x_1 + hv(x_1, x_2), x_2). \quad (2.61)$$

One immediately gets

$$F_h = \nabla\Phi_h = \mathbf{I} + h\nabla v = (1 + h\frac{\partial v}{\partial x_1})e_1 \otimes e_1 + h\frac{\partial v}{\partial x_2}e_1 \otimes e_2 + e_2 \otimes e_2$$

where $\mathbf{I}$ denotes the identity tensor.

The displacement $u(U,\delta,\ell+h)$ solution of the static problem associated with the loading U and the tips located at δ and $\ell+h$ is more shortly denoted by u^h,

$$u^h := u(U,\delta,\ell+h).$$

This displacement field defined on $\Omega_{\ell+h}$ is transported on Ω_ℓ and the transported displacement is denoted $\tilde{u}^h$:

$$\tilde{u}^h(x) = u^h(x^h) = u^h \circ \Phi_h(x).$$

Using these definitions and notations, the total energy of the body at equilibrium with the virtual crack $\Gamma_{\ell+h}$ reads as

$$\mathcal{E}(U,\delta,\ell+h) \;=\; \frac{\mu}{2}\int_{\Omega_{\ell+h}} \nabla u^h \cdot \nabla u^h dx^h + \int_{\Gamma_c^h} \sigma_c [\![u^h]\!] dx_1^h + \mathsf{G_c}\delta.$$

Introducing the change of variable $\mathbf{x}^h \mapsto \mathbf{x} = \Phi_h^{-1}(x^h)$, one has

$$\nabla u^h(\mathbf{x}^h) = F_h^{-T}(\mathbf{x})\nabla \tilde{u}^h(\mathbf{x}), \qquad dx^h = \det F_h(\mathbf{x})dx, \qquad dx_1^h = \left(1 + h\frac{\partial v}{\partial x_1}(\mathbf{x})\right) dx_1.$$

Inserting into the formula of the total energy $\mathcal{E}(U,\delta,\ell+h)$ leads to

$$\mathcal{E}(U,\delta,\ell+h) = \frac{\mu}{2}\int_{\Omega_\ell} \left(F_h^{-T}\nabla\tilde{u}^h \cdot F_h^{-T}\nabla\tilde{u}^h\right) \det F_h \, dx + \int_{\Gamma_c} \sigma_c [\![\tilde{u}^h]\!] \left(1 + h\frac{\partial v}{\partial x_1}\right) dx_1 + \mathsf{G_c}\delta.$$

We can now differentiate with respect to h in order to obtain $\mathcal{G}_\ell$. Indeed, $\mathcal{G}_\ell$ is nothing but the derivative of $\mathcal{E}(U,\delta,\ell+h)$ with respect to h at $h=0$. Noting that

$$\tilde{u}^h \mid_{h=0} = u, \quad F_h^{-1} \mid_{h=0} = \mathbf{I}, \quad \left.\frac{\partial F_h^{-T}}{\partial h}\right|_{h=0} = -e_1 \otimes \nabla v, \quad \frac{d}{dh}\det F_h \mid_{h=0} = \frac{\partial v}{\partial x_1},$$

and using the chain rule, we get

$$\begin{aligned}
\mathcal{G}_\ell &= -\frac{d}{dh}\,\mathcal{E}(U,\delta,\ell+h)|_{h=0} \\
&= \int_{\Omega_\ell} \mu\nabla u \cdot \nabla v \frac{\partial u}{\partial x_1} dx - \int_{\Omega_\ell} \frac{\mu}{2}\nabla u \cdot \nabla u \frac{\partial v}{\partial x_1} dx - \int_{\Gamma_c} \sigma_c [\![u]\!] \frac{\partial v}{\partial x_1} dx_1 \\
&\quad - \int_{\Omega_\ell} \mu\nabla u \cdot \nabla \dot{u} dx - \int_{\Gamma_c} \sigma_c [\![\dot{u}]\!] dx_1
\end{aligned}$$

where $\dot{u} = \dfrac{d\tilde{u}^h}{dh} \mid_{h=0}$. Since, owing to the transport, $\dot{u}$ belongs to $H^1(\Omega_\ell)$ and since $\dot{u}=0$ on $D^\pm \cup D_L$, it can be used as a function test in the variational equation giving u. Therefore, one gets

$$\int_{\Omega_\ell} \mu\nabla u \cdot \nabla \dot{u} dx + \int_{\Gamma_c} \sigma_c [\![\dot{u}]\!] dx_1 = 0$$

and finally $\mathcal{G}_\ell$ reads as

$$\mathcal{G}_\ell = \int_{\Omega_\ell} \mu \left(\frac{\partial u}{\partial x_j} \frac{\partial u}{\partial x_1} \frac{\partial v}{\partial x_j} - \frac{1}{2} \frac{\partial u}{\partial x_j} \frac{\partial u}{\partial x_j} \frac{\partial v}{\partial x_1} \right) dx - \int_{\Gamma_c} \sigma_c [\![u]\!] \frac{\partial v}{\partial x_1} dx_1. \tag{2.62}$$

This expression for $\mathcal{G}_\ell$ involves the field v and one could believe that $\mathcal{G}_\ell$ really depends on the choice of v. But we will see that it is not the case by reestablishing the Irwin's formula which gives $\mathcal{G}_\ell$ in terms of the stress intensity factor associated with the singularity at the tip ℓ. Indeed, for arbitrary values of U, δ and ℓ, the displacement field u is *a priori* singular (in the sense that it does not belong to $H^2(\Omega_\ell)$) and its singularity has the classical form

$$u(\mathbf{x}) = \frac{2\mathcal{K}}{\mu} \sqrt{\frac{r}{2\pi}} \sin \frac{\bar{\theta}}{2} + \dots \tag{2.63}$$

where $(r, \bar{\theta})$ denotes here the polar coordinates $x_1 - \ell = r \cos \bar{\theta}$, $x_2 = r \sin \bar{\theta}$. The coefficient $\mathcal{K}$ is the mode *III* stress intensity factor.

Let B_{r^*} be the ball with center $(\ell, 0)$ and radius r^* which is destined to goes to 0. Let C_{r^*} be its boundary, *i.e.* the circle centered at $(\ell, 0)$ with radius r^*. Let $\Gamma_{r^*} = \Gamma_\ell \cap B_{r^*}$, one has $\Gamma_{r^*} \subset \Gamma_c$ for r^* small enough. Setting $B^c_{r^*} = \Omega_\ell \setminus B_{r^*}$, the boundary of $B^c_{r^*}$ contains $\Gamma^\pm \cup N^\pm \cup D_L \cup D^\pm$ for r^* sufficiently small.

Then, decomposing the integral over Ω_ℓ into an integral over B_{r^*} and an integral over $B^c_{r^*}$, after integrating by parts the integral over B_{r^*}, the expression (2.62) for $\mathcal{G}_\ell$ becomes

$$\begin{aligned}
\mathcal{G}_\ell &= \int_{B_{r^*} \cup B^c_{r^*}} \mu \left(\frac{\partial u}{\partial x_j} \frac{\partial u}{\partial x_1} \frac{\partial v}{\partial x_j} - \frac{1}{2} \frac{\partial u}{\partial x_j} \frac{\partial u}{\partial x_j} \frac{\partial v}{\partial x_1} \right) dx - \int_{\Gamma_c} \sigma_c [\![u]\!] \frac{\partial v}{\partial x_1} dx_1 \\
&= \int_{B_{r^*}} \mu \left(\frac{\partial u}{\partial x_j} \frac{\partial u}{\partial x_1} \frac{\partial v}{\partial x_j} - \frac{1}{2} \frac{\partial u}{\partial x_j} \frac{\partial u}{\partial x_j} \frac{\partial v}{\partial x_1} \right) dx - \int_{\Gamma_c} \sigma_c [\![u]\!] \frac{\partial v}{\partial x_1} dx_1 \\
&+ \int_{B^c_{r^*}} \mu \left(- \frac{\partial}{\partial x_j} \left(\frac{\partial u}{\partial x_j} \frac{\partial u}{\partial x_1} \right) v + \frac{1}{2} \frac{\partial}{\partial x_1} \left(\frac{\partial u}{\partial x_j} \frac{\partial u}{\partial x_j} \right) v \right) dx \\
&+ \int_{\partial B^c_{r^*}} \mu \left(\frac{\partial u}{\partial n} \frac{\partial u}{\partial x_1} v - \frac{1}{2} \left(\frac{\partial u}{\partial x_j} \frac{\partial u}{\partial x_j} \right) v n_1 \right) ds
\end{aligned}$$

Considering the different terms above, we can remark that:

1. In the integral over B_{r^*}, the terms involving the gradient of u are singular as $1/\sqrt{r}$, while dx is proportional to r. Hence

$$\int_{B_{r^*}} \mu \left(\frac{\partial u}{\partial x_j} \frac{\partial u}{\partial x_1} \frac{\partial v}{\partial x_j} - \frac{1}{2} \frac{\partial u}{\partial x_j} \frac{\partial u}{\partial x_j} \frac{\partial v}{\partial x_1} \right) dx \sim O(r^*) \xrightarrow[r^* \to 0]{} 0.$$

2. The integral over $B^c_{r^*}$ vanishes by virtue of the equilibrium equation satisfied by u, *i.e.* $\Delta u = 0$. Indeed,

$$\int_{B^c_{r^*}} \Big(-\frac{\partial}{\partial x_j}\big(\frac{\partial u}{\partial x_j}\frac{\partial u}{\partial x_1}\big)v + \frac{1}{2}\frac{\partial}{\partial x_1}\big(\frac{\partial u}{\partial x_j}\frac{\partial u}{\partial x_j}\big)v\Big)dx = -\int_{B^c_{r^*}} \Delta u \frac{\partial u}{\partial x_1} v dx = 0.$$

3. The integral over $\partial B^c_{r^*}$ vanishes on $\Gamma^{\pm} \cup D^{\pm} \cup D_L \cup \Gamma_0$ because either $v = 0$ or $n_1 = 0$. It remains the integral over C_{r^*} and $\Gamma_c \setminus \Gamma_{r^*}$. Since $n_1 = 0$, the integral over $\Gamma_c \setminus \Gamma_{r^*}$ is reduced to

$$I_c(r^*) := \int_{\Gamma_c \setminus \Gamma_{r^*}} \mu\left(\frac{\partial u}{\partial n}\frac{\partial u}{\partial x_1}v - \frac{1}{2}\big(\frac{\partial u}{\partial x_j}\frac{\partial u}{\partial x_j}\big)v n_1\right) ds = \int_{\Gamma_c \setminus \Gamma_{r^*}} \mu \frac{\partial u}{\partial n}\frac{\partial u}{\partial x_1} v(x_1, 0) dx_1.$$

By virtue of the boundary condition $\mu \partial u/\partial x_2 = \sigma_c$ on Γ_c and recalling that u is discontinuous across Γ_c, one gets

$$I_c(r^*) = -\int_{\delta}^{\ell - r^*} \sigma_c \frac{\partial [\![u]\!](x_1)}{\partial x_1} v(x_1, 0) dx_1.$$

Integrating by parts and taking into account that $v(\delta, 0) = 0$ gives

$$I_c(r^*) = \int_{\delta}^{\ell - r^*} \sigma_c [\![u]\!] \frac{\partial v}{\partial x_1} dx_1 - \sigma_c [\![u]\!](\ell - r^*) v(\ell - r^*, 0).$$

Since $[\![u]\!](\ell - r) \sim \sqrt{r}$ for small r, one can pass to the limit when $r^* \to 0$. One finally obtains

$$\lim_{r^* \to 0} I_c(r^*) = \int_{\delta}^{\ell} \sigma_c [\![u]\!] \frac{\partial v}{\partial x_1} dx_1$$

and this term will compensate the already existing integral over Γ_c

At this stage, we have proved that

$$\mathcal{G}_\ell = \lim_{r^* \to 0} \int_{C_{r^*}} \Big(-\mu \frac{\partial u}{\partial r}\frac{\partial u}{\partial x_1} + \frac{\mu}{2} \nabla u \cdot \nabla u \, \mathsf{e}_r \cdot \mathsf{e}_1 \Big) ds \tag{2.64}$$

where we have used that the outer normal to $B^c_{r^*}$ on C_{r^*} is $\mathbf{n} = -\mathbf{e}_r$ and that $v(\ell, 0) = 1$. Therefore, $\mathcal{G}_\ell$ is really independent of v. It remains to express it in terms of the stress intensity factor $\mathcal{K}$. Using the polar coordinates, one gets $ds = r^* d\bar{\theta}$. Using the form of the singularity (2.63) for u, the different terms in the integrand above read as

$$\frac{\partial u}{\partial r} \approx \frac{\mathcal{K}}{\mu\sqrt{2\pi r^*}} \sin\frac{\bar{\theta}}{2}, \quad \frac{\partial u}{\partial x_1} \approx -\frac{\mathcal{K}}{\mu\sqrt{2\pi r^*}} \sin\frac{\bar{\theta}}{2}, \quad \nabla u \cdot \nabla u \approx \frac{\mathcal{K}^2}{2\pi r^* \mu^2}, \quad \mathsf{e}_r \cdot \mathsf{e}_1 = \cos\bar{\theta}.$$

Inserting into (2.64) finally yields the desired expression

$$\mathcal{G}_\ell = \frac{\mathcal{K}^2}{2\mu}.$$

Therefore, Irwin's formula is still valid at the tip of the crack.

Moreover, the condition (2.53) for $\mathcal{G}_\ell = 0$ requires that the stress intensity factor $\mathcal{K}$ vanishes at the tip of cohesive zone. This result is conform to the fact that σ_c plays the role of a critical stress for the material. The length of the cohesive crack must be adjusted so that the stress remains less than σ_c everywhere and of course a necessary condition is that the singularity disappears.

Let us summarize all the results relative to the energy release rates by the following Proposition:

Proposition 2.7. *By virtue of the* D-law*, the necessary conditions for δ and ℓ stated in Proposition 2.6 are finally equivalent to the two following ones:*

$$\textit{Condition for } \delta: \qquad \begin{cases} [\![u]\!](0) \leq \delta_c \quad \textit{if} \quad \delta = 0 \\ \\ [\![u]\!](\delta) = \delta_c \quad \textit{if} \quad \delta > 0 \end{cases}; \tag{2.65}$$

$$\textit{Condition for } \ell: \qquad \mathcal{K} = 0 \quad \textit{(no singularity).} \tag{2.66}$$

2.4.3 Approximation by the MAM

Dugdale's model contains the material characteristic length δ_c which gives the critical displacement jump beyond which the cohesive force vanishes. We can also define another characteristic length d_c as follows

$$d_c = \frac{\mu}{\sigma_c}\delta_c. \tag{2.67}$$

Since in practice the ratio μ/σ_c is large with respect 1 (around 10^3–10^4 for usual materials), d_c is much greater than δ_c. As we will see below, the length d_c gives the order of magnitude of the size of the cohesive crack. Accordingly, in order that we can apply the **MAM** for evaluating the evolution of the crack at the tip of the notch, d_c has to be small with respect to the size of the body. So, throughout the end of the chapter, we consider that the ratio $\eta = d_c/H$ is a small parameter, *i.e.*

$$\eta = \frac{d_c}{H} \ll 1. \tag{2.68}$$

This parameter is now made explicit in the notations and all quantities which are dependent on this parameter will be denoted with the subscript η. Accordingly, for a loading U_η which can depend itself on η, the position of the non cohesive crack tip and the position of the cohesive crack tip are denoted δ_η and ℓ_η, respectively. The associated displacement field and stress intensity factor at the tip of the cohesive crack are denoted $u_\eta(U_\eta, \delta_\eta, \ell_\eta)$ and $\mathcal{K}_\eta(U_\eta, \delta_\eta, \ell_\eta)$ or more shortly u_η and $\mathcal{K}_\eta$ according to whether one wants to make explicit their dependence on the loading and the crack state.

With the above notations, the problem of evolution of the crack with respect to the loading can read as follows:

$$\text{at given } U_\eta, \quad \text{find } \delta_\eta \text{ and } \ell_\eta \text{ such that } 0 \le \delta_\eta < \ell_\eta$$
$$\text{and} \quad \begin{cases} \text{if } \delta_\eta = 0, \quad \text{then} \quad [\![u_\eta(U_\eta, 0, \ell_\eta)]\!](0) \le \delta_c, \quad \mathcal{K}_\eta(U_\eta, 0, \ell_\eta) = 0 \\ \text{if } \delta_\eta > 0, \quad \text{then} \quad [\![u_\eta(U_\eta, \delta_\eta, \ell_\eta)]\!](\delta_\eta) = \delta_c, \quad \mathcal{K}_\eta(U_\eta, \delta_\eta, \ell_\eta) = 0 \end{cases}, \tag{2.69}$$

where, by virtue of (2.49), the displacement u_η is, at given $(U_\eta, \delta_\eta, \ell_\eta)$, the unique solution in $H^1(\Omega_{\ell_\eta})$ of

$$\begin{cases} \Delta u_\eta = 0 & \text{in} \quad \Omega_{\ell_\eta} \\ u_\eta = \pm U_\eta & \text{on} \quad D^\pm \\ u_\eta = 0 & \text{on} \quad D_L \\ \dfrac{\partial u_\eta}{\partial n} = 0 & \text{on} \quad \Big((0, \delta_\eta) \times \{0\}\Big) \cup \Gamma^\pm \cup N^\pm \\ \mu \dfrac{\partial u_\eta}{\partial x_2} = \sigma_c & \text{on} \quad (\delta_\eta, \ell_\eta) \times \{0\} \end{cases}. \tag{2.70}$$

We are interested only by the nucleation stage of the crack, *i.e.* when the lengths δ_η and ℓ_η are of the order of $d_c = \eta H$. So we are in a situation where the defect is small by comparison with the size of the body. (We will see that the loading is itself small and of the order of $\eta^{-\lambda}\delta_c$.) Accordingly, applying the **MAM**, it is sufficient to determine the leading term in the inner and outer expansions for having a good approximation of the solution.

Outer problem

Considering only the first order term of the outer expansion, u_η can read

$$u_\eta(\mathbf{x}) = U_\eta \tilde{u}^0(\tilde{\mathbf{x}}) + \cdots, \qquad \tilde{\mathbf{x}} = \frac{\mathbf{x}}{H}. \tag{2.71}$$

In (2.71), $\tilde{u}^0$ is defined on the rescaled (dimensionless) outer domain $\tilde{\Omega}_0$ which does not contain a crack. It is the unique solution in $H^1(\tilde{\Omega}_0)$ of the elementary outer problem of order 0:

$$\begin{cases} \Delta \tilde{u}^0 = 0 & \text{in} \quad \tilde{\Omega}_0 \\ \tilde{u}^0 = \pm 1 & \text{on} \quad \tilde{D}^\pm \\ \tilde{u}^0 = 0 & \text{on} \quad \tilde{D}_L \\ \dfrac{\partial \tilde{u}^0}{\partial n} = 0 & \text{on} \quad \tilde{\Gamma}^\pm \cup \tilde{N}^\pm \end{cases} \tag{2.72}$$

It is clear that $\tilde{u}^0$ is dimensionless, independent of the size of the body and of the elasticity of the material, but depends on the notch angle ω and the ratio L/H. By virtue of the results of the previous

chapter, the behavior of $\tilde{u}^0$ in the neighborhood of the tip of the notch can be read as

$$\tilde{u}^0(\tilde{r},\bar{\theta}) = b_1^1 \tilde{r}^\lambda \cos(\lambda\theta) + \cdots , \tag{2.73}$$

where $\tilde{r}$ denotes the rescaled distance to the tip of the notch, *i.e.* $\tilde{r} = \|\tilde{\mathbf{x}}\|$. Since $\lambda = \pi/\omega < 1$, the associated stress field $\mu\nabla\tilde{u}^0$ tends to infinity when $\tilde{r}$ tends to 0. So, $b_1^1\tilde{r}^\lambda\cos(\lambda\theta)$ can be seen as the singular part of $\tilde{u}^0$ (not in the sense of Definition 1.1 but in the sense that it belongs to $H^1(\tilde{\Omega}_0)$ but not to $H^2(\tilde{\Omega}_0)$) and the coefficient b_1^1 plays the role of a *stress intensity factor*. (When $\omega = 2\pi$, *i.e.* when the notch is a preexisting crack, then b_1^1 is really the usual stress intensity factor K_{III} up to a normalization.) In practice, the coefficient b_1^1 is obtained from $\tilde{u}^0$ by the path integral (see Proposition (1.4)):

$$b_1^1 = \frac{2\tilde{r}^{-\lambda}}{\omega}\int_0^\omega \tilde{u}^0(\tilde{r},\theta)\cos(\lambda\theta)d\theta. \tag{2.74}$$

Its value is given in Table 2.2 for several values of the angle of the notch. Note that b_1^1 is negative in all cases.

Inner problem

Let us now construct the first order inner problem. The lengths δ_η and ℓ_η giving the positions of the tips of the non cohesive and cohesive cracks are assumed to be of the order of ηH. That allows us to set at the first order

$$\delta_\eta = \bar{\delta}\,\eta H + \cdots , \qquad \ell_\eta = \bar{\ell}\,\eta H + \cdots \tag{2.75}$$

Moreover, the first order inner problem will be posed at the scale of d_c and hence we introduce the following dimensional coordinates $\mathbf{y}$ and $(\tilde{\rho},\theta)$

$$\mathbf{y} = \frac{\mathbf{x}}{d_c} = \frac{\tilde{\mathbf{x}}}{\eta}, \qquad \tilde{\rho} = \frac{\tilde{r}}{\eta}. \tag{2.76}$$

Inserting this new coordinates into (2.71) and taking account of (2.73), u_η in the neighborhood of the notch tip can read as

$$u_\eta(\mathbf{x}) = U_\eta \eta^\lambda b_1^1 \tilde{\rho}^\lambda \cos(\lambda\theta) + \cdots \tag{2.77}$$

This expansion is valid both for the inner and outer expansions in the intermediate zone, *i.e.* when $\tilde{r}$ is close to 0 and $\tilde{\rho}$ is close to infinity. Accordingly, the right hand side of (2.77) gives the behavior of the first order inner term at infinity. In the other hand, on account of (2.69), u_η must be of the order of δ_c in the neighborhood of the crack. That implies that U_η must be of the order of $\eta^{-\lambda}\delta_c$ and hence one can set

$$U_\eta = -\frac{\bar{V}}{b_1^1}\eta^{-\lambda}\delta_c + \cdots \tag{2.78}$$

where $\bar{V}$ will play the role of the rescaled (dimensionless) loading parameter of the inner problem.

Finally, the inner expansion of u_η at the first order can read as

$$u_\eta(\mathbf{y}) = \tilde{v}^1(\mathbf{y})\delta_c + \cdots \tag{2.79}$$

where $\tilde{v}^1$ is defined on the infinite rescaled inner domain $\tilde{\Omega}^\infty$, see Figure 2.9,

$$\tilde{\Omega}^\infty = \{(\tilde{\rho}, \theta) \in (0, +\infty) \times (0, \omega)\} \setminus \left\{\mathbf{y} \in (0, \bar{\ell}) \times \{0\}\right\}.$$

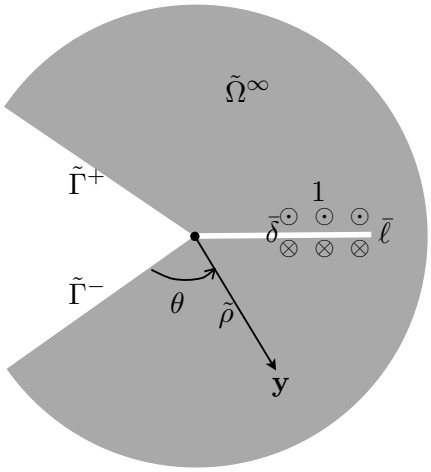

Figure 2.9: The rescaled inner domain

Inserting (2.79) into (2.70) and using the matching condition (2.77) give the problem that $\tilde{v}^1$ must satisfy. Specifically, one gets

$$\begin{cases} \Delta\tilde{v}^1 = 0 & \text{in} \quad \tilde{\Omega}^\infty \\ \dfrac{\partial\tilde{v}^1}{\partial y_2} = 1 & \text{on} \quad (\bar{\delta}, \bar{\ell}) \times \{0\} \\ \dfrac{\partial\tilde{v}^1}{\partial n} = 0 & \text{on} \quad \tilde{\Gamma}^\pm \cup \Big((0, \bar{\delta}) \times \{0\}\Big) \\ \tilde{v}^1 \sim -\bar{V}\tilde{\rho}^\lambda \cos(\lambda\theta) & \text{at} \quad \text{infinity} \end{cases}. \tag{2.80}$$

Remark 2.7. *For given $(\bar{V}, \bar{\delta}, \bar{\ell})$, we are in a situation similar but not identical to Chapter 1. Indeed, the problem* (2.80) *is a combination of the problem* (1.32) *and the problem* (1.33) *with $i = 1$, the force density g is given here by*

$$g(x) = \begin{cases} 0 & \text{on} \quad (\bar{\delta}, \bar{\ell}) \times \{0\pm\} \\ \mp 1 & \text{on} \quad (0, \bar{\delta}) \times \{0\pm\} \end{cases}$$

and the singular part of $\tilde{v}^1$ is

$$\tilde{v}^1_S(\mathbf{y}) = -\bar{V}\tilde{\rho}^\lambda \cos(\lambda\theta).$$

The fact that g appears here in the inner problem of order 1 while it appeared in the inner problem of order 0 in Chapter 1 is due to the fact that the density of forces were assumed to be of the order of $1/\ell$ *in Chapter 1, see* (1.4).

But we can still apply Proposition 1.3. Since the forces are equilibrated on the lips of the crack (the cohesive forces themselves are equilibrated from one lip to the other), the problem (2.80) *admits a unique solution that we will obtain in a closed form in the next subsection.*

The positions $\bar{\delta}$ and $\bar{\ell}$ of the non cohesive and cohesive crack tips are obtained in terms of the loading parameter $\bar{V}$ by using (2.69) which now read as

$$\begin{cases} \text{if} \quad \bar{\delta} = 0, \quad \text{then} \quad [\![\tilde{v}^1]\!](0) \leq 1, \quad \tilde{\mathcal{K}}^1 = 0 \\ \text{if} \quad \bar{\delta} > 0, \quad \text{then} \quad [\![\tilde{v}^1]\!](\bar{\delta}) = 1, \quad \tilde{\mathcal{K}}^1 = 0 \end{cases}, \tag{2.81}$$

where $\tilde{\mathcal{K}}^1$ denotes the stress intensity factor associated with the singularity of $\tilde{v}^1$ at $\bar{\ell}$.

2.4.4 Resolution of the inner problem in a closed form

It turns out that the solution of the problem (2.80) can be obtained in a closed form for arbitrary values of $\bar{V}$, $\bar{\delta}$ and $\bar{\ell}$ (with $0 \leq \bar{\delta} < \bar{\ell} < \infty$) by using the method of complex potentials [Muskhelishvili, 1963]. Indeed, $\tilde{v}^1$ is a harmonic function and hence can be considered as the real part of a holomorphic function in the complex plane $z = y_1 + iy_2$. Then, the problem (2.80) becomes an Hilbert' problem by using the following conformal mapping $z \mapsto Z$:

$$Z = z^{2\lambda}, \quad z = y_1 + iy_2, \qquad Z = Z_1 + iZ_2, \qquad Z_1 = R\cos\Theta, \quad Z_2 = R\sin\Theta.$$

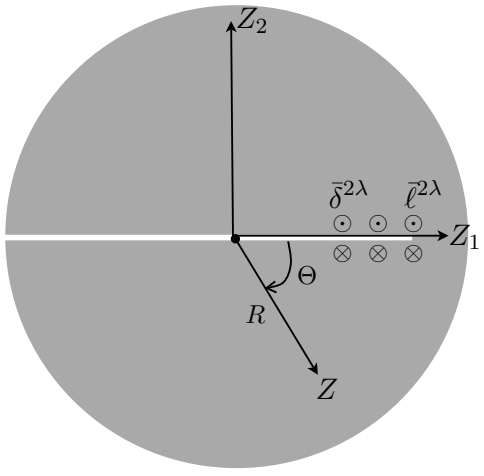

Figure 2.10: Setting of the inner plane in the Z-plane. The origin of the angle Θ is the axis Z_1 contrarily to the angle θ.

By this transform, the domain $\tilde{\Omega}^\infty$ is transformed into $\mathbb{R}^2 \setminus \big((-\infty, \bar{\ell}^{2\lambda}) \times \{0\}\big)$, the edges $\tilde{\Gamma}^\pm$ of the notch become the half line $(-\infty, 0) \times \{0\}$, the non cohesive crack is transformed into the line segment $(-0, \bar{\delta}^{2\lambda}) \times \{0\}$ and the cohesive crack is transformed into the line segment $(\bar{\delta}^{2\lambda}, \bar{\ell}^{2\lambda}) \times \{0\}$, see Figure 2.10. Denoting by V^1 the transformed of $\tilde{v}^1$, *i.e.*

$$V^1(Z_1, Z_2) = \tilde{v}^1(y_1, y_2),$$

V^1 is the unique solution of the following problem

$$\begin{cases} \Delta V^1 = 0 & \text{in} \quad \mathbb{R}^2 \setminus \big((-\infty, \bar{\ell}^{2\lambda}) \times \{0\}\big) \\ \dfrac{\partial V^1}{\partial Z_2} = \dfrac{1}{2\lambda} Z_1^{\frac{1}{2\lambda}-1} & \text{on} \quad (\bar{\delta}^{2\lambda}, \bar{\ell}^{2\lambda}) \times \{0\} \\ \dfrac{\partial V^1}{\partial n} = 0 & \text{on} \quad (-\infty, \bar{\delta}^{2\lambda}) \times \{0\} \\ V^1 \sim \bar{V}\sqrt{R}\sin\dfrac{\Theta}{2} & \text{at} \quad \text{infinity} \end{cases} . \tag{2.82}$$

Since V^1 is also a harmonic function, it is the real part of a holomorphic function f of the variable Z and one can set

$$f(Z) = V^1(Z_1, Z_2) + iW^1(Z_1, Z_2),$$

where W^1 is the imaginar part of $f(Z)$. Introducing $\Phi(Z) = if'(Z)$, one gets

$$\Phi(Z) := if'(Z) = \frac{\partial V^1}{\partial Z_2}(Z_1, Z_2) + i\frac{\partial V^1}{\partial Z_1}(Z_1, Z_2). \tag{2.83}$$

So we are in a situation where the real part of Φ, *i.e.* $\partial V^1/\partial Z_2$, is given on the half-line $(-\infty, \bar{\ell}^{2\lambda}) \times \{0\}$ and we can apply the usual results of Hilbert's problem, see Appendix 1.5. Specifically, since

$$\frac{\partial V^1}{\partial Z_2}(t, 0) = \begin{cases} 0 & \text{if} \quad -\infty < t < \bar{\delta}^{2\lambda} \\ \frac{1}{2\lambda} t^{\frac{1}{2\lambda}-1} & \text{if} \quad \bar{\delta}^{2\lambda} < t < \bar{\ell}^{2\lambda} \end{cases},$$

one obtains

$$\Phi(Z) = \frac{\bar{V}}{2\sqrt{Z - \bar{\ell}^{2\lambda}}} + \frac{1}{\pi\sqrt{Z - \bar{\ell}^{2\lambda}}} \int_{\bar{\delta}^{2\lambda}}^{\bar{\ell}^{2\lambda}} \frac{t^{\frac{1}{2\lambda}-1}}{2\lambda} \frac{\sqrt{\bar{\ell}^{2\lambda} - t}}{t - Z} dt. \tag{2.84}$$

In (2.84), the square root is defined by $\sqrt{Re^{i\Theta}} = \sqrt{R}\, e^{i\Theta/2}$. From the knowledge of Φ, one deduces f by integration (the constant of integration is obtained by the conditions at infinity) and hence V^1.

The condition on the tip of the cohesive zone: vanishing of the stress intensity factor $\tilde{\mathcal{K}}^1$

The tip of the cohesive zone is at $Z_c = \big(\bar{\ell}^{2\lambda}, 0\big)$. If one considers the behavior of $\Phi(Z)$ in the neighborhood of Z_c, (2.84) gives

$$\lim_{Z \to Z_c} \sqrt{Z - Z_c}\, \Phi(Z) = K := \frac{\bar{V}}{2} - \frac{1}{2\pi\lambda} \int_{\bar{\delta}^{2\lambda}}^{\bar{\ell}^{2\lambda}} \frac{t^{\frac{1}{2\lambda}-1}}{\sqrt{\bar{\ell}^{2\lambda} - t}} dt.$$

Hence, if $K \neq 0$, then the gradient of V^1 is singular and tends to infinity when Z tends to Z_c. In fact, K is proportional to the stress intensity factor $\mathcal{K}^1$ and therefore the condition (2.81) on $\bar{\ell}$ requires that $K = 0$. That leads to the first relation between $\bar{V}$, $\bar{\delta}$ and $\bar{\ell}$:

$$\bar{V} = \frac{1}{\pi\lambda} \int_{\bar{\delta}^{2\lambda}}^{\bar{\ell}^{2\lambda}} \frac{t^{\frac{1}{2\lambda}-1}}{\sqrt{\bar{\ell}^{2\lambda} - t}} dt. \tag{2.85}$$

After a change of variable in the integral, (2.85) becomes:

$$\bar{V} = \frac{2\bar{\ell}^{1-\lambda}}{\pi\lambda} \int_0^{\alpha_m} (\cos\alpha)^{\frac{1}{\lambda}-1} d\alpha \tag{2.86}$$

with

$$\alpha_m = \arccos\left(\frac{\bar{\delta}}{\bar{\ell}}\right)^{\lambda}. \tag{2.87}$$

Thus the parameter α_m gives the ratio between the length of the non cohesive crack and the total length of the crack.

In the first stage of the crack nucleation, when the non cohesive crack has not still appeared, $\bar{\delta} = 0$ and hence $\alpha_m = \pi/2$. Accordingly, during this stage where only the cohesive cracks exists, the length of the cohesive zone is given in terms of the load parameter $\bar{V}$ by the explicit relation:

$$\bar{V} = \frac{2\bar{\ell}^{1-\lambda}}{\pi\lambda} \int_0^{\pi/2} (\cos\alpha)^{\frac{1}{\lambda}-1} d\alpha. \tag{2.88}$$

Of course, this relation depends on the notch angle through the parameter $\lambda = \pi/\omega$. We can note that, as expected, $\bar{\ell}$ is a monotonically increasing function of $\bar{V}$ (provided that $\lambda < 1$, *i.e.* provided that $\omega > \pi$) which grows from 0 to ∞ when $\bar{V}$ does. However, this relation is only valid for $\bar{V}$ small enough because this stage will stop when the jump of the displacement at the tip of the notch reaches the critical value δ_c. To find the critical load $\bar{V}_c$ needs to determine this displacement jump. It is the goal of the next subsection.

Calculation of $[\![\tilde{v}^1]\!](\bar{\delta})$

Inserting (2.85) into (2.84), the function $\Phi(Z)$ reads now:

$$\Phi(Z) = -\frac{1}{2\pi\lambda} \sqrt{Z - \bar{\ell}^{2\lambda}} \int_{\bar{\delta}^{2\lambda}}^{\bar{\ell}^{2\lambda}} \frac{t^{\frac{1}{2\lambda}-1} dt}{(t - Z)\sqrt{\bar{\ell}^{2\lambda} - t}} \tag{2.89}$$

Let $Z_1 \in (\bar{\delta}^{2\lambda}, \bar{\ell}^{2\lambda})$ and $Z^{\pm} = Z_1 \pm i\,0$. Since $\sqrt{Z^{\pm} - \bar{\ell}^{2\lambda}} = \pm i\sqrt{\bar{\ell}^{2\lambda} - Z_1}$, Φ is discontinuous at $Z = Z_1$ and its jump reads as

$$[\![\Phi]\!](Z_1) = -\frac{i}{\pi\lambda} \sqrt{\bar{\ell}^{2\lambda} - Z_1} \int_{\bar{\delta}^{2\lambda}}^{\bar{\ell}^{2\lambda}} \frac{t^{\frac{1}{2\lambda}-1} dt}{(t - Z_1)\sqrt{\bar{\ell}^{2\lambda} - t}},$$

where the integral contains a kernel and hence must be understood in the sense of principal value. Using (2.83), one obtains the derivative of the jump of V across the cohesive crack. Specifically

$$\frac{d[\![V]\!]}{dZ_1}(Z_1) = -\frac{1}{\pi\lambda}\sqrt{\bar{\ell}^{2\lambda} - Z_1}\int_{\bar{\delta}^{2\lambda}}^{\bar{\ell}^{2\lambda}} \frac{t^{\frac{1}{2\lambda}-1}dt}{(t-Z_1)\sqrt{\bar{\ell}^{2\lambda}-t}}.$$

Using $[\![V^1]\!](\bar{\ell}^{2\lambda}) = 0$ and integrating the equation above over $(\bar{\delta}^{2\lambda}, \bar{\ell}^{2\lambda})$ give $[\![V^1]\!](\bar{\delta}^{2\lambda})$ and hence $[\![\tilde{v}^1]\!](\bar{\delta})$. Accordingly, one gets

$$[\![\tilde{v}^1]\!](\bar{\delta}) = [\![V^1]\!](\bar{\delta}^{2\lambda}) = \frac{1}{\pi\lambda}\int_{\bar{\delta}^{2\lambda}}^{\bar{\ell}^{2\lambda}}\int_{\bar{\delta}^{2\lambda}}^{\bar{\ell}^{2\lambda}} \frac{t^{\frac{1}{2\lambda}-1}}{\sqrt{\bar{\ell}^{2\lambda}-t}}\frac{\sqrt{\bar{\ell}^{2\lambda}-Z_1}}{t-Z_1}dtdZ_1$$

where the integral with respect to Z_1 is taken in the sense of the absolute value. This integral can be calculated in a closed form and one gets

$$[\![\tilde{v}^1]\!](\bar{\delta}) = \frac{1}{\pi\lambda}\int_{\bar{\delta}^{2\lambda}}^{\bar{\ell}^{2\lambda}} \frac{t^{\frac{1}{2\lambda}-1}}{\sqrt{\bar{\ell}^{2\lambda}-t}}\left(2\sqrt{\bar{\ell}^{2\lambda}-\bar{\delta}^{2\lambda}} + \sqrt{\bar{\ell}^{2\lambda}-t}\ \ln\frac{\sqrt{\bar{\ell}^{2\lambda}-\bar{\delta}^{2\lambda}} - \sqrt{\bar{\ell}^{2\lambda}-t}}{\sqrt{\bar{\ell}^{2\lambda}-\bar{\delta}^{2\lambda}} + \sqrt{\bar{\ell}^{2\lambda}-t}}\right)dt. \tag{2.90}$$

Making the change of variables $t = \bar{\ell}^{2\lambda}\cos^2\alpha$ into the integral above, one gets

$$[\![\tilde{v}^1]\!](\bar{\delta}) = \frac{4\bar{\ell}}{\pi\lambda}\int_0^{\alpha_m} \cos\alpha^{\frac{1}{\lambda}-1}\Big(\sin\alpha_m + \frac{\sin\alpha}{2}\ln\frac{\sin\alpha_m - \sin\alpha}{\sin\alpha_m + \sin\alpha}\Big)d\alpha, \tag{2.91}$$

where α_m is given by (2.87). To discuss the properties of the integral above, it is sometimes more convenient to make the change of variable $\alpha \mapsto \zeta = \sin\alpha/\sin\alpha_m$. That leads to

$$[\![\tilde{v}^1]\!](\bar{\delta}) = \frac{4\bar{\ell}\sin^2\alpha_m}{\pi\lambda}\int_0^1 (1-\zeta^2\sin^2\alpha_m)^{\frac{1}{2\lambda}-1}\Big(1+\frac{\zeta}{2}\ln\frac{1-\zeta}{1+\zeta}\Big)d\zeta. \tag{2.92}$$

The first stage of the nucleation of the crack, when $\bar{\delta} = 0$

Let us consider the first stage of the crack nucleation, when $\bar{\delta}$ is still equal to 0. Then, $\alpha_m = \pi/2$ and (2.91) gives

$$[\![\tilde{v}^1]\!](0) = \frac{4\bar{\ell}}{\pi\lambda}\int_0^{\frac{\pi}{2}} (\cos\alpha)^{\frac{1}{\lambda}-1}\Big(1+\frac{\sin\alpha}{2}\ln\frac{1-\sin\alpha}{1+\sin\alpha}\Big)d\alpha.$$

Hence $[\![\tilde{v}^1]\!](0)$ is proportional to the length of the cohesive crack with a coefficient of proportionality which is positive and depends on the notch angle through λ. By virtue of (2.81), $[\![\tilde{v}^1]\!](0)$ must be smaller than 1 as long as $\bar{\delta} = 0$. Therefore the first stage of the crack nucleation will finish when $[\![\tilde{v}^1]\!](0) = 1$ and hence when $\bar{\ell}$ reaches the critical value $\bar{\ell}_c$ given by

$$\bar{\ell}_c = \frac{\pi\lambda}{4\displaystyle\int_0^{\pi/2}(\cos\alpha)^{\frac{1}{\lambda}-1}\Big(1+\frac{\sin\alpha}{2}\ln\frac{1-\sin\alpha}{1+\sin\alpha}\Big)d\alpha}. \tag{2.93}$$

Since $\bar{\ell}$ is a monotonically increasing function of the loading parameter $\bar{V}$ during this stage, the first stage of the crack nucleation will finish when $\bar{V}$ reaches the critical value $\bar{V}_c$ given by

$$\bar{V}_c = \frac{2}{\pi\lambda}\bar{\ell}_c^{1-\lambda}\int_0^{\pi/2}(\cos\alpha)^{\frac{1}{\lambda}-1}d\alpha. \tag{2.94}$$

ω	π	$7\pi/6$	$4\pi/3$	$3\pi/2$	$5\pi/3$	$11\pi/6$	2π
λ	1	6/7	3/4	2/3	3/5	6/11	1/2
$\bar{\ell}_c$	∞	3.3332	1.8215	1.3110	1.0516	0.8931	0.7854
$\bar{V}_c$	1	1.2471	1.2756	1.2522	1.2128	1.1699	1.1284

Table 2.4: The values of $\bar{\ell}_c$ and $\bar{V}_c$ for some values of ω

Both critical values $\bar{\ell}_c$ and $\bar{V}_c$ only depend on the notch angle. Their values are given in Table 2.4 for some values of ω whereas the graphs giving their dependence on ω are plotted on Figure 2.11. It turns out that $\bar{\ell}_c$ decreases from infinity to $\pi/4$ when ω increases from π to 2π. On the other hand, the variations of $\bar{V}_c$ with ω is not monotonic. However, the dependence of $\bar{V}_c$ on ω is rather weak. Accordingly, its value for any notch is quite similar to the value for a prexisting crack (but the order of magnitude of the true critical loading U_η strongly depends on ω, see (2.78)).

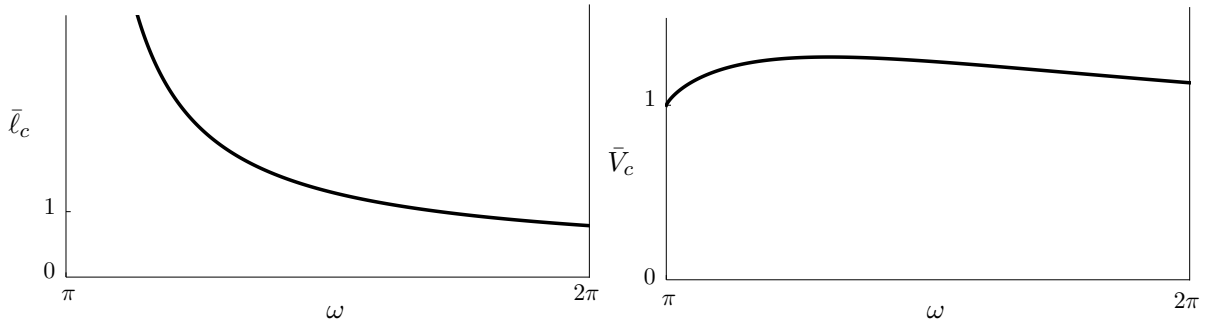

Figure 2.11: Graphs of the dependence of $\bar{\ell}_c$ and $\bar{V}_c$ on ω

Beyond the first stage of the crack nucleation

After the first stage, if one increases $\bar{V}$ beyond the critical value $\bar{V}_c$, a non cohesive crack necessarily appears at the angle of the notch. Let us try to find its evolution by assuming that the body is always in a stable equilibrium state. In that case $\bar{V}$, $\bar{\delta}$ and $\bar{\ell}$ must be such that $\tilde{\mathcal{K}}^1 = 0$ and $[\![\tilde{v}^1]\!](\bar{\delta}) = 1$.

Therefore, one deduces from (2.91) that $\bar{\ell}$ is given in terms of the parameter α_m by

$$\bar{\ell} = \frac{\pi\lambda}{4\displaystyle\int_0^{\alpha_m} (\cos\alpha)^{\frac{1}{\lambda}-1}\Big(\sin\alpha_m + \frac{\sin\alpha}{2}\ln\frac{\sin\alpha_m - \sin\alpha}{\sin\alpha_m + \sin\alpha}\Big)d\alpha}. \tag{2.95}$$

Using the definition (2.87) of α_m, one obtains $\bar{\delta}$ in terms of α_m

$$\bar{\delta} = \frac{\pi\lambda\ (\cos\alpha_m)^{\frac{1}{\lambda}}}{4\displaystyle\int_0^{\alpha_m} (\cos\alpha)^{\frac{1}{\lambda}-1}\Big(\sin\alpha_m + \frac{\sin\alpha}{2}\ln\frac{\sin\alpha_m - \sin\alpha}{\sin\alpha_m + \sin\alpha}\Big)d\alpha}. \tag{2.96}$$

Finally, (2.86) gives also $\bar{V}$ in terms of α_m by using (2.95):

$$\bar{V} = \frac{2\bar{\ell}^{1-\lambda}}{\pi\lambda}\int_0^{\alpha_m} (\cos\alpha)^{\frac{1}{\lambda}-1}d\alpha. \tag{2.97}$$

Therefore (2.95)–(2.97) give the evolution in terms of the parameter α_m. It turns out that $\bar{\delta}$ is a monotonically decreasing function of α_m which grows from 0 to ∞ when α_m decreases from $\pi/2$ to 0. Recalling that, by (2.87), $\cos\alpha_m$ represents the ratio between the length of the non cohesive crack and the total length of the crack (including its non cohesive part), this monotonicity property of $\bar{\delta}$ with respect to α_m means that the relative length of the cohesive crack with respect to the total crack length decreases and even goes to 0 when the crack propagates. On the other hand $\bar{V}$ is a monotonically increasing function of α_m which decreases from $\bar{V}_c$ to 0 when α_m decreases from $\pi/2$ to 0. That means that one must decrease the loading after the end of the first stage if one wants to control the growth of the non cohesive crack. Therefore, $\bar{V}_c$ is a limit loading beyond which the propagation of the non cohesive crack is necessarily unstable. One can consider that $\bar{V}_c$ is the critical load at which a macroscopic crack nucleates. Indeed, since $\bar{V}$ is decreasing to 0 when $\bar{\delta}$ goes to infinity, one can only recover a stable equilibrium state for values of δ_η which are of another order of magnitude than those used in this asymptotic approach. In fact the new equilibrium state must be such that the crack length is larger than ℓ_{m}, see Figure 2.5 and the analysis made in the Griffith setting at the beginning of this chapter. To illustrate these purposes, one plots on Figure 2.12 the curve $\bar{\delta}$–$\bar{V}$ parametrized by α_m for $\omega = 3\pi/2$. One represents also in this figure the relation between $\bar{\ell}$ and $\bar{V}$ during the first stage of nucleation of the crack. Moreover, the dashed line represents the critical load at which the *G-law* predicts that a preexisting crack of length $\bar{\delta}$ at the tip of the notch should propagate. One sees that the curve $\bar{\delta}$–$\bar{V}$ converges asymptotically to that predicted by *G-law* when the length of the preexisting tends to infinity (at this scale). This convergence is due to the fact that α_m goes to 0 and hence the length of the cohesive crack becomes small by comparison with the length of the non cohesive crack. Consequently, the influence of the cohesive crack becomes negligible and one recovers Griffith

law. However, this convergence has no practical interest because this part of the response cannot be observed. It remains the fundamental difference between *D-law* and *G-law*: the critical load at which a crack nucleates with the *D-law* is finite while it is infinite with the *G-law*.

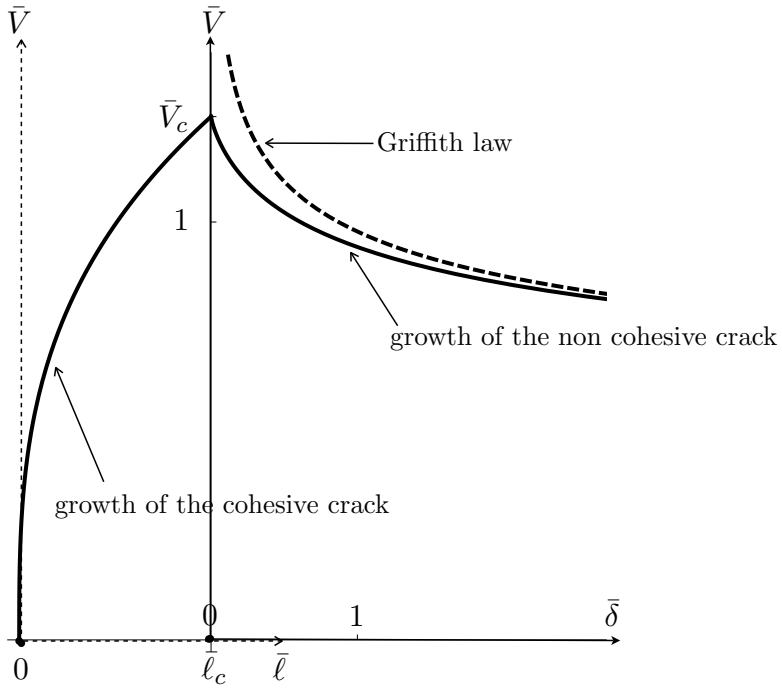

Figure 2.12: The curve on the negative side of the axis $\bar{\delta}$ corresponds to the relation between the load parameter $\bar{V}$ and the length of the cohesive crack $\bar{\ell}$ during the first stage of the crack nucleation (before the apparition of the non cohesive crack), see (2.88). The plain curve on the positive side of the axis $\bar{\delta}$ represents the graph of the relation between the load parameter $\bar{V}$ and the length of the non cohesive crack $\bar{\delta}$ (once the non cohesive crack is appeared) given by Dugdale's model for $\omega = 3\pi/2$, see (2.96)-(2.97). The dashed line represents the load at which the *G-law* predicts that a preexisting crack of length $\bar{\delta}$ should propagate.

On Figure 2.13 one plots the relation between the total length of the crack $\bar{\ell}$ and the loading parameter $\bar{V}$. Therefore the first part of the curve, starting at $(0, 0)$ and finishing at $(\bar{\ell}_c, \bar{V}_c)$, corresponds to the stage of the nucleation process where the cohesive crack alone exists. When the non cohesive crack appears, one sees that there is a snap-back which means that one must decrease the loading but also that the total length of the crack is decreasing. Comparing with Figure 2.12 where the non cohesive crack length is in the same time increasing, one concludes that the decreasing of the total length is due in fact to a decreasing of the cohesive crack length. Of course, such a behavior is not really compatible with an irreversibility principle and should disappear if one treated the problem by taking into account the irreversibility. But, since this part of the response is not really interesting in practice, such an extended study is unnecessary.

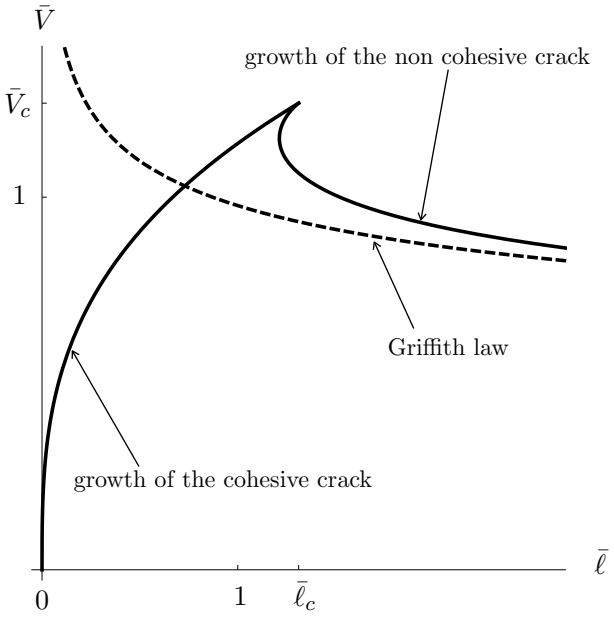

Figure 2.13: Graph of the relation between the load parameter $\bar{V}$ and the total length of the crack $\bar{\ell}$ given by Dugdale's model for $\omega = 3\pi/2$, see (2.95)-(2.97). The first part of the curve (until $(\bar{\ell}_c, \bar{V}_c)$) corresponds to the first stage of the nucleation when the non cohesive crack has not still appeared. Then the second part, when the non cohesive crack is appeared, presents a snap-back before to converge to the curve predicted by *G-law*(dashed line).

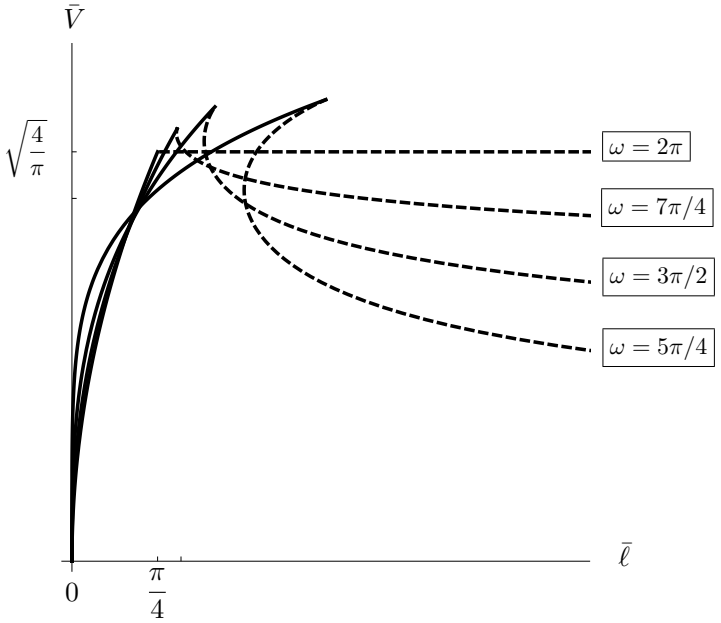

Figure 2.14: The two stages of the crack nucleation associated to several values of ω in a diagram $(\bar{\ell}, \bar{V})$ like in Figure 2.13.

Finally, the dependence of the response on the notch angle is illustrated on Figure 2.14. Note that in the case where $\omega = 2\pi$, *i.e.* when the notch is a crack, then the loading parameter remains constant and equal to $\bar{V}_c = \sqrt{4/\pi}$ when the non cohesive crack appears, in conformity with *G-law* and *FM-law*. Note also that the snap-back exists for sufficiently small values of ω only.

Remark 2.8. *In the case of a preexisting crack, i.e. when $\omega = 2\pi$, one can see on Figure 2.14 that $\bar{V}$ remains constant and equal to $\bar{V}_c$ when $\bar{\delta} \geq 0$. This result is in agreement with those obtained with* FM-law *(which is equivalent to* G-law *in that case). Moreover, the values of ℓ_c and $\bar{V}_c$ are obtained in a closed form. Specifically* (2.94) *and* (2.93) *give*

$$\bar{\ell}_c = \frac{\pi}{4}, \quad \bar{V}_c = \sqrt{\frac{4}{\pi}} \qquad \textit{when} \quad \omega = 2\pi.$$

2.4.5 Comparison of the crack nucleation criteria

This last section is devoted to the comparison of the crack nucleation predicted either by the cohesive model criterion or the FM-criterion. Let us recall that the former is based on local minimization of the energy while the latter needs to consider global minima of the energy. Moreover the two criteria differ by the form of the energy, the former one contains a cohesive surface energy while the latter uses Griffith's surface energy. In Section 2.3, by using the **MAM**, we have calculated the first crack ℓ_{i} and a corresponding critical load $U_i = \mathsf{t}_{\mathsf{i}} H$ predicted by FM-criterion. Specifically, Proposition 2.5 is repeated here with notations conform to those used in the cohesive case. It reads now as

Proposition 2.8. *For the* FM-law*: in the case of a genuine notch, i.e. when the notch angle $\omega \neq 2\pi$, then the displacement U_i at which the crack nucleates and the length ℓ_{i} of the nucleated crack at this time are approximated with the MAM 4 by*

$$\frac{\ell_{\mathsf{i}}}{H} \approx \left(\frac{(2\lambda-1)|P_2(\lambda)|}{(4\lambda-1)|P_4(\lambda)|}\right)^{\frac{1}{2\lambda}}, \qquad U_i^2 \approx \frac{\mathsf{G_c} H}{8\mu\lambda^3}\left(\frac{4\lambda-1}{|P_2(\lambda)|}\right)^{2-\frac{1}{2\lambda}}\left(\frac{4P_4(\lambda)}{2\lambda-1}\right)^{1-\frac{1}{2\lambda}}, \tag{2.98}$$

where $\lambda = \pi/\omega$ and the dimensionless coefficients P_2 and P_4 depend on ω only.

On the other hand, in Dugdale's approach, the nucleation of a non cohesive crack occurs when the load reaches a critical value given by (2.93) and (2.94).

Proposition 2.9. *For the* D-law*: when $\pi < \omega < 2\pi$, the critical load at which a macroscopic crack nucleates is given in terms of geometrical and material parameters by*

$$U_c = \frac{\bar{V}_c}{(-b_1^1)}\left(\frac{\sigma_c H}{\mu\delta_c}\right)^{\lambda}\delta_c \tag{2.99}$$

with

$$\bar{V}_c = \frac{4^{\lambda-\frac{1}{2}}}{(\lambda\pi)^{\lambda}} \frac{\displaystyle\int_0^{\pi/2} (\cos\theta)^{\frac{1}{\lambda}-1} d\theta}{\displaystyle\left(\int_0^{\pi/2} (\cos\theta)^{\frac{1}{\lambda}-1} \Big[1 + \frac{\sin\theta}{2} \ln\Big(\frac{1-\sin\theta}{1+\sin\theta}\Big) \Big] d\theta \right)^{1-\lambda}} \tag{2.100}$$

where the coefficient b_1^1 is obtained by determining the first outer term $\tilde{u}^0$. Moreover, at this critical loading, the length of the crack (which is still a "pure" cohesive crack) is given by

$$\ell_c = \frac{\pi\lambda}{4\displaystyle\int_0^{\pi/2} (\cos\alpha)^{\frac{1}{\lambda}-1} \Big(1 + \frac{\sin\alpha}{2} \ln\frac{1-\sin\alpha}{1+\sin\alpha}\Big) d\alpha} \frac{\mu}{\sigma_c} \delta_c. \tag{2.101}$$

Hence ℓ_c only depends on the angle of the notch and on the materials parameters. It is independent on the global geometry (and hence on the size of the body) provided that the characteristic material length d_c is small by comparison to the size H of the body.

In the formula for U_i in the virtue of FM-criterion which is obtained by MAM 4, we see that $U_i \sim \sqrt{H}$. On the other hand, in the formula (2.99) given by the *D-law*, $U_c^{\infty} \sim H^{\lambda}$. Comparing the two criteria leads to:

$$\frac{U_c}{U_i} = \Big(\frac{H}{d_c}\Big)^{\lambda-1/2} A(\lambda), \tag{2.102}$$

where $A(\lambda)$ is the function of λ given by

$$A(\lambda) = \frac{\bar{V}_c}{-b_1^1} \sqrt{8\lambda^3} \left(\frac{4\lambda-1}{|P_2(\lambda)|}\right)^{\frac{1}{4\lambda}-1} \left(\frac{4P_4(\lambda)}{2\lambda-1}\right)^{\frac{1}{4\lambda}-\frac{1}{2}}. \tag{2.103}$$

The values of $A(\lambda)$ for some values of λ are given in Table 2.5. From this numerical result, we see that the function $A(\lambda)$ is weakly decreasing in this range of values of λ (and for this particular geometry).

ϵ	0	0.05	0.1	0.15	0.2	0.25	0.3	0.35	0.4
λ	0.5	0.5081	0.5164	0.5249	0.5335	0.5423	0.5511	0.5600	0.5689
$A(\lambda)$	1.	0.9760	0.9617	0.9517	0.9444	0.9400	0.9364	0.9351	0.9342

Table 2.5: The value of function $A(\lambda)$ corresponding to some values of λ.

In Table 2.6, we give the values of U_i/δ_c and U_c/δ_c corresponding to the two methods when $H = d_c$. In that particular case, the values of U_i/δ_c and U_c/δ_c are close to each other.

ϵ	0	0.1	0.2	0.3	0.4
λ	0.5	0.5164	0.5335	0.5511	0.5689
U_i/δ_c by MAM 4	1.44038	1.58969	1.73182	1.88457	2.05813
U_c/δ_c by (2.99)	1.44039	1.52874	1.63563	1.76476	1.92274

Table 2.6: Comparison of the values of U_i/δ_c obtained by FM-criterion which are calculated by MAM 4, and those of U_c^∞/δ_c calculated by the analytic formula of Proposition 2.9 when $H = d_c$.

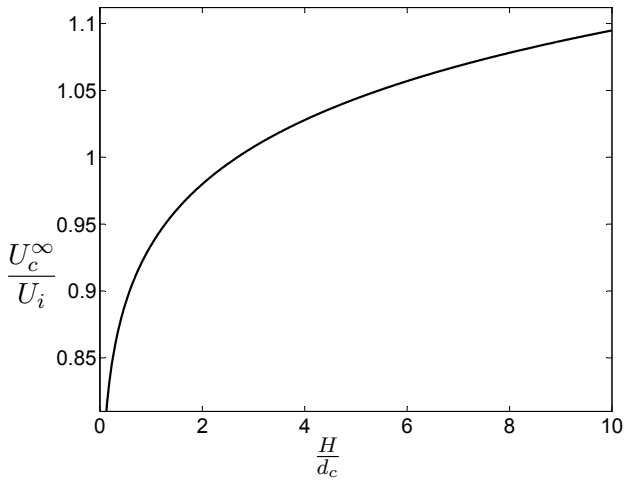

Figure 2.15: The comparison between U_c and U_i with respect to the value of H/d_c for $\omega = 5.5222$ and hence $\lambda = 0.5689$

The ratio U_c/U_i obviously depends on the ratio H/d_c at given ω. As we can see in Figure 2.15, when $H \gg d_c$, *i.e.* when the size of the body is large by comparison with the characteristic length of the material, *FM-law* predicts a crack nucleation earlier then *D-law*. Conversely, when $H \ll d_c$, *D-law* predicts a crack nucleation earlier than *FM-law*. These theoretical results should be compared with experimental results. In particular, the comparison of the measured critical load at which a macroscopic crack nucleates with those predicted by the two laws could allow one to discriminate between those laws and then to see which is the good law.

Chapter 3

Generalization to plane elasticity

3.1 Introduction

This chapter investigates the differences and the similarities between the properties of *FM-law* and *G-law* for the nucleation of a crack at the angle of a notch, in the plane elasticity setting. As in Chapter 2, the angle ω of the notch is given in terms of the parameter ϵ by

$$\omega = 2\pi - 2\arctan(\epsilon).$$

3.2 Case of a non cohesive crack

Let us recall the main assumptions associated with the Griffith setting of a non cohesive crack:

1. The elastic energy is supposed to be a 2-homogeneous function of the load t. So that, at equilibrium under the loading t when the crack length is ℓ, the potential energy reads as

$$\mathcal{P}_\epsilon(\mathsf{t}, \ell) = \mathsf{t}^2 \mathcal{P}_\epsilon(\ell).$$

2. The surface energy of the body depends only on the crack length, $\mathcal{S}(\ell)$, see (2.33). Therefore, the total energy of the body, at equilibrium under the loading t and with a crack of length ℓ, is given by

$$\mathcal{E}_\epsilon(\mathsf{t}, \ell) = \mathsf{t}^2 \mathcal{P}_\epsilon(\ell) + \mathcal{S}(\ell).$$

Under these assumptions, we can use the main theoretical results established in Chapter 2 and recalled hereafter, see Propositions 2.2, 2.3 and 2.4. When $\epsilon = 0$, *FM-law* and *G-law* have the same unique solution. When $\epsilon > 0$, *G-law* fails to predict the crack nucleation because $\mathcal{G}_\epsilon(0) := -\mathcal{P}'_\epsilon(0) = 0$. Indeed, the body is always in stable state and the crack will never appear. On the other hand, *FM-law* predicts that there exists a critical load, denoted t_i, at which the crack will jump from 0 to an finite length $\ell_\mathsf{i} > 0$. After this brutal nucleation, *FM-law* says that the evolution of the crack is continuous in time and follows the *G-law*. The aim of this section is to find a formula for the energy release rate $\mathcal{G}_\epsilon(\ell)$ as a function of ϵ and ℓ. It is based on the $G - \theta$ method developed in [Destuynder and Djaoua, 1981], see §2.2.1.

The geometry of the body is two-dimensional as in the previous sections and we adopt the framework of plane strain with small deformation in equilibrium state, see Figure 3.1. The origin of the coordinates $\mathbf{x} = (x_1, x_2)$ is placed at the tip of the notch. The axis $x_1$corresponds to the line segment of the crack Γ_ℓ. Thus, if one denotes $\Omega = (-H, L) \times (-H, +H)$, one removes from Ω the notch $\mathcal{N}$,

$$\mathcal{N} = \{\mathbf{x} = (x_1, x_2) \,:\, -H < x_1 \leq 0, |x_2| \leq \epsilon\,|x_1|)\}, \tag{3.1}$$

where ϵ is a given parameter in $(0,1)$. Finally the notch-shaped body is $\Omega_0 = \Omega \setminus \mathcal{N}$. The crack is $\Gamma_\ell = (0,\ell)\times\{0\}$ and the cracked body Ω_ℓ,

$$\Omega_\ell = \Omega_0 \setminus \Gamma_\ell.$$

The strain field, denoted by $\boldsymbol{\varepsilon}(\mathbf{u})$, has the form:

$$\boldsymbol{\varepsilon}(\mathbf{u}) = \varepsilon_{11}\big(\mathbf{e}_1 \otimes \mathbf{e}_1\big) + \varepsilon_{12}\big(\mathbf{e}_1 \otimes \mathbf{e}_2\big) + \varepsilon_{21}\big(\mathbf{e}_2 \otimes \mathbf{e}_1\big) + \varepsilon_{22}\big(\mathbf{e}_2 \otimes \mathbf{e}_2\big) \tag{3.2}$$

where all the components relative to x_3 vanish, *i.e.* $\varepsilon_{13} = \varepsilon_{31} = \varepsilon_{23} = \varepsilon_{32} = \varepsilon_{33} = 0$. The relations between the strain field and the displacement field are governed by the classical relation in the linear elasticity setting:

$$\boldsymbol{\varepsilon}(\mathbf{u}) = \frac{1}{2}(\nabla\mathbf{u} + \nabla^T\mathbf{u}). \tag{3.3}$$

The stress field obeys the Hooke's law:

$$\sigma_{ij}(\boldsymbol{\varepsilon}) = \lambda Tr(\boldsymbol{\varepsilon})\delta_{ij} + 2\mu\varepsilon_{ij}, \tag{3.4}$$

with λ and μ the two Lamé constants (λ is no more π/ω throughout chapter 3).

Supposing that the body forces are negligible, the equilibrium state $\mathbf{u}_\epsilon^\ell$ is a solution of the volumic equation where $\boldsymbol{\sigma}_\epsilon^\ell$ stands for the stress field associated to the displacement field $\mathbf{u}_\epsilon^\ell$:

$$\operatorname{div}\boldsymbol{\sigma}_\epsilon^\ell = 0 \quad \text{in} \quad \Omega_\epsilon^\ell. \tag{3.5}$$

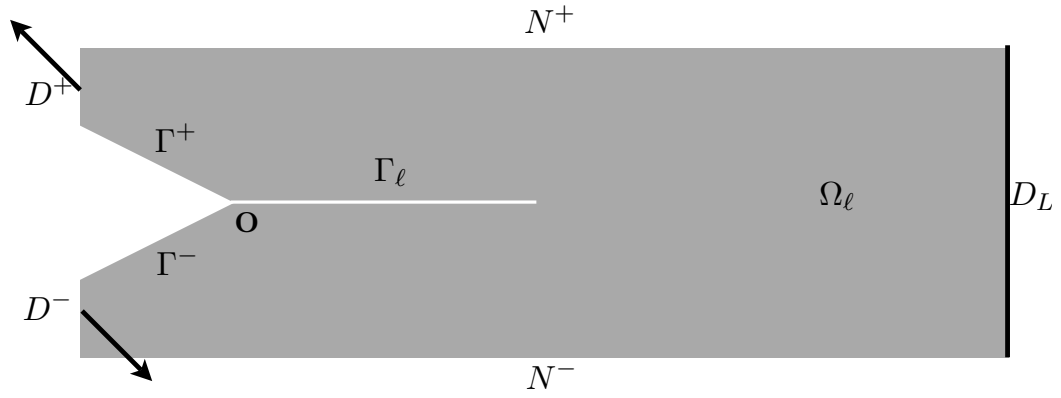

Figure 3.1: The domain Ω_ϵ^ℓ of the elasticity problem in 2D

Moreover, the body is submitted to a mixed mode loading on $D^\pm$ which is expressed by the Dirichlet's condition :

$$\mathbf{u}_\epsilon^\ell = \pm\mathsf{t}\big(\mathbf{e}_1 + \mathbf{e}_2\big) \quad \text{on} \quad D^\pm, \tag{3.6}$$

while the body is fixed on $D_L = \{L\} \times [-H, H]$ by the condition :

$$\mathbf{u}_\epsilon^\ell = \mathbf{0} \quad \text{on} \quad D_L. \tag{3.7}$$

The free stress condition $\boldsymbol{\sigma}\mathbf{n} = \mathbf{0}$ holds both on the lips of the crack Γ_ℓ and on the upper and the lower edges $N^+ \cup N^-$.

For $\mathbf{u} \in (H^1(\Omega_\epsilon^\ell))^2$, the associated elastic energy is given by

$$\mathcal{E}(\mathbf{u}) := \frac{1}{2}\int_{\Omega_\epsilon^\ell} \sigma_{ij}\varepsilon_{ij}\, d\mathbf{x} \quad \text{for } \boldsymbol{\varepsilon} := \varepsilon(\mathbf{u}) \text{ and } \boldsymbol{\sigma} := \boldsymbol{\sigma}(\boldsymbol{\varepsilon}).$$

Moreover, assuming that the material is isotropic, the energy takes the form

$$\mathcal{E}(\mathbf{u}) \;=\; \frac{1}{2}\int_{\Omega_\epsilon^\ell} \Big((\lambda + 2\mu)\big(u_{1,1}^2 + u_{2,2}^2\big) + \mu\big(u_{1,2} + u_{2,1}\big)^2 + 2\lambda u_{1,1}u_{2,2} \Big) d\mathbf{x}. \tag{3.8}$$

As far as the elastic energy at equilibrium is concerned, since the energy is a quadratic function of the loading, it is given by

$$\mathcal{P}_\epsilon(\mathsf{t}, \ell) := \mathcal{E}(\mathbf{u}_\epsilon^\ell) := \mathsf{t}^2 \mathcal{P}_\epsilon(\ell), \tag{3.9}$$

where $\mathcal{P}_\epsilon(\ell)$ denotes the elastic energy of the body at equilibrium under the external unit load $\pm\big(\mathbf{e}_1 + \mathbf{e}_2\big)$ on $D^\pm$.

The set of admissible displacements associated with a unit load reads as

$$\mathcal{U}_\epsilon^\ell = \{\mathbf{u} \in (H^1(\Omega_\epsilon^\ell))^2 : \mathbf{u} = \pm(\mathbf{e}_1 + \mathbf{e}_2) \quad \text{on} \quad D^\pm,\ \mathbf{u} = \mathbf{0} \quad \text{on} \quad D_L\}. \tag{3.10}$$

By the minimimum energy principle, $\mathbf{u}_\epsilon^\ell$ can read as $t\mathbf{U}_\epsilon^\ell$ where $\mathbf{U}_\epsilon^\ell$ realizes the minimum of the elastic energy on $\mathcal{U}_\epsilon^\ell$. Specifically,

$$\mathcal{P}_\epsilon(\ell) = \min_{\mathbf{u} \in \mathcal{U}_\epsilon^\ell} \mathcal{E}(\mathbf{u}). \tag{3.11}$$

The associated linear space associated with the affine space $\mathcal{U}_\epsilon^\ell$ is

$$\mathcal{V}_\epsilon^\ell = \{\mathbf{v} \in H^1(\Omega_\epsilon^\ell) \;:\; \mathbf{v} = \mathbf{0} \quad \text{on} \quad D^+ \cup D^- \cup D_L\}. \tag{3.12}$$

Define $\bar{\mathbf{U}}_0 = \operatorname{sign}(x_2) \max\Big\{ -\frac{x_1}{H}, 0 \Big\}\big(\mathbf{e}_1 + \mathbf{e}_2\big)$. Its restriction to Ω_ϵ^ℓ is in $\mathcal{U}_\epsilon^\ell$ for every $\epsilon \in [0, 1)$. Write $\mathbf{u} = \bar{\mathbf{U}}_0 + \mathbf{v}$ with $\mathbf{v} \in \mathcal{V}_\epsilon^\ell$. Consequently, the potential energy can be rewritten as a minimum over the linear space $\mathcal{V}_\epsilon^\ell$:

$$\begin{aligned} \mathcal{P}_\epsilon(\ell) \;&=\; \min_{\mathbf{v} \in \mathcal{V}_\epsilon^\ell} \frac{1}{2}\Big\{ \int_{\Omega_\epsilon^l} \Big((\lambda + 2\mu)\big(v_{1,1}^2 + v_{2,2}^2\big) + \mu\big(v_{1,2} + v_{2,1}\big)^2 + 2\lambda v_{1,1}v_{2,2} \Big) d\mathbf{x} \\ &-\; \int_{\mathcal{N}_\epsilon^c} \frac{\operatorname{sign}(x_2)}{H} \Big(2(\lambda + 2\mu)v_{1,1} + 2\mu\big(v_{1,2} + v_{2,1}\big) + 2\lambda v_{2,2} \Big) d\mathbf{x} + (\lambda + 3\mu)(2 - \epsilon) \Big\} \end{aligned} \tag{3.13}$$

Throughout the following sections we will use the following notations.

Notations We note $\mathcal{I}_\ell$ the cross-section of the body at $\ell \in [0, L]$, i.e. $\mathcal{I}_\ell = \{\ell\} \times (-H, H)$, and $\mathcal{R}^d_\ell$ the rectangle delimited by the cross-section $\mathcal{I}_\ell$ and $\mathcal{I}_d$, $0 \leq \ell < d \leq L$, and $\underline{\mathcal{I}}_\ell = \mathcal{I}_\ell \setminus \{0\} \times (-H, H)$, as well as $\underline{\mathcal{R}}^d_\ell = \mathcal{R}^d_\ell \setminus (\ell, d) \times \{0\}$. Firstly, we consider for the case that $\epsilon \in [0, 1)$ and $\ell \in (0, L)$, the derivative of $\mathcal{P}_\epsilon(\ell)$ w.r.t ℓ can be found as in the following proposition. This case corresponds to the preexisting crack inside the body.

Proposition 3.1. *(Case $0 \leq \epsilon < 1$ and $0 < \ell < L$) For each $\epsilon \in [0, 1)$, $\ell \mapsto P_\epsilon(\ell)$ is indefinitely differentiable on $(0, L)$. Moreover the first derivative P'_ϵ can read as :*

$$\begin{aligned} \mathcal{P}'_\epsilon(\ell) &= \frac{1}{\ell} \int_{\underline{R}^\ell_0} \left(\frac{\lambda + 2\mu}{2} \Big(U^2_{2,2} - U^2_{1,1} \Big) + \frac{\mu}{2} \Big(U^2_{1,2} - U^2_{2,1} \Big) \right) d\mathbf{x} \\ &- \frac{1}{L - \ell} \int_{R^L_\ell} \left(\frac{\lambda + 2\mu}{2} \Big(U^2_{2,2} - U^2_{1,1} \Big) + \frac{\mu}{2} \Big(U^2_{1,2} - U^2_{2,1} \Big) \right) d\mathbf{x}, \end{aligned} \tag{3.14}$$

where $\mathbf{U} = (U_1, U_2)$ stands for $\mathbf{U}^\ell_\epsilon$.

Proof. (See Appendix 3.A.1) The proof maps Ω^ℓ_ϵ into a fixed Ω^d_ϵ for $d \in (0, L)$. This leads to an explicit minimization problem in the variable ℓ. Applying the results of Lemma 3.2 gives us the derivability, and the formula (3.14) is easy to obtain. □

The computation of $\mathcal{P}'_\epsilon(\ell)$ involves a two-dimensional integral. In fact it can be simplified into the sum of two one-dimensional integrals, as stated in the next proposition.

Proposition 3.2. *For fixed $\ell \in (0, L)$, let $\mathcal{I}_\ell$ be the cross-section of Ω^ℓ_ϵ, and $\underline{\mathcal{I}}_\ell = \mathcal{I}_\ell \setminus \{0\} \times (-H, H)$ the cracked cross-section. Define*

$$\mathcal{J}_{\underline{\mathcal{I}}_l} = \int_{\underline{\mathcal{I}}_l} \left(\frac{\lambda + 2\mu}{2} (U^2_{2,2} - U^2_{1,1}) + \frac{\mu}{2} (U^2_{1,2} - U^2_{2,1}) \right) dx_2. \tag{3.15}$$

then $\mathcal{J}_{\underline{\mathcal{I}}_l}$ is independent of l for $l \in (0, \ell)$, the common value is denoted $J^-_\epsilon(\ell)$. Similarly, $\mathcal{J}_{\underline{\mathcal{I}}_l}$ is independent of l for $l \in (\ell, L)$, the common value is denoted $J^+_\epsilon(\ell)$. Therefore $P'_\epsilon(\ell) = J^-_\epsilon(\ell) - J^+_\epsilon(\ell)$ for all $\ell \in (0, L)$.

Proof. Taking $l_1 < l_2 < \ell$, it suffices to multiply the equilibrium equation $\mathrm{div}\boldsymbol{\sigma} = 0$ by $\mathbf{U}$ and integrate by parts over $R^{\ell_2}_{\ell_1}$ to see that $\mathcal{J}_{\underline{\mathcal{I}}_l}$ is independent of l. Inserting into (3.14) gives the last identity. □

The change of variable in Proposition 3.1 is no more valid when $\ell = 0$. However, when $\epsilon = 0$, *i.e.* when the body contains an initial crack of length H instead of a notch, we can define $\mathcal{P}_0$ on the whole interval $(-H, L)$, prove its regularity and compute its derivative.

Proposition 3.3. *(Case $\epsilon = 0$ and $\ell = 0$) $\mathcal{P}_0$ is indefinitely differentiable on (-H, L). Moreover, the first derivative ${\mathcal{P}'}_0$ is given by*

$$\begin{aligned} {\mathcal{P}'}_0(\ell) &= \frac{1}{H+\ell}\int_{\underline{R}^{\ell}_{-H}} \left(\frac{\lambda+2\mu}{2}\Big(U^2_{2,2}-U^2_{1,1}\Big)+\frac{\mu}{2}\Big(U^2_{1,2}-U^2_{2,1}\Big)\right)d\mathbf{x} \\ &- \frac{1}{L-\ell}\int_{\underline{R}^{L}_{\ell}} \left(\frac{\lambda+2\mu}{2}\Big(U^2_{2,2}-U^2_{1,1}\Big)+\frac{\mu}{2}\Big(U^2_{1,2}-U^2_{2,1}\Big)\right)d\mathbf{x} \end{aligned} \tag{3.16}$$

Proof. (See appendix 3.A.2) Similarly to Proposition 3.1. □

In the following proposition, we study the behavior of ${\mathcal{P}'}_\epsilon(\ell)$ when $\epsilon \not\equiv 0$. When $\epsilon > 0$, we have ${\mathcal{P}'}_\epsilon(0) = 0$ and even $\mathcal{P}'(\ell) \sim O(\ell^\beta)$ with $\beta = 2\alpha - 1 \in (0,1)$ as it is proved in the following

Proposition 3.4. *(Case $0 < \epsilon < 1$ and $\ell = 0$) The release of potential energy due to the a crack of small length ℓ is of the order of $\ell^{2\alpha}$, i.e there exists $C_\epsilon \geq 0$ such that*

$$0 \leq \limsup_{\ell \downarrow 0} \frac{\mathcal{P}_\epsilon(0) - \mathcal{P}_\epsilon(\ell)}{\ell^{2\alpha}} \leq C_\epsilon \tag{3.17}$$

Because $0 < \epsilon \leq 1$, the value of α is the solution of equation (3.20) such that $1 \geq \alpha > \frac{1}{2}$. Therefore, $\mathcal{P}'_\epsilon(0) = 0$. Moreover, $\mathcal{P}'_\epsilon$ is continuous at 0, and $\lim_{\ell\downarrow 0}\mathcal{P}'_\epsilon(\ell) = 0$.

Proof. See the appendix 3.A.3. □

Proposition 3.5. *(Case $0 \leq \varepsilon < 1$ and $\ell = L$) $\forall \varepsilon \in [0,1), \mathcal{P}_\varepsilon$ is continuously differentiable at L and $\mathcal{P}'_\varepsilon(L) = 0$.*

Proof. See the appendix 3.A.4. □

Proposition 3.6. *For each $\epsilon \in [0,1)$, $\ell \mapsto \mathcal{P}_\epsilon(\ell)$ is decreasing, and, for each $\ell \in [0,L]$, $\epsilon \mapsto \mathcal{P}_\epsilon(\ell)$ is decreasing.*

Proof. Let $0 \leq \ell_1 \leq \ell_2 \leq L$. Because $\mathcal{U}^{\ell_2}_\epsilon \supset \mathcal{U}^{\ell_1}_\epsilon$ and because $\mathcal{P}^\ell_\epsilon$ is the minimum of the elastic energy over $\mathcal{U}^\ell_\epsilon$, $\forall \ell$, hence, we have $\mathcal{P}^\ell_\epsilon(\ell_2) \leq \mathcal{P}^\ell_\epsilon(\ell_1)$. Now, we prove that this inequality is strict. Assuming that $\mathcal{P}^\ell_\epsilon(\ell_2) = \mathcal{P}^\ell_\epsilon(\ell_1)$. Because of the uniqueness of the minimizer of the elastic energy over $\mathcal{U}^\ell_\epsilon$ for each ℓ, we have that $\mathbf{U}^{\ell_1}_\epsilon = \mathbf{U}^{\ell_2}_\epsilon$. Setting $\Gamma^2_1 = (\ell_1, \ell_2) \times \{0\}$ as a line segment, we get

$$\mathcal{P}^\ell_\epsilon(\ell_2) - \mathcal{P}^\ell_\epsilon(\ell_1) = \frac{1}{2}\int_{\Gamma^2_1}\Big(\sigma^{\ell_2}_{ij} n_j U^{\ell_2}_i - \sigma^{\ell_1}_{ij} n_j U^{\ell_1}_i\Big)dx_1 = \frac{1}{2}\int_{\Gamma^2_1}\Big(\sigma^{\ell_2}_{ij} n_j U^{\ell_1}_i - \sigma^{\ell_1}_{ij} n_j U^{\ell_2}_i\Big)dx_1$$

where $(\sigma^{\ell_2}_{ij}, \mathbf{U}^{\ell_2}_\epsilon)$ and $(\sigma^{\ell_1}_{ij}, \mathbf{U}^{\ell_1}_\epsilon)$ are the stress field and the displacement field of the body at the state of crack respectively ℓ_2 and ℓ_1. Clearly, we can see that the first term $\sigma^{\ell_2}_{ij} n_j U^{\ell_1}_i = 0$ on Γ^2_1 but not the second term and it will not be zero. That concludes that $\mathcal{P}^\ell_\epsilon(\ell_2) - \mathcal{P}^\ell_\epsilon(\ell_1) \neq 0$. □

Conjecture 1. *$\mathcal{P}_0$ is strictly convex and $\mathcal{P}'_\epsilon \geq \mathcal{P}'_0,\ \forall \epsilon \in [0,1)$*

As regards convexity properties of $\mathcal{P}_\varepsilon$, the situation is quite different because such properties are strongly dependent on the geometry, the type of loading and even on the locus where the displacements or the forces are applied. So, their check is just done for this type of geometry numerically.

3.2.1 Numeric results obtained for $\mathcal{P}_\epsilon(\ell)$ and $\mathcal{G}_\epsilon(\ell)$ by FEM

Because of the formula for the energy release rate in the Proposition 3.A.1 being valid for mode I or mode II or mixed mode I and II. Notice that, the formula in Proposition 3.A.1 and Proposition 1.3, we can normalize by a $E/\big(1+\nu\big)$ where E is Young's modulus and ν is Poisson's ratio. For example, in the Proposition 3.A.1, the formula of $\mathcal{P}_\epsilon(\ell)$ can be written :

$$\begin{aligned}\frac{1+\nu}{E}\mathcal{P}'_\epsilon(\ell) &= \frac{1}{2\ell}\int_{\underline{R}_0^\ell}\left(\frac{1-\nu}{(1-2\nu)}\Big(U_{2,2}^2-U_{1,1}^2\Big)+\frac{1}{2}\Big(U_{1,2}^2-U_{2,1}^2\Big)\right)d\mathbf{x}\\ &- \frac{1}{2(L-\ell)}\int_{R_\ell^L}\left(\frac{\lambda+2\mu}{2}\Big(U_{2,2}^2-U_{1,1}^2\Big)+\frac{\mu}{2}\Big(U_{1,2}^2-U_{2,1}^2\Big)\right)d\mathbf{x} \qquad (3.18)\end{aligned}$$

In advance, the normalizing the dimensions of the the body, we introduce again the dimensionless quantities:

$$\ell = H\tilde{\ell},\quad \mathbf{u}_\epsilon(\ell) = H\tilde{\mathbf{u}}_\epsilon(\ell),\quad \mathcal{P}_\epsilon(\ell) = E/\big(1+\nu\big)H^2\tilde{\mathcal{P}}_\epsilon(\ell),\quad G_\epsilon(\ell) = E/\big(1+\nu\big)H\tilde{G}_\epsilon(\ell). \qquad (3.19)$$

It permits the generality of the study. In computation, the dimensions of the body are chosen $H = 1,\ L = 5$, the Poisson's ratio is taken for steel at -150^0. In that, $\tilde{\ell} \in (0,5)$ and $\epsilon \in (0,1)$.

The potential energy decreases w.r.t the length of the crack ℓ in this case, see Figure 3.2. Besides, it should be a decreased function of ϵ also. Its convexity will be checked by its derivative. The lost of convexity of the potential energy is visible in the graph of $\mathcal{G}_\epsilon(\ell)$, see Figure 3.3.

1. For $\epsilon = 0$, $\mathcal{G}_\epsilon/\Big(HE/(1+\nu)\Big)$ is monotonically decreasing from 0.1771 to 0 when ℓ/H grows from 0 to 5.

2. For $\epsilon > 0,\ \mathcal{G}_\epsilon/\Big(HE/(1+\nu)\Big)$ starts from 0 when $\ell/H = 0$, then is rapidly increasing. This growth is so important that it cannot be correctly captured by the FEM.

3. Still for $\epsilon > 0,\ \mathcal{G}_\epsilon/\Big(HE/(1+\nu)\Big)$ is monotonically increasing as long as $\ell \leq \ell_m$. At $\ell = \ell_m,\ \mathcal{G}_\epsilon$ takes its maximal value $\mathsf{G_m}$. Those values which depend on ϵ are given in the Table 3.1.

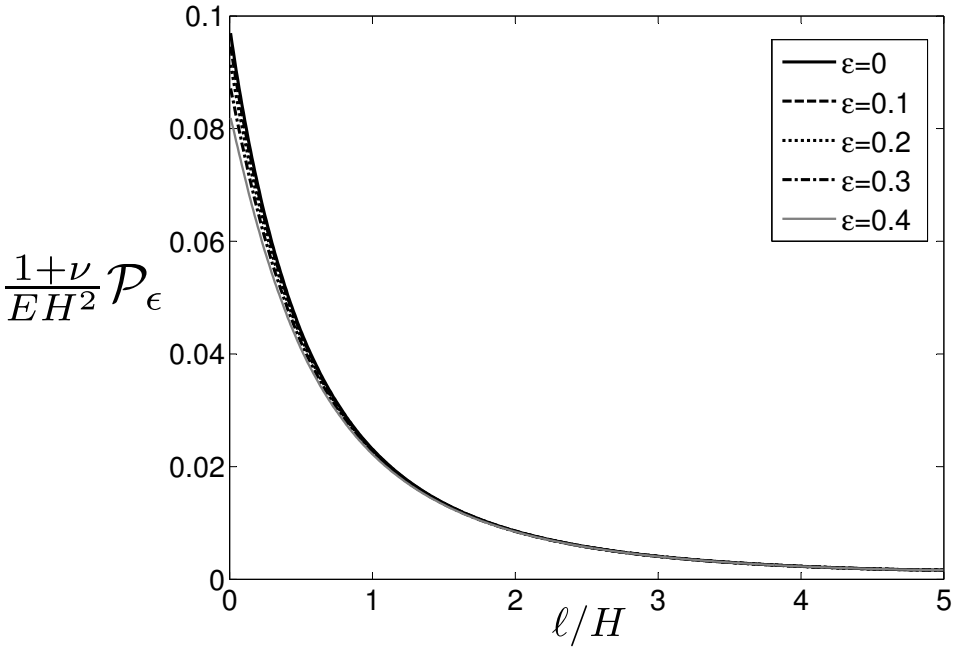

Figure 3.2: The potential energy of steel at -150^0C corresponding with different values of ϵ

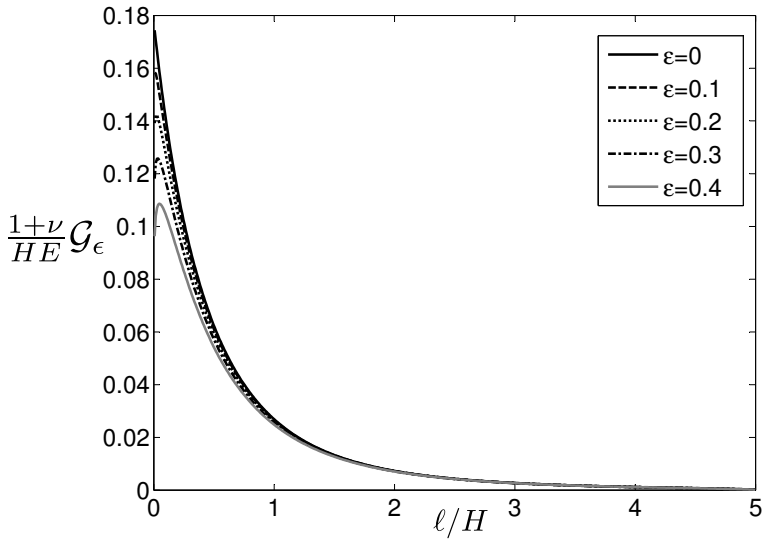

Figure 3.3: The energy release rate of steel at -150^0C corresponding with different values of ϵ

The influence of the notch to the potential energy $\mathcal{G}_\epsilon(\ell)$ for small crack can be seen in the Figure 3.4. When ϵ increases, the value of ℓ_{m} increases correspondingly. However, the value of G_{m} decreases

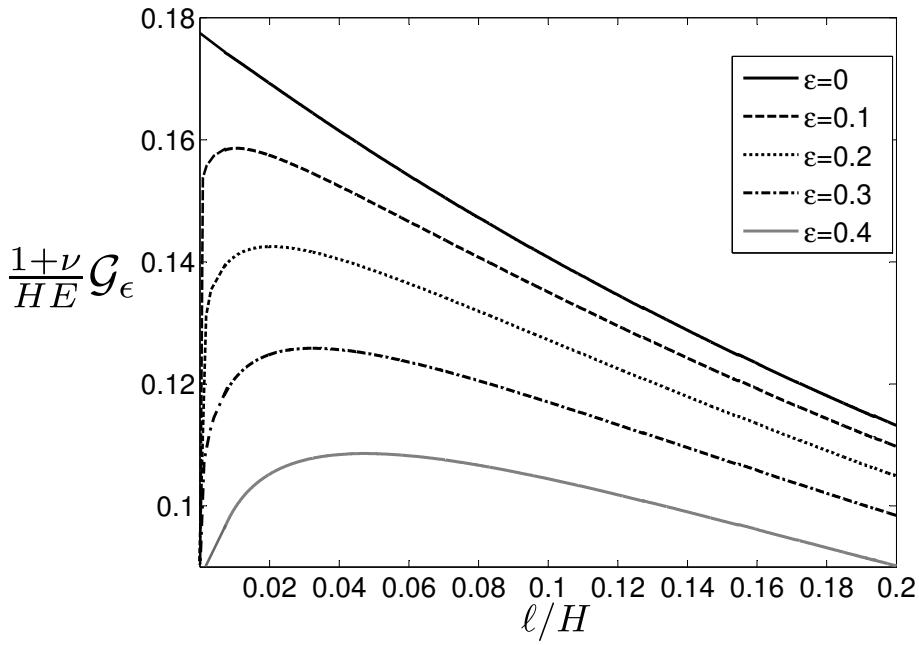

Figure 3.4: The energy release rate of steel at -150^0C corresponding with different values of ϵ in the case of small crack

ϵ	0.1	0.2	0.3	0.4
ℓ_m/H	0.0109	0.0213	0.0318	0.0467
$\mathsf{G_m}/H/\big(E/(1+\nu)\big)$	0.1586	0.1425	0.1258	0.1086
ℓ_i/H	0.0212	0.0566	0.0758	0.1033
$\mathsf{t_i}/\mathsf{t}_c$	2.8602	2.8473	2.8292	2.8215

Table 3.1: The value of ℓ_m/H, $\mathsf{G_m}/H/\big(E/(1+\nu)\big)$, ℓ_i/H and $\mathsf{t_i}/\mathsf{t}_c$ corresponding to *FM-law* with different values of ϵ

instead.

Recalling again the principal points of the agreement and the difference between FM-law and G-law. When $\epsilon = 0$, the notch is considered as a pre-existing crack. So that, in this case, the FM-law and G-law get the same unique solution. When $\epsilon > 0$, the crack will propagate continuously to $\ell(\mathsf{t}) \in (0, L)$ at load t such that $\mathsf{t}^2\mathcal{G}_\epsilon\ell(\mathsf{t}) = \mathsf{G_c}$. However, when $\epsilon > 0$, the body does not crack according to G-law, but it does in FM-law, see chapter [2]. The first crack ℓ_i will appear when $\ell_\mathsf{i}\mathcal{G}_\epsilon(\ell_\mathsf{i}) = \mathcal{P}_\epsilon(0) - \mathcal{P}_\epsilon(\ell_\mathsf{i})$ which obeys the Maxwell rule of equal areas, see Figure 2.5 at a certain critical load $\mathsf{t_i}$. The critical load $\mathsf{t_i}$ corresponds to ℓ_i is defined in a such way that $\mathsf{t_i}^2\mathcal{G}_\epsilon(\ell_\mathsf{i}) = \mathsf{G_c}$. In the dimensionless quantities, the length ℓ_i is defined so as to $\tilde{\ell}_\mathsf{i}\tilde{G}_\epsilon = \tilde{\mathcal{P}}_\epsilon(0) - \tilde{\mathcal{P}}_\epsilon$ and $\big(\mathsf{t_i}/\mathsf{t}_c\big)^2 = 1/\tilde{G}_\epsilon(\tilde{\ell}_\mathsf{i})$ with $(\mathsf{t}_c)^2 = \mathsf{G_c}/H(1+\nu)/E$.

The values of ℓ_{m}, G_{m} and also of ℓ_{i}, t_{i} corresponding to ϵ are given in Table 3.1.

3.3 Case of a cohesive crack

Using the Dugdale model in mode I or mode II. From the local minimization, the cohesive zone propagates until the singularity at its tip vanishes. Moreover, the non-cohesive zone will reach to a particular point where the jump of the displacement equals δ_c. The purpose here is to get the rupture response as in the chapter [2]. The result investigates for elasticity, especially in mode I or mode II in plane-strain state.

Firstly, the work requires to study the behaviors of the solution near the notch. The singularity will not have the form of $r^{\pi/\omega}$ for the displacement as in mode III anymore. Relying on the results of P. Grisvard for problem of elasticity in 2D, see [Grisvard, 1992], there exists (one or two) singular terms of order $0 < \alpha_1 < 1$ or $0 < \alpha_2 < 1$ which depends on the notch (which is characterized by ω). We call them (α_1 and α_2) the characteristic values. They are the solution of so-called 'characteristic equations'. The complexity of the solution in vicinity of the notch which contains a small crack requires a precise study locally. However, the solution in the region which is far from the crack and near the boundary is regular and can be approximated accurately by classical methods of approximation such as FEM.

The chapter firstly introduce the singularity around the notch for the problem of the elasticity in 2D. Then we introduce the matched asymptotic terms in the context of combining the analytic method of Muskhelishvili's in the inner problem $\mathbf{v}^0$ for deducing the relations between the load, and the two lengths of two zones of crack. From that point, the critical load under which, the crack will appear.

Firstly, let us introduce the characteristic equation which governs for the characteristic value α.

3.3.1 Analysis of characteristic equations

The characteristic values α_1 and α_2 have to satisfy the following equation :

$$\sin^2 \alpha\omega = \alpha^2 \sin^2 \omega \tag{3.20}$$

with the assumption that $\pi \leq \omega \leq 2\pi$. The equation (3.20) can be written as $\sin(\alpha\omega) = \pm\alpha \sin(\omega)$. The existence of α and how many values of α so that $\alpha \in (0, 1)$ depends on the value of ω, see Lemma 3.1.

Defining the angle $\omega_0 \in (\pi, 3\pi/2)$ such that $\omega_0 = \tan(\omega_0)$ or its value $\omega_0 \approx 4.4934$.

Opening angle ω	2π	$11\pi/6$	$7\pi/4$	$5\pi/3$	$3\pi/2$	$4\pi/3$
α_1	1/2	0.5014530	0.5050097	0.5122214	0.5444837	0.6157311
α_2	1/2	0.5981918	0.6597016	0.7309007	0.9085292	1.148913

Table 3.2: Values of α correspond to some values of ω

Lemma 3.1. *Equation (3.20) has no root in the strip $0 < Re\alpha < 1$ when $\omega < \pi$. It has only one single real root in that strip when $\pi < \omega < \omega_0$ and it has two distinct simple real roots in that strip when $\omega_0 < \omega \leq 2\pi$.*

Proof. The proof is cited in the Lemma 3.3.2 of [Grisvard, 1992] □

We take the numeric demonstration for some values of $\omega \in (\omega_0, 2\pi)$ and $\omega \in (\pi, \omega_0)$ in the Table 3.2. For $\omega \in (\omega_0, 2\pi]$ such as : $3\pi/2, \ldots, 2\pi$, value of α_1 and α_2 is real and is in the interval $[1/2, 1)$. While $\omega = 4\pi/3 \in (\pi, \omega_0)$, there is uniquely the value of $\omega_1 \in (1/2, 1)$ whereas $\alpha_2 > 1$.

Remark 3.1. *When $\omega \in (\pi, 2\pi]$, the value of α which is defined in Equation 3.20 is always greater than 1/2. In case of $\omega = \omega_0$, there exist only unique value of α, $\alpha_1 < 1$. This case is a limit case will be not considered in our context. Besides, when $\omega = 2\pi$, we get the real root for the characteristic equation (3.20) and clearly its value has the form of $n/2$ for $n \in \mathbb{N}_*$.*

3.3.2 Derivation of the singular solutions

Generally, let us define the vector field S_α for a given complex number α :

$$S_\alpha = r^\alpha \Phi_\alpha(\theta) \tag{3.21}$$

where Φ_α is the following vector field which depends on α and θ :

$$\Phi_\alpha = \{(\alpha-1)\sin(\alpha+1)\omega - (\alpha+1)\sin(\alpha-1)\omega\}\Phi_{\alpha,1} - (\alpha+1)\{\cos(\alpha+1)\omega - \cos(\alpha-1)\omega\}\Phi_{\alpha,2} \tag{3.22}$$

Two functions $\Phi_{\alpha,1}$, $\Phi_{\alpha,2}$ are such that $S_\alpha(r,\theta)$ has to satisfy the Lamé system and the homogeneous Neumann conditions on the edges of the notch $\Gamma^\pm$.

$$\Phi_{\alpha,1} = \begin{pmatrix} \{(\lambda+\mu)\alpha\cos(\alpha-2)\theta - [(\lambda+\mu)(\alpha+2)+2\mu]\cos(\alpha\theta)\} \\ -\{(\lambda+\mu)\alpha\sin(\alpha-2)\theta - [(\lambda+\mu)\alpha-2\mu]\sin(\alpha\theta)\} \end{pmatrix} \tag{3.23}$$

$$\Phi_{\alpha,2} = \begin{pmatrix} \{(\lambda+\mu)\alpha\sin(\alpha-2)\theta - [(\lambda+\mu)\alpha+2\mu]\sin(\alpha\theta)\} \\ \{(\lambda+\mu)\alpha\cos(\alpha-2)\theta - [(\lambda+\mu)(\alpha-2)-2\mu]\cos(\alpha\theta)\} \end{pmatrix} \tag{3.24}$$

The essential point is the Theorem 3.1 which gives us the behavior of $\mathbf{u}$ near the notch. The solution is not regular (which means belongs to $H^2(\Omega)^2$) anymore.

Theorem 3.1. *Assume that Ω is a bounded polygonal open subset of $\mathbb{R}^2$ with no corner of measure $\omega_0 = \tan\omega_0$. Let $u \in H^1(\Omega)^2$ be a variational solution of (3.5) with $f \in L^2(\Omega)^2$. Then there exists numbers c_α such that*

$$u - \sum_\alpha c_\alpha S_\alpha \in H^2(\Omega)^2 \tag{3.25}$$

where the sum is taken over the real solutions of $\sin^2\alpha\omega = \alpha^2\sin^2\omega$ in the interval $(0,1)$.

Proof. The proof is cited in Theorem 4.2.5 of [Grisvard, 1992]. □

Especially, when $\omega = 2\pi$, we have the following remark.

Remark 3.2. *When $\omega = 2\pi$, the roots of the characteristic equation $\sin^2\alpha\omega = \alpha^2\sin^2\omega$ are obviously the numbers $\alpha = n/2$ with $k \in \mathbb{N}_*$ and these are double roots. The statement of theorem (3.1) remains valid with the following modification near the corner :*

$$u - c_1\sqrt{r}\Phi_{1/2,1} - c_2\sqrt{r}\Phi_{1/2,2} \in H^2(V)^2 \tag{3.26}$$

where V is an open neighborhood of the corner (the notch) in $\bar{\Omega}$

Coming back to the problem of elasticity in the context of plane strain in the corner domain Ω_ϵ^ℓ as the same geometry in the first chapter. It contains a corner or a so-called notch which is characterized by an opening angular ω whose value is in the interval $(\pi, 2\pi]$.

While $\omega = 2\pi$, the notch becomes a pre-existing crack with a particular length not being small at all. The singularity study near the notch can be considered as the classic result also, specifically, it is mentioned in the Remark 3.2 with c_2 and c_1 correspond to K_I and K_{II} respectively in the well-known result in this case.

3.3.3 Problem of elasticity in 2D

Considering the elastic problem mode I and II in plane strain case deduced the problem into 2D problem. In the cohesive model, the crack Γ_ℓ of the length ℓ is divided into two zones : the non-cohesive zone of length l which is denoted by Γ_0 and the cohesive zone of length $\ell - l$ which is denoted by Γ_c.

In equilibrium state, the displacement field has to obey the Lamé system as mentioned before without the body forces imposing and concurrently, it has to satisfy the conditions imposed on the boundary as well as the compatible law. Namely, the displacement field is governed by the following

equations:

$$\begin{cases} D_j\sigma_{ij}(\mathbf{u}) = 0 & \text{in} \quad \Omega_\epsilon^\ell \\ \sigma_{ij}n_j = 0 & \text{on} \quad \Gamma^\pm \cup N^\pm \cup \Gamma_0 \\ \boldsymbol{\sigma}\mathbf{n} = \boldsymbol{\sigma}_c\mathbf{n} & \text{on} \quad \Gamma_c \\ \mathbf{u} = \pm \mathrm{t}(\mathbf{e}_1 + \mathbf{e}_2) & \text{on} \quad D^\pm \\ \mathbf{u} = \mathbf{0} & \text{on} \quad D_L \end{cases} \tag{3.27}$$

where $\boldsymbol{\sigma}_c = \sigma_c \mathbf{e}_2 \otimes \mathbf{e}_2 + \tau_c \mathbf{e}_1 \otimes \mathbf{e}_2$. In the condition of closed forces on cohesive part (Γ_c) of the crack, σ_c and τ_c correspond to mode I and mode II respectively. In case of linear isotropic and homogeneous material, the component of stress field satisfying the Hooke's law is supplied as following:

$$\sigma_{ij} = \lambda \mathrm{tr}\boldsymbol{\varepsilon}(\mathbf{u})\delta_{ij} + 2\mu\varepsilon_{ij} \tag{3.28}$$

with corresponding linearized strain tensor $\boldsymbol{\varepsilon}(\mathbf{u})$ is defined by :

$$\varepsilon_{ij}(\mathbf{u}) = \frac{1}{2}(D_j u_i + D_i u_j) \quad \text{with} \quad 1 \leq i, j \leq 2 \tag{3.29}$$

The existence of the notch and the small crack at the notch tip is necessary to consider the problem very carefully, especially, considering the problem in two different scales, the macroscopic scale and the microscopic scale. In the zone far from the crack, the solution is regular. While in the vicinity of the crack, the behavior of the solution is more complex. Using the matched asymptotic method, we suppose that the displacement $\mathbf{u}$ can be expanded into a matched asymptotic series, for instance, the outer expansion in macro-scale has the form:

$$\mathbf{u}(\mathbf{x}) = \mathbf{t}\mathbf{u}^0(\mathbf{x}) + \text{higher order terms} \tag{3.30}$$

where the first term $\mathbf{u}^0(\mathbf{x})$ is defined in the whole domain Ω_0 not containing the crack inside.

$$\Omega_0 = [-H, L] \times [-H, H] \setminus \mathcal{N}_\epsilon^c \tag{3.31}$$

The solution depends not only on the boundary condition, but also the geometry of Ω_0.

$$\begin{cases} D_j\sigma_{ij}(\mathbf{u}^0) = 0 & \text{in} \quad \Omega_0 \\ \sigma_{ij}(\mathbf{u}^0)n_j = 0 & \text{on} \quad \Gamma^\pm \cup N^\pm \\ \mathbf{u}^0 = \pm(\mathbf{e}_1 + \mathbf{e}_2) & \text{on} \quad D^\pm \\ \mathbf{u}^0 = 0 & \text{on} \quad D_L \end{cases} \tag{3.32}$$

Relying on the study of the solution in the corner domain which obtained in the Theorems 3.1 and Remark 3.2, the term $\mathbf{u}^0(\mathbf{x})$ can be decomposed into the singular term and the regular term $(\mathbf{u}_r^0(\mathbf{x}))$:

$$\mathbf{u}(\mathbf{x}) = \mathtt{t}\Big(\sum_{1/2\leq\alpha<1} c_\alpha S_\alpha(r,\theta) + \mathbf{u}_r^0(\mathbf{x})\Big) + \text{higher other terms} \tag{3.33}$$

where $\mathbf{u}_r^0(\mathbf{x}) \in H^2(\Omega_0)^2$ and the formula of $S_\alpha(r,\theta)$ defined in the theorem (3.1) can be rewritten as follows : setting that :

$$H_1 = \{(\alpha-1)\sin(\alpha+1)\omega - (\alpha+1)\sin(\alpha-1)\omega\} \tag{3.34}$$

$$\text{and} \quad H_2 = -(\alpha+1)\{\cos(\alpha+1)\omega - \cos(\alpha-1)\omega\} \tag{3.35}$$

We can write :

$$\begin{aligned} S_\alpha &= r^\alpha\Bigg[H_1\begin{pmatrix}\{(\lambda+\mu)\alpha\cos(\alpha-2)\theta - [(\lambda+\mu)(\alpha+2)+2\mu]\cos(\alpha\theta)\}\\ -\{(\lambda+\mu)\alpha\sin(\alpha-2)\theta - [(\lambda+\mu)\alpha-2\mu]\sin(\alpha\theta)\}\end{pmatrix} \\ &+ H_2\begin{pmatrix}\{(\lambda+\mu)\alpha\sin(\alpha-2)\theta - [(\lambda+\mu)\alpha+2\mu]\sin(\alpha\theta)\}\\ \{(\lambda+\mu)\alpha\cos(\alpha-2)\theta - [(\lambda+\mu)(\alpha-2)-2\mu]\cos(\alpha\theta)\}\end{pmatrix}\Bigg] \end{aligned} \tag{3.36}$$

The problem is considered in the context of very small crack length compared with the characteristic length of the geometry such as H, similarly, ℓ/H should be very small. In the larger scale $\mathbf{y} = \mathbf{x}/\ell$, the inner expansion is supposed to be have a following form :

$$\mathbf{u}(\mathbf{y}) = \mathbf{v}^0(\mathbf{y}) + \text{higher terms} \qquad \text{which is defined in } \Omega^\infty \tag{3.37}$$

Assuming that the load $\mathtt{t}$ is proportional to $\ell^{-\alpha}$, $(1/2 \leq \alpha < 1)$ and in case of existing two different values of α, we choose the smallest value or $\alpha = \alpha_1$. The load on the boundaries $\mathcal{D}^\pm$ is set to be $t = T\ell^{-\alpha_1}$. Hence, in the larger scale, at infinity, the solution $\mathbf{u}(\rho,\theta)$ reads as :

$$\mathbf{u}(\rho,\theta) = t\Big[c_{\alpha_1}\rho^{\alpha_1}\ell^{\alpha_1}(H_1\Phi_{\alpha,1} + H_2\Phi_{\alpha,2}) + \ldots\Big] = Tc_{\alpha_1}\rho^{\alpha_1}(H_1\Phi_{\alpha,1} + H_2\Phi_{\alpha,2}) + \ldots \tag{3.38}$$

Consequently, the term $Tc_{\alpha_1}\rho^{\alpha_1}(H_1\Phi_{\alpha,1} + H_2\Phi_{\alpha,2}) + \ldots$ will be the behavior of $\mathbf{v}^0$ at infinity. The equations govern for $\mathbf{v}^0(\mathbf{y})$ can be read as:

$$\begin{cases} D_j\sigma_{ij}(\mathbf{v}^0) = 0 & \text{in} \quad \Omega^\infty \\ \sigma_{ij}(\mathbf{v}^0)n_j = 0 & \text{on} \quad \Gamma^\pm \cup \Gamma_0 \\ \boldsymbol{\sigma}\mathbf{n} = \boldsymbol{\sigma}_c\mathbf{n} & \text{on} \quad \Gamma_c \\ \mathbf{v}^0 \to Tc_{\alpha_1}\rho^{\alpha_1}(H_1\Phi_{\alpha,1} + H_2\Phi_{\alpha,2}) & \text{at } \infty \end{cases} \tag{3.39}$$

Applying the conform mapping which is called $z = \omega(Z) = Z^{\frac{\omega}{2\pi}}$ to map the domain $\widetilde{\Omega}^{\infty}$ into Ω^{∞}. The domain $\tilde{\Omega}^{\infty}$ is defined by :

$$\tilde{\Omega}^{\infty} = \{(Z_1, Z_2) : \sqrt{Z_1^2 + Z_2^2} \to \infty\} \setminus (-\infty, \ell^{\frac{2\pi}{\omega}}] \times \{0\} \tag{3.40}$$

and $z = y_1 + iy_2$ $((y_1, y_2) \in \Omega^{\infty})$ and $Z = Z_1 + iZ_2$ $((Z_1, Z_2) \in \tilde{\Omega}^{\infty})$ as in the chapter [2]. Taking notice with the scalar ω denoted for the opening angle. Firstly, we consider the auxiliary problem of $\mathbf{v}^0(\mathbf{y})$ which is called $\mathbf{v}^0_{aux}(\mathbf{y})$ which satisfies the following equations:

$$\begin{cases} D_j \sigma_{ij}(\mathbf{v}^0_{aux}) = 0 & \text{in} \quad \Omega^{\infty} \\ \sigma_{ij}(\mathbf{v}^0_{aux}) n_j = 0 & \text{on} \quad \Gamma^{\pm} \cup \Gamma_0 \\ \boldsymbol{\sigma}\mathbf{n} = \boldsymbol{\sigma}_c \mathbf{n} & \text{on} \quad \Gamma_c \\ \mathbf{v}^0_{aux} \to 0 & \text{at } \infty \end{cases} \tag{3.41}$$

In the z-coordinates, the stress components of the stress field $\boldsymbol{\sigma}$ of the auxiliary problem are expressed by the potential functions $\varphi_{aux}(z)$ and $\psi_{aux}(z)$ as in [Muskhelishvili, 1963] :

$$\sigma_{yy} - i\sigma_{xy} = \overline{\varphi_{aux}{}'(z)} + \varphi_{aux}{}'(z) + z\overline{\varphi''_{aux}(z)} + \overline{\psi_{aux}{}'(z)} \tag{3.42}$$

with

$$\varphi_{aux}{}'(z) = \frac{d\varphi_{aux}}{dz} \quad \text{and} \quad \psi_{aux}{}'(z) = \frac{d\psi_{aux}}{dz} \tag{3.43}$$

Using the notation as in [Leblond, 2000], $\Omega_{aux}(z) = z\varphi_{aux}{}'(z) + \psi_{aux}(z)$, the equation (3.42) can be written as :

$$\sigma_{yy} - i\sigma_{xy} = \varphi_{aux}{}'(z) + \overline{\Omega_{aux}{}'(z)} + (z - \bar{z})\overline{\varphi''_{aux}(z)} \tag{3.44}$$

Then, in Z-coordinates it can be read as :

$$\Big[\sigma_{yy} - i\sigma_{xy}\Big] = \frac{1}{\omega'(Z)}\varphi_{aux}{}'(Z) + \frac{1}{\overline{\omega'(Z)}}\overline{\Omega_{aux}{}'(Z)} + \Big[\omega(Z) - \overline{\omega(Z)}\Big]\frac{1}{\overline{\omega'(Z)}}\overline{\Phi_{aux}{}'(Z)} \quad \text{with} \quad \Phi_{aux}(Z) = \varphi_{aux}{}'(z) \tag{3.45}$$

with

$$\varphi_{aux}{}'(Z) = \frac{d\varphi_{aux}}{dZ}, \quad \Omega_{aux}{}'(Z) = \frac{d\Omega_{aux}}{dZ} \quad \text{and} \quad \Phi_{aux}{}'(Z) = \frac{d\Phi_{aux}(Z)}{dZ} \tag{3.46}$$

Using the definition of Muskhelisvili for the conjugate of a function in complex plane, such that : $\bar{f}(z) = \overline{f(\bar{z})}$, setting $s^{\pm} \equiv s \pm i\varepsilon, \varepsilon > 0, \varepsilon \to 0$, we have:

$$\varphi_{aux}{}'(s^{\pm}) + \overline{\Omega_{aux}{}'}(s^{\mp}) = \begin{cases} 0 \quad \text{with} \quad \forall s \in (-\infty, l^{\frac{2\pi}{\omega}}] \\ \dfrac{1}{2k} s^{\frac{\omega}{2\pi}-1}\Big[\sigma_c - i\tau_c\Big] \quad \text{with} \quad \forall s \in (l^{\frac{2\pi}{\omega}}, \ell^{\frac{2\pi}{\omega}}) \end{cases} \tag{3.47}$$

Hence, we can obtain that :

$$\big({\varphi_{aux}}' - \overline{\Omega_{aux}{}'}\big)(s^+) - \big({\varphi_{aux}}' - \overline{\Omega_{aux}{}'}\big)(s^-) = 0 \tag{3.48}$$

The results here are related to the auxiliary problem with vanished boundary condition at infinity. So that, ${\varphi_{aux}}' - \overline{\Omega_{aux}{}'}$ will be bounded at infinity, by the Cauchy integral derived in Hilbert's problem, it can be concluded to be equal zero. In other words,

$$\overline{\Omega_{aux}{}'} = {\varphi_{aux}}' \quad \leftrightarrow \quad {\Omega_{aux}}' = \overline{\varphi_{aux}{}'} \tag{3.49}$$

Finally, the limit conditions on the crack lips become :

$${\varphi_{aux}}'(s^{\pm}) + {\varphi_{aux}}'(s^{\mp}) = \begin{cases} 0 \quad \text{with} \quad \forall t \in (-\infty, l^{\frac{2\pi}{\omega}}] \\ \dfrac{\omega}{2\pi} s^{\frac{\omega}{2\pi}-1}\Big(\sigma_c - i\tau_c\Big) \quad \text{with} \quad \forall t \in (l^{\frac{2\pi}{\omega}}, \ell^{\frac{2\pi}{\omega}}) \end{cases} \tag{3.50}$$

This is a Hilbert's problem. Choosing a function analytic as the same for mode III which mentioned in the previous chapter:

$$F(Z) = \frac{1}{\sqrt{Z - \ell^{\frac{2\pi}{\omega}}}}$$

Finally, the function ${\varphi_{aux}}'(Z)$ will be :

$${\varphi_{aux}}'(Z) = \frac{\sigma_c - i\tau_c}{2\pi\sqrt{Z - \ell^{\frac{2\pi}{\omega}}}} \int_{l^{\frac{2\pi}{\omega}}}^{\ell^{\frac{2\pi}{\omega}}} \frac{\omega}{2\pi} s^{\frac{\omega}{2\pi}-1} \frac{\sqrt{\ell^{\frac{2\pi}{\omega}} - s}}{s - Z} ds + \frac{C^*}{\sqrt{Z - \ell^{\frac{2\pi}{\omega}}}} \tag{3.51}$$

At infinity of the function ${\varphi_{aux}}'(Z)$ in the new domain behaves like $C^* Z^{-1/2}$, in the auxiliary problem, the coefficient C^* is chosen to be zero. Hence, the function of $\varphi'(Z)$ of the original problem can be read as :

$$\varphi'(Z) = \frac{\sigma_c - i\tau_c}{2\pi\sqrt{Z - \ell^{\frac{2\pi}{\omega}}}} \int_{l^{\frac{2\pi}{\omega}}}^{\ell^{\frac{2\pi}{\omega}}} \frac{\omega}{2\pi} s^{\frac{\omega}{2\pi}-1} \frac{\sqrt{\ell^{\frac{2\pi}{\omega}} - s}}{t - Z} ds + \frac{C^*}{\sqrt{Z - \ell^{2k}}} \tag{3.52}$$

where C^* is defined from behavior of the original problem of $\mathbf{v}^0(\mathbf{y})$ at infinity.

Coming back to the previous part mentioned about the behavior of $\mathbf{v}^0(\mathbf{y})$ at infinity, we have the solution behaves like :

$$\begin{aligned} \mathbf{v}^0(\mathbf{y}) = T c_{\alpha_1} \rho^{\alpha_1} \Bigg[& H_1 \begin{pmatrix} \{(\lambda+\mu)\alpha_1 \cos(\alpha_1 - 2)\theta - [(\lambda+\mu)(\alpha_1+2) + 2\mu]\cos(\alpha_1\theta)\} \\ -\{(\lambda+\mu)\alpha_1 \sin(\alpha_1 - 2)\theta - [(\lambda+\mu)\alpha_1 - 2\mu]\sin(\alpha_1\theta)\} \end{pmatrix} \\ + & H_2 \begin{pmatrix} \{(\lambda+\mu)\alpha \sin(\alpha - 2)\theta - [(\lambda+\mu)\alpha + 2\mu]\sin(\alpha\theta)\} \\ \{(\lambda+\mu)\alpha \cos(\alpha - 2)\theta - [(\lambda+\mu)(\alpha-2) - 2\mu]\cos(\alpha\theta)\} \end{pmatrix} \Bigg] \end{aligned} \tag{3.53}$$

From that, we have the stress behavior which is generated by the behavior at infinity of $\mathbf{v}^0(\mathbf{y})$ denoted by $\boldsymbol{\sigma}^\infty$, with:

$$\begin{aligned}\sigma_{yy}^\infty - i\sigma_{xy}^\infty &= -2Tc_{\alpha_1}\rho^{\alpha_1-1}\alpha_1\mu(\lambda+\mu)\Big[\Big((\alpha_1-1)H_1\big[\cos(\alpha_1-3)\theta-\cos(\alpha_1-1)\theta\big]\\ &+ H_2\big[(\alpha_1-1)\sin(\alpha_1-3)\theta-(\alpha_1-3)\sin(\alpha_1-1)\theta\big]\Big)\\ &- i\Big(H_1\big[(\alpha_1-1)\sin(\alpha_1-3)\theta-(\alpha_1+1)\sin(\alpha_1-1)\theta\big]\\ &+ H_2(\alpha_1-1)\big[\cos(\alpha_1-1)\theta-\cos(\alpha_1-3)\theta\big]\Big)\Big] \qquad (3.54)\end{aligned}$$

We can deduce the value of C^* in the real line $(Z_1, 0)$ by matching the condition $\boldsymbol{\sigma}^\infty$ with the condition of σ at infinity derived from $\varphi(Z)$:

$$C^* = -Tc_{\alpha_1}\alpha_1\mu(\lambda+\mu)\frac{\omega}{2\pi}R^{\alpha_1\frac{\omega}{2\pi}-\frac{1}{2}}\Big[Q_1 - iQ_2\Big] \qquad (3.55)$$

with

$$\begin{aligned}Q_1 &= (\alpha_1-1)H_1\big[\cos(\alpha_1-3)\frac{\omega}{2}-\cos(\alpha_1-1)\frac{\omega}{2}\big]\\ &+ H_2\big[(\alpha_1-1)\sin(\alpha_1-3)\frac{\omega}{2}-(\alpha_1-3)\sin(\alpha_1-1)\frac{\omega}{2}\big] \qquad (3.56)\\ Q_2 &= H_1\big[(\alpha_1-1)\sin(\alpha_1-3)\frac{\omega}{2}-(\alpha_1+1)\sin(\alpha_1-1)\frac{\omega}{2}\big]\\ &+ H_2(\alpha_1-1)\big[\cos(\alpha_1-1)\frac{\omega}{2}-\cos(\alpha_1-3)\frac{\omega}{2}\big] \qquad (3.57)\end{aligned}$$

With the Remark 3.2 in the case when $\omega = 2\pi$, H_1 and H_2 is chosen to be equal to 1 and we have :

$$Q_1 = -2 \quad \text{and} \quad Q_2 = 2 \qquad (3.58)$$

Finally, we get the function of $\varphi'(Z)$ valid on the real line $(Z_1, 0)$:

$$\varphi'(Z) = \frac{\sigma_c - i\tau_c}{2\pi\sqrt{Z-\ell^{\frac{2\pi}{\omega}}}}\int_{l^{\frac{2\pi}{\omega}}}^{\ell^{\frac{2\pi}{\omega}}}\frac{\omega}{2\pi}s^{\frac{\omega}{2\pi}-1}\frac{\sqrt{\ell^{\frac{2\pi}{\omega}}-s}}{s-Z}ds - \frac{\omega}{2\pi}\frac{Tc_{\alpha_1}\alpha_1\mu(\lambda+\mu)R^{\alpha_1\frac{\omega}{2\pi}-\frac{1}{2}}\Big(Q_1-iQ_2\Big)}{\sqrt{Z-\ell^{\frac{2\pi}{\omega}}}} \qquad (3.59)$$

From the function of $\varphi'(Z)$ in (3.59), we see there exists a singularity at $\ell^{\frac{2\pi}{\omega}}$. Clearly, because $(\ell^{\frac{2\pi}{\omega}}, 0)$ is the corresponding tip of the crack in the coordinates Z. So that, there exits the singularity there. However, in the model of Dugdale, the singularity at the crack tip will reach to the a point provided that the stress intensity factors $(K_I - iK_{II})$ vanish.

3.3.4 The stress intensity factor

Being similar work for mode III in the chapter [2], the stress intensity factors $K_I - iK_{II}$ in Z-coordinates are proportional to $\sqrt{Z - \ell^{\frac{2\pi}{\omega}}}\varphi'(Z)$. The condition

$$\lim_{Z \to (\ell^{\frac{2\pi}{\omega}}, 0)} \Big[\sqrt{Z - \ell^{\frac{2\pi}{\omega}}}\varphi'(Z)\Big] = 0 \tag{3.60}$$

deduces

$$-\frac{\sigma_c - i\tau_c}{2\pi}\frac{\omega}{2\pi}\int_{l^{\frac{2\pi}{\omega}}}^{\ell^{\frac{2\pi}{\omega}}} \frac{s^{\frac{\omega}{2\pi}-1}}{\sqrt{\ell^{\frac{2\pi}{\omega}} - s}}ds - \frac{\omega}{2\pi}Tc_{\alpha_1}\alpha_1\mu(\lambda+\mu)\ell^{\alpha_1 - \frac{\pi}{\omega}}\Big[Q_1 - iQ_2\Big] = 0 \tag{3.61}$$

Finally, we get the relations between the external load and the lengths of crack so that the intensity factors will be eliminated. Such as, for mode I :

$$c_{\alpha_1}T = -\frac{\sigma_c}{2\pi}\frac{\ell^{\frac{\pi}{\omega}-\alpha_1}}{\alpha_1\mu(\lambda+\mu)Q_1}\int_0^{\sqrt{\ell^{\frac{2\pi}{\omega}} - l^{\frac{2\pi}{\omega}}}} 2\big[\ell^{\frac{2\pi}{\omega}} - s^2\big]^{\frac{\omega}{2\pi}-1}ds \tag{3.62}$$

Putting $\theta_m = \arcsin\sqrt{1 - \left(\frac{l}{\ell}\right)^{\frac{2\pi}{\omega}}}$, the generalize load call $-c_{\alpha_1}T$ can read as :

$$-\frac{\mu(\lambda+\mu)}{\sigma_c}c_{\alpha_1}T = \frac{\ell^{1-\alpha_1}}{\pi\alpha_1 Q_1}\int_0^{\theta_m}\big(\cos\theta\big)^{\frac{\omega}{\pi}-1}d\theta \tag{3.63}$$

and for mode II, this relation becomes :

$$-\frac{\mu(\lambda+\mu)}{\tau_c}c_{\alpha_1}T = \frac{\ell^{1-\alpha_1}}{\pi\alpha_1 Q_2}\int_0^{\theta_m}\big(\cos\theta\big)^{\frac{\omega}{\pi}-1}d\theta \tag{3.64}$$

Being similar to mode III, corresponding to a external load, the tip of cohesive zone will be up to the value ℓ which satisfies equation 3.63 for mode I or equation 3.64 for mode II.

Moreover, the length of the non-cohesive zone is defined such that the jump at its tip reach to the critical value δ_c.

3.3.5 The jump of the displacement

The displacement is expressed in the function $\varphi(Z)$ can be written as in the formula of Muskehlishvili:

$$2\mu(u_1 + iu_2)(\mathbf{x}) \approx 2\mu(v_1^0 + iv_2^0) = \kappa\varphi(z) - z\overline{\varphi'(z)} - \overline{\psi(z)}, \quad \text{with} \quad \kappa = \frac{\lambda+3\mu}{\lambda+\mu} \tag{3.65}$$

Here, the formula of $\varphi(z)$, $\psi(z)$ or $\Omega(z)$ are taken into account for the problem $\mathbf{v}^0(\mathbf{y})$ and they include the behavior at infinity. They are not just the solution for auxiliary problem of $\mathbf{v}^0(\mathbf{y})$ but all the

relations between them will be kept in the context of the original problem $\mathbf{v}^0(\mathbf{y})$. So that, the tip of non-cohesive zone $(l,0)$ in the coordinates (y_1,y_2) becomes $(l^{\frac{2\pi}{\omega}},0)$ in the new coordinates (Z_1,Z_2) and the jump of the displacement at $(l^{\frac{2\pi}{\omega}},0)$:

$$[\![u_2]\!](l^{\frac{2\pi}{\omega}},0)=\frac{1}{2\mu i}[\![\kappa\varphi(z)-z\overline{\varphi'(z)}-\overline{\psi(z)}]\!] \tag{3.66}$$

Besides, we have :

$$\psi'(z)=\Omega'(z)-\varphi'(z)-z\varphi^{''}(z) \tag{3.67}$$

with

$$\Omega'(z)=\frac{d\Omega}{dz}=\frac{\Omega'(Z)}{\omega'(Z)}=\frac{\overline{\varphi'}(Z)}{\omega'(Z)}=\frac{\overline{\varphi}'(Z)}{\omega'(Z)}=\frac{d\overline{\varphi}}{dz}=\overline{\varphi}'(z)$$

So that,

$$\psi'(z)=\overline{\varphi}'(z)-\varphi'(z)-z\varphi^{''}(z) \tag{3.68}$$

We can obtain :

$$\psi(z)=\overline{\varphi}(z)-z\varphi'(z) \tag{3.69}$$

Besides, from the formula of the displacement (3.65), we have the jump of the component $u_2(y_1,y_2)$ can be read as following :

$$[\![u_2(z)]\!](l,0)=\frac{1}{2\mu i}[\![\kappa\varphi(z)-z\overline{\varphi'(z)}-\overline{\psi(z)}]\!]=\frac{\kappa+1}{2\mu i}[\![\varphi(Z)]\!]_{Z=(l^{\frac{2\pi}{\omega}},0)}$$

On the lips of the crack in Z-domain, we have :

$$\begin{aligned}
\varphi'(Z) &= \frac{\sigma_c}{2\pi i\sqrt{\ell^{\frac{2\pi}{\omega}}-Z}}\frac{\omega}{2\pi}\int_{l^{\frac{2\pi}{\omega}}}^{\ell^{\frac{2\pi}{\omega}}} s^{\frac{\omega}{2\pi}-1}\Big[\frac{\sqrt{\ell^{\frac{2\pi}{\omega}}-s}}{s-Z}+\frac{1}{\sqrt{\ell^{\frac{2\pi}{\omega}}-s}}\Big]ds\\
&= \frac{\sigma_c\sqrt{\ell^{\frac{2\pi}{\omega}}-Z}}{4\pi i}\frac{\omega}{\pi}\int_{l^{\frac{2\pi}{\omega}}}^{\ell^{\frac{\omega}{2\pi}}}\frac{s^{\frac{\omega}{2\pi}-1}}{(s-Z)\sqrt{\ell^{\frac{\omega}{2\pi}}-s}}ds\\
&= \frac{\sigma_c\sqrt{\ell^{\frac{\omega}{2\pi}}-Z}}{2\pi i}\frac{\omega}{\pi}\int_0^{\theta_m}\ell^{1-\frac{\pi}{\omega}}\frac{(\cos\theta)^{\frac{\omega}{\pi}-1}}{\ell^{\frac{\omega}{2\pi}}(\cos\theta)^2-Z}d\theta
\end{aligned} \tag{3.70}$$

Consequently, the jump of the displacement at the tip of non-cohesive zone as follow :

$$\begin{aligned}
[\![u_2(Z)]\!](l^{\frac{2\pi}{\omega}},0) &= -\frac{\sigma_c(\kappa+1)}{\mu}\frac{1}{4\pi}\frac{\omega}{\pi}\int_{\ell^{\frac{\omega}{2\pi}}}^{l^{\frac{\omega}{2\pi}}}\sqrt{\ell^{\frac{\omega}{2\pi}}-Z}\int_0^{\theta_m}\ell^{1-\frac{\pi}{\omega}}\frac{(\cos\theta)^{\frac{1}{k}-1}}{\ell^{\frac{\omega}{2\pi}}(\cos\theta)^2-Z}d\theta dZ\\
&= \frac{\sigma_c(\kappa+1)}{\mu}\frac{\ell}{2\pi}\frac{\omega}{\pi}\int_0^{\theta_m}\sin^2\sigma\cos\sigma\int_0^{\theta_m}\frac{(\cos\theta)^{\frac{1}{k}-1}}{\cos^2\theta-\cos^2\sigma}d\theta d\sigma\\
&= \frac{\sigma_c(\kappa+1)}{\mu}\frac{\ell}{2\pi}\frac{\omega}{\pi}\int_0^{\theta_m}(\cos\theta)^{\frac{\omega}{\pi}-1}\Big[\sin\theta_m+\frac{\sin\theta}{2}\ln\frac{\sin\theta_m-\sin\theta}{\sin\theta_m+\sin\theta}\Big]d\theta
\end{aligned} \tag{3.71}$$

Finally, we obtain the second equation governs for the length of the non-cohesive crack :

$$\frac{\delta_c \mu}{\sigma_c(\kappa+1)} = \frac{\ell}{2\pi}\frac{\omega}{\pi}\int_0^{\theta_m} (\cos\theta)^{\frac{\omega}{\pi}-1}\Big[\sin\theta_m + \frac{\sin\theta}{2}\ln\frac{\sin\theta_m - \sin\theta}{\sin\theta_m + \sin\theta}\Big]d\theta \tag{3.72}$$

Setting

$$\varepsilon = \frac{\delta_c \mu}{\sigma_c(\kappa+1)}, \text{ and } \quad \tilde{\ell} = \ell/\varepsilon, \quad \text{as well as } \quad \tilde{l} = l/\varepsilon \tag{3.73}$$

The so-called general load is denoted by $\mathcal{F} = -\frac{2(\lambda+2\mu)}{\delta_c} c_{\alpha_1} T \varepsilon^{\alpha_1}$. And finally, we get the two equations govern for the law of cracking.

$$\begin{cases} \mathcal{F} = & \dfrac{\tilde{\ell}^{1-\alpha_1}}{\pi\alpha_1 Q_1}\displaystyle\int_0^{\theta_m} \big(\cos\theta\big)^{\frac{1}{k}-1} d\theta \\ 1 = & \dfrac{\tilde{\ell}}{2\pi}\dfrac{\omega}{\pi}\displaystyle\int_0^{\theta_m} (\cos\theta)^{\frac{\omega}{\pi}-1}\Big[\sin\theta_m + \dfrac{\sin\theta}{2}\ln\dfrac{\sin\theta_m - \sin\theta}{\sin\theta_m + \sin\theta}\Big]d\theta \end{cases} \tag{3.74}$$

The quantity $\mathcal{F}$ is relative to t by the formula $\mathsf{t} = T\ell^{-\alpha_1}$. Therefore, we have:

$$\mathsf{t} = -\frac{\delta_c}{2(\lambda+2\mu)}\frac{\mathcal{F}}{c_{\alpha_1}\varepsilon^{2\alpha_1}}\tilde{\ell}^{-\alpha_1} \tag{3.75}$$

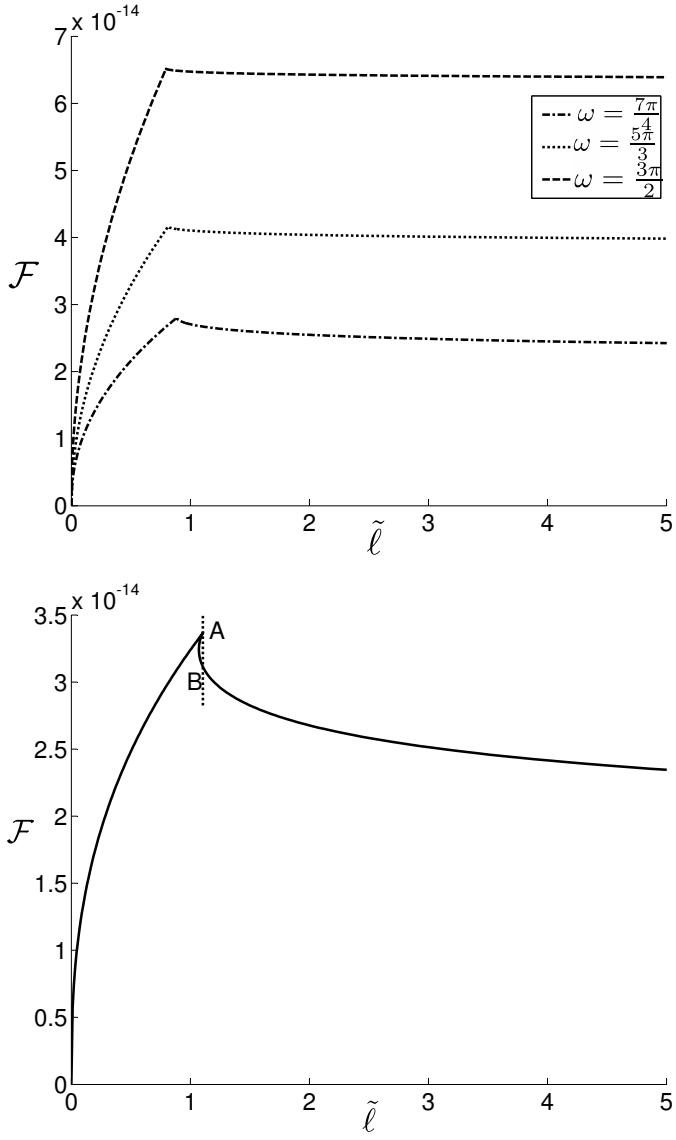

Figure 3.5: The relations between the applied load $\mathcal{F}$ and the position of the crack tip. Upper: in case of ω greater than ω_0; Lower: in case of ω less than ω_0

The relation between $\mathcal{F}$ and the position of the tip of the cohesive zone will be expressed in the Figure 3.5. We observe that, when $\omega > \omega_0$, the snap through behavior appears in the rupture, see upper one in the Figure 3.5. But when $\omega < \omega_0$, we get the snap-back phenomena because there exists a turning curve which is between A and B in the lower one in the Figure 3.5. In the both cases, there exists the limit point A as the critical value such that when the value of $\mathcal{F}$ (relative to $\mathtt{t}$) reaches A, the structure takes off dynamically. However, when the applied load below this value, the first cohesive

zone appear and propagate only at the beginning. Similarly, when the length of crack is not small any more, the hardening phenomena will appear in the behavior of the rupture. So that, when the applied load reaches the limit point A, the brutal crack of the length differs to 0 will initiate very rapidly.

3.3.6 Conclusion

The final result which contains in the equations (3.74) gives us the rupture law of the material. The difference between Griffith's model and cohesive's model relies on the beginning of the curve $\ell - \mathcal{F}$. By adding one cohesive zone in front of the crack tip, it generates the first hardening curve of the behavior of rupture in the cohesive model. Combining unstable phase with the hardening after unstable phase, cohesive's model allows to predict the crack nucleation.

3.A Appendix

3.A.1 Proof of Proposition 3.1

Proposition 3.1. *(Case $0 \leq \epsilon < 1$ and $0 < \ell < L$) For each $\epsilon \in [0,1)$, $\ell \mapsto P_\epsilon(\ell)$ is indefinitely differentiable on $(0,L)$. Moreover the first derivative P'_ϵ can read as :*

$$\begin{aligned}\mathcal{P}'_\epsilon(\ell) &= \frac{1}{\ell}\int_{\underline{R}_0^\ell}\left(\frac{\lambda+2\mu}{2}\Big(U_{2,2}^2-U_{1,1}^2\Big)+\frac{\mu}{2}\Big(U_{1,2}^2-U_{2,1}^2\Big)\right)d\mathbf{x}\\ &- \frac{1}{L-\ell}\int_{R_\ell^L}\left(\frac{\lambda+2\mu}{2}\Big(U_{2,2}^2-U_{1,1}^2\Big)+\frac{\mu}{2}\Big(U_{1,2}^2-U_{2,1}^2\Big)\right)d\mathbf{x}\end{aligned} \tag{3.76}$$

Proof. We make a change of variables to send the ℓ-dependent domain Ω_ϵ^ℓ into a fixed domain Ω_ϵ^d. Let choose $d \in (0,L)$ and let ϕ_ℓ be the following map:

$$\widetilde{\mathbf{x}} := \phi_\ell(\mathbf{x}) = \mathbf{x} + \begin{cases}\mathbf{0} & \text{if } x_1 < 0\\ (d-\ell)\dfrac{x_1}{\ell}\mathbf{e}_1 & \text{if } 0 \leq x_1 \leq \ell\\ (d-\ell)\dfrac{L-x_1}{L-\ell}\mathbf{e}_1 & \text{if } \ell \leq x_1 < L\end{cases} \tag{3.77}$$

with

$$F_\ell := \nabla\phi_\ell = \mathbf{e}_2\otimes\mathbf{e}_2 + \begin{cases}\mathbf{e}_1\otimes\mathbf{e}_1 & \text{if } x_1 < 0\\ \dfrac{d}{\ell}\mathbf{e}_1\otimes\mathbf{e}_1 & \text{if } 0 \leq x_1 \leq \ell\\ \dfrac{L-d}{L-\ell}\mathbf{e}_1\otimes\mathbf{e}_1 & \text{if } \ell \leq x_1 < L\end{cases} \tag{3.78}$$

Inserting (3.77), and (3.78) into (3.13), we obtain :

$$\mathcal{P}_\epsilon(\ell) = \min_{\widetilde{v}\in\mathcal{V}_\epsilon^d}\left\{\frac{1}{2}\sum_{i=1}^{18}a_\ell^i \mathrm{p}^i(\widetilde{\mathbf{v}},\widetilde{\mathbf{v}}) + \sum_{i=1}^{4}b_\ell^i \mathrm{q}^i(\widetilde{\mathbf{v}}) + c\right\} \tag{3.79}$$

with $c = (\lambda+3\mu)(2-\epsilon)$ while the coefficients $\{a_\ell^i\}_{1\leq i\leq 18}$ are in Table 3.3, $\{\mathsf{p}_\ell^i\}_{1\leq i\leq 18}$ in Table 3.5, $\{b_\ell^i\}_{1\leq i\leq 4}$ and $\{\mathsf{q}^i\}_{1\leq i\leq 4}$ in Table 3.4.

The minimizer in (3.79) is $\tilde{\mathbf{V}}_\epsilon^\ell$, the push-forward of $\mathbf{V}_\epsilon^\ell$, with $\tilde{\mathbf{V}}_\epsilon^\ell = \tilde{\mathbf{U}}_\epsilon^\ell - \bar{\mathbf{U}}_\epsilon$ because $\tilde{\bar{\mathbf{U}}}_\epsilon = \bar{\mathbf{U}}_\epsilon$.

Moreover, $p^\ell(\mathbf{u},\mathbf{u})$ satisfies the coercive condition, $\mathsf{p}^\ell = \sum_{i=1}^{18}a_\ell^i\mathsf{p}^i$. Choosing the positive the coefficient D such that :

$$\mathsf{C} = \min_{0<\ell<L}\left\{\frac{1}{2}a_\ell^1, 2a_\ell^2, 2a_\ell^3, \frac{1}{2}a_\ell^4, \frac{1}{2}a_\ell^5, a_\ell^6, \frac{1}{2}a_\ell^7, 2a_\ell^8, 2a_\ell^9, \frac{1}{2}a_\ell^{10}, \frac{1}{2}a_\ell^{13}, 2a_\ell^{14}, 2a_\ell^{15}, \frac{1}{2}a_\ell^{16}\right\} \tag{3.80}$$

i	1	2	3	4	5	6	7	8	9
a^i_ℓ	$\lambda+2\mu$	μ	μ	$\lambda+2\mu$	2λ	2μ	$(\lambda+2\mu)\frac{d}{\ell}$	$\mu\frac{\ell}{d}$	$\mu\frac{d}{\ell}$
i	10	11	12	13	14	15	16	17	18
a^i_ℓ	$(\lambda+2\mu)\frac{\ell}{d}$	2λ	2μ	$(\lambda+2\mu)\frac{L-d}{L-\ell}$	$\mu\frac{L-\ell}{L-d}$	$\mu\frac{L-d}{L-\ell}$	$(\lambda+2\mu)\frac{L-\ell}{L-d}$	2λ	2μ

Table 3.3: The coefficients $\{a^i_\ell\}_{1\le i\le 18}$ for the case $0\le\epsilon<1$ and $0<\ell<L$ in the formula (3.79)

i	1	2	3	4
b^i_ℓ	$\lambda+2\mu$	μ	μ	λ
$\mathsf{q}^i(\mathbf{v})$	$\int_{N^c_\epsilon}-\frac{\text{sign}(x_2)}{H}v_{1,1}d\mathbf{x}$	$\int_{N^c_\epsilon}-\frac{\text{sign}(x_2)}{H}v_{1,2}d\mathbf{x}$	$\int_{N^c_\epsilon}-\frac{\text{sign}(x_2)}{H}v_{2,1}d\mathbf{x}$	$\int_{N^c_\epsilon}-\frac{\text{sign}(x_2)}{H}v_{2,2}d\mathbf{x}$

Table 3.4: The coefficients $\{b^i_\ell\}_{1\le i\le 4}$ and $\{\mathsf{q}^i\}_{1\le i\le 4}$ for the case $0\le\epsilon<1$ and $0<\ell<L$ in the formula (3.79)

i	1	2	3
$\mathsf{p}^i(\mathbf{u},\mathbf{v})$	$\int_{\mathcal{N}^c_\epsilon}u_{1,1}v_{1,1}d\mathbf{x}$	$\int_{\mathcal{N}^c_\epsilon}u_{1,2}v_{1,2}d\mathbf{x}$	$\int_{\mathcal{N}^c_\epsilon}u_{2,1}v_{2,1}d\mathbf{x}$
i	4	5	6
$\mathsf{p}^i(\mathbf{u},\mathbf{v})$	$\int_{\mathcal{N}^c_\epsilon}u_{2,2}v_{2,2}d\mathbf{x}$	$\frac{1}{2}\int_{N^c_\epsilon}\Big(u_{1,1}v_{2,2}+v_{1,1}u_{2,2}\Big)d\mathbf{x}$	$\frac{1}{2}\int_{N^c_\epsilon}\Big(u_{1,2}v_{2,1}+v_{1,2}u_{2,1}\Big)d\mathbf{x}$
i	7	8	9
$\mathsf{p}^i(\mathbf{u},\mathbf{v})$	$\int_{\underline{R}^d_0}u_{1,1}v_{1,1}d\mathbf{x}$	$\int_{\underline{R}^d_0}u_{1,2}v_{1,2}d\mathbf{x}$	
i	10	11	12
$\mathsf{p}^i(\mathbf{u},\mathbf{v})$	$\int_{\underline{R}^L_0}u_{2,2}v_{2,2}d\mathbf{x}$	$\frac{1}{2}\int_{\underline{R}^L_0}\Big(u_{1,1}v_{2,2}+v_{1,1}u_{2,2}\Big)d\mathbf{x}$	$\frac{1}{2}\int_{\underline{R}^L_0}\Big(u_{1,2}v_{2,1}+v_{1,2}u_{2,1}\Big)d\mathbf{x}$
i	13	14	15
$\mathsf{p}^i(\mathbf{u},\mathbf{v})$	$\int_{R^L_d}u_{1,1}v_{1,1}d\mathbf{x}$	$\int_{R^L_d}u_{1,2}v_{1,2}d\mathbf{x}$	$\int_{R^L_d}u_{2,1}v_{2,1}d\mathbf{x}$
i	16	17	18
$\mathsf{p}^i(\mathbf{u},\mathbf{v})$	$\int_{R^L_d}u_{2,2}v_{2,2}d\mathbf{x}$	$\frac{1}{2}\int_{R^L_d}\Big(u_{1,1}v_{2,2}+v_{1,1}u_{2,2}\Big)d\mathbf{x}$	$\frac{1}{2}\int_{R^L_d}\Big(u_{1,2}v_{2,1}+v_{1,2}u_{2,1}\Big)d\mathbf{x}$

Table 3.5: The family of continuous bilinear symmetric forms $\{q^i(\mathbf{u},\mathbf{v})\}_{1\le i\le 18}$ for the case $0\le\epsilon<1$ and $0<\ell<L$ in the formula (3.79)

Obviously, we have :

$$\begin{aligned}\mathsf{p}^{\ell}(\mathbf{u},\mathbf{u}) &\geq \mathsf{C}\int_{\Omega_\epsilon^\ell}\Big(2(u_{1,1}^2+u_{2,2}^2)+\frac{1}{2}(u_{1,2}^2+u_{2,1}^2)+u_{1,2}u_{2,1}+2u_{1,1}u_{2,2}\Big)d\mathbf{x}\\ \mathsf{p}^{\ell}(\mathbf{u},\mathbf{u}) &\geq \mathsf{C}\int_{\Omega_\epsilon^\ell}\Big(u_{1,1}^2+u_{2,2}^2+\Big(\frac{1}{2}(u_{1,2}+u_{2,1})\Big)^2+\Big(\frac{1}{2}(u_{2,1}+u_{1,2})\Big)^2\Big)d\mathbf{x}\end{aligned}\tag{3.81}$$

Relying upon the Korn's inequality, there exists a constant $c_K>0$, known as Korn's constant such that

$$\int_{\Omega_\epsilon^\ell}\sum_{i,j=1}^{2}\Big(|u_i(\mathbf{x})|^2+|\varepsilon_{ij}(\mathbf{x})|^2\Big)d\mathbf{x} \;\geq\; \frac{1}{c_K}\|u\|^2_{H^1(\Omega_\epsilon^\ell)} \quad\text{with}\quad \varepsilon_{ij}(\mathbf{x})=\frac{1}{2}\Big(\frac{\partial u_j}{\partial x_i}+\frac{\partial u_i}{\partial x_j}\Big)$$

Then, putting $c^*=\max\{c_K-1,c_K\}>0$, we can deduce that :

$$\int_{\Omega_\epsilon^\ell}\sum_{i,j=1}^{2}|\varepsilon_{ij}(\mathbf{x})|^2d\mathbf{x}\geq\frac{1}{c^*}\int_{\Omega_\epsilon^\ell}\Big(|u_{1,1}|^2+|u_{1,2}|^2+|u_{2,1}|^2+|u_{2,2}|^2\Big)d\mathbf{x}\tag{3.82}$$

Finally, we get :

$$\mathsf{p}^{\ell}(\mathbf{u},\mathbf{u})\geq\frac{1}{c^*}\int_{\Omega_\epsilon^\ell}\Big(|u_{1,1}|^2+|u_{1,2}|^2+|u_{2,1}|^2+|u_{2,2}|^2\Big)d\mathbf{x}\tag{3.83}$$

Thanks to the Poincare's inequality, there exists a positive real number called c_P such that :

$$\int_{\Omega_\epsilon^\ell}\Big(u_{1,1}|^2+|u_{1,2}|^2+|u_{2,1}|^2+|u_{2,2}|^2\Big)d\mathbf{x}\geq c_P\|u\|_{H^1(\Omega_\epsilon^\ell)}\tag{3.84}$$

Eq (3.83) and Eq (3.84) show that p^ℓ is coercive. Using the Schwarz's inequality and Poincare's inequality, we see that $\{\mathsf{p}^i\}_i$ and $\{q^i\}_i$ are bounded. The family $\{\mathsf{q}^i\}_i$ is continuous bilinear symmetric forms in $\mathcal{H}^1(\Omega_\epsilon^\ell)$, and $\{\mathsf{q}^i\}_{1\leq i\leq n}$ is a family of continuous linear forms in $\mathcal{H}^1(\Omega_\epsilon^\ell)$. In order to make the notations more simple, we write that $\tilde{\mathbf{U}}_\epsilon^\ell=\tilde{\mathbf{U}}$. Applying Lemma 3.2 given at the end of the appendix, the derivative of the elastic energy $\mathcal{P}_\epsilon(\ell)$ w.r.t ℓ can be expressed as follows:

$$\begin{aligned}\mathcal{P}_\epsilon{}'(\ell) &= \frac{1}{d}\int_{\underline{R}_0^d}\Big[\frac{\lambda+2\mu}{2}\widetilde{U}_{2,2}^2+\frac{\mu}{2}\widetilde{U}_{1,2}^2-\frac{\mu}{2}\Big(\frac{d}{\ell}\Big)^2\widetilde{U}_{2,1}^2-\frac{\lambda+2\mu}{2}\Big(\frac{d}{\ell}\Big)^2\widetilde{U}_{1,1}^2\Big]d\mathbf{x}\\ &+\;\frac{1}{L-d}\int_{R_d^L}\Big[\frac{\mu}{2}\Big(\frac{L-d}{L-\ell}\Big)^2\widetilde{U}_{2,1}^2+\frac{\lambda+2\mu}{2}\Big(\frac{L-d}{L-\ell}\Big)^2\widetilde{U}_{1,1}^2-\frac{\lambda+2\mu}{2}\widetilde{U}_{2,2}^2-\frac{\mu}{2}\widetilde{U}_{1,2}^2\Big]d\mathbf{x}\end{aligned}\tag{3.85}$$

Making the inverse change of variable $\mathbf{x}\mapsto\phi_\ell^{-1}(\mathbf{x})$ inside the integral of Eq (3.85) and taking into account that $\bar{\mathbf{U}}_\epsilon=0$ when $x_1>0$ lead to the conclusion. □

i	1	2	3	4	5	6
a^i_ℓ	$(\lambda+2\mu)\frac{H}{H+\ell}$	$\mu\frac{L+\ell}{H}$	$\mu\frac{H}{H+\ell}$	$(\lambda+2\mu)\frac{H+\ell}{H}$	2λ	2μ
i	7	8	9	10	11	12
a^i_ℓ	$\lambda+2\mu$	$\mu\frac{L-\ell}{L}$	$\mu\frac{L}{L-\ell}$	$(\lambda+2\mu)\frac{L-\ell}{L}$	2λ	2μ

Table 3.6: The coefficients $\{a^i_\ell\}_{1\le i\le 12}$ for the case $\epsilon=0$ and $\ell=0$ in the formula (3.89)

3.A.2 Proof of Proposition 3.3

Proposition 3.3. *(Case $\epsilon=0$ and $\ell=0$) $\mathcal{P}_0$ is indefinitely differentiable on (-H, L). Moreover, the first derivative $\mathcal{P}'_0$ can read as*

$$\begin{aligned}\mathcal{P}'_0(\ell) &= \frac{1}{H+\ell}\int_{\underline{R}^\ell_{-H}}\Big(\frac{\lambda+2\mu}{2}\Big(U^2_{2,2}-U^2_{1,1}\Big)+\frac{\mu}{2}\Big(U^2_{1,2}-U^2_{2,1}\Big)\Big)d\mathbf{x}\\ &- \frac{1}{L-\ell}\int_{\underline{R}^L_\ell}\Big(\frac{\lambda+2\mu}{2}\Big(U^2_{2,2}-U^2_{1,1}\Big)+\frac{\mu}{2}\Big(U^2_{1,2}-U^2_{2,1}\Big)\Big)d\mathbf{x}\end{aligned} \tag{3.86}$$

Proof. When $\epsilon=0$, the notch becomes a preexisting crack of length H. The change of variable in Eq (3.77) is not valid any more when $\ell=0$. Here, we choose a different function $\phi_\ell(\mathbf{x})$:

$$\phi_\ell(\mathbf{x})=\mathbf{x}-\begin{cases}\ell\dfrac{H+x_1}{H+\ell}\mathbf{e}_1 & \text{if } -H\le x_1\le\ell\\ \ell\dfrac{L-x_1}{L-\ell}\mathbf{e}_1 & \text{if } \ell\le x_1\le L\end{cases} \tag{3.87}$$

$$\nabla\phi_\ell=\mathbf{e}_2\otimes\mathbf{e}_2+\begin{cases}\dfrac{H}{H+\ell}\mathbf{e}_1\otimes\mathbf{e}_1 & \text{if } -H\le x_1\le\ell\\ \dfrac{L}{L-\ell}\mathbf{e}_1\otimes\mathbf{e}_1 & \text{if } \ell\le x_1\le L\end{cases} \tag{3.88}$$

Similarly, inserting (3.87) and (3.88) into (3.13), we obtain :

$$\mathcal{P}_0(\ell)=\min_{\tilde{\mathbf{v}}\in\mathcal{V}^\ell_\epsilon}\Big\{\frac{1}{2}\sum_{i=1}^{12}a^i_\ell\mathsf{p}^i(\tilde{\mathbf{v}},\tilde{\mathbf{v}})+\sum_{i=1}^{4}b^i_\ell\mathsf{q}^i(\tilde{\mathbf{v}})+c\Big\} \tag{3.89}$$

with $c=(\lambda+3\mu)(2-\epsilon)$, while the coefficients $\{a^i_\ell\}_{1\le i\le 12}$ are in Table 3.6, the family of functions $\{\mathsf{q}^i(\mathbf{u},\mathbf{v})\}_{1\le i\le 12}$ and the coefficients $\{b^i_\ell\}_{1\le i\le 4}$ in Table 3.7.

Showing coercive condition for $p_l=\sum_{i=1}^{10}a^i_l p^i$ is done similarly as in the Proposition 3.A.1. Then applying the Lemma 3.2 again, gives us :

$$\begin{aligned}\mathcal{P}_0{}'(\ell) &= \frac{1}{H}\int_{\underline{R}^l_{-H}}\Big[\frac{\lambda+2\mu}{2}\widetilde{U}^2_{2,2}+\frac{\mu}{2}\widetilde{U}^2_{1,2}-\frac{\mu}{2}\frac{H^2}{(H+\ell)^2}\widetilde{U}^2_{2,1}-\frac{\lambda+2\mu}{2}\frac{H^2}{(H+\ell)^2}\widetilde{U}^2_{1,1}\Big]d\mathbf{x}\\ &- \frac{1}{L}\int_{R^L_\ell}\Big\{\frac{\lambda+2\mu}{2}\widetilde{U}_{2,2}+\frac{\mu}{2}\widetilde{U}^2_{1,2}-\frac{\mu}{2}\frac{L^2}{(L-\ell)^2}\widetilde{U}^2_{2,1}-\frac{\lambda+2\mu}{2}\frac{L^2}{(L-\ell)^2}\widetilde{U}^2_{1,1}\Big\}d\mathbf{x}\end{aligned}$$

i	1	2	3	4
b^i_ℓ	$(\lambda+2\mu$	μ	μ	λ
$\mathsf{q}^i_\ell(\mathbf{v})$	$\int_{N_0^c} -\frac{\text{sign}(x_2)}{H} v_{1,1} d\mathbf{x}$	$\int_{N_0^c} -\frac{\text{sign}(x_2)}{H} v_{1,2} d\mathbf{x}$	$\int_{N_0^c} -\frac{\text{sign}(x_2)}{H} v_{2,1} d\mathbf{x}$	$\int_{N_0^c} -\frac{\text{sign}(x_2)}{H} v_{2,2} d\mathbf{x}$

Table 3.7: The coefficients $\{b^i_\ell\}_{1\le i\le 4}$ and $\{\mathsf{q}^i_\ell\}_{1\le i\le 4}$ for the case $0 \le \epsilon = 0$ and $\ell = 0$ in the formula (3.89)

i	1	2	3
$\mathsf{p}^i_\ell(\mathbf{u},\mathbf{v})$	$\int_{\underline{R}^\ell_{-H}} u_{1,1}v_{1,1} d\mathbf{x}$	$\int_{\underline{R}^\ell_{-H}} u_{1,2}v_{1,2} d\mathbf{x}$	$\int_{\underline{R}^\ell_{-H}} u_{2,1}v_{2,1} d\mathbf{x}$
i	4	5	6
$\mathsf{p}^i_\ell(\mathbf{u},\mathbf{v})$	$\int_{\underline{R}^\ell_{-H}} u_{2,2}v_{2,2} d\mathbf{x}$	$\int_{\underline{R}^\ell_{-H}} \frac{1}{2}\Big(u_{1,1}v_{2,2} + v_{1,1}u_{2,2}\Big) d\mathbf{x}$	$\int_{\underline{R}^\ell_{-H}} \frac{1}{2}\Big(u_{1,2}v_{2,1} + v_{1,2}u_{2,1}\Big) d\mathbf{x}$
i	7	8	9
$\mathsf{p}^i_\ell(\mathbf{u},\mathbf{v})$	$\int_{R^L_\ell} u_{1,1}v_{1,1} d\mathbf{x}$	$\int_{R^L_\ell} u_{1,2}v_{1,2} d\mathbf{x}$	$\int_{R^L_\ell} u_{2,1}v_{2,1} d\mathbf{x}$
i	10	11	12
$\mathsf{p}^i_\ell(\mathbf{u},\mathbf{v})$	$\int_{R^L_\ell} u_{2,2}v_{2,2} d\mathbf{x}$	$\int_{R^L_\ell} \frac{1}{2}\Big(u_{1,1}v_{2,2} + v_{1,1}u_{2,2}\Big) d\mathbf{x}$	$\int_{R^L_\ell} \frac{1}{2}\Big(u_{1,2}v_{2,1} + v_{1,2}u_{2,1}\Big) d\mathbf{x}$

Table 3.8: The coefficients $\{\mathsf{p}^i_\ell\}_{1\le i\le 12}$ for the case $0 \le \epsilon = 0$ and $\ell = 0$ in the formula (3.89)

making the inverse change variable $\mathbf{x} \mapsto \phi_\ell^{-1}(\mathbf{x})$, we get Eq (3.16). □

3.A.3 Proof of Proposition 3.4

Proposition 3.4. *(Case $0 < \epsilon < 1$ and $\ell = 0$) The release of potential energy due to the a crack small length ℓ is of the order of $\ell^{2\alpha}$, i.e there exists $C_\epsilon \ge 0$ such that*

$$0 \le \limsup_{\ell \downarrow 0} \frac{\mathcal{P}_\epsilon(0) - \mathcal{P}_\epsilon(\ell)}{\ell^{2\alpha}} \le C_\epsilon \tag{3.90}$$

Because $0 < \epsilon \le 1$, the value of α is the solution of Equation (3.20) such that $1 \ge \alpha > \frac{1}{2}$. Therefore, $\mathcal{P}'_\epsilon(0) = 0$. Moreover, $\mathcal{P}'_\epsilon$ is continuous at 0, and

$$\lim_{\ell \downarrow 0} \mathcal{P}'_\epsilon(\ell) = 0$$

Proof. The proof is divided into 4 steps.

Step 1 : Let $\ell > 0$ small enough. Calling that $\mathcal{S}^\ell_\epsilon$ stands for the set of statically admissible stress fields, i.e.

$$\mathcal{S}^\ell_\epsilon = \{\boldsymbol{\tau} \in L^2(\Omega^\ell_\epsilon;\ \mathbb{R}^4)\ :\ \int_{\Omega^\ell_\epsilon} \boldsymbol{\tau} \nabla \mathbf{v} d\mathbf{x} = 0,\ \forall \mathbf{v} \in \mathcal{V}^\ell_\epsilon\} \tag{3.91}$$

Generally, the tensor $\mathbf{A}$ is an elastic matrix characterizing for the material, then the elastic energy of the body can be read as :

$$\begin{aligned}
\mathcal{P}_\epsilon(\ell) &= \min_{\mathbf{u}\in\mathcal{U}_\epsilon^\ell}\int_{\Omega_\epsilon^\ell}\frac{1}{2}\mathbf{A}\boldsymbol{\epsilon}(\mathbf{u})\boldsymbol{\epsilon}(\mathbf{u})d\mathbf{x}\\
&= \min_{\mathbf{u}\in\mathcal{U}_\epsilon^l}\max_{\boldsymbol{\tau}\in L^2(\Omega_\epsilon^l;\mathbb{R}^4)}\int_{\Omega_\epsilon^\ell}\big[\boldsymbol{\tau}\boldsymbol{\varepsilon}(\mathbf{u})-\frac{1}{2}\mathbf{A}^{-1}\boldsymbol{\tau}\boldsymbol{\tau}\big]d\mathbf{x}\\
&= \max_{\boldsymbol{\tau}\in L^2(\Omega_\varepsilon^\ell;\mathbb{R}^4)}\min_{\mathbf{u}\in\mathcal{U}_\varepsilon^\ell}\int_{\Omega_\varepsilon^\ell}\big[\boldsymbol{\tau}\boldsymbol{\varepsilon}(\mathbf{u})-\frac{1}{2}\mathbf{A}^{-1}\boldsymbol{\tau}\boldsymbol{\tau}\big]d\mathbf{x}\\
&= \max_{\boldsymbol{\tau}\in\mathcal{S}_\varepsilon^\ell}\int_{\Omega_\varepsilon^\ell}\big[\boldsymbol{\tau}\boldsymbol{\varepsilon}(\mathbf{U}_\varepsilon^0)-\frac{1}{2}\mathbf{A}^{-1}\boldsymbol{\tau}\boldsymbol{\tau}\big]d\mathbf{x} \qquad (3.92)
\end{aligned}$$

Using the Airy function Φ in plane-strain case, we have

$$\begin{cases}
\sigma_{rr} = & \frac{1}{r^2}\Phi_{,\theta\theta}+\frac{1}{r}\Phi_{,\theta}\\
\sigma_{\theta\theta} = & \Phi_{,rr} \qquad\qquad \text{in } B_{2\ell}\cap\Omega_\varepsilon^\ell\\
\sigma_{r\theta} = & -(\frac{1}{r}\Phi_{,\theta})_{,r}
\end{cases} \qquad (3.93)$$

Now, we construct a statically admissible stress field $\boldsymbol{\tau}$ by introducing the function $f(r)=r/\ell-1$ for $r\in[\ell,2\ell]$ as following :

$$\begin{cases}
\boldsymbol{\tau}=0 \quad \text{in} \quad \Omega_\varepsilon^\ell\cap B_\ell\\
\tau_{rr}=\dfrac{f(r)}{r^2}\Phi_{,\theta\theta}+\dfrac{1}{r}(f(r)\Phi)_{,\theta},\ \tau_{\theta\theta}=(f(r)\Phi(r))_{,rr},\ \tau_{r\theta}=-\big(\dfrac{1}{r}f(r)\Phi_{,\theta}\big)_{,r} \text{ in } \Omega_\varepsilon^\ell\cap B_{2\ell}\\
\boldsymbol{\tau}=\boldsymbol{\sigma}_\varepsilon \quad \text{in} \quad \Omega_\varepsilon^\ell\setminus B_{2\ell}
\end{cases} \qquad (3.94)$$

belongs to $\mathcal{S}_\varepsilon^\ell$.

$$\mathcal{P}_\varepsilon(\ell)=\max_{\boldsymbol{\tau}\in\mathcal{S}_\varepsilon^\ell}\int_{\Omega_\varepsilon^l}\Big(\boldsymbol{\tau}\boldsymbol{\varepsilon}_0-\frac{1}{2}\mathbf{A}^{-1}\boldsymbol{\tau}\boldsymbol{\tau}\Big)d\mathbf{x} \qquad (3.95)$$

$$\mathcal{P}_\varepsilon(\ell)=\max_{\boldsymbol{\tau}\in\mathbf{S}_\varepsilon^\ell}\int_{\Omega_\varepsilon^l}\left[\boldsymbol{\tau}\boldsymbol{\varepsilon}_0-\frac{1}{2}\big(-\frac{\nu}{E}\tau_{kk}\tau_{ii}+\frac{1+\nu}{E}\tau_{ij}\tau_{ij}\big)\right]d\mathbf{x} \qquad (3.96)$$

So, we can get :

$$\begin{aligned}
\mathcal{P}_\varepsilon(0)-\mathcal{P}_\varepsilon(\ell) &\le \frac{1}{2}\int_{\Omega_\varepsilon^\ell}\|-\frac{\nu}{E}\mathrm{tr}^2(\boldsymbol{\sigma}-\boldsymbol{\tau})+\frac{1+\nu}{E}(\boldsymbol{\sigma}-\boldsymbol{\tau}):(\boldsymbol{\sigma}-\boldsymbol{\tau})\|d\mathbf{x}\\
&\le \frac{1}{2}\int_{\Omega_\epsilon^\ell\cap B_\ell}\|-\frac{\nu}{E}\mathrm{tr}^2\boldsymbol{\sigma}+\frac{1+\nu}{E}\boldsymbol{\sigma}:\boldsymbol{\sigma}\|d\mathbf{x}\\
&+ \int_{\Omega_\epsilon^\ell\cap(B_{2\ell}\setminus B_\ell)}\frac{1}{2}\max_{r\in[\ell,2\ell]}\Big\{-\frac{\nu}{E}\big[\sigma_{rr}-\tau_{rr}+\sigma_{\theta\theta}-\tau_{\theta\theta}\big]^2\\
&+ \frac{1+\nu}{E}\big[(\sigma_{rr}-\tau_{rr})^2+(\sigma_{\theta\theta}-\tau_{\theta\theta})^2+2(\sigma_{r\theta}-\tau_{r\theta})^2\big]\Big\}d\mathbf{x}
\end{aligned}$$

Using the formula of $\boldsymbol{\tau}$ as in (3.94), we have the right terms can be read as :

$$\begin{aligned}
&\int_{\Omega_\epsilon^\ell\cap B_\ell}\frac{1}{2}\big[-\frac{\nu}{E}(\sigma_{\theta\theta}+\sigma_{rr})^2+\frac{1+\nu}{E}(\sigma_{\theta\theta}^2+\sigma_{rr}^2+2\sigma_{r\theta}^2)\big]d\mathbf{x}\\
+\quad&\int_{\Omega_\epsilon^\ell\cap(B_{2\ell}\setminus B_\ell)}\frac{1}{2}\max_{r\in[\ell,2\ell]}\Big\{-\frac{\nu}{E}\big[\big(1-f(r)\big)\sigma_{rr}-\frac{1}{r\ell}\Phi+\big(1-f(r)\big)\sigma_{\theta\theta}-\frac{2}{\ell}\Phi_{,r}\big]^2 \qquad (3.97)\\
+\quad&\frac{1+\nu}{E}\Big[\big[\big(1-f(r)\big]\sigma_{rr}-\frac{1}{r\ell}\Phi\Big]^2+\big[\big(1-f(r)\big)\sigma_{\theta\theta}-\frac{2}{\ell}\Phi_{,r}\big]^2+2\big(2\sigma_{r\theta}+\frac{1}{\ell}\Phi_{,r\theta}\big)^2\Big\}d\mathbf{x}
\end{aligned}$$

because $\boldsymbol{\sigma}$ behaves like $r^{\alpha-1}$, Φ behaves like $r^{\alpha+1}$ and $\Phi_{,r}$ behaves like r^α, after taking the integrals, they behave like $\ell^{2\alpha}$. So we can say that

$$0\leq\limsup_{\ell\downarrow 0}\frac{\mathcal{P}_\epsilon(0)-\mathcal{P}_\epsilon(\ell)}{\ell^{2\alpha}}\leq C_\epsilon \qquad (3.98)$$

besides, we have $1>\alpha>\frac{1}{2}$, Lemma (3.1). That means $\mathcal{P}'_\epsilon(0)=0$

Step 2 : Transport of $\mathbf{U}_\epsilon^0$ into $\mathcal{U}_\epsilon^d$.

For $\ell>0$, $\widetilde{\mathbf{U}}_\epsilon^\ell$ of $\mathbf{U}_\epsilon^\ell$ is an element of $\mathcal{U}_\epsilon^d=\overline{\mathbf{U}}_\epsilon+\mathcal{V}_\epsilon^d$. In order to compare it with $\mathbf{U}_\epsilon^0$, we have to transport it into $\mathcal{U}_\epsilon^d$. Calling that $\phi_0 : R_0^L\to R_d^L$ be linear bijection $\tilde{\mathbf{x}}=\phi_0(\mathbf{x})=\big[d+\big(1-\frac{d}{L}\big)x_1\big]\mathbf{e}_1+x_2\mathbf{e}_2$ and with $\mathbf{v}:\Omega_\epsilon\to\mathbb{R}$ is associated $\widehat{\mathbf{v}}:\Omega_\epsilon^d\to\mathbb{R}$ by :

$$\widehat{\mathbf{v}}(\mathbf{x})=\begin{cases}\mathbf{v}(\mathbf{x}) & \text{in } N_\epsilon^c\\ \mathbf{v}(0,x_2) & \text{in } \underline{R}_0^d\\ \mathbf{v}\circ\phi_0^{-1}(\mathbf{x}) & \text{in } R_d^L\end{cases} \qquad (3.99)$$

the image of $\mathcal{V}_\epsilon^0$ by this isomorphism is $\widehat{\mathcal{V}}_\epsilon^0$. The elements of $\widehat{\mathcal{V}}_\epsilon^0$ which are in $\mathcal{V}_\epsilon^d$ constitute its (weakly) closed subspace $\widehat{\mathcal{V}}_\epsilon^0=\{\mathbf{v}\in\mathcal{V}_\epsilon^d:\mathbf{v}_{,1}=\mathbf{0}\text{ in }\underline{R}_0^d\}$. Because the singularity of $\mathbf{V}_\epsilon^0$ at $\mathbf{O}$ is weak, so $\int_{I_0}\mathbf{V}_{\epsilon,2}^{0^2}dx_2<+\infty$, so that $\widehat{\mathbf{V}}_\epsilon^0\in\mathcal{V}_\epsilon^d$.

Step 3 : Convergence of $\widetilde{\mathbf{U}}_\epsilon^\ell$ to $\widehat{\mathbf{U}}_\epsilon^0$ when $\ell\to 0$. Putting

$$I=\int_{\Omega_\epsilon^0}\Big[(\lambda+2\mu)(u_{1,1}^2+u_{1,2}^2)+\mu(u_{1,2}+u_{2,1})^2+2\lambda u_{1,2}u_{2,2}\Big]d\mathbf{x} \qquad (3.100)$$

Taking the integral on Ω_ϵ^d because $\widehat{\mathbf{V}}(x)$ is defined in Ω_ϵ^d, we have :

$$\begin{aligned}
I\quad=\quad&\int_{\Omega_\epsilon^d}\Big\{(\lambda+2\mu)\Big[\Big(\frac{\partial u_1}{\partial\tilde{x}_1}\frac{\partial\tilde{x}_1}{\partial x_1}\Big)^2+\Big(\frac{\partial u_2}{\partial\tilde{x}_2}\frac{\tilde{x}_2}{\partial x_2}\Big)^2\Big]+\mu\Big(\frac{\partial u_1}{\partial\tilde{x}_2}\frac{\partial\tilde{x}_2}{\partial x_2}+\frac{\partial u_2}{\partial\tilde{x}_1}\frac{\partial\tilde{x}_1}{\partial x_1}\Big)^2\\
+\quad&2\lambda\Big(\frac{\partial u_1}{\partial\tilde{x}_1}\frac{\partial\tilde{x_1}}{\partial x_1}\Big)\Big(\frac{\partial u_2}{\partial\tilde{x}_2}\frac{\partial\tilde{x}_2}{\partial x_2}\Big)\Big\}\frac{1}{\det\phi_0}d\mathbf{x}
\end{aligned}$$

with $\nabla\phi_0 = \frac{L-d}{L}\mathbf{e}_1\otimes\mathbf{e}_1 + \mathbf{e}_2\otimes\mathbf{e}_2$ from $R_0^L \to R_d^L$. We rewrite :

$$\begin{aligned}\mathcal{P}_\epsilon(0) &= \min_{\widehat{\mathbf{v}}\in\mathcal{V}_\epsilon^0}\Big\{\frac{1}{2}a_0^1\mathrm{p}^1(\widehat{\mathbf{v}}+\overline{\mathbf{U}}_\epsilon,\widehat{\mathbf{v}}+\overline{\mathbf{U}}_\epsilon)+\frac{1}{2}a_0^5\mathrm{p}^5(\widehat{\mathbf{v}}+\overline{\mathbf{U}}_\epsilon,\widehat{\mathbf{v}})+\frac{1}{2}\sum_{i=2,i\neq5}^{6}a_0^i\mathrm{p}(\widehat{\mathbf{v}},\widehat{\mathbf{v}})\\ &+ \frac{1}{2}\sum_{i=13}^{18}a_0^i\mathrm{p}^i(\widehat{\mathbf{v}},\widehat{\mathbf{v}})\Big\}\end{aligned}$$

The minimizer of $\mathcal{P}_\epsilon(0)$ is $\widehat{\mathbf{V}}_\epsilon^0$ and $\widehat{\mathbf{U}}_\epsilon^0$ which have the relation of $\widehat{\mathbf{U}}_\epsilon^0 = \overline{\mathbf{U}}_\epsilon + \widehat{\mathbf{V}}_\epsilon^0$ satisfying : $\mathrm{A}(\widehat{\mathbf{U}}_\epsilon^0,\mathbf{v}-\widehat{\mathbf{U}}_\epsilon^0) = \mathrm{L}(\mathbf{v}),\ \forall\mathbf{v}$ if and only if $\hat{\mathbf{U}}_\epsilon^0$ minimizes $\big\{\frac{1}{2}\mathrm{A}(\widehat{\mathbf{U}}_\epsilon^0,\widehat{\mathbf{U}}_\epsilon^0)-\mathrm{L}(\widehat{\mathbf{U}}_\epsilon^0)\big\}$, A is a positive bi-symmetric operator and L is a linear operator. The elastic energy $\mathcal{P}_\epsilon(0)$ can be expressed as :

$$\sum_{i=1}^{6}a_0^i\mathrm{p}^i(\widehat{\mathbf{U}}_\epsilon^0,\widehat{\mathbf{v}})+\sum_{i=13}^{18}a_0^i\mathrm{p}(\widehat{\mathbf{U}}_\epsilon^0,\widehat{\mathbf{v}})=0 \qquad \forall\widehat{\mathbf{v}}\in\mathcal{V}_\epsilon^0 \tag{3.101}$$

In (3.101),we consider $\sum_{i=1}^{6}a_0^i\mathrm{p}^i(\widehat{\mathbf{U}}_\epsilon^0,\widehat{\mathbf{v}})$ firstly,

$$\begin{aligned}\sum_{i=1}^{6}a_0^i\mathrm{p}^i(\widehat{\mathbf{U}}_\varepsilon^0,\widehat{\mathbf{v}}) &= \int_{N_\varepsilon^c}\Big[a_0^1\widehat{U}^0_{\varepsilon1,11}\widehat{v}_1+a_0^2\widehat{U}^0_{\varepsilon1,22}\widehat{v}_1+a_0^3\widehat{U}^0_{\varepsilon2,11}\widehat{v}_2+a_0^4\widehat{U}^0_{\varepsilon2,22}\widehat{v}_2\\ &+ a_0^5\big(\frac{1}{2}\widehat{U}^0_{\varepsilon1,12}\widehat{v}_2+\frac{1}{2}\widehat{U}^0_{\varepsilon2,21}\widehat{v}_1\big)+a_0^6\big(\frac{1}{2}\widehat{U}^0_{\varepsilon1,21}\widehat{v}_2+\frac{1}{2}\widehat{U}^0_{\varepsilon2,12}\widehat{v}_1\big)\Big]d\mathbf{x}\\ &= \int_{N_\varepsilon^c}\Big[\big(a_0^1\widehat{U}^0_{\varepsilon1,11}\widehat{v}_1+a_0^2\widehat{U}^0_{\varepsilon1,22}+\frac{1}{2}a_0^5\widehat{U}^0_{\varepsilon2,21}+\frac{1}{2}a_0^6\widehat{U}^0_{\varepsilon2,12}\big)\widehat{v}_1\\ &+ \big(a_0^3\widehat{U}^0_{\varepsilon2,11}+a_0^4\widehat{U}^0_{\varepsilon2,22}+\frac{1}{2}a_0^5\widehat{U}^0_{\varepsilon1,12}+\frac{1}{2}a_0^6\widehat{U}^0_{\varepsilon1,21}\big)\widehat{v}_2\Big]d\mathbf{x}\end{aligned} \tag{3.102}$$

Deriving from above, because for arbitrary $\widehat{\mathbf{v}}\in\mathcal{V}_\varepsilon^0$, in N_ε^c we get that :

$$\begin{cases}a_0^1\widehat{U}^0_{\varepsilon1,11}\widehat{v}_1+a_0^2\widehat{U}^0_{\varepsilon1,22}+\frac{1}{2}a_0^5\widehat{U}^0_{\varepsilon2,21}+\frac{1}{2}a_0^6\widehat{U}^0_{\varepsilon2,12}= & 0\\ a_0^3\widehat{U}^0_{\varepsilon2,11}+a_0^4\widehat{U}^0_{\varepsilon2,22}+\frac{1}{2}a_0^5\widehat{U}^0_{\varepsilon1,12}+\frac{1}{2}a_0^6\widehat{U}^0_{\varepsilon1,21}= & 0\end{cases} \tag{3.103}$$

Similarly, for the second sum of (3.101) :

$$\begin{aligned}\sum_{i=13}^{18}a_0^i\mathrm{p}(\widehat{\mathbf{U}}_\varepsilon^0,\widehat{\mathbf{v}}) &= \int_{R_d^L}\Big[a_0^{13}\widehat{U}^0_{\varepsilon1,11}\widehat{v}_1+a_0^{14}\widehat{U}^0_{\varepsilon1,22}\widehat{v}_1+a_0^{15}\widehat{U}^0_{\varepsilon2,11}\widehat{v}_2+a_0^{16}\widehat{U}^0_{\varepsilon2,22}\widehat{v}_2 \qquad (3.104)\\ &+ a_0^{17}\big(\frac{1}{2}\widehat{U}^0_{\varepsilon1,12}\widehat{v}_2+\frac{1}{2}\widehat{U}^0_{\varepsilon2,21}\widehat{v}_1\big)+a_0^{18}\big(\frac{1}{2}\widehat{U}^0_{\varepsilon1,21}\widehat{v}_2+\frac{1}{2}\widehat{U}^0_{\varepsilon2,12}\widehat{v}_1\big)\Big]d\mathbf{x}=0\end{aligned}$$

then, we obtain in the R_d^L that :

$$\begin{cases}a_0^{13}\widehat{U}^0_{\varepsilon1,11}+a_0^{14}\widehat{U}^0_{\varepsilon1,22}+\frac{1}{2}a_0^{17}\widehat{U}^0_{\varepsilon2,21}+\frac{1}{2}a_0^{18}\widehat{U}^0_{\varepsilon2,12}= & 0\\ a_0^{15}\widehat{U}^0_{\varepsilon2,11}+a_0^{16}\widehat{U}^0_{\varepsilon2,22}+\frac{1}{2}a_0^{17}\widehat{U}^0_{\varepsilon1,12}+\frac{1}{2}a_0^{18}\widehat{U}^0_{\varepsilon1,21}= & 0\end{cases} \tag{3.105}$$

From (1.2) and (1.3), we multiply two these equations with $\mathbf{v} = (v_1, v_2)$ in $\mathcal{V}_\varepsilon^d$, then integrate over $N_\varepsilon^c \cup R_d^L$, we can get :

$$\sum_{i=1}^{6} \mathrm{p}^i(\widehat{\mathbf{U}}_\varepsilon^0, \mathbf{v}) + \sum_{i=13}^{18} a_0^i \mathrm{p}^i(\widehat{\mathbf{U}}_\varepsilon^0, \mathbf{v}) = \mathrm{q}_1^0(\mathbf{v}) \tag{3.106}$$

where

$$\mathrm{q}_1^0(\mathbf{v}) = -\int_{\underline{R}_0^d} \big(\sigma_{11}^0 v_{1,1} + \sigma_{12}^0 v_{2,1}\big) d\mathbf{x}$$

$$\sigma_{11}^0(x_2) = (\lambda + 2\mu)\widehat{U}_{\varepsilon 1,1}^0(0-, x_2) + \lambda \widehat{U}_{\varepsilon 2,2}^0(0-, x_2) = (\lambda + 2\mu) a_0^{13} \widehat{U}_{\varepsilon 1,11}^0(d+, x_2) + \lambda a_0^{17} \widehat{U}_{\varepsilon 2,2}^0(d+, x_2)$$

$$\sigma_{12}^0(x_2) = \mu\big[\widehat{U}_{\varepsilon 2,1}^0(0-, x_2) + \widehat{U}_{\varepsilon 1,2}^0(0-, x_2)\big] = \mu\big[a_0^{15} \widehat{U}_{\varepsilon 2,1}^0(d+, x_2) + a_0^{18} \widehat{U}_{\varepsilon 1,2}^0(d+, x_2)\big]$$

Recalling $\widetilde{\mathbf{U}}_\varepsilon^\ell$ which satisfies :

$$\sum_{i=1}^{18} a_\ell^i \mathrm{p}^i(\widetilde{\mathbf{U}}_\varepsilon^\ell, \mathbf{v}) = 0 \qquad \forall \mathbf{v} \in \mathcal{V}_\varepsilon^d \tag{3.107}$$

Setting $\mathbf{w}_\ell = (w_{\ell 1}, w_{\ell 2}) = \widetilde{\mathbf{U}}_\varepsilon^\ell - \widehat{\mathbf{U}}_\varepsilon^0$ and taking $\mathbf{v} = \mathbf{w}_\ell$ in Eq (3.107), we get :

$$\begin{aligned} 0 = &\sum_{i=1}^{18} a_\ell^i \mathrm{p}^i(\mathbf{w}_\ell, \mathbf{w}_\ell) + \sum_{i=1}^{18} \mathrm{p}^i(\widehat{\mathbf{U}}_\varepsilon^0, \mathbf{w}_\ell) = \sum_{i=1}^{18} a_\ell^i \mathrm{p}^i(\mathbf{w}_\ell, \mathbf{w}_\ell) + a_\ell^8 \mathrm{p}^8(\widehat{\mathbf{U}}_\varepsilon^0, \mathbf{w}_\ell) + a_\ell^{10} \mathrm{p}(\widehat{\mathbf{U}}_\varepsilon^0, \mathbf{w}_\ell) \\ &+ \sum_{i=11}^{12} a_\ell^i \mathrm{p}^i(\widehat{\mathbf{U}}_\varepsilon^0, \mathbf{w}_\ell) + \sum_{i=13}^{18} (a_\ell^i - a_0^i) \mathrm{p}^i(\widehat{\mathbf{U}}_\varepsilon^0, \mathbf{w}_\ell) + q_1^0(\mathbf{w}_\ell) = 0 \end{aligned} \tag{3.108}$$

with the behavior of the coefficients as following :

$$\begin{aligned} a_\ell^1 = a_\ell^2 = a_\ell^3 = a_\ell^4 = a_\ell^5 = a_\ell^6 = 1, a_\ell^7 = O(\ell^{-1}),\ a_\ell^8 = O(\ell),\ a_\ell^9 = O(\ell^{-1}),\ a_\ell^{10} = O(\ell) \\ a_\ell^{11} = a_\ell^{12} = 1 a_\ell^{13} = a_\ell^{14} = a_\ell^{15} = a_\ell^{16} = a_\ell^{17} = a_\ell^{18} = O(1), a_\ell^{13} - a_0^{13} = a_\ell^{14} - a_0^{14} \\ = a_\ell^{15} - a_0^{15} = a_\ell^{16} - a_0^{16} = O(\ell) a_\ell^{17} - a_0^{17} = a_\ell^{18} - a_0^{18} = 0 \end{aligned}$$

Finally, (3.108) can be written as :

$$\begin{aligned} \sum_{i=1}^{18} a_\ell^i \mathrm{p}^i(\mathbf{w}_\ell, \mathbf{w}_\ell) + a_\ell^8 \mathrm{p}^8(\widehat{\mathbf{U}}_\varepsilon^0, \mathbf{w}_\ell) + a_\ell^{10} \mathrm{p}^{10}(\widehat{\mathbf{U}}_\varepsilon^0, \mathbf{w}_\ell) + \sum_{i=11}^{12} a_\ell^i \mathrm{p}^i(\widehat{\mathbf{U}}_\varepsilon^0, \mathbf{w}_\ell) \\ + \sum_{i=13}^{16} (a_\ell^i - a_0^i) \mathrm{p}^i(\widehat{\mathbf{U}}_\varepsilon^0, \mathbf{w}_\ell) + \mathrm{q}_1^0(\mathbf{w}_\ell) = 0 \end{aligned} \tag{3.109}$$

Deriving from (3.109), we obtain :

$$\begin{aligned} \|w_{\ell 1}\|_{N_\varepsilon^c}^2 + \|w_{\ell 2}\|_{N_\varepsilon^c}^2 + \int_{N_\varepsilon^c} \big(w_{\ell 1,1} w_{\ell 2,2} + w_{\ell 1,2} w_{\ell 2,1}\big) d\mathbf{x} + \int_{R_0^d \cup R_d^L} (\tilde{U}_{\varepsilon 1,1}^\ell w_{\ell 2,2} + \tilde{U}_{\varepsilon 1,2} w_{\ell 2,1}\big) d\mathbf{x} \\ + \frac{1}{\ell} |w_{\ell 1,1}|_{\underline{R}_0^d}^2 + \ell |w_{\ell 1,2}|_{R_d^L}^2 + \frac{1}{\ell} |w_{\ell 2,1}|_{\underline{R}_0^d}^2 + \ell |w_{\ell 2,2}|_{\underline{R}_0^d}^2 + |w_{l1}|_{R_d^L}^2 + |w_{l2}|_{R_d^L}^2 \le C\ell \big(|w_{l,2}|_{\underline{R}_0^d} \\ + |w_{l2,2}|_{\underline{R}_0^d} + \|w_{l1}\|_{R_d^L} + \|w_{l2}\|_{R_d^L}\big) + C|w_{l1,1}|_{\underline{R}_0^d} + C|w_{l2,1}|_{\underline{R}_0^d} \end{aligned}$$

It gives that :

$$\begin{aligned}&\|w_{\ell 1}\|_{N_\varepsilon^c} \leq C\sqrt{\ell};\ \|w_{\ell 2}\|_{N_\varepsilon^c} \leq C\sqrt{\ell};\ \|w_{\ell 1}\|_{R_d^L} \leq C\sqrt{\ell};\ \|w_{\ell 2}\|_{R_d^L} \leq C\sqrt{\ell}\\&|w_{\ell 1,1}|_{\underline{R}_0^d} \leq C\ell;\ |w_{\ell 2,1}|_{\underline{R}_0^d} \leq C\ell;\ |w_{\ell 1,2}| \leq C;\ |w_{\ell 2,2}| \leq C\end{aligned} \tag{3.110}$$

The equation (3.110) shows the weakly convergence of $\tilde{\mathbf{U}}_\varepsilon^\ell$ to $\widehat{\mathbf{U}}_\varepsilon^0$ in $\widehat{\mathcal{V}}_\varepsilon^0$. Besides, (3.107) passes to its limit when $\ell \to 0$. Assuming that $(\lambda+2\mu)\tilde{U}_{\varepsilon 1,1}^\ell/\ell \rightharpoonup *$ and $\mu\tilde{U}_{\varepsilon 2,1}^\ell/\ell \rightharpoonup **$, we have :

$$\begin{aligned}\sum_{i=1}^{6} \mathrm{p}^i(\widehat{\mathbf{U}}_\varepsilon^0, \mathbf{v}) + \sum_{i=13}^{18} a_0^i \mathrm{p}^i(\widehat{\mathbf{U}}_\varepsilon^0, \mathbf{v}) + \int_{\underline{R}_0^d} \big(\lambda \widehat{U}_{\varepsilon 2,2}^0 v_{1,1} + \mu \widehat{U}_{\varepsilon 1,2}^0 v_{2,1}\big) d\mathbf{x}\\ + \int_{\underline{R}_0^d} (\lambda+2\mu) \frac{d\tilde{U}_{\varepsilon 2,1}^\ell}{\ell} v_{1,1} d\mathbf{x} + \int_{\underline{R}_0^d} \mu \frac{d\tilde{U}_{\varepsilon 2,1}^l}{\ell} v_{2,1} d\mathbf{x} = 0\end{aligned} \tag{3.111}$$

or it can be read as :

$$\begin{aligned}\sum_{i=1}^{6} \mathrm{p}^i(\widehat{\mathbf{U}}_\varepsilon^0, \mathbf{v}) + \sum_{i=13}^{18} a_0^i \mathrm{p}^i(\widehat{\mathbf{U}}_\varepsilon^0, \mathbf{v}) + \int_{\underline{R}_0^d} \big\{(\lambda+2\mu) \frac{d\tilde{U}_{\varepsilon 1,1}^l}{l} + \lambda \widehat{U}_{\varepsilon 2,2}^0\big\} v_{1,1} d\mathbf{x}\\ + \int_{\underline{R}_0^d} \big\{\mu \frac{d\tilde{U}_{\varepsilon 2,1}^l}{l} + \mu \widehat{U}_{\varepsilon 1,2}^0\big\} v_{2,1} d\mathbf{x} = 0\end{aligned}$$

Comparing with (3.106), we get that :

$$\begin{cases}(\lambda+2\mu) \dfrac{d\tilde{U}_{\varepsilon 1,1}^\ell}{\ell} + \lambda \widehat{U}_{\varepsilon 2,2}^0 \rightharpoonup_{\ell\to 0} \sigma_{11}^0\\ \mu \dfrac{d\tilde{U}_{\varepsilon 2,1}^\ell}{\ell} + \mu \widehat{U}_{\varepsilon 1,2}^0 \rightharpoonup_{\ell\to 0} \sigma_{12}^0\end{cases} \tag{3.112}$$

or

$$\begin{cases}\dfrac{d\tilde{U}_{\varepsilon 1,1}^\ell}{\ell} \rightharpoonup_{\ell\to 0} \underbrace{\dfrac{1}{(\lambda+2\mu)}\big(\sigma_{11}^0 - \lambda \widehat{U}_{\varepsilon 2,2}^0\big)}_{\sigma_{11}^*}\\ \dfrac{d\tilde{U}_{\varepsilon 2,1}^\ell}{\ell} \rightharpoonup_{\ell\to 0} \underbrace{\dfrac{1}{\mu}\big(\sigma_{12}^0 - \mu \widehat{U}_{\varepsilon 1,2}^0\big)}_{\sigma_{12}^*}\end{cases} \tag{3.113}$$

The limit is unique, so all the sequence converges weakly. Using the coercive of $\mathrm{p}^i(\mathbf{w}_\ell, \mathbf{w}_\ell)$, in order to obtain the strong convergence, we will consider :

$$\ell \mathrm{E}_\ell = \sum_{i \notin \{7;9\}} a_\ell^i \mathrm{p}^i(\mathbf{w}_\ell, \mathbf{w}_\ell) + \frac{\ell}{d} \int_{\underline{R}_0^d} (\lambda+2\mu) \big[\frac{d\tilde{U}_{\varepsilon 1,1}^\ell}{\ell} - \frac{\sigma_{11}^*}{(\lambda+2\mu)}\big]^2 d\mathbf{x} + \frac{\ell}{d} \int_{\underline{R}_0^d} \mu \big[\frac{d\tilde{U}_{\varepsilon 2,1}^\ell}{\ell} - \frac{\sigma_{12}^*}{\mu}\big]^2 d\mathbf{x} \tag{3.114}$$

We have

$$\mathrm{E}_\ell = \sum_{i=1}^{18} \frac{a_\ell^i}{\ell} \mathrm{p}^i(\mathbf{w}_\ell, \mathbf{w}_\ell) + \frac{1}{d}\int_{\underline{R}_0^d} \frac{\sigma_{11}^{*2}}{(\lambda+2\mu)} d\mathbf{x} + \frac{1}{d}\int \underline{R}_0^d \frac{\sigma_{12}^{*2}}{\mu} d\mathbf{x} - 2\int_{\underline{R}_0^d} \sigma_{11}^* \Big(\frac{\tilde{U}_{\varepsilon 1,1}^\ell - \widehat{U}_{\varepsilon 1,1}^0}{\ell}\Big) d\mathbf{x}$$
$$-2\int_{\underline{R}_0^d} \sigma_{12}^* \Big(\frac{\tilde{U}_{\varepsilon 2,1}^\ell - \widehat{U}_{\varepsilon 2,1}^0}{\ell}\Big) d\mathbf{x}$$

Or

$$\mathrm{E}_\ell = -\frac{1}{d}\mathrm{p}^8(\widehat{\mathbf{U}_\varepsilon^0}, \mathbf{w}_\ell) - \frac{1}{d}\mathrm{p}^{10}(\widehat{\mathbf{U}_\varepsilon^0}, \mathbf{w}_\ell) - \sum_{i=13}^{16} \frac{a_\ell^i - a_\ell^0}{\ell} \mathrm{p}^i(\widehat{\mathbf{U}_\varepsilon^0}, \mathbf{w}_\ell) + \frac{1}{d}\int_{\underline{R}_0^d} \sigma_{11}^* \Big(\frac{\sigma_{11}^*}{\lambda+2\mu} - \frac{d\tilde{U}_{\varepsilon 1,1}^\ell}{\ell}\Big) d\mathbf{x}$$

Since $\mathrm{E}_\ell \to_{\ell\to 0}$, we can conclude that $\dfrac{d\tilde{U}_{\varepsilon 1,1}^\ell}{\ell} \to_{\ell\to 0} \dfrac{\sigma_{11}^*}{\lambda+2\mu}$ and $\dfrac{d\tilde{U}_{\varepsilon 2,1}^\ell}{\ell} \to_{\ell\to 0} \dfrac{\sigma_{12}^*}{\mu}$ in $L^2(\underline{R}_0^d)$, $\quad \widetilde{\mathbf{U}}_\varepsilon^\ell \to \widehat{\mathbf{U}}_\varepsilon^0$ strongly in $\mathcal{V}_\varepsilon^0$.

Step 4 : We have that $\mathcal{P}'_\varepsilon(\ell) = J_\varepsilon^-(\ell) - J_\varepsilon^+(\ell)$

$$J_\varepsilon^-(\ell) = \frac{1}{d}\int_{\underline{R}_0^d} \Big[\frac{\lambda+2\mu}{2}\tilde{U}_{\varepsilon 2,2}^{\ell 2} + \frac{\mu}{2}\widetilde{U}_{\varepsilon 1,2}^{\ell 2} - \frac{\mu}{2}\big(\frac{d}{\ell}\big)^2 \widetilde{U}_{\varepsilon 2,1}^{\ell 2} - \frac{\lambda+2\mu}{2}\big(\frac{d}{\ell}\big)^2 \widetilde{U}_{\varepsilon 1,1}^{\ell 2}\Big] d\mathbf{x}$$
$$J_\varepsilon^+(\ell) = \frac{1}{L-d}\int_{R_d^L} \Big[\frac{\lambda+2\mu}{2}\widetilde{U}_{\varepsilon 2,2}^{\ell 2} + \frac{\mu}{2}\tilde{U}_{\varepsilon 1,2}^{\ell 2} - \frac{\mu}{2}\big(\frac{L-d}{L-\ell}\big)^2 \widetilde{U}_{\varepsilon 2,1}^{\ell 2} - \frac{\lambda+2\mu}{2}\big(\frac{L-d}{L-\ell}\big)^2 \widetilde{U}_{\varepsilon 1,1}^{\ell 2}\Big] d\mathbf{x}$$

then passing to the limit when $\ell \to 0$, we obtain :

$$\begin{aligned}
\lim_{l\to 0} J_\varepsilon^-(\ell) &= \frac{1}{d}\int_{\underline{R}_0^d} \Big[\frac{\lambda+2\mu}{2}\big(\widehat{U}_{\varepsilon 2,2}^{0\,2} - \frac{1}{\lambda+2\mu}(\sigma_{11}^0 - \lambda\widehat{U}_{\varepsilon 2,2}^0)^2\big) + \frac{\mu}{2}\big(\widehat{U}_{\varepsilon 1,2}^{0\,2} - \frac{1}{\mu}(\sigma_{12}^0 - \mu\widehat{U}_{\varepsilon 1,2}^0)^2\big)\Big] d\mathbf{x} \\
&= \frac{1}{d}\int_{\underline{R}_0^d} \Big[\frac{\lambda+2\mu}{2}\big(\widehat{U}_{\varepsilon 2,2}^{0\,2} - \widehat{U}_{\varepsilon 1,1}^{0\,2}\big) + \frac{\mu}{2}\Big(\widehat{U}_{\varepsilon 1,2}^{0\,2} - \widehat{U}_{\varepsilon 2,1}^{0\,2}\big)\Big] d\mathbf{x} \\
&= \int_{\mathcal{I}_0} \Big[\frac{\lambda+2\mu}{2}\big(U_{\varepsilon 2,2}^{0\,2} - U_{\varepsilon 1,1}^{0\,2}\big) + \frac{\mu}{2}\big(U_{\varepsilon 1,2}^{0\,2} - U_{\varepsilon 2,1}^{0\,2}\big)\Big] d\mathbf{x} \\
\lim_{\ell\to 0} J_\varepsilon^-(\ell) &= \frac{1}{L-d}\int_{R_d^L} \Big[\frac{\lambda+2\mu}{2}\big(\widehat{U}_{\varepsilon 2,2}^{0\,2} - \big(\frac{L-d}{L}\big)^2 \widehat{U}_{\varepsilon 1,1}^{0\,2}\big) + \frac{\mu}{2}\big(\widehat{U}_{\varepsilon 1,2}^{0\,2} - \big(\frac{L-d}{L}\big)^2 U_{\varepsilon 2,1}^{0\,2}\Big)\Big] d\mathbf{x}
\end{aligned}$$

Making the inverse change of variable, $\phi_0^{-1} : R_d^L \to R_0^L$, and using the proposition 3.1, we have

$$\lim_{\ell\to 0} \mathcal{P}'_\varepsilon(0) = 0 \tag{3.115}$$

□

3.A.4 Proof of Proposition 3.5

Proposition 3.5. *(Case $0 \leq \epsilon < 1$ and $\ell = L$) $\forall \varepsilon \in [0,1), \mathcal{P}_\varepsilon$ is continuously differentiable at L and $\mathcal{P}'_\varepsilon(L) = 0$.*

Proof. The proof of the regularity of $\mathcal{P}_\varepsilon$ at $\ell = L$ is quite similarly to the case of $\ell = 0$. The proof is devided into 2 steps.

Step 1 : Making the transport of $\mathbf{U}_\varepsilon^L$ into $\mathcal{U}_\varepsilon^d$ by using the map $\phi_L : R_0^L \to R_0^d, \quad \mathbf{x} \to \dfrac{d}{L} x_1 \mathbf{e}_1 + x_2 \mathbf{e}_2$. With $\mathbf{v} : \Omega_\varepsilon^L \to \mathbb{R}$ is associated with $\widehat{\mathbf{v}} : \Omega_\varepsilon^d \to \mathbb{R}$ by :

$$\widehat{\mathbf{v}}(\mathbf{x}) = \begin{cases} \mathbf{v}(\mathbf{x}) & \text{in } N_\varepsilon^c \\ \mathbf{v} \circ \phi_L^{-1}(\mathbf{x}) & \text{in } \underline{R}_0^d \\ 0 & \text{in } R_d^L \end{cases} \tag{3.116}$$

The image of $\mathcal{V}_\varepsilon^L$ by this isomorphism is $\widehat{\mathcal{V}_\varepsilon^L}$, a (weakly) closed subspace of $\mathcal{V}_\varepsilon^d$. We still have $\widehat{\mathbf{U}}_\varepsilon^L = \overline{\mathbf{U}}_\varepsilon + \widehat{\mathbf{V}}_\varepsilon^L$. Similarly, inserting the change of variable into Eq (3.13) leads to :

$$\mathcal{P}_\varepsilon^L = \min_{\mathbf{v} \in \mathcal{V}_\varepsilon^L} \Big\{ \frac{1}{2} \sum_{i=1}^{6} \mathrm{p}^i(\mathbf{v} + \overline{\mathbf{U}}_\varepsilon, \mathbf{v} + \overline{\mathbf{U}}_\varepsilon) + \frac{1}{2} \sum_{i=7}^{12} a_L^i \mathrm{p}^i(\mathbf{v}, \mathbf{v}) \Big\} \tag{3.117}$$

The minimizer in (54) is $\mathbf{V}_\varepsilon^L$ and $\mathbf{U}_\varepsilon^L$ which satisfies :

$$\forall \mathbf{v} \in \mathcal{V}_\epsilon^L, \quad \sum_{i=1}^{12} a_L^i \mathrm{p}^i(\mathbf{U}_\epsilon^L, \mathbf{v}) = 0 \tag{3.118}$$

Computing in N_ϵ^c, we have

$$\mathrm{p}^1(\mathbf{U}_\epsilon^L, \mathbf{v}) = \int_{\partial N_\epsilon^c} U_{\epsilon 1,1}^L v_1 n_1 ds - \int_{N_\epsilon^c} U_{\epsilon 1,11}^L v_1 d\mathbf{x}, \quad \mathrm{p}^2(\mathbf{U}_\epsilon^L, \mathbf{v}) = \int_{\partial N_\epsilon^c} U_{\epsilon 1,2}^L v_1 n_2 ds - \int_{N_\epsilon^c} U_{\epsilon 1,22}^L v_1 d\mathbf{x}$$

$$\mathrm{p}^3(\mathbf{U}_\epsilon^L, \mathbf{v}) = \int_{\partial N_\epsilon^c} U_{\epsilon 2,1}^L v_2 n_1 ds - \int_{N_\epsilon^c} U_{\epsilon 2,11}^L v_2 d\mathbf{x}, \quad \mathrm{p}^4(\mathbf{U}_\epsilon^L, \mathbf{v}) = \int_{\partial N_\epsilon^c} U_{\epsilon 2,2}^L v_2 n_2 ds - \int_{N_\epsilon^c} U_{\epsilon 2,22}^L v_2 d\mathbf{x}$$

$$\mathrm{p}^5(\mathbf{U}_\epsilon^L, \mathbf{v}) = \int_{\partial N_\epsilon^c} U_{\epsilon 1,1}^L v_2 n_2 ds - \int_{N_\epsilon^c} U_{\epsilon 1,12}^L v_2 d\mathbf{x} + \int_{\partial N_\epsilon^c} U_{\epsilon 2,2}^L v_1 n_1 ds - \int_{N_\epsilon^c} U_{\epsilon 2,21}^L v_1 d\mathbf{x}$$

$$\mathrm{p}^6(\mathbf{U}_\epsilon^L, \mathbf{v}) = \int_{\partial N_\epsilon^c} U_{\epsilon 1,2}^L v_2 n_1 ds - \int_{N_\epsilon^c} U_{\epsilon 1,21}^L v_2 d\mathbf{x} + \int_{\partial N_\epsilon^c} U_{\epsilon 2,1}^L v_1 n_2 ds - \int_{N_\epsilon^c} U_{\epsilon 2,12}^L v_1 d\mathbf{x}$$

We can deduce from that :

$$\sum_{i=1}^{6} \mathrm{p}^i(\mathbf{U}_\epsilon^L, \mathbf{v}) = 0 \quad \text{and} \quad \sum_{i=7}^{12} a_L^i \mathrm{p}^i(U_\epsilon^L, \mathbf{v}) = 0 \tag{3.119}$$

Or it can be read as in $(\ \Omega_\epsilon^L \setminus N_\epsilon^c\ ) \cup I_0$

$$\begin{cases} (\lambda+2\mu)U^L_{\epsilon 1,11} + \mu U^L_{\epsilon 1,22} + \lambda U^L_{\epsilon 2,21} + \mu U^L_{\epsilon 2,12} = 0 \\ \mu U^L_{\epsilon 2,11} + (\lambda+2\mu)U^L_{\epsilon 2,22} + \lambda U^L_{\epsilon 1,12} + \mu U^L_{\epsilon 1,21} = 0 \end{cases} \tag{3.120}$$

and also in $\Omega_\epsilon^L \setminus R_0^d$,

$$\begin{cases} (\lambda+2\mu)\dfrac{d}{L}U^L_{\epsilon 1,11} + \mu\dfrac{d}{L}U^L_{\epsilon 1,22} + \lambda U^L_{\epsilon 2,21} + \mu U^L_{\epsilon 2,12} = 0 \\ \mu\dfrac{d}{L}U^L_{\epsilon 2,11} + (\lambda+2\mu)\dfrac{L}{d}U^L_{\epsilon 2,22} + \lambda U^L_{\epsilon 1,12} + \mu U^L_{\epsilon 1,21} = 0 \end{cases} \tag{3.121}$$

Multiplying the two previous equations with $\mathbf{v} \in \mathcal{V}_\epsilon^d$, then integrate over $N_\epsilon^c \cup \underline{R}_0^d$, we obtain :

$$\sum_{i=1}^{6} \mathrm{p}^i(\mathbf{U}_\epsilon^L, \mathbf{v}) + \sum_{i=7}^{12} a_L^i \mathrm{p}^i(\mathbf{U}_\epsilon^L, \mathbf{v}) = \int_{\mathcal{I}_d} \big(\sigma_{11}^L v_1 + \sigma_{12}^L v_2\big) ds = \underbrace{-\int_{R_d^L} \big(\sigma_{11}^L v_{1,1} + \sigma_{12}^L v_{2,1}\big) d\mathbf{x}}_{\mathrm{q}_1^L(\mathbf{v})}$$

We define

$$\sigma_{11}^L(x_2) = (\lambda+2\mu)U^L_{\epsilon 1,1}(0+,x_2) + \lambda U^L_{\epsilon 2,2}(0+,x_2) = (\lambda+2\mu)\frac{d}{L}U^L_{\epsilon 1,1}(d-,x_2) + \lambda U^L_{\epsilon 2,2}(d-,x_2)$$

$$\sigma_{12}^L(x_2) = \mu\big[U^L_{\epsilon 1,1}(0+,x_2) + U^L_{\epsilon 1,2}(0+,x_2)\big] = \mu\big[\frac{d}{L}U^L_{\epsilon 2,1}(d-,x_2) + U^L_{\epsilon 1,2}(d-,x_2)\big]$$

with $\sigma_{11}^L,\ \sigma_{12}^L \in L^2(\mathcal{I}_L)$ because there is no singularity at $(L,0)$. Besides, we also have $\sum_{i=1}^{18} a_\ell^i \mathrm{p}^i(\tilde{\mathbf{U}}_\epsilon^\ell, \mathbf{v}) = 0,\ \forall \mathbf{v} \in \mathcal{V}_\epsilon^d$, setting $\mathbf{w}_\ell = \widetilde{\mathbf{U}}_\epsilon^\ell - \mathbf{U}_\epsilon^\ell$ and choosing $\mathbf{v} = \mathbf{w}_\ell$, we get

$$\sum_{i=1}^{18} a_\ell^i \mathrm{p}^i(\mathbf{w}_\ell, \mathbf{w}_\ell) + \sum_{i=1}^{18} a_\ell^i \mathrm{p}^i(\mathbf{U}_\epsilon^L, \mathbf{w}_\ell) = 0$$

or

$$\sum_{i=1}^{18} a_\ell^i \mathrm{p}^i(\mathbf{w}_\ell, \mathbf{w}_\ell) + \sum_{i=1}^{6} \mathrm{p}^i(\mathbf{U}_\epsilon^L, \mathbf{w}_\ell) + \sum_{i=7}^{12} a_L^i \mathrm{p}^i(\mathbf{U}_\epsilon^L, \mathbf{w}_\ell) + \sum_{i=7}^{12} (a_\ell^i - a_L^i) \mathrm{p}^i(\mathbf{U}_\epsilon^L, \mathbf{w}_\ell) = 0$$

. Finally, we have :

$$\sum_{i=1}^{18} a_\ell^i \mathrm{p}^i(\mathbf{w}_\ell, \mathbf{w}_\ell) + \sum_{i=7}^{12} (a_\ell^i - a_L^i) \mathrm{p}^i(\mathbf{U}_\varepsilon^L, \mathbf{w}_\ell) + \mathrm{q}_1^L(\mathbf{w}_\ell) = 0 \tag{3.122}$$

When $\ell \to L$, the behaviors of the coefficients as following :

$$a_\ell^1 = a_\ell^2 = a_\ell^2 = a_\ell^3 = a_\ell^4 = a_\ell^5 = a_\ell^6 = 1,\ a_\ell^7 = a_\ell^8 = a_\ell^9 = a_\ell^{10} = O(1),\ a_\ell^{11} = a_\ell^{12} = 1$$

$$a_\ell^{13} = O\big((L-\ell)^{-1}\big),\ a_\ell^{14} = O(L-\ell),\ a_\ell^{15} = O\big(O(L-\ell)^{-1}\big),\ a_\ell^{16} = O(L-\ell),\ a_\ell^{17} = a_\ell^{18} = 1$$

$$a_\ell^7 - a_L^7 = \ a_\ell^8 - a_L^8 = \ a_\ell^9 - a_L^9 = \ a_\ell^{10} - a_L^{10} = O(L-\ell),\ a_\ell^{11} - a_L^{11} = a_\ell^{12} - a_L^{12} = 0$$

Therefore,

$$\sum_{i=1}^{18} a_\ell^i \mathrm{p}^i(\mathbf{w}_\ell, \mathbf{w}_\ell) + \sum_{i=7}^{10}(a_\ell^i - a_L^i)\mathrm{p}^i(\mathbf{U}_\varepsilon^L, \mathbf{w}_\ell) + \mathrm{q}_1^L(\mathbf{w}_\ell) = 0 \tag{3.123}$$

So, we can have

$$\begin{aligned}&\|\mathbf{w}_\ell\|^2_{\Omega_\varepsilon^d \setminus R_d^L} + \frac{1}{L-\ell}|w_{\ell 1,1}|^2_{R_d^L} + (L-\ell)|w_{\ell 1,2}|^2_{R_d^L} + \frac{1}{L-\ell}|w_{\ell 2,1}|^2_{R_d^L} + (L-\ell)|w_{\ell 2,2}|^2_{R_d^L}\\ &+ \int_{R_d^L}\big(w_{\ell 1,1}w_{\ell 2,2} + w_{\ell 1,2}w_{\ell 2,1}\big)d\mathbf{x} \le C(L-\ell)\|\mathbf{w}_\ell\|_{\Omega_\varepsilon^d\setminus R_d^L} + C\big(|w_{\ell 1,1}|_{R_d^L} + |w_{\ell 2,1}|_{R_d^L}\big)\end{aligned}$$

can imply :

$$\begin{cases} \|\mathbf{w}_\ell\|_{\Omega_\varepsilon^d\setminus R_d^L} \le C\sqrt{L-\ell},\ |w_{l1,1}|_{R_d^L} \le C(L-\ell) \\ |w_{l2,1}|_{R_d^L} \le C(L-l),\ |w_{\ell 1,2}|_{R_d^L} \le C|w_{\ell 2,2}|_{R_d^L} \le C \end{cases} \tag{3.124}$$

It concludes that $\widetilde{\mathbf{U}}_\varepsilon^\ell - \mathbf{U}_\varepsilon^L$ converges weakly to 0 in $\mathcal{V}_\varepsilon^L$. Moreover, we have a (sub-sequence of) $(\lambda+2\mu)\dfrac{\widetilde{U}_{\varepsilon 1,1}^\ell}{L-\ell} \rightharpoonup *$ and $\mu\dfrac{\tilde{U}_{\varepsilon 2,1}^\ell}{L-\ell} \rightharpoonup **$ when $\ell \to L$ in $L^2(R_d^L)$. However, the equation

$$\sum_{i=1}^{18} a_\ell^i \mathrm{p}^i(\widetilde{\mathbf{U}}_\varepsilon^\ell, \mathbf{v}),\ \forall \mathbf{v} \in \mathcal{V}_\varepsilon^d = 0$$

then passing to the limit when $\ell \to L$, we obtain :

$$\begin{aligned}\sum_{i=1}^{6}\mathrm{p}^i(\mathbf{U}_\varepsilon^L, \mathbf{v}) + \sum_{i=7}^{12} a_L^i \mathrm{p}^i(\mathbf{U}_L^\varepsilon, \mathbf{v}) + \int_{R_d^L}(\lambda+2\mu)\frac{L-d}{L-\ell}\widetilde{U}_{\varepsilon 1,1}^\ell v_{1,1}d\mathbf{x} + \int_{R_d^L}\mu\frac{L-d}{L-\ell}\widetilde{\mathbf{U}}_{\varepsilon 2,1}^\ell v_{2,1}d\mathbf{x}\\ + \int_{R_d^L}\big(\lambda\widetilde{U}_{\varepsilon 1,1}^l v_{2,2} + \mu\widetilde{U}_{\varepsilon 2,1}^l v_{1,2}\big)d\mathbf{x} = 0\end{aligned}$$

then comparing with Eq (3.123), we have

$$\begin{cases} (\lambda+2\mu)\dfrac{L-d}{L-\ell}\tilde{U}_{\varepsilon 1,1}^\ell \rightharpoonup_{\ell\to L} \sigma_{11}^L \\ \mu\dfrac{L-d}{L-\ell}\tilde{U}_{\varepsilon 2,1}^\ell \rightharpoonup_{\ell\to L} \sigma_{12}^L \end{cases} \tag{3.125}$$

$$\text{Or it can be read as} \quad \begin{cases} \dfrac{L-d}{L-\ell}\tilde{U}_{\varepsilon 1,1}^\ell \rightharpoonup_{\ell\to L} = \underbrace{\dfrac{1}{\lambda+2\mu}\sigma_{11}^L}_{\sigma_{11}^*} \\ \dfrac{L-d}{L-\ell}\tilde{U}_{\varepsilon 2,1}^\ell \rightharpoonup_{\ell\to L} = \underbrace{\dfrac{1}{\mu}\sigma_{12}^L}_{\sigma_{12}^*} \end{cases} \tag{3.126}$$

The limit is unique, so all the sequence convergences weakly. In order to obtain the strong convergence, similarly we consider :

$$(L-\ell)\mathrm{E}_\ell = \sum_{i\notin\{13,15\}} a_\ell^i \mathrm{p}(\mathbf{w}_\ell,\mathbf{w}_\ell) + \frac{L-\ell}{L-d}\int_{R_d^L}(\lambda+2\mu)\big[\frac{L-d}{L-\ell}\widetilde{U}^\ell_{\varepsilon 1,1} - \frac{1}{\lambda+2\mu}\sigma^*_{11}\big]^2 d\mathbf{x}$$
$$+\frac{L-\ell}{L-d}\int_{R_d^L}\mu\big[\frac{L-d}{L-\ell}\widetilde{U}^\ell_{\varepsilon 2,1} - \frac{1}{\mu}\sigma^*_{12}\big]^2 d\mathbf{x}$$

From that, we have

$$\mathrm{E}_\ell = \sum_{i=1}^{18}\frac{a_\ell^i}{\ell}\mathrm{p}^i(\mathbf{w}_\ell,\mathbf{w}_\ell) + \frac{1}{L-d}\int_{R_d^L}\frac{1}{\mu}\sigma^*_{11}d\mathbf{x} - 2\int_{R_d^L}\frac{\tilde{U}^\ell_{\varepsilon 1,1}-U^\ell_{\varepsilon 1,1}}{L-\ell}d\mathbf{x} - 2\int_{R_d^L}\frac{\tilde{U}^\ell_{\varepsilon 2,1}-U^\ell_{\varepsilon 2,1}}{L-\ell}\sigma^*_{12}d\mathbf{x}$$

Otherwise , because of $\sum_{i=1}^{18} a_\ell^i \mathrm{p}^i(\mathbf{w}_\ell,\mathbf{w}_\ell) + \sum_{i=7}^{10}(a_\ell^i - a_L^i)\mathrm{p}^i(\mathbf{U}^\ell_\varepsilon,\mathbf{w}_\ell) + \mathrm{q}_1^L(\mathbf{w}_\ell) = 0$, E_ℓ can be read as :

$$\begin{aligned}
\mathrm{E}_\ell &= -\sum_{i=7}^{10}\frac{a_\ell^i - a_L^i}{L-\ell}\mathrm{p}^i(\mathbf{U}^L_\varepsilon,\mathbf{w}_\ell) - \int_{R_d^L}\frac{\tilde{U}^L_{\varepsilon 1,1}-U^L_{\varepsilon 1,1}}{L-\ell}\sigma^*_{11}d\mathbf{x} - \int_{R_d^L}\frac{\tilde{U}^L_{\varepsilon 2,1}-U^L_{\varepsilon 2,1}}{L-\ell}\sigma^*_{12}d\mathbf{x}\\
&+\frac{1}{L-d}\int_{R_d^L}\Big(\frac{1}{\lambda+2\mu}{\sigma^*_{11}}^2 + \frac{1}{\mu}{\sigma^*_{12}}^2\Big)d\mathbf{x}\\
&= -\sum_{i=7}^{10}\frac{a_\ell^i - a_L^i}{L-\ell}\mathrm{p}^i(\mathbf{U}^L_\varepsilon,\mathbf{w}_\ell) + \frac{1}{L-d}\int_{R_d^L}\sigma^*_{11}\Big(\frac{1}{\lambda+2\mu}\sigma^*_{11} - \frac{L-d}{L-l}\tilde{U}^l_{\varepsilon 1,1}\Big)d\mathbf{x}\\
&+\frac{1}{L-d}\int_{R_d^L}\sigma^*_{12}\Big(\frac{1}{\mu}\sigma^*_{12} - \frac{L-d}{L-l}\tilde{U}^1_{\varepsilon 2,1}\Big)d\mathbf{x}
\end{aligned} \tag{3.127}$$

Besides, we have $\mathrm{E}_\ell \to 0$, when $\ell \to L$, so, we also have $\dfrac{L-d}{L-\ell}\tilde{U}^\ell_{\varepsilon 1,1}$ converges strongly to $\dfrac{\sigma^*_{11}}{\lambda+2\mu}$ in $L^2(R_d^L)$ and $\dfrac{L-d}{L-\ell}\widetilde{U}^\ell_{\varepsilon 2,1}$ converges strongly to $\dfrac{\sigma^*_{12}}{\mu}$ in $L^2(R_d^L)$, $\widetilde{\mathbf{U}}^\ell_\varepsilon - \mathbf{U}^L_\varepsilon$ converges strongly to $\mathbf{0}$ in $\mathcal{V}_\varepsilon$ and $\dfrac{\mathbf{U}^L_\varepsilon - \tilde{\mathbf{U}}^\ell_\varepsilon}{\sqrt{L-\ell}}$ converges strongly in $H^1(\ \Omega^d_\varepsilon \setminus R_d^L\ )$.

Step 2 : In order to prove that $\lim_{\ell\to L}\mathcal{P}'_\varepsilon(\ell) = 0$, we start from $\mathcal{P}'_\varepsilon(\ell) = \mathcal{J}^-_\varepsilon(\ell) - \mathcal{J}^+_\varepsilon(\ell)$ with $\mathcal{J}^\pm_\varepsilon(\ell)$ is given by :

$$\begin{aligned}
\mathcal{J}^-_\varepsilon(\ell) &= \frac{1}{d}\int_{\underline{R}_0^d}\Big[\frac{\lambda+2\mu}{2}\big(\tilde{U}^{\ell 2}_{\varepsilon 2,2} - \frac{d^2}{\ell^2}\widetilde{U}^{\ell 2}_{\varepsilon 1,2}\big) + \frac{\mu}{2}\big(\tilde{U}^{\ell 2}_{\varepsilon 1,2} - \frac{d^2}{\ell^2}\widetilde{U}^{\ell 2}_{\varepsilon 2,1}\big)\Big]d\mathbf{x}\\
&\to_{\ell\to L}\frac{1}{d}\int_{\underline{R}_0^d}\Big[\frac{\lambda+2\mu}{2}\big(U^{\ell 2}_{\varepsilon 2,2} - \frac{d^2}{\ell^2}U^{\ell 2}_{\varepsilon 1,2}\big) + \frac{\mu}{2}\big(U^{\ell 2}_{\varepsilon 1,2} - \frac{d^2}{\ell^2}U^{\ell 2}_{\varepsilon 2,1}\big)\Big]d\mathbf{x}\\
\mathcal{J}^+_\varepsilon(l) &= \frac{1}{L-d}\int_{\underline{R}_d^L}\Big[\frac{\lambda+2\mu}{2}\big(\widetilde{U}^{l\ 2}_{\varepsilon 2,2} - \frac{(L-d)^2}{(L-l)^2}\widetilde{U}^{l\ 2}_{\varepsilon 1,2}\big) + \frac{\mu}{2}\big(\tilde{U}^{l\ 2}_{\varepsilon 1,2} - \frac{(L-d)^2}{(L-l)^2}\widetilde{U}^{l\ 2}_{\varepsilon 2,1}\big)\Big]d\mathbf{x}\\
&\to_{\ell\to L}\frac{1}{L-d}\int_{\underline{R}_d^L}\Big[\frac{\lambda+2\mu}{2}\Big(U^{L\ 2}_{\varepsilon 2,2} - \big(\frac{\sigma^*_{11}}{\lambda+2\mu}\big)^2\Big) + \frac{\mu}{2}\Big(U^{L\ 2}_{\varepsilon 1,2} - \big(\frac{\sigma^*_{12}}{\mu}\big)^2\Big)\Big]d\mathbf{x}
\end{aligned}$$

Because $U^L_{\varepsilon 2,2}=0$ and $U^L_{\varepsilon 1,2}=0$, $\mathcal{J}^{\pm}_{\varepsilon}(\ell)$ can be read as :

$$\mathcal{J}^{+}_{\varepsilon}(\ell) = -\int_{\mathcal{I}_L}\Big[\frac{{\sigma^*_{11}}^2}{2(\lambda+2\mu)}+\frac{{\sigma^*_{12}}^2}{2\mu}\Big]dx_2 \tag{3.128}$$

by inversed changing the variable $\mathbf{x}\to\phi_L^{-1}(\mathbf{x})$ from $R^d_0\longrightarrow R^L_0$,

$$\begin{aligned}\mathcal{J}^{-}_{\varepsilon}(\ell) &= \frac{1}{L}\int_{\underline{R}^L_0}\Big[\frac{\lambda+2\mu}{2}(U^{L\,2}_{\varepsilon 2,2}-U^{L\,2}_{\varepsilon 1,1})+\frac{\mu}{2}(U^{L\,2}_{\varepsilon 1,2}-U^{L\,2}_{\varepsilon 2,1})\Big]d\mathbf{x}\\ &= \int_{\mathcal{I}_L}\Big[\frac{\lambda+2\mu}{2}(U^{L\,2}_{\varepsilon 2,2}-U^{L\,2}_{\varepsilon 1,1})+\frac{\mu}{2}(U^{L\,2}_{\varepsilon 1,2}-U^{L\,2}_{\varepsilon 2,1})\Big]dx_2 \end{aligned}\tag{3.129}$$

then, using the proposition 3.1, $\mathcal{J}^{+}_{\varepsilon}(\ell)=\mathcal{J}^{-}_{\varepsilon}(\ell)$, so we have $\lim_{\ell\to L}P'_{\varepsilon}(\ell)=0$.

Now, we have to prove that $P'_{\varepsilon}(L)=0$.
Considering $\mathcal{P}_{\varepsilon}(L)-\mathcal{P}_{\varepsilon}(\ell)=\frac{1}{2}\sum_{i=1}^{12}a^i_L\mathrm{p}^i(\mathbf{U}^L_{\varepsilon},\mathbf{U}^L_{\varepsilon})-\frac{1}{2}\sum_{i=1}^{18}a^i_{\ell}\mathrm{p}^i(\tilde{\mathbf{U}}^{\ell}_{\varepsilon},\tilde{\mathbf{U}}^{\ell}_{\varepsilon})$, with $\mathbf{w}_{\ell}=\tilde{\mathbf{U}}^{\ell}_{\varepsilon}-\mathbf{U}^{\ell}_{\varepsilon}$, we obtain :

$$\begin{aligned}P_{\varepsilon}(L)-P_{\varepsilon}(\ell) &= \frac{1}{2}\Big[\sum_{i=1}^{12}a^i_L\mathrm{p}^i(\mathbf{U}^L_{\varepsilon},\widetilde{\mathbf{U}}^L_{\varepsilon})-\sum_{i=1}^{12}a^i_L\mathrm{p}^i(\mathbf{U}^L_{\varepsilon},\mathbf{w}_{\ell})-\sum_{i=1}^{12}a^i_{\ell}\mathrm{p}^i(\mathbf{U}^L_{\varepsilon},\widetilde{\mathbf{U}}^L_{\varepsilon})\\ &- \sum_{i=1}^{18}a^i_{\ell}\mathrm{p}^i(\mathbf{U}^L_{\varepsilon},\mathbf{w}_{\ell})\Big]\end{aligned}\tag{3.130}$$

However, because $\frac{1}{2}\sum_{i=1}^{18}a^i_{\ell}\mathrm{p}^i(\mathbf{U}^L_{\varepsilon},\mathbf{w}_{\ell})=0$ and $\sum_{i=1}^{12}a^i_L\mathrm{p}^i(\mathbf{U}^L_{\varepsilon},\mathbf{w}_{\ell})=\mathrm{q}^L_1(\mathbf{w}_{\ell})=\mathrm{q}^L_1(\tilde{\mathbf{U}}^{\ell}_{\varepsilon})$, $\mathcal{P}_{\varepsilon}{}'(L)$ can be read as :

$$\begin{aligned}\mathcal{P}_{\varepsilon}{}'(L) &= \lim_{\ell\to L}\frac{1}{2}\sum_{i=7}^{10}\frac{a^i_L-a^i_{\ell}}{L-\ell}\mathrm{p}^i(\mathbf{U}^L_{\varepsilon},\widetilde{\mathbf{U}}^L_{\varepsilon})-\mathrm{q}^L_1\big(\frac{\widetilde{\mathbf{U}}^{\ell}_{\varepsilon}}{L-\ell}\big) \qquad (3.131)\\ &= -\frac{d}{2L^2}\mathrm{p}^7(\mathbf{U}^L_{\varepsilon},\mathbf{U}^L_{\varepsilon})+\frac{1}{2d}\mathrm{p}^8(\mathbf{U}^L_{\varepsilon},\mathbf{U}^L_{\varepsilon})-\frac{d}{2L^2}\mathrm{p}^9(\mathbf{U}^L_{\varepsilon},\mathbf{U}^L_{\varepsilon})+\frac{1}{2d}\mathrm{p}^{10}(\mathbf{U}^L_{\varepsilon},\mathbf{U}^L_{\varepsilon})\\ &+ \frac{1}{L-d}\int_{R^L_d}\Big[\frac{{\sigma^L_{11}}^2}{2(\lambda+2\mu)}+\frac{{\sigma^L_{12}}^2}{2\mu}\Big]d\mathbf{x}\end{aligned}$$

Finally, from (3.128) and (3.129), we can conclude that $\mathcal{P}'_{\varepsilon}(L)=\lim_{\ell\to L}\Big[\mathcal{J}^{-}_{\varepsilon}(\ell)-\mathcal{J}^{+}_{\varepsilon}(\ell)\Big]=0$.

□

3.A.5 Lemma 3.2 and its proof

Lemma 3.2. *Let $\mathcal{H}$ be a Hilbert space with norm $\|.\|$ and let Λ be a real interval. Let $\{p^i\}_{1\le i\le m}$ be a family of continuous bilinear symmetric forms on $\mathcal{H}$ and $\{q^i\}_{1\le i\le n}$ a family of continuous linear forms*

on $\mathcal{H}$. Let $\{a_\lambda^i\}_{1\le i\le m}, \{b_\lambda^i\}_{1\le i\le n}$ and c_λ be a real-valued functions of λ, differentiable in Λ.

If $p_\lambda := \sum_{i=1}^m a_\lambda^i p^i$ is coercive on $\mathcal{H}$, uniformly with respect to λ, i.e.

$$\exists \alpha > 0 \quad \forall \lambda \in \Lambda \qquad p_\lambda(\mathbf{u},\mathbf{u}) \ge \alpha \|u\|^2 \qquad \forall u \in \mathcal{H}$$

then the three following properties hold

1. For every $\lambda \in \Lambda$, the minimization problem $min_{u\in\mathcal{H}}\Big\{\frac{1}{2}p_\lambda(\mathbf{u},\mathbf{u})+q_\lambda(u)+c_\lambda\Big\}$ with $q_\lambda := \sum_{i=1}^n b_\lambda^i q^i$ admits a unique solution u_λ;

2. The minimizer u_λ is a differentiable function of λ on Λ and its derivative $\dot{u}_\lambda \in \mathcal{H}$ is given by

$$p_{\lambda(\dot{u}_\lambda,v)} + \sum_{i=1}^m \dot{a}_\lambda^i p^i(u_\lambda, v) + \sum_{i=1}^n \dot{b}_\lambda^i(v) = 0 \qquad \forall v \in \mathcal{H} \tag{3.132}$$

where the dot denotes the derivative with respect to λ.

3. The minimum $P_\lambda := \frac{1}{2}p_\lambda(u_\lambda,u_\lambda) + q_\lambda(u_\lambda) + c_\lambda$ is a differentiable function of λ on Λ and its derivative is given by

$$\dot{P}_\lambda = \frac{1}{2}\sum_{i=1}^m \dot{a}_\lambda^i p^i(u_\lambda,u_\lambda) + \sum_{i=1}^n \dot{b}_\lambda^i q^i(u_\lambda) + \dot{c}_\lambda \tag{3.133}$$

Proof. The proof uses the following Theorem, see [Brezis, 1983].

Theorem . *Let D be a bounded open subset with smooth boundary in $\mathbb{R}^n, p \in (1,+\infty)$, and $\{u_m\}$ be a bounded sequence in $W^{1,p}(D)$. Then there are u in $W^{1,p}(D)$ and a subsequence $\{u_{m_k}\}$ such that $\{u_{m_k}\}$ weakly converges to u.*

1. $\{q^i\}_{1\le i\le n}$ a family of continuous linear forms on $\mathcal{H}$, so q_λ is continuous and linear on $\mathcal{H}$. Using the Riesz theorem, $\exists!\ a\ \in \mathcal{H}$, such that :

$$q_\lambda(u) = \langle u, a\rangle \qquad \forall u \in \mathcal{H}$$

Moreover, $p_\lambda(\mathbf{u},\mathbf{v}) = \sum_{i=1}^m a_\lambda^i p^i(\mathbf{u},\mathbf{v})$ is continuous bilinear and symmetric forms on $\mathcal{H}$, and it is coercive on $\mathcal{H}$ implies $\exists!\ \ u^*$ in $\mathcal{H}$ such that $p_\lambda(u^*,v) = \langle -a, v\rangle \quad \forall v \in \mathcal{H}$ or $p_\lambda(u^*,v) + q_\lambda(v) = 0$ and u^* is the solution of the minimized problem $\min_{u\in\mathcal{H}}\{\frac{1}{2}p_\lambda(\mathbf{u},\mathbf{u}) - \langle a, u\rangle\}$

$$\frac{1}{2}p_\lambda(u^*,u^*) + q_\lambda(u^*) = \min_{u\in\mathcal{H}}\{\frac{1}{2}p_\lambda(\mathbf{u},\mathbf{u}) + q_\lambda(u)\}$$

$\forall \lambda \in \Lambda, \exists u_\lambda$ such that u_λ is the unique solution of $\min_{u\in\mathcal{H}}\{\frac{1}{2}p_\lambda(\mathbf{u},\mathbf{u}) + q_\lambda(u) + c_\lambda\}$ and

$$\begin{cases} p_\lambda(u_\lambda, v) + q_\lambda(v) = 0 & \forall v \in \mathcal{H} \\ p_{\lambda+h}(u_{\lambda+h}, v) + q_{\lambda+h}(v) = 0 & \forall v \in \mathcal{H} \end{cases}$$

$$\Leftrightarrow \quad \sum_{i=1}^m a_\lambda^i p^i(u_\lambda, v) + \sum_{i=1}^n b_\lambda^i q^i(v) = 0 \qquad \forall v \in \mathcal{H} \tag{3.134}$$

$$\sum_{i=1}^m a_{\lambda+h}^i p^i(u_{\lambda+h}, v) + \sum_{i=1}^n b_{\lambda+h}^i q^i(v) = 0 \quad \forall v \in \mathcal{H} \tag{3.135}$$

Let $v_h = \dfrac{u_{\lambda+h} - u_\lambda}{h}$, we have :

$$\begin{aligned} \frac{(3.135)-(3.134)}{h} =& \frac{1}{h}\sum_{i=1}^m a_{\lambda+h}^i p^i(u_{\lambda+h}, v) - \frac{1}{h}\sum_{i=1}^m a_\lambda^i p^i(u_\lambda, v) + \sum_{i=1}^n \frac{b_{\lambda+h}^i - b_\lambda^i}{h} q^i(v) = 0 \\ & \sum_{i=1}^m a_{\lambda+h}^i p^i(v_h, v) + \sum_{i=1}^n \frac{a_{\lambda+h}^i - a_\lambda^i}{h} p^i(u_\lambda, v) + \sum_{i=1}^n \frac{b_{\lambda+h}^i - b_\lambda^i}{h} q^i(v) = 0 \qquad (3.136) \\ & p_{\lambda+h}(v_h, v) + \sum_{i=1}^m \frac{a_{\lambda+h}^i - a_\lambda^i}{h} p^i(u_\lambda, v) + \sum_{i=1}^n \frac{b_{\lambda+h}^i - b_\lambda^i}{h} q^i(v) = 0 \end{aligned}$$

from which, we see that $p_{\lambda+h}(v_h, v)$ converges to $\sum_{i=1}^m \dot{a}_\lambda^i p^i(u_\lambda, v) + \sum_{i=1}^n q^i(v)$ when $h \mapsto 0$. $\forall v \in \mathcal{H},\ \exists C_v$ such that $\|p_{\lambda+h}(v_h, v)\| \leq C_v$ (because $p_{\lambda+h}(v_h, .)$ is a convergent sequence in $\mathbb{R}$, it will be bounded in $\mathbb{R}$). We choose $v = v_h$, so we have $p_{\lambda+h}(v_h, v_h) \leq C_{v_h}$. Using the coercive properties of p_λ, we find out that the sequence v_h is bounded ($\|v_h\|^2 \leq \dfrac{C_{v_h}}{\alpha}$). The theorem above allows us to conclude that there is a subsequence weakly converges in $\mathcal{H}$. Passing to the limit in (5), we obtain that the limit $\dot{u}_\lambda$ satisfies (1) and hence is unique. Because of the unique of the limit $p_\lambda(\dot{u}_\lambda, v)$, all the sequence v_h weakly converges to $\dot{u}_\lambda$.

Then we will prove that v_h converges strongly to $\dot{u}_\lambda$. Because $v_h \rightharpoonup \dot{u}_\lambda$, we have $\lim_{h\mapsto 0} p_\lambda(v_h, v) = p_\lambda(\dot{u}_\lambda, v), \quad \forall v \in \mathcal{H} \Rightarrow \lim_{h\mapsto 0} p_\lambda(v_h - \dot{u}_\lambda, v) = 0 \quad \forall v \in \mathcal{H}$. We also choose that $v = v_h - \dot{u}_\lambda$, that leads to $\lim_{h\mapsto 0} p_\lambda(v_h - \dot{u}_\lambda, v_h - \dot{u}_\lambda) = 0$, using the coercive property of p_λ again, we have $\lim_{h\mapsto 0} \|v_h - \dot{u}_\lambda\|^2 = 0$, concludes that v_h strongly converges to $\dot{u}_\lambda$.

3. Caculating the $\dot{P}_\lambda$ We have $P_\lambda = \frac{1}{2}p_\lambda(u_\lambda, u_\lambda) + q_\lambda + c_\lambda$. Differentating P_λ leads to

$$\dot{P}_\lambda = \underbrace{p_\lambda(\dot{u}_\lambda, u_\lambda) + q_\lambda(\dot{u}_\lambda)}_{0} + \frac{1}{2}\sum_{i=1}^m \dot{a}_\lambda^i p^i(u_\lambda, u_\lambda) + \sum_{i=1}^n \dot{b}_\lambda^i q^i(u_\lambda) + \dot{c}_\lambda$$

Calculation of $\dot{P}_\lambda$ does not require the calculation of $\dot{u}_\lambda$, but only that of u_λ. □

Conclusion and Perspectives

We have presented here a general method based on matched asymptotic expansions which can be applied to determine the mechanical fields and all related mechanical quantities in the case of a defect located at the tip of a notch.

Applying first this method to the case of a non cohesive crack, it turns out that it is sufficient to solve few inner and outer problems to obtain with a very good accuracy the dependence of the energy and the energy release rate on the length of the crack. Moreover, this approximation can be used for very small values of the length of the crack and hence for determining the onset of the cracking whereas a classical finite element method gives rise to inaccurate results. In particular, the matched asymptotic method allowed us to compare the nucleation process of a crack at the tip of the notch which is predicted by the classical Griffith criterion with that predicted by the principle of energy minimization proposed in [Francfort and Marigo, 1998]. It turns out that the latter principle gives rise to much more relevant results than the former from a physical viewpoint.

A natural extension of this work is to consider situations where the geometry and the loading have no symmetry and hence one has also to predict the direction that the nucleated crack will choose. Let us note that the *G-law* alone is not able to give an answer, one must add another criterion for determining the direction. In an anti-plane setting one cannot use the principle of local symmetry which is by essence made for an isotropic plane setting. It turns out that the *FM-law* in its general statement can also predict the direction and more generally the path of the crack, see [Chambolle et al., 2009; Chambolle et al., 2010; Francfort and Marigo, 1998]. So, an interesting challenge should be to use the **MAM** and the *FM-law* in a non symmetric case to predict also the direction of nucleation.

The method was then applied to the case of a cohesive crack. That essentially consists in changing the form of the surface energy. Indeed, the non cohesive case is based on the crucial Griffith assumption that the surface energy is proportional to the crack area and independent of the jump discontinuity of the displacement. This assumption has very important consequences on the nucleation as we have seen in chapter 2. With this hypothesis, there is no cohesive force and hence the model does not

contain the concept of critical stress. An important step will be to apply the **MAM** in the case of a cohesive crack [Barenblatt, 1962; Dugdale, 1960; Del Piero and Raous, 2010] which automatically contains a critical stress and even a characteristic length. The goal will be to study the influence of those critical stress and characteristic length on the nucleation and the propagation of a crack in the spirit of the previous works based on the variational approach to fracture [Abdelmoula et al., 2010; Bourdin et al., 2008; Charlotte et al., 2006; Del Piero and Truskinovsky, 2009; Ferdjani et al., 2007; Giacomini, 2005; Jaubert and Marigo, 2006; Marigo and Truskinovky, 2004].

Bibliography

[Abdelmoula and Marigo, 2000] Abdelmoula, R. and J. J. Marigo: 2000, 'The effective behavior of a fiber bridged crack'. *J. Mech. Phys. Solids* **48**(11), 2419–2444.

[Abdelmoula et al., 2010] Abdelmoula, R., J.-J. Marigo, and T. Weller: 2010, 'Construction and justification of Paris-like fatigue laws from Dugdale-type cohesive models'. *Annals of Solid and Structural Mechanics* **1**(3-4), 139–158.

[Barenblatt, 1962] Barenblatt, G. I.: 1962, 'The mathematical theory of equilibrium cracks in brittle fracture'. *Adv. Appl. Mech.* **7**, 55–129.

[Bilteryst and Marigo, 2003] Bilteryst, F. and J.-J. Marigo: 2003, 'An energy based analysis of the pull-out problem'. *Eur. J. Mech. A-Solid* **22**(1), 55–69.

[Bonnaillie-Noel et al., 2010] Bonnaillie-Noel, V., M. Dambrine, F. Herau, and G. Vial: 2010, 'On generalized Ventcel's type boundary conditions for Laplace operators in a bounded domain'. *SIAM J. Math. Anal.* **42**(2), 931–945.

[Bonnaillie-Noel et al., 2011] Bonnaillie-Noel, V., M. Dambrine, and G. Vial: 2011, 'Small Defects in Mechanics'. In: Simos, T E (ed.): *Internation Conference on Numerical Analysis and Applied Mathematics ICNAAM 2011, Vols A-C*. International Conference on Numerical Analysis and Applied Mathematics (ICNAAM), Halkidiki, Greece, September 19-25, 2011.

[Bourdin et al., 2008] Bourdin, B., G. A. Francfort, and J.-J. Marigo: 2008, 'The variational approach to fracture'. *J. Elasticity* **91**(1-3), 5–148.

[Brezis, 1983] Brezis, H.: 1983, *Analyse fonctionnelle*. Paris: Masson.

[Brezis, 2010] Brezis, H.: 2010, *Functional analysis, Sobolev spaces and partial differential equations*. Springer.

[Bui, 1978] Bui, H. D.: 1978, *Mécanique de la rupture fragile*. Paris: Masson.

[Chambolle et al., 2009] Chambolle, A., G. A. Francfort, and J.-J. Marigo: 2009, 'When and how do cracks propagate?'. *J. Mech. Phys. Solids* **57**(9), 1614–1622.

[Chambolle et al., 2010] Chambolle, A., G. A. Francfort, and J.-J. Marigo: 2010, 'Revisiting energy release rates in brittle fracture'. *J. Nonlinear Sci.* **20**(4), 395–424.

[Chambolle et al., 2008] Chambolle, A., A. Giacomini, and M. Ponsiglione: 2008, 'Crack initiation in brittle materials'. *Arch. Ration. Mech. An.* **188**(2), 309–349.

[Charlotte et al., 2006] Charlotte, M., J. Laverne, and J.-J. Marigo: 2006, 'Initiation of cracks with cohesive force models: a variational approach'. *Eur. J. Mech. A-Solid* **25**(4), 649–669.

[Cherepanov, 1979] Cherepanov, G. P.: 1979, *Mechanics of Brittle Fracture*. McGraw-Hill International Book Company.

[Dal Maso et al., 2005] Dal Maso, G., G. A. Francfort, and R. Toader: 2005, 'Quasistatic crack growth in nonlinear elasticity'. *Arch. Ration. Mech. An.* **176**(2), 165–225.

[Dal Maso and Toader, 2002] Dal Maso, G. and R. Toader: 2002, 'A Model for the Quasi-Static Growth of Brittle Fractures: Existence and Approximation Results'. *Arch. Ration. Mech. An.* **162**, 101–135.

[Dauge, 1988] Dauge, M.: 1988, *Elliptic Boundary Value Problems in Corner Domains — Smoothness and Asymptotic of Solutions*, Lectures Notes in Mathematics. Springer Verlag.

[Dauge et al., 2010] Dauge, M., S. Tordeux, and G. Vial: 2010, 'Selfsimilar perturbation near a corner: matching versus multiscale expansions for a model problem'. In: *Around the research of Vladimir Maz'ya. II*, Vol. 12 of *Int. Math. Ser. (N. Y.)*. Springer, pp. 95–134.

[David et al., 2012] David, M., J.-J. Marigo, and C. Pideri: 2012, 'Homogenized Interface Model Describing Inhomogeneities Localized on a Surface'. *J. Elasticity* **109**(2), 153–187.

[Del Piero, 1999] Del Piero, G.: 1999, 'One-Dimensional ductile-brittle transition, yielding and structured deformations'. *in: P. Argoul, M. Frémond (Eds.), Proceedings of IUTAM Symposium "Variations de domaines et frontières libres en mécanique", Paris, 1997, Kluwer Academic.*

[Del Piero and Raous, 2010] Del Piero, G. and M. Raous: 2010, 'A unified model for adhesive interfaces with damage, viscosity, and friction'. *Eur. J. Mech. A-Solid* **29**(4), 496–507.

[Del Piero and Truskinovsky, 2001] Del Piero, G. and L. Truskinovsky: 2001, 'Macro- and micro-cracking in one-dimensional elasticity'. *Int. J. Solids Struct.* **38**(6), 1135–1138.

[Del Piero and Truskinovsky, 2009] Del Piero, G. and L. Truskinovsky: 2009, 'Elastic bars with cohesive energy'. *Continuum Mech. Therm.* **21**(2), 141–171.

[Destuynder and Djaoua, 1981] Destuynder, P. and M. Djaoua: 1981, 'Sur une interprétation mathématique de l'intégrale de Rice en théorie de la rupture fragile'. *Math. Met. Appl. Sc* **3**, 70–87.

[Dugdale, 1960] Dugdale, D. S.: 1960, 'Yielding of steel sheets containing slits'. *J. Mech. Phys. Solids* **8**, 100–108.

[Ferdjani et al., 2007] Ferdjani, H., R. Abdelmoula, and J.-J. Marigo: 2007, 'Insensitivity to small defects of the rupture of materials governed by the Dugdale model'. *Continuum Mech. Therm.* **19**(3-4), 191–210.

[Francfort and Larsen, 2003] Francfort, G. A. and C. Larsen: 2003, 'Existence and convergence for quasi-static evolution in brittle fracture'. *Commun. Pur. Appl. Math.* **56**(10), 1465–1500.

[Francfort and Marigo, 1998] Francfort, G. A. and J.-J. Marigo: 1998, 'Revisiting brittle fracture as an energy minimization problem'. *J. Mech. Phys. Solids* **46**(8), 1319–1342.

[G.Duvaut, 1990] G.Duvaut: 1990, *Mécanique des milieux continus*. Masson.

[Geymonat et al., 2011] Geymonat, G., F. Krasucki, S. Hendili, and M. Vidrascu: 2011, 'The matched asymptotic expansion for the computation of the effective behavior of an elastic structure with a thin layer of holes'. *Int. J. Multiscale Comput. Eng.* **9**(5), 529–542.

[Giacomini, 2005] Giacomini, A.: 2005, 'Size effects on quasi-static growth of cracks'. *SIAM J. Math. Anal.* **36**(6), 1887–1928.

[Griffith, 1920] Griffith, A.: 1920, 'The phenomena of rupture and flow in solids'. *Phil. Trans. Roy. Soc. London* **CCXXI**(A), 163–198.

[Grisvard, 1985] Grisvard, P.: 1985, *Elliptic problems in non smooth domains*, No. 24 in Monographs and Studies in Mathematics. Pitman.

[Grisvard, 1986] Grisvard, P.: 1986, 'Problèmes aux limites dans les polygones; Mode d'emploi'. *EDF, Bulletin de la Direction des Études et Recherches* **Série C**(1), 21–59.

[Grisvard, 1992] Grisvard, P.: 1992, *Singularities in boundary value problems.* Masson.

[Irwin, 1958] Irwin, G. R.: 1958, 'Fracture'. *In Handlbuch des Physik, Springer Verlag* **6**, 551–590.

[Jaubert and Marigo, 2006] Jaubert, A. and J.-J. Marigo: 2006, 'Justification of Paris-type Fatigue Laws from Cohesive Forces Model via a Variational Approach'. *Continuum Mech. Therm.* **V18**(1), 23–45.

[Kevorkian and Cole, 1996] Kevorkian, J. and J. Cole: 1996, *Multiple scale and singular perturbation methods.* Springer.

[Laverne and Marigo, 2004] Laverne, J. and J.-J. Marigo: 2004, 'Global approach, relative minima and yield criterion in Fracture Mechanics'. *Comptes Rendus Mécanique* **332**(4), 313–318.

[Lawn, 1993] Lawn, B.: 1993, *Fracture of Brittle Solids - Second Edition*, Cambridge Solid State Science Series. Cambridge: Cambridge University press.

[Leblond, 2000] Leblond, J.-B.: 2000, *Mécanique de la rupture fragile et ductile*, Collection Études en mécanique des matériaux et des structures. Editions Lavoisier.

[Leguillon, 1990] Leguillon, D.: 1990, 'Calcul du taux de restitution de l'énergie au voisinage d'une singularité'. *C. R. Acad. Sci. II b* **309**, 945–950.

[Marigo, 2010] Marigo, J.-J.: 2010, 'Initiation of cracks in Griffith's theory: an argument of continuity in favor of global minimization'. *J. Nonlinear Sci.* **20**(6), 831–868.

[Marigo and Pideri, 2011] Marigo, J.-J. and C. Pideri: 2011, 'The effective behavior of elastic bodies containing microcracks or microholes localized on a surface'. *Int. J. Damage Mech.* **20**, 1151–1177.

[Marigo and Truskinovky, 2004] Marigo, J.-J. and L. Truskinovky: 2004, 'Initiation and propagation of fracture in the models of Griffith and Barenblatt'. *Continuum Mech. Therm.* **16**(4), 391–409.

[Marsden and Hughes, 1983] Marsden, J. and T. Hughes: 1983, *Mathematical foundations of elasticity.* Prentice Hall.

[Muskhelishvili, 1963] Muskhelishvili, N.: 1963, *Some basic problems of mathematical theory of elasticity.* P. Noordhoff Ltd, Groningen.

[Needleman, 1992] Needleman, A.: 1992, 'Micromechanical modelling of interface decohesion'. *Ultramicroscopy* **40**, 203–214.

[Negri, 2008] Negri, M.: 2008, 'A comparative analysis on variational models for quasi-static brittle crack propagation'. *Advances in Calculus of Variations* **3**(2), 149—212.

[Negri and Ortner, 2008] Negri, M. and C. Ortner: 2008, 'Quasi-static crack propagation by Griffith's criterion'. *Math. Mod. Meth. Appl. S.* **18**, 1895–1925.

[Nguyen, 2000] Nguyen, Q. S.: 2000, *Stability and Nonlinear Solid Mechanics*. London: Wiley & Son.

[Recho, 2012] Recho, N.: 2012, *Fracture Mechanics and crack growth*. Wiley-ISTE.

[Rice, 1968] Rice, J. R.: 1968, 'A path independent integral and the approximate analysis of strain concentration by notches and cracks'. *J. Appl. Mech.* **35**, 379–386.

[Vidrascu et al., 2012] Vidrascu, M., G. Geymonat, S. Hendili, and F. Krasucki: 2012, 'Matched asymptotic expansion and domain decomposition for an elastic structure'. In: *21st International Conference on Domain Decomposition Methods*. Rennes, France.

[Willis, 1967] Willis, J. R.: 1967, 'A comparison of the fracture criteria of Griffith and Barenblatt'. *J. Mech. Phys. Solids* **15**, 151–162.

List of Figures

List of Tables

Contents